Functional Impact of Phosphodiesterase 4 (PDE4) Subtypes in Human Primary Immune Cells

DISSERTATION

zur
Erlangung des akademischen Grades eines
Doktors der Naturwissenschaften (Dr. rer. nat.)
des Fachbereichs für Biologie
an der Universität Konstanz

vorgelegt von

Daniel Peter

Tag der mündlichen Prüfung: 12.12.2006
1. Referent: Prof. Dr. Marcus Groettrup
2. Referent: Priv. Doz. Dr. Christian Schudt

Acknowledgments

The present dissertation was performed from May 2003 - October 2006 in the Department of Biochemistry 2 (RPR/B2) at ALTANA Pharma AG, Konstanz and was encouraged and assisted by numerous people. For the extensive support that I received during the study I would like to express my sincere gratitude and respect, especially to:

Dr. Armin Hatzelmann for offering the attractive project in his department, for critical surveillance and support of the study, and for the outstanding scientific expertise.
Dr. Christof Zitt for his excellent supervision, the friendly atmosphere in his group, the helpful advice for the progress of the study, but also for facilitating self-directed work.
Prof. Dr. Marcus Groettrup for the continuous evaluation of the study and inspiring ideas for the scientific concept.
Dr. Hermann Tenor for diverse contributions and for initiating the cooperation with Prof. Dr. Marco Conti.
Sandra Hamm and Bettina Eidmann for the cordially teamwork in the lab and all other colleagues from the biochemistry departments for appreciated help in various concerns.
Barbara Burgbacher for support with immunoblot experiments.
Drs. Volker Gekeler and Hans-Peter Hoffmann and colleagues from the oncology department for valuable help in establishing the knockdown technique in the A549 cell line.
Dr. Oliver Steinbach and Jonathan Gilbert for helpful advice concerning the siRNA technology.
Prof. Dr. Marco Conti and Dr. Catherine Jin for the excellent research training in their laboratory in Stanford and for their scientific contributions to the study.
Priv. Doz. Dr. Christian Schudt for insight into the large field of inflammation and for evaluation of the study.
Prof. Dr. Albrecht Wendel and Prof. Dr. Klaus Schaefer for having organized and Dr. Priv. Doz. Jutta Schlepper-Schaefer for having coordinated the unique graduate program ‘Biomedical Drug Research’. I was very honored to participate in this program.

I would like to thank all colleagues and friends from work and social life, who altogether multifariously contributed to transform challenging ‘everyday’ work into a pleasant and motivating activity.

My special thanks go to my parents, who always supported me on my way and gave me faith in what I was doing. Finally, I am deeply indepted to Eva for her love and encouragement.

TABLE OF CONTENTS

List of abbreviations……..……...IV

1 INTRODUCTION....1
1.1 The second messenger cAMP....1
1.2 Phosphodiesterases (PDEs): a superfamily inactivating cyclic nucleotides....3
1.3 The phosphodiesterase 4 family comprises a variety of isoforms....7
1.3.1 Structural properties of PDE4 isoforms....7
1.3.2 Upstream conserved regions (UCRs): unique regulatory motifs of PDE4 isoforms....9
1.3.3 Phosphorylation controls PDE4 activity....11
1.4 cAMP exhibits many inhibitory properties in immune cells....11
1.5 PDE4 isoforms are widely expressed in inflammatory and immunocompetent cells....13
1.6 PDE4 inhibition has anti-inflammatory and immunomodulatory properties....14
1.7 Functional impact of PDE4 subtypes in human immune cells....17
1.8 Aims of the study....19

2 MATERIALS AND METHODS....20
2.1 Materials....20
2.1.1 Chemicals....20
2.1.2 Reagents and kits....20
2.1.3 Radioactive materials....20
2.1.4 Buffers and solutions....20
2.1.5 Phosphodiesterase inhibitors....21
2.1.6 Oligonucleotides....21
2.1.7 DNA and RNA modifying enzymes....23
2.1.8 Antibodies....23
2.1.9 Cytokines and lipopolysaccharide....24
2.1.10 Kits for enzyme-linked immunosorbent assays (ELISA)....24
2.1.11 Primary cells and cell lines....24
2.1.12 Cell isolation reagents....24
2.1.13 Cell culture media....24
2.1.14 Cell transfection reagents....25
2.1.15 Devices and software....25
2.2 Molecular biology methods....26
2.2.1 RNA isolation and quantification....26
2.2.2 cDNA synthesis and quantitative PCR....26
2.2.3 Relative expression calculated by the $\Delta\Delta C_t$ method....27
2.3 Biochemical methods....27
2.3.1 Protein determination....27
2.3.2 SDS-Polyacrylamide gel electrophoresis (SDS-PAGE)....28
2.3.3 PDE activity assay....29
2.3.4 Proliferation assay....30
2.4 Immunological methods....31
2.4.1 Immunoprecipitation....31
2.4.2 Immunodetection of blotted proteins....31
2.4.3 Flow cytometry....32
2.4.4 Enzyme-linked immunosorbent assay (ELISA)....33
2.5 Eukaryotic cell culture....33
2.6 Isolation of human primary immune cells....33

2.6.1 Isolation of untouched $CD4^+$ T cells....33
2.6.2 Isolation of untouched $CD4^+$ T cells positive for CD45RA or CD45RO....34
2.6.3 Isolation of untouched $CD8^+$ T cells....34
2.6.4 Isolation of human peripheral $CD14^+$ monocytes....34
***2.7 In vitro* generation of macrophages and dendritic cells....35**
2.7.1 Differentiation of $CD14^+$ cells to monocyte-derived macrophages (Mo$M\phi$)....35
2.7.2 Differentiation of $CD14^+$ cells to monocyte-derived dendritic cells (MoDCs)....35
2.8 Transfection of cells....36
2.8.1 Transfection of A549 cells with the cationic lipid argfectin-50....36
2.8.2 Electroporation of $CD4^+$ T cells using the amaxa nucleofector (nucleofection)....36
2.9 Stimulation of human primary immune cells....37
2.9.1 Anti-CD3/CD28 stimulation of T cells....37
2.9.2 LPS stimulation of macrophages (Mo$M\phi$) and dendritic cells (MoDCs)....38
2.10 Bioinformatics....38

3 RESULTS....39
3.1 Validation of PCR primer and probes....39
3.2 Selection of target cells and stimulation conditions....41
3.3 Expression profiling in human primary $CD4^+$ T cells....42
3.3.1 Isolation and stimulation of human primary $CD4^+$ T cells....42
3.3.2 PDE4 subtype mRNA expression and regulation in human primary $CD4^+$ T cells....43
3.3.3 Regulation of PDE4 subtypes after stimulation with different anti-CD3/CD28 ratios....45
3.3.4 Regulation of PDE4 subtypes in human primary naïve and memory $CD4^+$ T cells....46
3.3.5 PDE4 activity in human primary $CD4^+$ T cells....47
3.3.6 Immunodetection of PDE4 subtypes in human primary $CD4^+$ T cells....48
3.4 Expression profiling in $CD8^+$ T cells, monocytes, and monocyte-derived cells....50
3.4.1 PDE4 subtype mRNA expression and regulation in $CD8^+$ T cells....50
3.4.2 PDE4 subtype mRNA expression in monocytes, Mo$M\phi$, and MoDCs....51
3.4.3 PDE4 subtype mRNA regulation after LPS stimulation in Mo$M\phi$ and MoDCs....53
3.5 Validation of PDE4 subtype-specific knockdown tools in A549....55
3.5.1 Delivery of antisense and small interfering RNA into A549 cells via lipofection....56
3.5.2 Validation of knockdown constructs directed against PDE4 subtypes in A549 cells....57
3.5.3 mRNA knockdown of PDE4 subtypes in transfected A549 cells....59
3.5.4 PDE4 activity knockdown in transfected A549 cells....61
3.5.5 Immunodetection of PDE4D splice variants in untreated and transfected A549 cells....63
3.5.6 Summary: Antisense versus siRNA in transfected A549 cells....65
3.6 Validation of PDE4 subtype-specific siRNAs in $CD4^+$ T cells....65
3.6.1 Delivery of a GFP-plasmid and of FITC-siRNA into $CD4^+$ T cells via nucleofection....66
3.6.2 Selection of individual PDE4 subtype-specific siRNAs....66
3.6.3 Tolerability of amaxa nucleofection in $CD4^+$ T cells....67
3.6.4 PDE4 subtype-specific mRNA knockdown in nucleofected $CD4^+$ T cells....70
3.6.5 siRNA-mediated PDE4 activity knockdown in nucleofected $CD4^+$ T cells....71
3.7 Anti-CD3/CD28 induced release of cytokines and the effect of PDE inhibition on T cells....72
3.7.1 Time-dependent release of cytokines after anti-CD3/CD28 stimulation of $CD4^+$ T cells....72
3.7.2 Suppression of cytokine release and proliferation by PDE4 and/or PDE3 inhibition....74
3.7.3 Suppression of cytokine release and proliferation by Itk-specific siRNA....75
3.8 Impact of PDE4 subtype-specific siRNAs on T cell functions....76
3.8.1 Functional impact of PDE4 subtype-specific siRNAs on IL-2 release in $CD4^+$ T cells....77
3.8.2 Functional impact of PDE4 subtype-specific siRNAs on IFN-γ release in $CD4^+$ T cells....78
3.8.3 Functional impact of PDE4 subtype-specific siRNAs on IL-5 release in $CD4^+$ T cells....79
3.8.4 Functional impact of PDE4 subtype-specific siRNAs on proliferation in $CD4^+$ T cells....80

3.8.5 Summary: Impact of PDE4 subtype-specific siRNAs on T cell function 81

4 DISCUSSION 82

4.1 PDE4 subtype expression and regulation in human primary CD4$^+$ T cells 82

4.1.1 PDE4 subtype mRNA expression and regulation in CD4$^+$ T cells 83

4.1.2 Protein activity of PDE4 subtypes in CD4$^+$ T cells 85

4.1.3 Protein expression of PDE4 subtypes in CD4$^+$ T cells 86

4.1.4 Long- and short-term regulation of PDE4 subtypes 87

4.2 PDE4 subtype expression and regulation in human primary CD8$^+$ T cells 88

4.3 PDE4 subtype expression and regulation in human primary monocytes, macrophages, and dendritic cells 89

4.3.1 PDE4 subtype mRNA expression in monocytes 89

4.3.2 PDE4 subtype mRNA expression in monocyte-derived macrophages (MoMϕ) 90

4.3.3 PDE4 subtype mRNA expression in monocyte-derived dendritic cells (MoDCs) 91

4.4 Application of mRNA knockdown strategies 92

4.4.1 Lipofection of A549 cells with antisense-constructs 92

4.4.2 Lipofection of A549 cells with siRNAs 93

4.4.3 Amaxa nucleofection of CD4$^+$ T cells with siRNAs 94

4.5 Functional impact of PDE4 subtypes in CD4$^+$ T cells 96

4.5.1 Anti-CD3/CD28 activation of CD4$^+$ T cells and IL-2, IFN-γ, and IL-5 synthesis 96

4.5.2 Anti-inflammatory effects of PDE4 inhibitors and the consequences of PDE3 inhibition 98

4.5.3 The impact of PDE4 subtype-specific siRNAs on CD4$^+$ T cell functions 99

4.5.4 The role of PDE4 subtypes for T cell function: Comparison to other studies 102

4.6 Beyond CD4$^+$ T cells: Functional impact of PDE4 subtypes 103

4.7 Future options for the development of PDE4 inhibitors 105

4.8 Compartmentalization of PDE4 subtypes 106

4.9 Conclusions 108

5 SUMMARY 109

6 ZUSAMMENFASSUNG 112

7 REFERENCES 115

LIST OF ABBREVIATIONS

Abbreviation	Full name	Abbreviation	Full name
18S rRNA	18S ribosomal RNA	FITC	Fluorescein isothiocyanate
5'AMP	Adenosine 5' monophosphate	FSH	Follicle stimulating hormone
5'GMP	Guanosine 5' monophosphate	g	Gravitational constant, 9.81 m/s^2
Ab	Antibody	GAF	cGMP binding domain, found in cGMP-regulated PDEs, ACs, and FhlA
AC	Adenylyl cyclase	GEF	Guanine-nucleotide exchange factor
AEBSF	4-(2-Aminoethyl)-benzenesulfonyl fluoride	GM-CSF	Granulocyte-macrophage colony-stimulating factor
Akt	Protein kinase B	GPCR	G protein-coupled receptor
AMV	Avian myeloblastosis virus	GSK-3	Glycogen synthase kinase-3
AP-1	Activator protein-1	GTP	Guanosine 5'-triphosphate
APS	Ammonium peroxodisulfate	h	Hour
AR	Adrenergic receptor	HARBS	High-affinity rolipram-binding state
AS^{1st}	First generation antisense (oligophosphorothioates)	HAT	Histone acetyltransferase
AS^{2nd}	Second generation antisense (2'-alkoxy modified chimeric phosphorothioate oligonucleotides)	HEPES	4-(2-Hydroxyethyl)-1-piperazineethanesulfonic acid
ATF1	Activating transcription factor 1	IBD	Inflammatory bowel disease
ATP	Adenosine 5'-triphosphate	IBMX	3-Isobutyl-1-methylxanthine
Bcl10	B-cell leukaemia protein 10	IFN	Interferon
BSA	Bovine serum albumin	IKK	IκB kinase
CaMKII	Calcium/calmodulin-dependent protein kinase II	IL	Interleukin
cAMP	Adenosine 3'-5' cyclic monophosphate	IMDM	Iscove's modified Dulbecco's medium
CARMA1	Caspase recruitment domain-containing membrane-associated guanylate kinase protein-1	IP3	Inositol-1,4,5-tris-phosphate
CBP	CREB-binding protein	Itk	IL-2 inducible T cell kinase
Cbp/PAG	Csk-binding protein/phosphoprotein associated with glycosphingolipid-enriched micro domains	kDa	Kilo Dalton, molecular weight
cDNA	Copy deoxyribonucleic acid	LAT	Linker for activation of T cells
cGMP	Guanosine 3'-5' cyclic monophosphate	LARBS	Low-affinity rolipram-binding state
CNG	Cyclic nucleotide gated channel	Lck	Src-family tyrosine kinase
COPD	Chronic obstructive pulmonary disease	LTB	Leukotriene B
COT	Cancer osaka thyroid mitogen-activated protein (MAP3) kinase	LTC	Leukotriene C
Cpm	Counts per minute	LPS	Lipopolysaccharide
CRE	cAMP response element	MALT-1	Mucosa-associated lymphoid tissue 1
CREB	CRE-binding protein	MEK	MAPK (mitogen-activated protein kinase)/ERK kinase
CREM	cAMP-responsive element modulator	MGB	Minor groove binder (Applied Biosystem TaqMan probe stabilizer)
Csk	C-terminal Src kinase	min	Minute
DAG	Diacylglycerine	MIP	Macrophage inflammatory protein
DMEM	Dulbecco's modification of Eagle's medium	MoDC	Monocyte-derived dendritic cell
DMSO	Dimethylsulfoxide	MoMΦ	Monocyte-derived macrophage
DNA	Deoxyribonucleic acid	mRNA	Messenger ribonucleic acid
dNTP	2'-Deoxy-nucleoside triphosphate	MUC5AC	Mucin 5AC
ECL	Enhanced chemiluminescence	Nck	Noncatalytic region of tyrosine kinase adaptor protein 1
EDTA	Ethylenediaminetetraacetic acid	NF	Nucleofection
EGTA	Ethylene glycol-bis(2-aminoethylether)-tetraacetic acid	NFAT	Nuclear factor of activated T cells
ELISA	Enzyme-linked immunosorbent assay	NFκB	Nuclear factor κB
ERK	Extracellular signal-regulated kinase	NP-40	Nonionic detergent P-40
FAM	Reporter dye: 6-carboxy-fluorescein	PA	Phosphatidic acid
FCS	Fetal calf serum	PAF	Platelet-activating factor
FEV1	Forced expiratory volume in one sec	PAGE	Polyacrylamide gel electrophoresis

Abbreviation	Full name	Abbreviation	Full name
PAS	Domain found in Per, ARNT, and Sim proteins	RT	Room temperature
PBS	Phosphate buffered saline	RT-PCR	Reverse transcriptase - PCR
PCR	Polymerase chain reaction	SDS	Sodium dodecyl sulfate
PDE	Phosphodiesterase	sec	Second
PE	Phycoerythrin	siRNA	Small interfering RNA
PGD	Prostaglandin D	SLP-76	SH2-domain-containing leukocyte protein of 76 kDa
PGE	Prostaglandin E	SMARTpool	Pool of 4 siRNAs
PHA	Phytohaemagglutinin	TAPAS-1	Tryptophan anchoring phosphatidic acid selective-binding domain 1
PI3K	Phosphatidylinositol-3 kinase	TEMED	Tetramethylethylenediamine
PIP2	Phosphatidylinositol-4,5-bisphosphate	TNF	Tumor necrosis factor
PIP3	Phosphatidylinositol-3,4,5-trisphosphate	Tris	2-Amino-2-(hydroxymethyl)propane-1,3-diol
PKA	Protein kinase A, cAMP-protein kinase	U	Uracil
PKC	Protein kinase C	Ub	Ubiquitin
PLC	Phospholipase C	UBC13	Ubiquitin-conjugating enzyme
RACK	Receptor for activated C-kinase	UCR	Upstream conserved region
RANTES	Regulated on activation, normal T cell expressed and secreted	Vav-1	Guanine exchange factor
RasGRP	Guanine exchange factor	VCAM	Vascular cell adhesion molecule
RISC	RNA-induced silencing complex		
RNAi	RNA interference	VIC	Reporter dye, proprietary to Applied Biosystems
ROS	Reactive oxygen species	v/v	Volume by volume
RP73401	Piclamilast, PDE4 inhibitor	w/v	Weight by volume
rpm	Rotation per minute	XAP2	X-associated protein 2, immunophilin
RPMI	Roswell park memorial institute medium	ZAP70	Zeta-associated protein 70

If not listed here, abbreviations are explained in the text or figures.

1 INTRODUCTION

The transduction of extracellular signals into the cell interior is an important prerequisite for the exertion of various cell functions as well as for cell-to-cell communications. The specific binding of 'first messengers' to cell-surface receptors can trigger the generation of intracellular 'second messengers', such as adenosine 3'-5' cyclic monophosphate (cAMP), which process the signals and direct various cellular responses.

1.1 The second messenger cAMP

Since the first description of cAMP in 1957 (Sutherland and Rall, 1958), a large number of scientific reports have exemplified the profound effects of cAMP action (Beavo and Brunton, 2002; Kopperud et al., 2003). Initially, cAMP signaling involves the specific extracellular ligand binding to G protein-coupled receptors (GPCR), which form one of the largest protein families with more than 1000 variant forms (Hermans, 2003) and can be classified into four major classes (Wess, 1998):

(i) The rhodopsin-type receptor subfamily (Class I) is the largest receptor subfamily, which binds structurally very diverse ligands. This class comprises receptors for sensory stimuli (e.g. rhodopsin), ligands such as glycoprotein hormones (e.g. follicle stimulating hormone [FSH] and luteinizing hormone [LH]), peptides (e.g. angiotensin II, chemokines, and vasopressin), or biogenic amines (e.g. acetylcholine, dopamine, adrenalin/noradrenalin, and histamine), and various signaling molecules (e.g. adenosine, leukotrienes, and prostanoids).

(ii) The Class II subfamily comprises secretin/glucagon receptors.

(iii) The Class III subfamily includes metabiotrophic glutamate receptors, calcium sensors, γ-aminobutyric acid (GABA) receptors, and putative pheromone receptors.

(iv) The Class IV subfamily comprises a small group of other putative pheromone receptors.

While ligands and receptor types are diverse, the molecular mechanism through which all G protein-coupled receptors transduce extracellular signals into the cell is similar. GPCRs can associate with distinct heterotrimeric G proteins (GTP binding protein), which generally consist of a subunit Gα bound to a β/γ complex (Hermans, 2003). Four classes of Gα subunits have been characterized (Neer, 1995): α_S stimulates adenylyl cyclase (AC), α_i inhibits adenylyl cyclase, α_q activates phospholipase C (PLC), and α_{12} regulates Na^+/K^+ exchange. The mode of action of all G proteins can be exemplified for $G\alpha_S$: Interaction of the ligand-activated receptor with a G protein promotes the exchange of GTP for GDP within the active site of $G\alpha_S$ and triggers the dissociation of $G\alpha_S$-GTP from the β/γ complex. As a consequence, $G\alpha_S$-GTP and

the β/γ complex are released and $G\alpha_S$-GTP can transmit signals to effector systems, most notably to distinct isoforms of adenylyl cyclases (Bourne, 1997; Wess, 1998; Hanoune and Defer, 2001). Adenylyl cyclases are anchored in the plasma membrane by two α-helical segments each spanning six transmembranes. The two cytoplasmatic regions host the catalytic apparatus, which is responsible for ATP and $G\alpha_S$ binding and the conversion of ATP into cAMP (Tesmer et al., 1997; Hurley, 1999; Simonds, 1999). cAMP exerts its effect on cellular signaling processes in different ways (Figure 1).

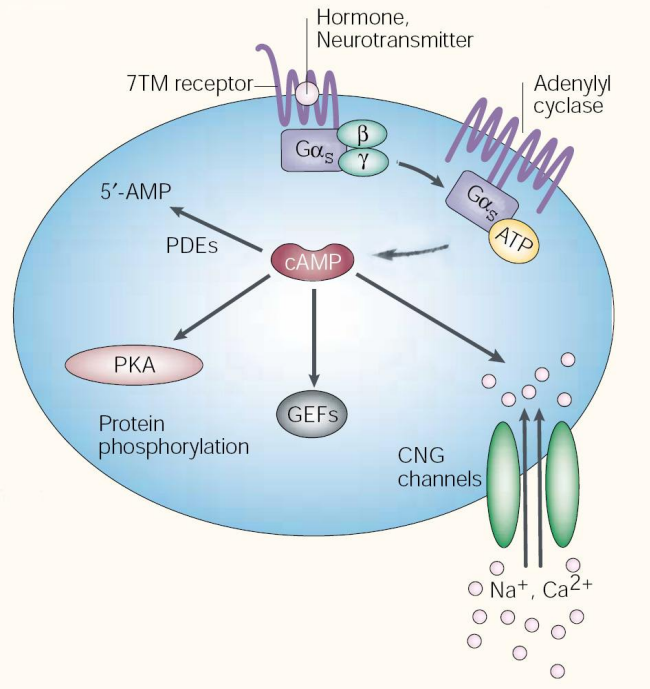

Figure 1. Basic mechanisms of cAMP regulation and function. The cartoon depicts the basic pathways for cAMP metabolism. Upon stimulation of seven transmembrane (7TM) receptors (GPCRs) by hormones or neurotransmitters, G protein subunit $G\alpha_S$ can translocate and activate adenylyl cyclase, which converts ATP into cAMP. cAMP can orchestrate signaling processes via protein kinase A (PKA), guanine-exchange factors (GEFs), and cyclic-nucleotide gated channels (CNG channels). Phosphodiesterases (PDEs) biologically inactivate cAMP. Modified from Beavo and Brunton, 2002.

The direct activation of the cAMP-protein kinase (protein kinase A, PKA) via cAMP is generally considered as the principle mode of cAMP action. The PKA holoenzyme consists of a regulatory (R) subunit dimer and two catalytic (C) subunits and was first biochemically classified as PKA type I and type II (PKAI and PKAII, respectively), according to their order of elution by ion-exchange chromatography (Reimann et al., 1971; Corbin et al., 1975). The large molecular heterogeneity in both R- and C-subunits allows a multiplicity of PKA isoforms with different biochemical properties (Skalhegg and Tasken, 2000). The common mode of action for all PKA isoenzymes is that, upon binding of cAMP to the regulatory domain, active C subunits are released, facilitating the phosphorylation of serine and threonine residues on specific

substrate proteins via transfer of the γ-phosphate of PKA-bound ATP (Taylor et al., 2004). Effects of PKA action are very diverse and can involve the activation of multiple splice variants of nuclear cAMP responsive element (CRE)-binding proteins (CREB) and other closely related gene products, such as activating transcription factor 1 (ATF1) or cAMP-responsive element modulator (CREM), resulting in the activation of a large pool of transcription factors with pleiotropic biological effects (Gonzalez and Montminy, 1989; Lee and Masson, 1993; Shaywitz and Greenberg, 1999). For example, phosphorylated CREB can recruit a co-activator, the CREB-binding protein (CBP), which has an intrinsic histone acetyltransferase (HAT) activity and interacts with RNA polymerase II (Pol II), resulting in the enhanced transcription of many genes that have the cAMP responsive element (CRE) as sequence motif in their promoter regions (Chrivia et al., 1993; Mayr and Montminy, 2001; Vo and Goodman, 2001).

cAMP can also activate effector systems that are independent of PKA. Cyclic nucleotide-gated (CNG) channels, which are directly activated by binding guanosine 3'-5' cyclic monophosphate (cGMP) and cAMP to channel proteins, can control the membrane potential and intracellular Ca^{2+} or Na^{+} levels, and are involved in the photoreceptor cell and olfactory sensory neuron signaling (Wei et al., 1998; Kaupp and Seifert, 2002; Bradley et al., 2005). Cyclic nucleotide-binding sites on guanine-nucleotide-exchange factors (GEFs) can serve as additional effector systems of cAMP action. Bos, Graybiel and coworkers first described the activation of small G-proteins by cAMP-activated GEFs, called Epacs (exchange proteins directly activated by cAMP) (de Rooij et al., 1998; Kawasaki et al., 1998). Epacs have been described to advance the active GTP-bound state of the small G proteins Rap1 and Rap2, which can activate various downstream effector proteins (Kopperud et al., 2003; Bhattacharya et al., 2004).

In summary, cAMP can profoundly influence cellular functions via several effector systems and plays a crucial role for the transduction of extracellular signals. Considering the multitude of cAMP signals, one can postulate that the regulation of cAMP levels has to be similarly complex. Indeed, when Sutherland and Rall first described cAMP (Sutherland and Rall, 1958), they reported the presence of cyclic nucleotide hydrolyzing activity in their cell extracts. Their assumption that phosphodiesterases (PDEs) are responsible for the inactivation of cyclic nucleotides was confirmed in the early 1970s by several reports revealing that PDEs comprise a large enzyme family with kinetically distinct isoforms that are differently expressed in various tissues (Beavo et al., 1970; Thompson and Appleman, 1971a; Thompson and Appleman, 1971b).

1.2 Phosphodiesterases (PDEs): a superfamily inactivating cyclic nucleotides

The characterization of genetic, biochemical, pharmacological, and structural profiles has identified 11 different gene families of PDEs in mammals termed PDE1 - PDE11 (Conti and

Jin, 1999; Francis et al., 2001; Essayan, 2001; Lugnier, 2006; Bender and Beavo, 2006). PDEs inactivate 3'-5' cyclic nucleotides by hydrolytically cleaving the 3'-phosphodiester bound, thus generating the corresponding 5'-nucleotide monophosphate (see Figure 2).

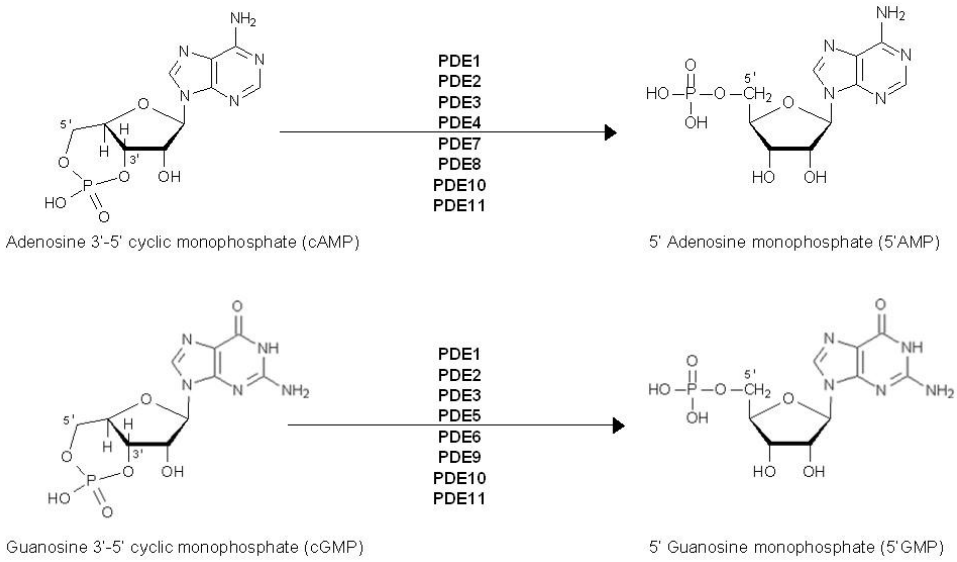

Figure 2. Phosphodiesterases biologically inactivate cyclic nucleotides. The 3'-phosphodiester bound of cAMP and cGMP is hydrolytically cleaved, generating 5'AMP and 5'GMP, respectively. Some of the PDEs have dual substrate specificity and can inactivate cAMP and cGMP (PDE1, PDE2, PDE3, PDE10, and PDE11), other PDEs are specific for the hydrolysis of cAMP (PDE4, PDE7, and PDE8) or cGMP (PDE5, PDE6, and PDE9).

The PDE families can be differentiated functionally on the basis of substrate specificity, i.e., their relative affinities for cAMP and cGMP. Moreover, PDEs can be distinguished by their sensitivity to endogenous/exogenous regulators and their genetic sequence homology. Six of the eleven PDE families include more than one gene, called subtype - overall more than 20 genes/subtypes were found. The subtypes are designated with a letter following the family number (e.g. PDE4A). Additionally, multiple splice variants of the PDE subtypes can be expressed that further increase the high level of complexity. The splice variants are generated by alternative splicing or by multiple transcriptional start sites and are designated with a number following the subtype letter (e.g. PDE4A1). In total, the PDE superfamily comprises more than 50 isoforms of PDE proteins that show differences in their tissue distribution, subcellular localization, and post-translational modification. Of the eleven PDEs thus far identified, PDE4, PDE7, and PDE8 are specific for cAMP, whereas PDE1, PDE2, PDE3, PDE10, and PDE11 are able to hydrolyze both cAMP and cGMP, with different selectivities and kinetics (Torphy, 1998; Lugnier, 2006; Bender and Beavo, 2006).

The current classification scheme including some characteristics (biochemical parameters, subtype number, and domain and motif organization) of the mammalian PDEs are shown in Table 1 and Figure 3.

Table 1. Characteristics of cyclic nucleotide phosphodiesterase families. The subtypes of each isoenzyme family represent different genes. Given are some characteristics and exemplary substrate concentrations at half maximum velocity (Michaelis constant K_m) for cAMP and cGMP hydrolysis, respectively. IBMX = 3-isobutyl-1-methylxanthine; GAF domains = cGMP-binding regulatory domains; UCR = upstream conserved region.

Isoenzyme family	Characteristics	Subtypes	~K_m [µM] cAMP	~K_m [µM] cGMP	Ref.
PDE1	Ca^{2+}/CaM-stimulated	3	1 - 50	0.6 - 3	*, $
PDE2	cGMP-stimulated, GAF domains	1	50	50	*
PDE3	cGMP-inhibited, cAMP selective	2	0.2	0.3	*
PDE4	cAMP specific, UCR1 & UCR2 domains	4	2 - 4	> 1000	*, °
PDE5	cGMP-specific, GAF domains	1	150	1	*
PDE6	cGMP-specific, Photoreceptor, GAF domains	3	2000	60	*
PDE7	high affinity cAMP-specific	2	0.2	> 1000	*
PDE8	cAMP specific, IBMX insensitive	2	0.1	124	§
PDE9	cGMP specific, IBMX insensitive	1	230	0.2	#
PDE10	GAF domains, V_{max} for GMP hydrolysis higher	1	0.3	7	+
PDE11	GAF domains	1	1 - 5.7	0.5 - 4.2	++,**

* Torphy, 1998; $ Loughney et al., 1996; ° Lugnier, 2006 ; § Fisher et al., 1998b; # Fisher et al., 1998a; + Fujishige et al., 1999; ++ Fawcett et al., 2000; ** Hetman et al., 2000b.

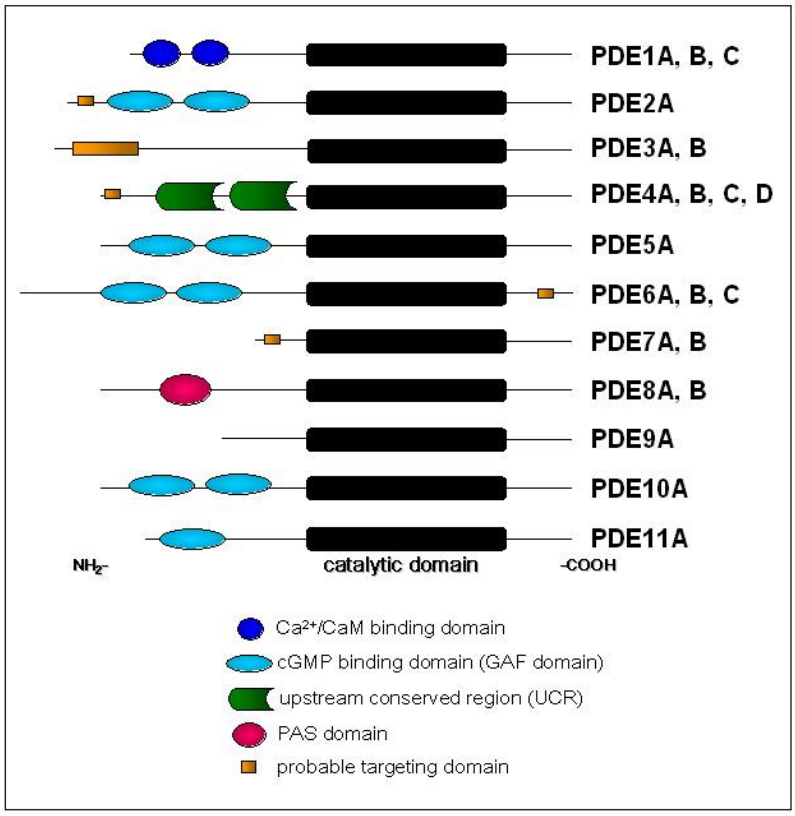

Figure 3. Schematic overview of the PDE superfamily. The diagram pictures the domain and motif organization of the eleven families of phosphodiesterases (PDEs). All PDEs share a conserved catalytic domain, but differ in their N- and C-terminal regions. The Ca^{2+}/Calmodulin binding domain is found only in PDE1. The GAF domain (found in cGMP-regulated PDEs, adenylyl cyclases, and FhlA), which can bind cGMP, is located at N-terminal regions of PDE2, PDE5, PDE6, PDE10, and PDE11. The UCR (upstream conserved region) is a characteristical motif found only in PDE4. PDE8 can be distinguished by a PAS domain (found in Per, ARNT, and Sim proteins). Probable targeting domains are putative membrane-association domains or other targeting motifs. Modified from Soderling and Beavo, 2001.

Phosphodiesterase 1 was the first human PDE to be discovered (Kakiuchi and Yamazaki, 1970). Today, three distinct subtypes (PDE1A, PDE1B, and PDE1C) have been characterized, which differ in their tissue distribution, substrate affinities, splice variants, and regulatory properties (Loughney et al., 1996; Kakkar et al., 1999). The human cGMP-stimulated PDE2 has similar K_m-values for the hydrolysis of both cAMP and cGMP, and comprises one gene with one human splice variant (PDE2A3) described so far (Rosman et al., 1997). The PDE3 family contains the two subtypes PDE3A and PDE3B, which are high affinity phosphodiesterase for both cGMP and cAMP (Meacci et al., 1992; Taira et al., 1993). However, the maximal velocity for cAMP hydrolysis can be 4 - 10 times higher than for cGMP (Manganiello et al., 1995). Considering the competition of cGMP with cAMP at the catalytic site, cGMP can act as a transient inhibitor of cAMP hydrolytic activity until cGMP itself is hydrolyzed; thus, PDE3 was initially termed cGMP-inhibited PDE (Degerman et al., 1997). Characteristic for PDE3 are N-terminal hydrophobic domains, which allow membrane association (Shakur et al., 2000; Kenan et al., 2000). The PDE4 family contains four genes, the subtypes PDE4A - PDE4D. Their structure, biochemical characterization and potential biological functions are summarized in chapter 1.3. PDE5 is encoded by one single gene, but three splice variants have been described (Lin et al., 2002). PDE5 is a cGMP-binding, cGMP-specific homodimeric phosphodiesterase, and is widely expressed in most smooth muscle tissues as well as in platelets, gastrointestinal epithelial cells, and Purkinje cells of the cerebellum (Burnett, 2005). Besides homologies to other PDE families (PDE5 and PDE11), PDE6 has unique characteristics: PDE6 is directly activated by transducin (a G protein), specifically hydrolyzes cGMP, and is expressed in vertebrate photoreceptor cells as a critical processor of phototransduction (Yarfitz and Hurley, 1994; Norton et al., 2000; Fain et al., 2001). PDE7 has been characterized as a high-affinity cAMP-hydrolyzing phosphodiesterase, which contains two subtypes, PDE7A and PDE7B, and several splice variants (Bloom and Beavo, 1996; Hetman et al., 2000a). PDE8 contains two subtypes, PDE8A and PDE8B, which specifically hydrolyze cAMP (Fisher et al., 1998b; Soderling et al., 1998a). PDE9 is, along with PDE5 and PDE6, cGMP-specific. One subtype, PDE9A, has been described so far (Fisher et al., 1998a; Guipponi et al., 1998; Soderling et al., 1998b). PDE10 contains a single subtype, PDE10A, which can hydrolyze both cAMP and cGMP, but kinetic data indicate that PDE10 might have the properties of a cAMP-inhibited cGMP phosphodiesterase (Fujishige et al., 1999; Soderling et al., 1999). PDE11, the most recently described phosphodiesterase, is a single gene, but transcripts of multiple splice variants have been detected in various tissues (Fawcett et al., 2000; Hetman et al., 2000b; Yuasa et al., 2001). Although the catalytic domain of PDE11 has the closest homology with PDE5 (Fawcett et al., 2000), PDE11 hydrolyzes both cAMP and cGMP with similar affinity.

Despite the functional and structural diversity, all phosphodiesterases show a multidomain structure composed of three functional domains: a regulatory N-terminus, a central catalytical domain, and a regulatory C-terminus (Figure 3). The catalytical domain with the size of about 270 amino acids has a considerable sequence similarity of at least ~50% on the amino acid level, whereas the C- and N-termini are heterologous (Torphy, 1998). N-termini of PDEs contain unique binding sites for small messenger molecules (such as Ca^{2+}/Calmodulin, cGMP, or phosphatic acid), motifs for membrane targeting, phosphorylation sites, and metal ion binding sites (Conti and Jin, 1999; Francis et al., 2001; Essayan, 2001; Lugnier, 2006; Bender and Beavo, 2006). N-termini can therefore determine the activity status of phosphodiesterases, their dimerization, and their cellular compartmentalization. In general, the occupancy of the respective N-terminal binding site or the phosphorylation at the N-terminus mediates activation of the corresponding phosphodiesterase (Richter and Conti, 2004).
Contrary to the N-terminus, only little is known about the regulatory role of the C-terminus of PDEs, but reports indicate that C-termini may be involved in dimerization (Kovala et al., 1997) and phosphorylation (MacKenzie et al., 2000).

1.3 The phosphodiesterase 4 family comprises a variety of isoforms

In 1989, several groups reported the identification and cloning of high-affinity rat cAMP specific phosphodiesterases (Swinnen et al., 1989a; Davis et al., 1989; Colicelli et al., 1989). These cAMP-phosphodiesterases were homologous to the cAMP-PDE encoded by the *dunce* locus of *Drosophila melanogaster*. Mutation of the *dunce* gene in *D. melanogaster* results in defects in learning and memory (Dudai et al., 1976; Tempel et al., 1983). Shortly after, human cAMP-phosphodiesterases (designated to be type IV = cAMP-specific PDE = PDE4) have been cloned from monocytes, lymphocytes, and brain tissue, and the subtype notation A, B, C, and D was introduced (Beavo and Reifsnyder, 1990).

1.3.1 Structural properties of PDE4 isoforms

PDE4 is the only human PDE family that comprehends four genes coding for the subtypes PDE4A, PDE4B, PDE4C, and PDE4D. By the complex arrangement of transcriptional units, multiple promoters, and resulting splice variants, more than 20 isoforms have been described (Conti and Jin, 1999). PDE4 isoforms have a high similarity both in their sequence and in the complex range across different species, indicating the evolutionary pressure on the conservation of PDE4 isoforms and underlining their important functional role (Houslay, 2001). Compared to PDE4A, the human subtypes PDE4B, PDE4C, and PDE4D have amino acid identities of 70 - 74% across entire sequence and 80 - 84% within the catalytic domain (Torphy, 1998).

Various reports indicate that isoforms of the PDE4 family often account for most of the cAMP hydrolyzing activity of a cell (Conti et al., 2003). All PDE4 isoforms have similar affinities for cAMP (K_m 2 - 4 µM), but exhibit weak affinity for cGMP (K_m > 1000 µM) (Torphy, 1998). Kinetic analyses revealed that the maximal velocity (V_{max}) for cAMP hydrolysis markedly differs between PDE4 isoforms, pointing to the N-terminal region functioning as regulator of catalytical activity. As metallohydrolases, PDE4 isoforms are Mg^{2+}-dependent, but the two identified metal ion binding sites (Me1 and Me2) in the catalytical core may also be occupied by Zn^{2+} or Mn^{2+}, i.e., by different bivalent metal ions (Laliberte et al., 2000; Xu et al., 2000).

The four PDE4 subtypes are each encoded by large complex genes of around 50 kb and can have more than 18 transcriptional units (exons) (Houslay and Adams, 2003). All PDE4 isoforms are widely expressed, with primary tissue distribution in kidney, brain, liver, lung, and immunocytes (Essayan, 2001). Unlike the other PDE4 subtypes, PDE4C seems to have a restricted expression, but is abundant in neuronal tissue (Sullivan et al., 1999). The use of multiple transcriptional start sites as well as alternative splice events generate a variety of transcripts with unique 5' ends, as depicted in Figure 4.

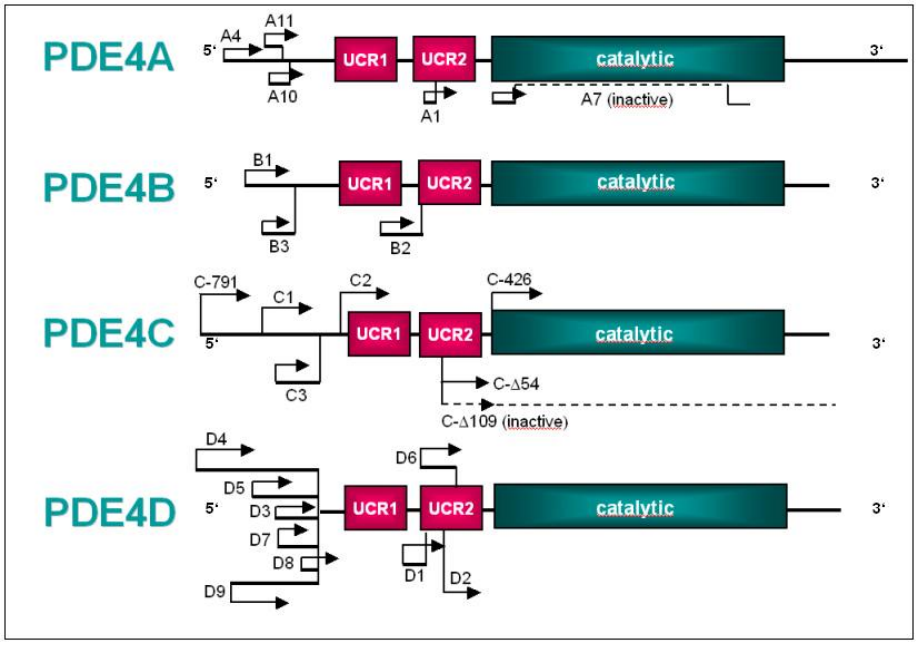

Figure 4. Schematic representation of the 5'-3' genetic structure of human *PDE4A*, *PDE4B*, *PDE4C*, and *PDE4D* mRNA transcripts. PDE4 splice variants are either the result of different starting sites or alternative splice events. PDE4 isoforms can be divided into long forms (e.g. PDE4A4) or short forms (e.g. PDE4D1). UCR1 and UCR2 = upstream conserved region 1 and 2, respectively. Modified from a figure kindly provided by Dr. Quintini (ALTANA Pharma AG, Konstanz).

The PDE4 genes are localized on three chromosomes. Based on the *PDE4A* gene, which is located at the human chromosome 19p13.1, five human *PDE4A* splice variants (*PDE4A1, PDE4A4, PDE4A7, PDE4A10*, and *PDE4A11*) have been identified to date (Wallace et al.,

2005). All transcripts are the result of 5' splicing and form catalytically active isoforms, with *PDE4A7* being an exception with an additional 3' truncated end, coding a catalytically inactive isoform (Johnston et al., 2004). The human *PDE4B* gene (located at the chromosome 1p31-32) encodes the transcripts *PDE4B1, PDE4B2,* and *PDE4B3*, with PDE4B1 and PDE4B2 isoforms being strongly conserved among species (Shepherd et al., 2003). However, the rat PDE4B4 isoform has not been identified in humans so far. By determination of the human *PDE4C* gene (chromosome 19p13.1), several groups reported the identification and molecular cloning of various *PDE4C* transcripts, such as *PDE4C1, PDE4C2, PDE4C3, PDE4C-791, PDE4C-426, PDE4Cdelta54,* and *PDE4Cdelta109* (Obernolte et al., 1997; Owens et al., 1997). Yet, Houslay and colleagues argue that the latter three transcripts may represent incompletely or incorrectly spliced variants that are nonfunctional (Sullivan et al., 1999). Nine transcripts of the human *PDE4D* gene (chromosome 5q12) have been described, PDE4D1 - PDE4D9 (Wang et al., 2003; Gretarsdottir et al., 2003). All nine PDE4D splice variants are also expressed in rat tissue, where they are, like in humans, differently expressed and regulated (Richter et al., 2005).

1.3.2 Upstream conserved regions (UCRs): unique regulatory motifs of PDE4 isoforms

Structurally, all PDE4 isoforms can be divided into two major categories, termed long and short forms (Figure 5) (Conti et al., 2003). The classification is based on the presence of two modules that are highly conserved in PDE4 subtypes, namely upstream conserved regions 1 and 2 (UCR1 and UCR2, respectively) (Bolger et al., 1993). In contrast to PDE4 long isoforms, which are characterized by two complete UCR motifs (UCR1 and UCR2), short isoforms lack UCR1. UCR1 and UCR2 (~60 and ~80 amino acids in size, respectively) are linked with subtype-specific, ~24 amino acid long linker regions (Houslay and Adams, 2003). Another subtype-specific linker region (~10 - 28 amino acids) is located in between the UCR2 and the catalytic domain. Whereas many studies are underway to reveal the impact of the N-termini on PDE4 function, the role of the subtype-specific C-terminal region is not well understood so far.

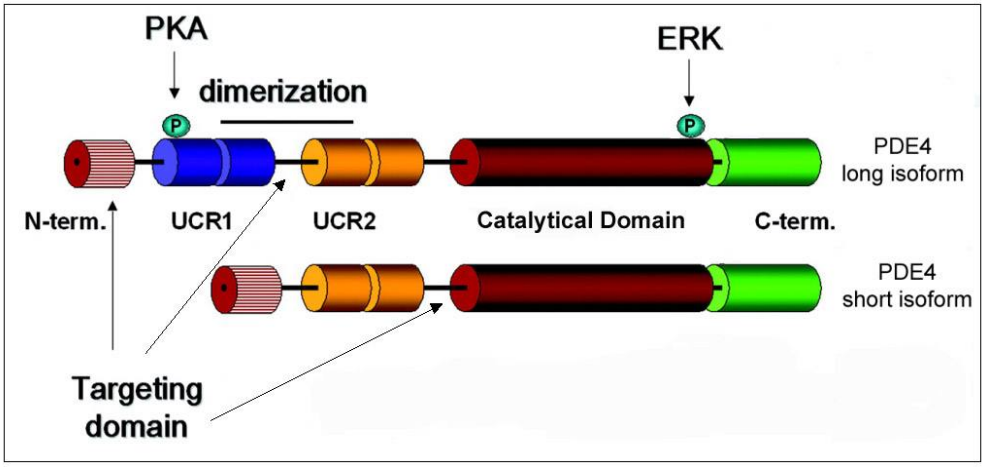

Figure 5. Domain organization of PDE4 long and short isoforms. The classification is based on the unique N-terminal region of PDE4 splice variants. Depicted are different domains, which are linked by putative targeting elements. PDE isoforms are subject to phosphorylation by PKA (only long forms) and by ERK (long and short forms, but not PDE4A isoforms). Two upstream conserved regions (UCR1 and UCR2) regulate dimerization and are involved in PDE4 activation and intracellular localization. Modified from Conti et al., 2002.

The presence and arrangement of the UCR motifs can influence PDE4 function in different ways. UCR motifs were shown to be involved in (i) PDE4 dimerization, (ii) PDE4 activation or inhibition, and (iii) intracellular targeting of PDE4.

(i) The C-terminal half of UCR1 and the N-terminal half of UCR2 have been found to mediate dimerization in long forms, whereas short forms behave as monomers (Richter and Conti, 2002). The oligomerization state was shown to determine several regulatory properties, such as activation by PKA (see chapter 1.3.3) or facilitating special conformations of the catalytic site (Richter and Conti, 2004).

(ii) Independent of their role for oligomerization in long forms, the UCR1 and UCR2 motifs show intramolecular interaction (Beard et al., 2000). Several reports revealed that UCR2 exhibits an autoinhibitory effect on the catalytical core and proposed that PKA phosphorylation at the extreme N-terminal end of UCR1 leads to an altered UCR1-UCR2 interaction that removes the inhibitory effect (Sette and Conti, 1996; Lim et al., 1999; Beard et al., 2000). Additionally, the ERK-mediated inhibition of the catalytical activity (see chapter 1.3.3) in long forms seems to be mediated via UCR1 (MacKenzie et al., 2000).

(iii) Myomegalin, a protein of the Golgi/Centrosome region, was shown to interact with PDE4D3, thereby targeting the phosphodiesterase to a particulate structure (Verde et al., 2001) and pointing to a role of UCR1/UCR2 in intracellular targeting.

1.3.3 Phosphorylation controls PDE4 activity

As depicted in Figure 5, phosphorylation sites for PKA and ERK have been found in PDE4 isoforms. Long PDE4 isoforms can be activated through PKA phosphorylation of a single serine residue located at the N-terminal end of UCR1 (Sette and Conti, 1996; Ekholm et al., 1997; MacKenzie et al., 2002; Laliberte et al., 2002). This catalytic activation may be mediated by phosphorylation-induced destabilization of the intrinsic 'low' activity state of PDE4 isoforms, by enhancing the sensitivity to Mg^{2+}, and/or by disrupting potential inhibitory effects of the UCR2 motif (Houslay and Adams, 2003). Besides, in all PDE4 subtypes except PDE4A, a serine residue in the third subdomain of the catalytic core can be phosphorylated by the extracellular signal-related kinase 2 (ERK2), establishing a cross talk between cAMP and ERK signaling pathways (Houslay and Baillie, 2003). The phosphorylation via ERK has dual properties: On the one hand, ERK phosphorylation of PDE4 long forms leads to inhibition (Hoffmann et al., 1999), but additional phosphorylation via PKA causes a net activation of the PDE4 isoforms (Baillie et al., 2001). On the other hand, in short forms, an ERK-mediated phosphorylation causes activation (Baillie et al., 2000). Thus, long and short forms can be differently regulated, allowing a complex network of cAMP and ERK signaling systems that give a rationale for the existence of multiple long and short forms.

Moreover, not only phosphorylation, but also negatively charged phosphatidic acid (PA), discussed as second messenger in response to various stimuli (e.g. growth factors or hormones), can regulate the activity of PDE4 long forms, as exemplified by the binding of PA at the N-terminal domain of PDE4D3 (Grange et al., 2000).

1.4 cAMP exhibits many inhibitory properties in immune cells

As already detailed in chapter 1.1, cAMP action has profound effects on cell function (Beavo and Brunton, 2002; Kopperud et al., 2003). In immune cells, the complexity of cAMP signaling is reflected in cAMP having dual properties. On the one hand, cAMP has been described to initiate and activate inflammatory cell functions (pro-inflammatory effects). On the other hand, the majority of reports indicate that cAMP has inhibitory properties, promoting an inhibitory constraint on immune cell functions with anti-inflammatory effects (Tasken and Aandahl, 2004; Hata and Breyer, 2004). The first messengers, initiating the transduction signals and the generation of cAMP, have major impact in configuring the complexity of cAMP action in immune cells. For example, the well-characterized prostaglandin E_2 (PGE_2)-induced upregulation of intracellular cAMP levels (Honda et al., 1993; Regan et al., 1994) was shown to be required for human dendritic cell migration and maturation and for enhanced capacity to stimulate naïve T cells (Steinbrink et al., 2000; Scandella et al., 2002; Legler et al., 2006). Contrary, PGE_2 mediated signaling can inhibit T cell proliferation and macrophage cytokine

release (Hata and Breyer, 2004) and can also have inhibitory properties on monocyte differentiation to dendritic cells (Kalinski et al., 1997; Sombroek et al., 2002).
Because the other two common downstream effector systems of cAMP action, cyclic nucleotide gated channels (CNG) and Epac guanin-exchange factors, have not yet been linked with a central role in human primary immune cells, it is likely that PKA mainly exerts cAMP action in immune cells. In T cells, various negative regulators of immunoreceptor signaling ensure that T cells either maintain the quiescent state of unstimulated, mature T cells or limit and terminate the activating signal, restoring the dormant state of T cells (Veillette et al., 2002; Liu, 2005). Interestingly, cAMP has been recognized as an important mediator of such inhibitory signaling mechanisms by activation of PKA, with PKA functioning as gatekeeper of tonic inhibition in T cells, restraining proliferation and cytokine release (Kammer, 1988; Skalhegg et al., 1992; Tamir and Isakov, 1994; Selliah et al., 1995; Loza et al., 2006). The inhibitory effects of PKA on inflammatory cell functions can be mediated via several molecular mechanisms (Torgersen et al., 2002), and are exemplified for T cells in Figure 6.

For instance, PKA can phosphorylate NFAT, a transcription factor that is implicated in the expression of several cytokine genes, and subsequently inhibits its translocation into the nucleus (Chow and Davis, 2000). Besides, PKA has been shown to be localized with the TCR-CD3 complex (Skalhegg et al., 1994), and PKA-dependent serine phosphorylation and activation of Csk was shown to inhibit Lck action and subsequently proximal TCR signaling (Aandahl et al., 2002). Several reports correlated inhibition of members of the phospholipase family with PKA phosphorylation (Liu and Simon, 1996; Yue et al., 1998). Also, PKA can act as a negative modulator of adhesion (Laudanna et al., 1997), is involved in cytoskeleton organization (Lang et al., 1996), and was found to inhibit the ERK pathway by phosphorylation of Raf-1 (Dhillon et al., 2002). However, the impact of PKA phosphorylation on the ERK pathway has been shown to be similarly versatile as the impact of PKA phosphorylation on NFkB signals, ranging from activating to inhibitory effects (Torgersen et al., 2002; Takahashi et al., 2002).
The complexity of cAMP action, exemplified in Figure 6 for T cells, is pronounced in many inflammatory cells. For example, cAMP has been shown to be involved in cytokine synthesis in monocytes, macrophages, and dendritic cells, e.g., by upregulating IL-10 release or by lowering TNF-α and IL-12 synthesis after lipopolysaccharide (LPS) stimulation (Eigler et al., 1998; Platzer et al., 1999; Procopio et al., 1999; Vassiliou et al., 2003). Furthermore, amongst others, inhibition of monocyte adhesion and migration (Fine et al., 2001) and decreased neutrophil responses (Harvath et al., 1991; Derian et al., 1995) have been linked to cAMP action.

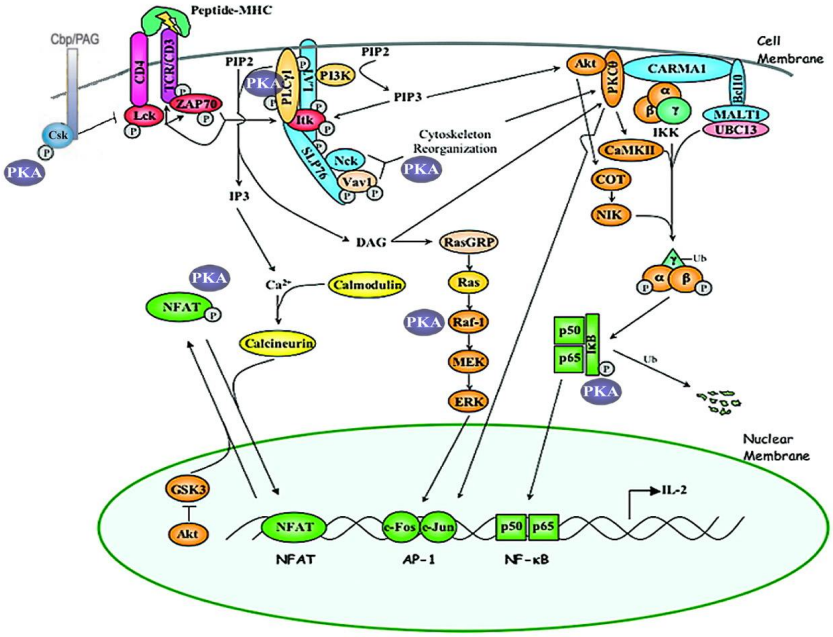

Figure 6. Schematic overview of potential PKA interaction interfaces with TCR signaling pathways. Depicted are some key signaling events of T cell activation after CD4, TCR/CD3, and peptide-MHC binding, resulting in the activation of transcription factors and the induction of cytokines. Shown are some potential interfaces of PKA and TCR signaling pathways. Csk = C-terminal Src kinase, Cbp/PAG = Csk-binding protein/phosphoprotein associated with glycosphingolipid-enriched microdomains, Lck = Src-family tyrosine kinase, ZAP70 = zeta-associated protein 70, PIP2 = phosphatidylinositol-4,5-bisphosphate, IP3 = inositol-1,4,5-tris-phosphate, DAG = diacylglycerine, PLCγ1 = phospholipase Cγ1, LAT = linker for activation of T cells, PI3K = phosphatidylinositol-3 kinase, PIP3 = phosphatidylinositol-3,4,5-trisphosphate, Itk = IL-2 inducible T cell kinase, SLP-76 = SH2-domain-containing leukocyte protein of 76 kDa, Vav-1 = guanine exchange factor, Nck = noncatalytic region of tyrosine kinase adaptor protein 1, Akt = protein kinase B, PKCθ = protein kinase Cθ, CARMA1 = caspase recruitment domain-containing membrane-associated guanylate kinase protein-1, IKK = IκB kinase, Bcl10 = B-cell leukaemia protein 10, MALT-1 = mucosa-associated lymphoid tissue 1, UBC13 = ubiquitin-conjugating enzyme, CaMKII = calcium/calmodulin-dependent protein kinase II, COT = cancer osaka thyroid mitogen-activated protein (MAP3) kinase, NIK = NF-κB inducing kinase, Ub = ubiquitin, RasGRP = guanine exchange factor, ERK = extracellular signal-regulated kinase, MEK = MAPK (mitogen-activated protein kinase)/ERK kinase, NFAT = nuclear factor of activated T cells, GSK-3 = glycogen synthase kinase-3, AP-1 = activator protein-1, NFκB = nuclear factor κB. Modified from Huang, Y. and Wange, R., 2003 with modifications from Torgersen et al., 2002 and Abrahamsen et al., 2004.

1.5 PDE4 isoforms are widely expressed in inflammatory and immunocompetent cells

By activating PKA, as detailed in chapter 1.4, cAMP signals manifoldly control immune functions and can inhibit various inflammatory responses of T cells, monocytes, macrophages, or dendritic cells, subsequently exhibiting an inhibitory constraint on these cells.

Paradoxically, crosslinking of the TCR was shown to initially elevate intracellular cAMP levels in T cells (Ledbetter et al., 1986; Kammer et al., 1988), as did LPS stimulation in macrophages (Jin et al., 2005). As a consequence, to abolish the inhibitory tone of cAMP and for cell activation to occur, cell signaling must involve effective local cAMP hydrolyzing capacities. In T cells and T cell lines, several cAMP-hydrolizing PDEs have been found, namely PDE1, PDE3,

PDE4, PDE7, and PDE8 (Tenor et al., 1995b; Giembycz et al., 1996; Li et al., 1999; Glavas et al., 2001). As detailed in chapter 1.3, the cAMP-specific phosphodiesterase 4 (PDE4) family has been recognized as a pivotal regulator of cAMP signals by inactivating cAMP. Various reports indicate that isoforms of the PDE4 family often account for most of the cAMP hydrolyzing activity in immune cells (Essayan, 1999; Souness et al., 2000; Conti et al., 2003). Several studies revealed an induction of PDE4 expression or activity in T cells as a result of different receptor-mediated stimuli, for instance phytohemagglutinin (PHA) (Jiang et al., 1998; Kanda and Watanabe, 2001), β_2-agonists (Seybold et al., 1998), or anti-CD3/CD28 stimulation (Kanda and Watanabe, 2001). Similar results were obtained with cAMP-analogs such as 8-bromo-cAMP (Seybold et al., 1998).

PDE4 is also the predominant phosphodiesterase family in a variety of other human inflammatory and immunocompetent cells, such as in neutrophils, eosinophils, endothelial cells, epithelial cells, B cells, and smooth muscle cells (Rabe et al., 1994; Schudt et al., 1995; Weston et al., 1997; Dent et al., 1998; Gantner et al., 1998). In human monocytes, Gantner et al. (Gantner et al., 1997a) reported a predominant activity of PDE4, which was downregulated during the differentiation of monocytes to macrophages. Similar observations were made during the differentiation of monocytes to dendritic cells (Gantner et al., 1999). Likewise to T cells, PDE4 expression in monocytic cells was found to be upregulated in response to the cAMP-analog dibutyryl-cAMP (Verghese et al., 1995), in response to β_2-agonists (Torphy et al., 1995; Manning et al., 1996), or in response to LPS stimulation (Ma et al., 1999).

The predominant, tightly regulated expression and activity of PDE4 isoforms in many inflammatory and immunocompetent cells and the notion that cAMP exhibits many anti-inflammatory effects led to the concept that the PDE4 family might be a predestinated target for the development of PDE4 inhibitors for the treatment of chronic inflammatory diseases.

1.6 PDE4 inhibition has anti-inflammatory and immunomodulatory properties

The medicinal use of PDE inhibitors was initiated more than 60 years ago by the discovery that a caffeine-relative, the xanthine theophylline, was effective for the treatment of asthma. Theophylline is a weak, nonselective PDE inhibitor (Aubier and Barnes, 1995) that exerts bronchodilating properties in patients with asthma and chronic obstructive pulmonary disease (COPD) and has also additional anti-inflammatory effects (Barnes and Pauwels, 1994). Moreover, recent data proposes that theophylline exhibits PDE-independent mechanisms of actions, e.g. the activation of histone deacetylase (HDAC) activity, and might thus mimic the effects of corticosteroids (Barnes, 2003b). Three decades ago, Schwabe and coworkers (Schwabe et al., 1976) reported the development of a PDE4 inhibitor, rolipram, as anti-

depressant drug (ZK 62711, Schering AG). Rolipram showed potent and selective PDE4 inhibition and became the archetypical PDE4 inhibitor (Figure 7).

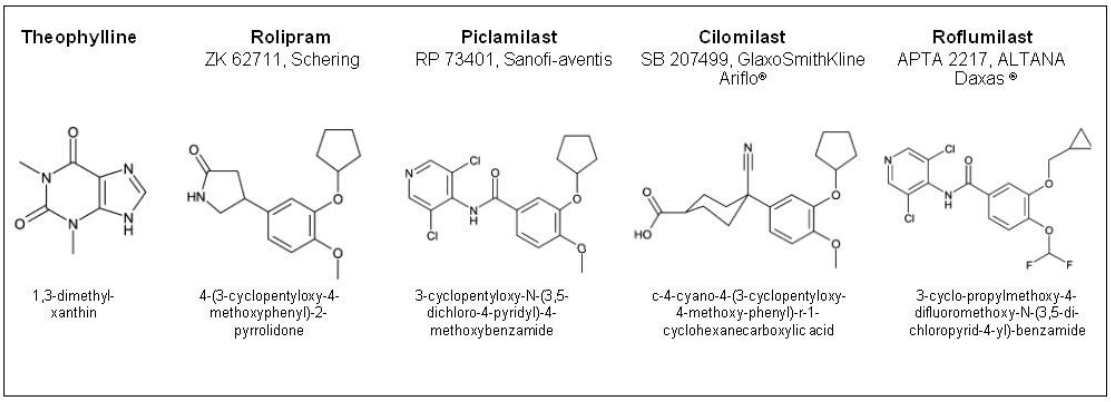

Figure 7. The development of PDE4 inhibitors. Theophylline is a non-selective PDE inhibitor used for the treatment of asthma and COPD. The development of the archetypical PDE4 inhibitor rolipram (ZK 62711, Schering) was reported three decades ago. Other PDE4 inhibitors are exemplified by piclamilast (RP 73401, Sanofi-aventis) and the second generation PDE4 inhibitors cilomilast (Ariflo®, GlaxoSmithKline) and roflumilast (Daxas®, ALTANA Pharma AG).

Intense research efforts led to the development of various PDE4 inhibitors, such as piclamilast (RP73401, Sanofi-aventis, formerly Rhône-Poulenc Rorer) (Raeburn et al., 1994) for the treatment of chronic inflammatory diseases. However, early PDE4 inhibitors failed in clinical studies due to their adverse gastrointestinal and emetic side effects or due to the lack of clinical efficacy. Currently, various PDE4 inhibitors are in the development for the treatment of a growing number of diseases, however, the development of PDE4 inhibitors as anti-inflammatory drugs for the treatment of asthma and COPD is most progressed (Giembycz, 2002; Lipworth, 2005; Boswell-Smith et al., 2006). The most advanced second generation PDE4 inhibitors under clinical investigation are cilomilast (Ariflo®, GlaxoSmithKline) (Barnette et al., 1998) and roflumilast (Daxas®, ALTANA Pharma AG) (Hatzelmann and Schudt, 2001).

Many *in vitro* experiments with PDE4 specific inhibitors demonstrate the profound anti-inflammatory and immunomodulatory effects of PDE4 inhibition on diverse inflammatory cell functions (Torphy, 1998; Souness et al., 2000). As depicted in Figure 8, PDE4 inhibition can repress the activation and recruitment of key inflammatory and immunocompetent cells involved in the pathophysiology of chronic inflammatory diseases.

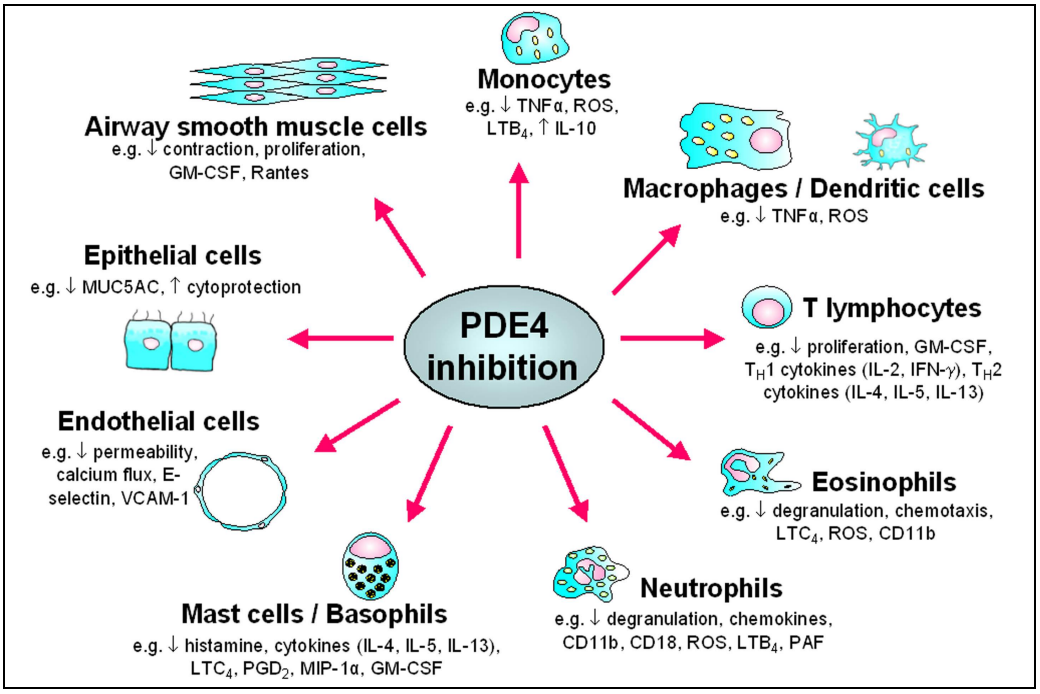

Figure 8. PDE4 inhibitors broadly target inflammatory and immunocompetent cells. PDE4 inhibition was shown to suppress the activation and recruitment of key cells involved in chronic inflammatory diseases such as asthma and COPD. TNF = tumor necrosis factor, ROS = reactive oxygen species, LTB = leukotriene B, GM-CSF = granulocyte-macrophage colony-stimulating factor, IL = interleukin, IFN = interferon, LTC = leukotriene C, PAF = platelet-activating factor, PGD = prostaglandin, MIP = macrophage inflammatory protein, VCAM = vascular cell adhesion molecule, MUC5AC = mucin 5AC, Rantes = regulated on activation, normal T cell expressed and secreted (chemokine), ↓ = suppression of cellular parameter by PDE4 inhibition, ↑ = upregulation of cellular parameter by PDE4 inhibition. For review, see Torphy, 1998; Souness et al., 2000; Essayan, 2001. Modified from a figure kindly provided by Dr. A. Hatzelmann (ALTANA Pharma AG, Konstanz).

Several preclinical *in vivo* models, such as antigen-induced bronchoconstriction, eosinophil/neutrophil influx, airway hyperreactivity, and microvascular leakage in mouse, rat, rabbit, guinea pig, and monkey showed efficacy of PDE4 inhibitors in pulmonary inflammation (Torphy, 1998; Souness et al., 2000). In line with the concept of beneficial PDE4 inhibition, many *in vitro* and *in vivo* findings confirmed the anti-inflammatory and immunomodulatory properties of roflumilast (Hatzelmann and Schudt, 2001; Bundschuh et al., 2001; Kumar et al., 2003; Martorana et al., 2005), giving the rationale for clinical trials for the treatment of asthma and COPD. For instance, 500 µg roflumilast given once daily efficiently decreased exercise-induced asthma and suppressed LPS-stimulated TNF-α secretion *ex vivo* (Timmer et al., 2002). In another study, roflumilast significantly attenuated early and late allergen-induced asthmatic responses (van Schalkwyk et al., 2005). Regarding COPD, significant improvements in forced expiratory volume in one second (FEV_1) and in morning peak expiratory flow were observed after treatment with roflumilast (Bredenbröker et al., 2002; Rabe et al., 2005). Taken together, data derived from clinical studies showed both efficacy and safety of roflumilast (Lipworth, 2005; Karish and Gagnon, 2006; Bateman et al., 2006).

In contrast to these results, the development of early PDE4 inhibitors was paralleled and discouraged by gastrointestinal- and CNS-related adverse effects related to PDE4 inhibition (Torphy, 1998; Souness et al., 2000). However, compelling evidence supports the idea that such side effects can be separated from anti-inflammatory effects. The catalytical unit of PDE4 splice variants can adopt at least two conformational states, termed high-affinity rolipram-binding state (HARBS) and low-affinity rolipram-binding state (LARBS) (Souness and Rao, 1997; Houslay and Adams, 2003; Conti et al., 2003). The HARBS conformer was linked to the CNS and parietal glands (probably mediating undesired effects), whereas LARBS may be predominantly present in immune cells (likely mediating desired anti-inflammatory therapeutic effects) (Souness and Rao, 1997; Torphy, 1998; Souness et al., 2000). Whether a PDE4 splice variant may adopt HARBS or LARBS conformation was shown to be dependent on various molecular mechanisms, such as involvement of bivalent-metal-ions, of phosphorylation events, and/or of the amino termini of PDE4 isoforms (Houslay and Adams, 2003; Conti et al., 2003). Remarkably, it was also suggested that individual PDE4 subtypes may have different relevance in mediating side effects, and PDE4D has been linked to the emetogenic basis of PDE4 inhibitors (Robichaud et al., 2002). Collectively, these data point to the necessity to better understand the functional roles of distinct PDE4 subtypes in human primary immune cells. In this regard, an improved knowledge of the functions of PDE4 subtypes would certainly help to improve future drug discovery strategies.

1.7 Functional impact of PDE4 subtypes in human immune cells

Current PDE4 inhibitors do not discriminate between distinct PDE4 subtypes and are subsequently not an appropriate tool to study the functional role of individual PDE4 subtypes. However, evidence derived from PDE4 knockout mice and from biochemical studies demonstrate that PDE4 subtypes are not redundant, indicating that distinct PDE4 subtypes can have distinct functional impact in inflammatory and immunocompetent cells (Figure 9). For example, in murine monocytes, macrophages, and dendritic cells, Conti and coworkers showed an exclusive role of PDE4B for LPS-induced TNF-α release because PDE4B ablation, but not PDE4A or PDE4D ablation, suppressed TNF-α (Jin and Conti, 2002; Jin et al., 2005). In human monocytes, PDE4B2 was identified as the predominantly regulated PDE4 subtype after LPS stimulation (Wang et al., 1999), but also other PDE4 isoforms have been shown to be differentially regulated after stimulation in these cells (Verghese et al., 1995; Torphy et al., 1995; Manning et al., 1996). Whilst smooth muscle cells are generally not considered as inflammatory cells, they can act as immunocompetent cells and have functional relevance in chronic inflammatory diseases (Panettieri, 2003; Lazaar and Panettieri, Jr., 2006). Experiments performed with knockout mice demonstrated that PDE4D likely is the subtype that

exerts functional effects for airway smooth muscle contraction, pointing to a role of PDE4D in regulating smooth muscle contraction in the lung (Hansen et al., 2000; Mehats et al., 2003). In mice deficient in PDE4B or PDE4D, neutrophil recruitment to the site of inflammation was substantially impaired, with deletion of PDE4D having predominant effects (Ariga et al., 2004). In human eosinophils, a recent study correlated suppression of eosinophil chemotaxis with the inhibition of PDE4D activity (Chambers et al., 2006).

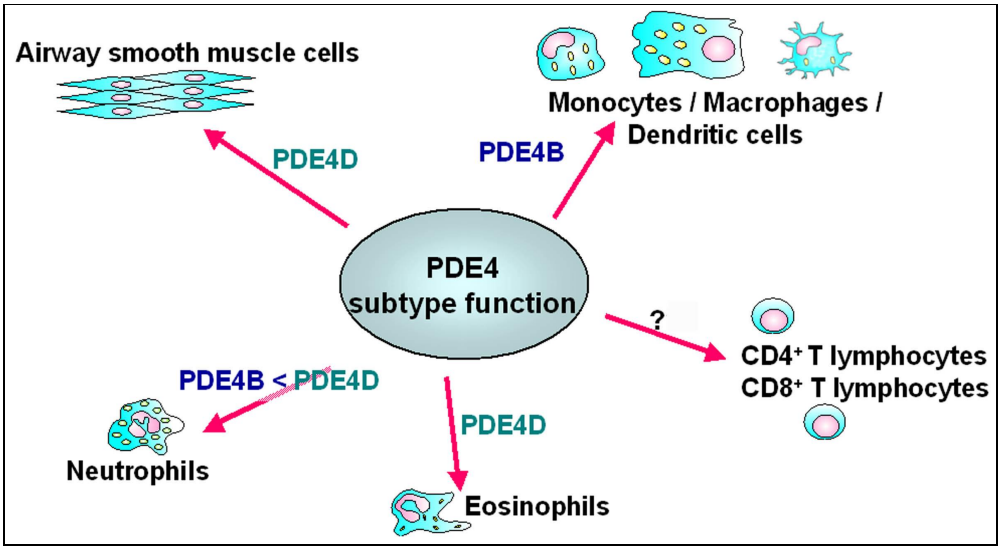

Figure 9. PDE4 subtypes have different functional impact in inflammatory and immunocompetent cells. Schematically depicted are the PDE4 subtype(s) that have been suggested to have functional roles in distinct cellular settings based on data derived from knockout mice and from biochemical studies. For instance, LPS-induced TNF-α release is suppressed in monocytes, macrophages, and dendritic cells from PDE4B$^{-/-}$ knockout mice (Jin and Conti, 2002; Jin et al., 2005). Moreover, the human *PDE4B* gene was exclusively found to be LPS-inducible (Wang et al., 1999). Airways of PDE4D$^{-/-}$ knockout mice are refractory to muscarinic cholinergic stimulation (Hansen et al., 2000; Méhats et al. 2003). The recruitment of neutrophils was shown to be impaired in PDE4B$^{-/-}$ and PDE4D$^{-/-}$ mice, with PDE4D effects being more pronounced (Ariga et al., 2004). In human eosinophils, a recent study linked eosinophil chemotaxis to PDE4D (Chambers et al., 2006). In human primary CD4^{+} and CD8^{+} T cells, the relevance of PDE4 subtypes has to be clarified.

Remarkably, in human primary T cells, such as helper (CD4^{+}) and cytotoxic (CD8^{+}) T cells, which have a major pathophysiological relevance in chronic inflammatory diseases (Tattersfield et al., 2002; Skapenko et al., 2005; Barczyk et al., 2006), the functional impact of PDE4 subtypes is still unclear and no data from knockout mice is available to date. PDE4B2 has been found to be associated with the CD3ε chain of the human TCR complex (Baroja et al., 1999), and overexpression of PDE4B2 in Jurkat cells localizes to the immunological synapse upon activation, correlating with an increase in IL-2 production (Arp et al., 2003). In another study, Taskén and coworkers (Abrahamsen et al., 2004) reported that TCR and CD28 stimulation in human peripheral T cells recruits PDE4A4, PDE4B2, PDE4D1, and PDE4D2 in complex with β-arrestin to lipid rafts, pointing to a potential role of individual PDE4 isoforms in opposing the TCR-induced production of cAMP.

However, the precise expression patterns of PDE4 subtypes and particularly their functional consequences for cell responses in T cells and in human primary immune cells in general remain speculative.

1.8 Aims of the study

The second messenger cAMP has been recognized as critical regulator of the immune system by its ability to suppress various inflammatory cell responses. By inactivating cAMP, isoforms of the phosphodiesterase 4 (PDE4) family are capable to attenuate the negative, inhibitory threshold of cAMP. Thus, PDE4s are key enzymes controlling immune cell functions and have pathophysiological relevance in chronic inflammatory diseases such as asthma or COPD. The PDE4 family comprises four distinct genes/subtypes, which code for multiple splice variants that are widely expressed in inflammatory and immunocompetent cells and set up a complex regulatory repertoire. Whereas studies with knockout mice revealed that individual PDE4 subtypes can have distinct functional impact in defined cellular settings, it is largely unknown whether these findings can be extended to immune cells of human origin. Furthermore, the functional relevance of PDE4 subtypes in $CD4^+$ T cells is unclear, although T cells are of pivotal importance in orchestrating inflammatory responses. Due to the lack of PDE4 subtype-specific inhibitors, the functional impact of PDE4 subtypes cannot be addressed pharmacologically. Thus, a molecular knockdown strategy would be a feasible tool to study the functional role of PDE4 subtypes in human primary immune cells.

The intention of the present study was to demonstrate that distinct PDE4 subtypes exert distinct cellular functions in human primary immune cells, especially in human primary $CD4^+$ T cells. For this purpose, following stepwise approaches were proposed:

(i) Elucidation of PDE4 subtype expression profiles in several human primary immune cells by quantitative PCR, PDE activity assays, and immunodetection experiments.
(ii) Validation of a PDE4 subtype-specific, antisense- and siRNA-mediated knockdown technique in a cell line and transfer of the superior knockdown technique to hard-to-transfect human primary $CD4^+$ T cells.
(iii) Examination of the impact of PDE4 subtype-specific knockdown on cell functions such as cytokine release and proliferation in human primary $CD4^+$ T cells.

A better understanding of the function of individual PDE4 subtypes may help to explain the biological role of the plethora of PDE4 family members. Furthermore, detailed information about functionally relevant PDE4 subtypes may help to define the rationale for the development of PDE4 inhibitors that have an improved therapeutic profile.

2 MATERIALS AND METHODS

2.1 Materials

2.1.1 Chemicals

All chemicals not specifically mentioned were of analytical grade and were obtained from Sigma-Aldrich (Steinheim, Germany).

2.1.2 Reagents and kits

Bradford reagent (Bio-Rad protein assay dye reagent concentrate) and Pierce reagent (Micro BCA protein assay kit) for the determination of protein quantity were purchased from Bio-Rad Laboratories (Muenchen, Germany) and from Pierce (Rockford, USA), respectively. Sepharose A/G and ECL Advance Western Blotting detection kit were obtained from Amersham Biosciences (GE Healthcare, Uppsala, Sweden). RNeasy mini kit and QIAshredder columns for the isolation of RNA were from Qiagen (Hilden, Germany). Lumi light plus western blotting substrate was purchased from Roche (Mannheim, Germany).

2.1.3 Radioactive materials

[5,8-^{3}H]-cAMP and [^{3}H]-thymidine were obtained from Amersham Biosciences.

2.1.4 Buffers and solutions

Buffers and solutions were either provided by the manufacturer as content of diverse kits or were prepared according to Table 2.

Table 2. Buffers and solutions used for experiments. % = w/v for solid substances and v/v for liquid substances. If not otherwise stated, buffers were prepared at room temperature.

Buffer / Solution	Composition
RNA lysis buffer	RLT buffer (Qiagen), 1% 2-mercaptoethanol
Lysis buffer I	50 mM Tris-HCl pH 7.4, 250 mM sodium chloride, 10 mM sodium fluoride, 1 mM EDTA, 0.2 mM EGTA, 10 mM sodium pyrophosphate, 5% glycerol, 1 mM AEBSF (Roche), 1 tablet/10 ml protease inhibitor mixture (Roche), 1 mM sodium orthovanadate, 1% NP-40 (Calbiochem, San Diego, USA), 15 mM 2-mercaptoethanol
Lysis buffer II	20 mM Tris-HCl pH 7.6, 140 mM sodium chloride, 3.8 mM potassium chloride, 1 mM EGTA, 1 mM magnesium chloride, 0.5 mM AEBSF (Roche), 10 µM leupeptin, 2 mM benzamidine, 10 µM pepstatin A, 5 µM soybean trypsin inhibitor, 1 mM 2-mercaptoethanol

Lysis buffer III (RIPA lysis buffer)	50 mM Tris-HCl pH 7.5, 120 mM sodium chloride, 20 mM sodium fluoride, 0.5% sodium deoxycholate, 0.1% SDS, 200 µM sodium ortho-vanadate, 1 mM AEBSF (Roche), 1% Triton X-100
Lysis buffer IV (Western lysis buffer)	50 mM Tris-HCl pH 7.4, 150 mM sodium chloride, 5 mM EDTA, 0.1% sodium azide, 0.5% Triton X-100, 0.5 mM AEBSF (Roche), 10 µM leupeptin, 2 mM benzamidine, 10 µM pepstatin A, 5 µM soybean trypsin inhibitor
Laemmli running buffer	25 mM Tris-HCl pH 6.8, 192 mM glycin, 0.1% SDS
5 x SDS sample buffer	50 mM Tris-HCl pH 6.8, 12% glycerol, 4% SDS, 0.01% Coomassie Brilliant Blue G-250, 4% 2-mercaptoethanol
TBE	100 mM Tris-HCl pH 7.5, 100 mM boric acid, 2.5 mM EDTA
TBS	20 mM Tris-HCl pH 7.5, 100 mM sodium chloride
TBS-T	20 mM Tris-HCl pH 7.5, 100 mM sodium chloride, 0.05% Tween 20
10 x blotting buffer	250 mM Tris-HCl pH 8.3, 1.92 M glycin, 10% methanol, 0.01% SDS
Stripping buffer	5 mM sodium phosphate pH 7.5, 2 mM 2-mercaptoethanol, 2% SDS
PBS	Dulbecco's phosphate buffered saline pH 7.4, GIBCO, Invitrogen
MACS buffer	PBS, 0.5% FCS, 2 mM EDTA

2.1.5 Phosphodiesterase inhibitors

The PDE4 inhibitor rolipram was purchased from Sigma-Aldrich. The PDE3 inhibitor motapizone was a generous gift from formerly Nattermann (Rhone-Poulenc Rorer, Koeln, Germany). The PDE4 inhibitor RP73401 (piclamilast) (WO9212961) was synthesized at the chemical facilities of ALTANA Pharma AG (Konstanz, Germany).

2.1.6 Oligonucleotides

Antisense oligophosphorothioates (AS^{1st}) and 2'-alkoxy modified chimeric phosphorothioate oligonucleotides (AS^{2nd}) were kindly provided by Drs. Gekeler and Hofmann (ALTANA Pharma AG, Konstanz). Complementary sequences were designed to 3' ends of individual PDE4 subtype mRNA regions, at positions where all known splice variants of one subtype are identical, but distinct from other PDE4 subtypes. The sequences were proposed by Prof. Sczakiel (DGS Consulting e.K., Luebeck) and are proprietary to ALTANA Pharma AG. AS^{1st} were 17 - 20 bases in length containing a phosphorothioate backbone without further modifications. AS^{2nd} were 17 - 20 bases in length containing a phosphorothioate backbone and 2'-alkoxy modifications on the ribose residues at the first and last 4 - 6 bases. AS^{1st} and AS^{2nd} were solved in PBS and the stock solutions were stored at -80°C until use.

Small interfering RNAs (siRNAs) were from Dharmacon (Lafayette, USA), as listed in Table 3. All siRNAs have two symmetrical UU overhangs and a 5' phosphorylated antisense strand.

Dharmacon siRNAs were delivered desalted, were reconstituted in 1 x siRNA buffer (Dharmacon), and were stored at -80°C.

Table 3. siRNA sequences. Name, order number, and sequence (5'-3') of used Dharmacon siRNAs. 'SMARTpool' siRNAs are a pooled set of 4 individual siRNAs targeting the same transcript.

Name and order number	Description or siRNA-sequence (5'-3')	Reference sequence
PDE4A_SMARTpool M-007647	set of four siRNAs targeting PDE4A	NM_006202
PDE4B_SMARTpool M-007648	set of four siRNAs targeting PDE4B	NM_002600
PDE4C_SMARTpool M-007649	set of four siRNAs targeting PDE4C	NM_000923
PDE4D_SMARTpool M-004757	set of four siRNAs targeting PDE4D	NM_006203
NEG_SMARTpool D-001206-13	set of four non-targeting siRNAs, with >4 mismatches to every known human gene	
PDE4A_si1, D-007647-04	GUAACAGCCUGAACAACUC	NM_006202
PDE4B_si1, D-007648-04	GAAAGAGACCUCCUAAAGA	NM_002600
PDE4D_si1, D-004757-05	GAAAUCAAGUGUCAGAGUU	NM_006203
PDE4D_si2, D-004757-06	GAACUUGCCUUGAUGUACA	NM_006203
NEG_si, D-001210-01	non-targeting siRNA, >4 mismatches to every known human gene	
Itk_si, D-003144-09	GAACAAUCCCUGUAUAAAG	NM_005546

PDE4D_si1 and PDE4D_si2 were shown to have the same efficacy and were both used in experiments and were labeled PDE4D_si in the text and figures. To test for transfection efficiency, FITC-labeled non-targeting siRNA was purchased from Sequitur (BLOCK-iT fluorescent oligo, Sequitur, Invitrogen, Carlsbad, USA). FITC-labeled non-targeting antisense (AS^{2nd}) constructs were provided from Dr. H.-P. Hofmann (ALTANA Pharma AG, Konstanz).

Forward/reverse primer and probe sets for quantitative PCR were purchased from Applied Biosystems (Foster City, USA) and are shown in Table 4.

Hexanucleotides as primers for the synthesis of cDNA were from Roche. dNTPs were purchased from Larova (Teltow, Germany).

Table 4. Primer and probe sets. Name, sequence (5'-3'), and final concentration in PCR reactions are indicated. Probes were either VIC- or FAM-labeled. FAM-probes have a minor groove binder (MGB) protein at their 3' end to improve binding.

Name	Sequence (5'-3')	Final conc. [nM]
18S rRNA	Forward: CGGCTACCACATCCAAGGAA	50
	Reverse: GCTGGAATTACCGCGGCT	50
	Probe: VIC-TGCTGGCACCAGACTTGCCCTC	50
PDE4A	Forward: GTGGCTCCGGATGAGTTCTC	900
	Reverse: GGGCTGCTGTGGCTTACAG	900
	Probe: FAM-CCGGGAGGAATTCGTGGT-MGB	200
PDE4B	Forward: AGCAGCACAAAGACGCTTTGT	300
	Reverse: TCAGTCTCTCCCAGGGAATCTC	600
	Probe: FAM-TGATTGATCCAGAAAAC-MGB	200
PDE4C	Forward: ACTCTGGAGGAGGCAGAGGAA	900
	Reverse: AGGCAACTCCAAGGCCTCTT	900
	Probe: FAM-AAGAGACAGCTTTAGCC-MGB	200
PDE4D	Forward: GGCAGGGTCAAACTGAGAAATT	900
	Reverse: TGACTGCCACTGTCCTTTTCC	900
	Probe: FAM-TAGAGGAAGATGGTGAGTCAG-MGB	200

2.1.7 DNA and RNA modifying enzymes

DNAse I, used for on-column DNA digestion, was from Qiagen. Reverse transcriptase AMV, used for synthesis of cDNA, was purchased from Roche. 2 x TaqMan universal PCR master mix, containing AmpliTaq Gold DNA polymerase, was obtained from Applied Biosystems.

2.1.8 Antibodies

For the stimulation of human primary $CD4^+$ and $CD8^+$ T cells, anti-CD3 mAb (Orthoclone OKT-3, Janssen-Cilag, Neuss, Germany) and anti-CD28 mAb (clone CD28.2, Immunotech, Marseille, France) were used. For flow cytometry, murine antibodies recognizing human surface expression markers, such as CD4, CD8, CD14, CD83, or CD25 (PE or FITC labeled) were purchased from Immunotech. Antibodies recognizing CCR7 were from R&D systems (Minneapolis, USA). Nonspecific murine IgG1, IgG2a, and IgG2b antibodies were used as respective isotype controls (Immunotech, R&D systems). For immunoprecipitation experiments, rabbit polyclonal antibodies AC55 (anti-PDE4A) and K118 (anti-PDE4B) and the murine monoclonal antibody m3S1 (anti-PDE4D) (Iona et al., 1998) were generously provided from Prof. Conti (Stanford University School of Medicine, Stanford, USA). Purified mouse myeloma IgG1 as isotype control was purchased from Zymed (Invitrogen, Carlsbad, USA). For immunoblotting experiments in A549 cells, affinity purified polyclonal rabbit antibodies directed against PDE4A, PDE4B, and PDE4D (PD4-112AP, PD4-401AP, PD4-201AP, respectively) were obtained from FabGennix Inc. (Shreveport, USA). For immunoblotting experiments in human primary $CD4^+$ T cells, rabbit polyclonal antibodies raised against PDE4A, PDE4B, and

PDE4D (Tenor et al., 2002) were provided from Dr. H. Tenor (ALTANA Pharma AG, Konstanz). Mouse monoclonal anti-β-Actin was used to verify that the same amounts of protein were loaded onto the gel (loading control) and was purchased from Sigma-Aldrich. Secondary antibodies were peroxidase-conjugated goat anti-mouse and anti-rabbit IgG (H+L) from Dianova (Hamburg, Germany).

2.1.9 Cytokines and lipopolysaccharide

For the *in vitro* differentiation of human peripheral monocytes to dendritic cells, interleukin-4 (IL-4) was purchased from R&D systems. Granulocyte macrophage-colony stimulating factor (GM-CSF) was obtained from Biozol (Eching, Germany). Lipopolysaccharide (LPS) was from Sigma-Aldrich.

2.1.10 Kits for enzyme-linked immunosorbent assays (ELISA)

Cytokine levels in the culture medium were measured using specific enzyme-linked immunosorbent assays for IL-2, IL-5, and IFN-γ, purchased from Immunotech.

2.1.11 Primary cells and cell lines

Primary cells were obtained by negative selection of $CD4^+$, $CD8^+$, or $CD14^+$ cells of freshly taken human peripheral blood. Alternatively, $CD14^+$ cells were isolated by positive selection. The local ethics committee has approved this study with human material. The human lung adenocarcinoma epithelial cell line A549 (CCL-185) was obtained from LGC Promochem (Wesel, Germany).

2.1.12 Cell isolation reagents

For the isolation of distinct subpopulations of human peripheral cells, magnetic cell isolation kits were purchased from Miltenyi Biotec (Bergisch Gladbach, Germany): $CD4^+$ T cell isolation kit II, $CD8^+$ T cell isolation kit II, monocyte T cell isolation kit II, CD45RA microbeads, CD45RO microbeads, and CD14 microbeads.

2.1.13 Cell culture media

A549 medium, complemented: DMEM (GIBCO, Invitrogen), 10% FCS.

T cell medium, complemented: RPMI 1640 (GIBCO, Invitrogen), 10% FCS, 1% L-glutamine, 100 units/ml penicillin, 0.1 mg/ml streptomycin.

Macrophage medium, complemented: RPMI 1640 (GIBCO, Invitrogen), 10% human AB serum, 1% sodium pyruvate, 1% L-glutamine, 1% essential amino-acids, 100 units/ml penicillin, 0.1 mg/ml streptomycin.
Monocyte medium, complemented: IMDM (GIBCO, Invitrogen), 10% FCS, 80 µg/ml gentamycin.
Before use, serum was heat-inactivated by incubation at 56°C for 30 min.

2.1.14 Cell transfection reagents

For transfection of A549 cells, the cationic lipid argfectin-50 was provided from Atugen (Berlin-Buch, Germany). Unstimulated human primary $CD4^+$ T cells were transfected with the human T cell nucleofector kit from Amaxa (Koeln, Germany).

2.1.15 Devices and software

Data collection and analysis were performed using a SpectraMax Plus photometer and the SoftMax Pro software (Molecular Devices, Sunnyvale, USA), an ABI Prism 7900 HT sequence detection system and the SDS 2.1 software (Applied Biosystems), an EPICS-XL cytometer and the Expo32 1.2 software (Beckman Coulter, Fullerton, USA), a SPECTRA Rainbow reader and the easyWIN fitting 6.0a software (Tecan, Mannedorf, Switzerland), an LAS-1000 luminescence image analyzer (Fujifilm, Duesseldorf, Germany) and the Aida image analyzer 3.22 software (Raytest, Straubenhardt, Germany), a TopCount NXT and the NXT 2.14 software (Perkin Elmer, Boston, USA), and an LS6500 scintillation counter (Beckman Coulter). Human primary cells were isolated using an autoMACS system (Miltenyi Biotec). Transfections of T cells were performed using the nucleofector device I (Amaxa). Homogenization of cells was carried out with Sonopuls ultrasonic homogenizers (Bandelin, Berlin, Germany). Microsoft Excel (Microsoft, Redmond, USA) and GraphPad Prism (GraphPad Software, San Diego, USA) were used for data management. Immunoblotting autoradiographies were assembled using Adobe Photoshop 6 (Adobe Systems, San Jose, USA). The primer and probe sets for quantitative PCR analysis were designed using Primer Express 2.0 (Applied Biosystems). Microscopy was performed using an Axiovert 25 inverse microscope (Carl Zeiss MicroImaging GmbH, Goettingen, Germany) or a DMIL 1000 inverse microscope (Leica Microsystems, Wetzlar, Bensheim, Germany).

2.2 Molecular biology methods

2.2.1 RNA isolation and quantification

Before RNA isolation, cells were washed in PBS, lysed with 350 µl or 700 µl RLT buffer (Qiagen) supplemented with 1% 2-mercaptoethanol, and homogenized with QIAshredder spin columns (Qiagen). Subsequently, total RNA was isolated using RNeasy mini columns with silica-gel membranes, according to the instructions of the manufacturer (Qiagen). Briefly, the homogenized lysate was diluted with 1 volume of ice cold 70% ethanol, mixed, and transferred to RNeasy columns. All subsequent steps were performed at RT. After centrifugation and a washing step with 400 µl RW1 buffer, 30 units of RNase-free DNase in 80 µl RDD buffer (Qiagen) were applied for on-column digestion of DNA (20 min). The columns were washed once with 400 µl RW1 buffer and twice with 500 µl RPE buffer. RNA was eluted by pipetting 15 µl of nuclease-free water (Eppendorf, Hamburg, Germany) onto the dried membrane, followed by an incubation period of 5 min and subsequent centrifugation for 1 min at 8000 x g. This elution step was repeated with fresh water. Finally, RNA concentration was determined by OD_{260} measurement using a SpectraMax Plus photometer (Molecular Devices).

2.2.2 cDNA synthesis and quantitative PCR

In this study, gene expression quantification was carried out using two-step reverse transcription-polymerase chain reactions (RT-PCR) in which the PCR step was coupled with a 5' fluorogenic nuclease assay (Heid et al., 1996). For reverse transcription of RNA, 0.5 - 1 µg RNA in a volume of 12.5 µl nuclease-free water (Eppendorf) was incubated for 60 min at 42°C with 1 µl dNTPs (final 0.5 mM each; Larova), 1.5 µl hexanucleotide mix (final 0.8 x, Roche), 1 µl AMV reverse transcriptase (final 20 units, Roche), and 4 µl incubation buffer (Roche). Thus, the total volume of the reaction was 20 µl. The cDNA was diluted in nuclease-free water (Eppendorf) to a concentration of 2 ng cDNA/µl. Total RNA and cDNA were stored at -80°C.

Quantitative PCR reactions were performed on an ABI Prism 7900 HT sequence detection system (Applied Biosystems) with primer and probe sets detecting *18S rRNA* as internal standard and one of the four subtypes of PDE4 as target gene. In order to detect all transcripts of one subtype with one primer and probe set, all known splice variants of one subtype have been bioinformatically aligned. Then, the PDE4 subtype primer and probe sets have been designed to bind at the 3' end of the open reading frame of each subtype, at positions where individual splice variants of one subtype are identical. Primer and probe sets were tested for specificity and were optimized to have similar amplification efficiencies in duplex reactions (i.e., combined detection of *18S rRNA* and a target gene), as verified with a series of validation experiments. Standard quantitative PCR reactions were performed in a total volume of 25 µl in triplicates, each containing 5 µl cDNA (10 ng), 1.25 µl per primer and probe detecting

18S rRNA, 1.25 µl per primer and probe detecting the target gene, and 12.5 µl of 2x TaqMan universal PCR master mix (Applied Biosystems). The thermal cycler protocol was standardized and consisted of a 2 min period at 50°C (uracil removal for PCR carryover protection), a 10 min period at 95°C (denaturation of native DNA), and of 40 cycles of 15 sec at 95°C (denaturation of PCR product) followed by 1 min at 60°C (annealing/extension). DNA contamination was controlled by taking total RNA as template. Additionally, water was used as 'template' to test whether the primer and probe sets were DNA-free. For control experiments, plasmids were used containing conserved C-terminal parts of the subtypes PDE4A, PDE4B, PDE4C, and PDE4D.

2.2.3 Relative expression calculated by the $\Delta\Delta C_t$ method

Quantification of PCR experiments was based on the comparative $\Delta\Delta C_t$ method as described elsewhere (Livak and Schmittgen, 2001). Briefly, the measured fluorescent signal intensities of both the probe detecting *18S rRNA* and the probe detecting the target gene were semilogarithmically plotted against the number of PCR cycles, generating C_t values (cycle at threshold). To normalize for input amounts of RNA within one sample, the C_t of *18S rRNA* was subtracted from the corresponding target C_t, generating the normalized ΔC_t. Either untreated cells or nucleofection (NF) control cells were then defined as calibrator, and the normalized ΔC_t value of the calibrator was subtracted from all other normalized ΔC_t values of the other samples, generating $\Delta\Delta C_t$ values. As final output, the expression of each sample relative to the calibrator was obtained by calculating $2^{-\Delta\Delta Ct}$ (Livak and Schmittgen, 2001).

2.3 Biochemical methods

2.3.1 Protein determination

If not otherwise stated, protein determination was performed according to a method described by Bradford (Bradford, 1976). 1 µl of lysate was diluted in 160 µl H_2O and 40 µl of protein assay dye reagent concentrate (Bio-Rad). For normalization, 1 - 6 µg of BSA stock solution (1 µg/µl, Bio-Rad) in a 1:160 dilution of the respective lysis buffer were used as standard. Samples were shaken vigorously, incubated for 5 min at RT, and analyzed in a 96-well microplate reader at 595 nm (Rainbow reader, Tecan, Mannedorf, Switzerland). Alternatively, for immunoblotting experiments with lysates from human primary $CD4^+$ T cells, a BCA protein assay was performed according to the instructions of the manufacturer (Pierce).

2.3.2 SDS-Polyacrylamide gel electrophoresis (SDS-PAGE)

For immunoblotting experiments with lysates from A549 cells, SDS-PAGE was performed using 10% polyacrylamide separating gels and 4% polyacrylamide stacking gels (see Table 5), adapted from a method described by Laemmli (Laemmli, 1970).

Table 5. Constituents of SDS-PAGE stacking and separating gels for immunoblotting experiments with A549 cell lysates. Shown are the volumes for 2 gels.

Constituent	Stacking gel (4%)	Seperating gel (10%)
Acrylamide/Bis (30%/0.8%)	0.67 ml	3.33 ml
0.5 M Tris/HCl, pH 6.8	1.25 ml	-
1.5 M Tris/HCl, pH 8.8	-	2.5 ml
10% SDS	0.1 ml	0.1 ml
Glycerol	-	1.2 ml
H_2O	3 ml	2.79 ml
TEMED	3.8 µl	7.5 µl
APS	37.5 µl	75 µl

Gels were prepared and run in a Mini-PROTEAN II electrophoresis system (Bio-Rad). 17 - 30 µg of protein in 20 µl lysis buffer III (RIPA buffer) were mixed with 5 µl 5 x SDS sample buffer and incubated at 95°C for 5 min. Samples were loaded onto the gels and were separated with 120 V for 1 h in Laemmli running buffer. Full range rainbow molecular weight marker (10 - 250 kDa Rainbow 800, Amersham) was used as protein standard.

For immunoblotting experiments with lysates from human primary $CD4^+$ T cells, SDS-PAGE was performed using 10% polyacrylamide separating gels and 5% polyacrylamide stacking gels (see Table 6).

Table 6. Constituents of SDS-PAGE stacking and separating gels for immunoblotting experiments with human primary $CD4^+$ T cell lysates. Shown are the volumes for 2 gels.

Constituent	Stacking gel (5%)	Seperating gel (10%)
Acrylamide/Bis (30%/0.8%)	4.95 ml	20 ml
0.625 M Tris/HCl, pH 6.8	6 ml	-
1.8 M Tris/HCl, pH 8.8	-	12 ml
0.5% SDS	6 ml	12 ml
H_2O	13.05 ml	16 ml
TEMED	30 µl	50 µl
10% APS	150 µl	300 µl

Gels were prepared and run in a Hoefer SE600 electrophoresis system (Hoefer Inc., San Francisco, USA). Washed cell pellets were incubated for 30 min in ice cold lysis buffer IV, mixed, and subject for centrifugation at 4°C for 15 min at 1000 x g. 50 µg of protein of the supernatant were mixed 3:1 with Roti Load I (Carl Roth GmbH, Karlsruhe, Germany) and were denaturated at 95°C for 7 min. Samples were loaded onto the gels and were separated with 80 V for 30 min and 200 V for 75 min in Laemmli running buffer. A 1:1 mixture of unstained

and prestained Precision Plus Protein Standards (Bio-Rad) in Precision Protein™ StrepTactin-HRP Conjugate (Bio-Rad, 1:10 diluted) was used as protein standard.

2.3.3 PDE activity assay

All PDE activity measurements were based on a procedure described by Thompson et al. (Thompson et al., 1979). In this study, PDE activity assays were performed a) in accordance to a protocol (= PDE activity assay I) described by Conti and coworkers (Conti et al., 1984; Jin et al., 2005) or b) in accordance to a protocol (= PDE activity assay II) modified by Bauer and Schwabe (Bauer and Schwabe, 1980), and further detailed by Hatzelmann and Schudt (Hatzelmann and Schudt, 2001).

a) PDE activity assay I:

Unstimulated and anti-CD3/CD28 treated human primary $CD4^+$ T cells were washed in PBS and were resuspended for 10 min in ice cold lysis buffer I. After sonication with 25 bursts (continuously, duty cycle 30, output control 3, power 20%, Sonopuls, Bandelin), the lysate was centrifuged at 4°C for 20 min at 16000 x g. For determination of total cAMP hydrolyzing PDE activity in the supernatant, 10 - 20 µg of protein were diluted in glass tubes (Fisherbrand, Los Angeles, USA) in 150 µl Tris/HCl pH 8, 1% BSA. Then, 50 µl assay mixture (40 mM Tris/HCl pH 8, 40 mM magnesium chloride, 5 mM 2-mercaptoethanol, 4 µM cAMP, and 100000 cpm/assay [^{3}H]-cAMP) were added and the reaction was started by incubating the PDE assay mixture at 34°C in a water bath for 10 min. For determination of rolipram-insensitive cAMP hydrolyzing PDE activity, 10 µM rolipram were included in the PDE assay mixture prior incubation. The PDE reaction was stopped on ice by addition of 200 µl stop solution (40 mM Tris/HCl pH 7.4, 100 mM EDTA). Subsequently, the mixture was boiled for 1 min, was incubated with 50 µl 5'-nucleotidase (*Crotalus atrox* snake venom, Sigma-Aldrich, 1 mg/ml in H_2O) at 34°C for 20 min, and was left on ice for 10 min. After adding 1 ml of methanol, the samples were mixed and loaded on anion exchange columns filled with 1 ml 20% AG 1 x 8 resin (Bio-Rad). The eluted [^{3}H]-adenosine was mixed with 7 ml scintillation fluid (Econosafe, Research Products International, Mt. Prospect, USA) and measured for total radioactivity on a scintillation counter (Beckman Coulter). Results were corrected for blank values (measured in the absence of protein) and the PDE4 activity was calculated as the difference of total PDE activity and rolipram-insensitive PDE activity.

b) PDE activity assay II:

Cells grown in suspension were washed in PBS (4°C) and then resuspended for 10 min in ice cold lysis buffer II. Adherent A549 cells were washed once with PBS (4°C), incubated with lysis buffer II, and collected using cell scrapers. After sonication with 3 x 15 bursts (duty cycle 10,

output control 2, power 20%, Sonopuls, Bandelin), lysates were centrifuged at 4°C for 20 min at 1000 x g. From the supernatant, 5 - 20 µg of protein (T cells) or 3 - 5 µg of protein (A549 cells) in 100 µl lysis buffer II were diluted on 96-well plates with 20 mM Tris/HCl pH 7.8 to a final volume of 140 µl. Afterwards, 10 µl of 20 mM Tris/2% DMSO or 10 µl of 20 µM RP73401 (piclamilast, 1 mM stock solution in 100% DMSO diluted 1:50 in 20 mM Tris/HCl pH 7.8) were added for the determination of total cAMP hydrolyzing PDE activity or piclamilast-insensitive cAMP hydrolyzing PDE activity, respectively. After preincubation at 37°C for 5 min, the reaction was started by adding 50 µl assay mixture (20 mM Tris/HCl pH 7.8, 20 mM magnesium chloride, 2 µM cAMP, 400 µM EGTA, and ~30000 cpm/assay [^{3}H]-cAMP) and the assays were incubated for 20 - 25 min at 37°C. To stop the reaction, 50 µl 0.2 N HCl (4°C) were added and the assays were left on ice for 10 min. Following incubation at 37°C for 15 min with 50 µl 5'-nucleotidase (*Crotalus atrox* snake venom, Sigma-Aldrich, 0.5 mg/ml in 400 mM Tris/HCl pH 8.5 [37°C]), the assays were loaded on Poly-Prep chromatography columns (Bio-Rad) filled with 1 ml of QAE Sephadex A-25 (Sigma-Aldrich). [^{3}H]-Adenosine was eluted with 2 ml of 30 mM ammonium formiate pH 6.0, mixed with 3 ml scintillation fluid (Lumasafe Plus, Lumac, Groningen, The Netherlands), and measured for total radioactivity in a scintillation counter (Beckman Coulter). Results were corrected for blank values (measured in the presence of denatured protein) and the PDE4 activity was calculated as the difference of total PDE activity and piclamilast-insensitive PDE activity.

In all PDE assay experiments, the amount of cAMP hydrolyzed was below 25% of the original substrate concentration.

2.3.4 Proliferation assay

The incorporation of [^{3}H]-thymidine was taken as a parameter to determine CD4$^+$ T cell proliferation and was determined in duplicate reactions. After 48 h of stimulation, 10 µl of [^{3}H]-thymidine were added to the cells (0.2 µCi/well) for a period of 18 h. Cell transfer to filter plates (UniFilter-96, Perkin Elmer, Boston, USA) was performed by using a cell harvester (Tomtec cell harvester 96, Dunn Labortechnik, Asbach, Germany). The filter plates were washed three times with water at RT and then dried at 60°C for 1.5 h. To detect the radioactivity of the cells as count per minute (cpm), 40 µl scintillator (Microscint O, Perkin Elmer) was added, the plates were sealed, and the radioactivity was finally measured using a TopCount microplate scintillation counter (Perkin Elmer).

2.4 Immunological methods

2.4.1 Immunoprecipitation

For immunoprecipitation, 30 µl Sepharose-A and -G (Immunoprecipitation Starter Kit, Amersham Biosciences) were washed once with cold 200 µl PBS pH 7.4 and twice with 200 µl PBS containing 0.05% BSA. 10 µl PDE4A- or PDE4B-specific Ab (AC55 or K118, respectively) or 10 µl preimmune-serum (as nonspecific precipitation control) were preincubated at 4°C for 1 h with protein A-sepharose (Amersham Biosciences) and 90 µl PBS containing 0.05% BSA. Likewise, 25 µg PDE4D-specific Ab (m3S1) or IgG1 (Zymed, as nonspecific precipitation control) were preincubated with protein G-sepharose (Amersham Biosciences). After incubation, the sepharose-antibody complexes were washed once with 200 µl ice cold 20mM Tris/HCl pH 7.8, 0.5 M NaCl and twice with ice cold 200 µl Tris/HCl pH 7.8. The supernatant of lysed T cells was equally aliquoted (50 - 150 µg of protein per aliquot, in a volume of 500 µl lysis buffer I) and incubated for 90 min at 4°C with the sepharose-antibody preparations. After washing twice in ice cold PBS containing 0.05% BSA, the sepharose-antibody-antigen complexes were either washed in 500 µl 40 mM Tris/HCl pH 8 containing 1% BSA or in 500 µl PDE assay buffer II. Afterwards, sepharose-antibody-antigen complexes were transferred to PDE assay tubes for determining PDE activity, as described above.

2.4.2 Immunodetection of blotted proteins

After separation of A549 protein lysates on SDS-PAGE minigels (as described in chapter 2.3.2), a wet blotting system (Transphor Electrophoresis Unit, Hoefer Inc., San Francisco, USA) was used to transfer the proteins to Protran nitrocellulose membranes (Schleicher and Schuell, Dassel, Germany). After washing in 1 x blotting buffer, minigels were adjusted in the wet blotting system and proteins were transferred with 950 mA for 45 min to the nitrocellulose membrane. After transfer, membranes were washed in TBS buffer and blocked for 2 h at RT with TBS containing 5% BSA by shaking. For detection of target proteins, membranes were incubated overnight at 4°C with antibodies recognizing PDE4A, PDE4B, or PDE4D, diluted in TBS containing 0.05% BSA according to the suppliers' manuals (Fabgennix). Subsequently, membranes were washed three times for 10 min with TBS-T and incubated for 2 h at RT with a 1:50000 dilution of a horseradish peroxidase-conjugated secondary antibody (Dianova) in TBS-T. After incubation, membranes were washed three times for 10 min with TBS-T. For chemiluminescence detection, membranes were incubated for 1 min with 3 ml of a 1:1 dilution of Lumi-LightPLUS Stable Peroxid Solution and Lumi-LightPLUS Luminol/Enhancer (Roche) and were analyzed using the LAS-1000 Luminescence Image system (Fuji Film).

For the immunodetection of ß-Actin, used as internal standard, membranes were incubated at 60°C for 30 min in stripping buffer to remove bound antibodies. Membranes were then washed

three times for 5 min at RT with TBS-T and were incubated for 4 h at 4°C with a 1:5000 dilution of monoclonal mouse anti-ß-Actin antibody (Sigma-Aldrich) in TBS, 0.05% BSA. Subsequent steps were performed as described above.

After separation of human primary $CD4^+$ T cell protein lysates on SDS-PAGE gels (as described in chapter 2.3.2), a semi-dry blotting system (Bio-Rad) was used for the transfer of separated proteins to nitrocellulose membranes (BA 85), according to the instructions of the manufacturer. After transfer, membranes were blocked in PBS containing 5% skim milk by shaking for 2 h at RT. After washing for 10 min with 50 mM Tris-HCl pH 7.6 containing 150 mM sodium chloride and 0.5% BSA, membranes were incubated overnight at 4°C with antibodies recognizing PDE4A, PDE4B, or PDE4D (Tenor et al., 2002), diluted in the latter Tris buffer. Dilutions were: anti-PDE4A antibody 1:2000, anti-PDE4B antibody 1:2000, or anti-PDE4D antibody 1:5000. In parallel, anti-ß-Actin antibodies (Sigma-Aldrich) were added (1:100000). Subsequently, membranes were washed six times for 5 min with 50 mM Tris-HCl pH 7.6 containing 150 mM sodium chloride and 0.05% Tween 20. After washing, membranes were incubated for 1 h at RT with a 1:100000 dilution of goat anti-rabbit and goat anti-mouse IgG-HRP (Dianova), respectively, in the latter Tris buffer. Additionally, StrepTacin-HRP conjugate was added (Bio-Rad, 1:50000). After incubation, membranes were washed six times for 5 min with 50 mM Tris-HCl pH 7.6 containing 150 mM sodium chloride and 0.05% Tween 20 and once for 5 min with 50 mM Tris-HCl pH 7.6 containing 150 mM sodium chloride. For chemiluminescence detection, membranes were incubated for 2 min with ECL Advance Western blotting reagent (Amersham) and analyzed using the LAS-1000 Luminescence Image system (Fuji Film).

2.4.3 Flow cytometry

For flow cytometrical analysis, 1 - 5 x 10^5 cells were washed twice in staining buffer (PBS, 2% FCS) and resuspended in 100 µl of ice cold staining buffer. Labeling was carried out using 10 µl of antibodies directed against surface markers. As viability dye, 5 µl propidium iodide (100 µg/ml, Sigma-Aldrich) or 10 µl 7-aminoactinomycine D solution (Immunotech) were used. After incubation at 4°C for 15 min in the dark, the labeled cells were diluted with 400 µl staining buffer and subject for analysis on a Coulter Epics XL-MCL flow cytometer, according to the instructions of the manufacturer (Beckman-Coulter). Isotype controls were used to detect unspecific binding of antibodies. For the analysis of monocytes, dendritic cells, and macrophages, 5 µl Fc-blocking reagent (Miltenyi Biotec) were included in the assays to increase the specificity of antibody binding.

2.4.4 Enzyme-linked immunosorbent assay (ELISA)

For the determination of cytokine levels in the culture medium, $CD4^+$ T cell supernatants were removed after 24 h, 48 h, or 72 h, and stored at -80°C until specific commercially available enzyme-linked immunosorbent assays (IFN-γ, IL-2, and IL-5 assay kits, Immunotech) were performed. Due to the high variability of cytokine levels from different blood donors, but the comparable narrow linear range of the enzyme-linked immunosorbent assay standard curve, appropriate dilution factors have been determined prior to the analysis. Dilutions were performed in the buffers contained in the assay kits. All cytokines were determined from the pool fraction in duplicate in accordance to the manufacturer's instructions (Immunotech) on a 96 well microplate reader at 450 nm (Tecan).

2.5 Eukaryotic cell culture

Adherent A549 cells were cultivated in T-175 culture flasks in A549 medium in a humidified incubator at 37°C, 5% CO_2. At 80 - 90% confluence, the medium was removed and the cells were washed with 10 ml PBS. For detaching, cells were treated for 3 min with 5 ml trypsin (0.05% trypsin with EDTA, 1 x solution, Invitrogen). The trypsin incubation was stopped with fresh medium, and the cells were centrifuged for 10 min at 200 x g. One third of the cells was resuspended in fresh medium and subject for further cultivation.

Frozen cells (stored in liquid nitrogen) were thawed in a water bath, quickly removed from the cryovial, and transferred to 10 ml complemented A549 medium (4°C). The cells were pelleted, resuspended in prewarmed medium (37°C), and cultivated in cell culture flasks, as described above. For long-term storage of A549 cells, 2.5×10^5 cells were pelleted and resuspended in 1 ml medium containing 40% DMEM, 40% FCS, and 20% DMSO. Cells were frozen in cryovials with ~ -1°C/min at -80°C and were then transferred to the nitrogen storage unit.

2.6 Isolation of human primary immune cells

2.6.1 Isolation of untouched $CD4^+$ T cells

Human peripheral blood $CD4^+$ T cells were purified by negative selection, adapted to a method described elsewhere (Zitt et al., 2004). Briefly, 250 ml blood from normal, healthy donors were taken by antecubital venipuncture. The blood was citrate-treated (0.3% w/v) and diluted 1.6-fold with PBS before centrifugation at RT for 10 min at 220 x g. The lower phase was layered on a percoll gradient (ρ = 1.077 g/ml) and was subject for centrifugation at RT for 25 min at 800 x g. The interphase containing the peripheral blood mononuclear cells (PBMCs) was harvested, washed twice in PBS containing 2 mM EDTA and was then resuspended in ice cold

MACS buffer to a cell density of 1 x 10^7 cells per 40 µl. Antibody binding of the cells was performed by adding 10 µl biotin-antibody cocktail per 1 x 10^7 cells (directed against CD8, CD14, CD16, CD19, CD36, CD56, CD123, TCRγ/δ, and glycophorin A; $CD4^+$ T Cell isolation kit II, Miltenyi Biotec), followed by incubation for 15 min at 4°C. Before magnetical labeling with 20 µl anti-biotin microbeads (Miltenyi Biotec) per 1 x 10^7 cells for 15 min at 4°C, 30 µl MACS buffer per 1 x 10^7 cells were added. After labeling, the cells were washed in MACS buffer, centrifuged at 4°C for 10 min at 300 x g, and resuspended in 50 µl MACS buffer per 1 x 10^7 cells. The cells were magnetically separated using the autoMACS system (separation strategy 'deplete', Miltenyi Biotec), yielding untouched human peripheral blood $CD4^+$ T cells. Freshly isolated $CD4^+$ T cells were cultured in cell culture flasks in T cell medium at a cell density of 1 x 10^6 cells/ml at 37°C, 5% CO_2 in a humidified incubator. The purity of isolated cells was assessed by flow cytometry, as described in chapter 2.4.3.

2.6.2 Isolation of untouched $CD4^+$ T cells positive for CD45RA or CD45RO

Untouched $CD4^+$ T cells of one donor were separated into two parts, and each part was labeled with anti-CD45RA or anti-CD45RO microbeads (Miltenyi Biotec), respectively. Per 1 x 10^7 pelleted $CD4^+$ T cells, 80 µl MACS buffer and 20 µl microbeads were added. Cells were incubated at 4°C for 15 min. After labeling, the cells were washed in MACS buffer, centrifuged at 4°C for 10 min at 300 x g, and resuspended in 50 µl MACS buffer per 1 x 10^7 cells. The cells were magnetically separated using the autoMACS system (separation strategy 'deplete', Miltenyi Biotec), yielding untouched human $CD4^+CD45RA^+$ (naïve) and $CD4^+CD45RO^+$ (memory) T cells. Naïve and memory T cells were checked for purity and cultured as described in chapter 2.6.1.

2.6.3 Isolation of untouched $CD8^+$ T cells

Human peripheral blood $CD8^+$ T cells were purified by negative selection, as described in chapter 2.6.1. However, the $CD8^+$ T cell isolation kit II (Miltenyi Biotec) was used. The biotin-antibody cocktail used was directed against CD4, CD14, CD16, CD19, CD36, CD56, CD123, TCRγ/δ, and glycophorin A.

2.6.4 Isolation of human peripheral $CD14^+$ monocytes

Human peripheral blood $CD14^+$ cells (monocytes) were either isolated by negative selection or by positive selection. Untouched $CD14^+$ cells were purified by negative selection, as detailed in chapter 2.6.1. However, the $CD14^+$ monocyte isolation kit II (Miltenyi Biotec) was used. Thus, antibody binding of PBMC cells was performed in 30 µl ice cold MACS buffer, 10 µl FcR

blocking reagent, and 10 µl biotin-antibody cocktail (directed against CD3, CD7, CD16, CD19, CD56, CD123, and glycophorin A) per 1 x 10^7 cells. Magnetical labeling and separation were carried out as described in chapter 2.6.1. Positive selection of $CD14^+$ cells was performed using anti-CD14 microbeads (Miltenyi Biotec). Per 1 x 10^7 pelleted PBMCs, 80 µl MACS buffer and 20 µl microbeads were added. Cells were incubated at 4°C for 15 min. After labeling, the cells were washed in ice cold MACS buffer, centrifuged at 4°C for 10 min at 300 x g, and resuspended in 50 µl MACS buffer per 1 x 10^7 cells. The cells were magnetically separated using the autoMACS system (separation strategy 'positive selection', Miltenyi Biotec).

2.7 *In vitro* generation of macrophages and dendritic cells

2.7.1 Differentiation of $CD14^+$ cells to monocyte-derived macrophages (MoMϕ)

For the *in vitro* differentiation of monocytes to monocyte-derived macrophages (MoMϕ), freshly isolated monocytes were resuspended in endotoxin-free macrophage medium (5 x 10^5 cells/ml), as detailed elsewhere (Gantner et al., 1997a). To increase the purity of untouched isolated monocytes, 1.5 ml of cell suspension were plated on Falcon Primaria 3846 6-well tissue culture plates (Becton Dickinson) and were incubated at 37°C, 5% CO_2 to allow adherence. After 1.5 h, medium was changed to eliminate non-adherent cells. Monocytes were further incubated at 37°C, 5% CO_2. Due to the high purity after isolation, positive selected cells were not subject for the adherence step. Medium was changed every 3 days until the end of the differentiation period (6 - 8 days), which was phenotypically controlled by inverse microscopy.

2.7.2 Differentiation of $CD14^+$ cells to monocyte-derived dendritic cells (MoDCs)

Similar to the *in vitro* differentiation of monocytes to MoMϕ, freshly isolated monocytes were resuspended in endotoxin-free monocyte medium (5 x 10^5 cells/ml) for the differentiation of monocytes to monocyte-derived dendritic cells (MoDCs) (Gantner et al., 1999). To increase the purity of untouched isolated monocytes, 1.5 ml of cell suspension were plated on Costar 3506 6-well tissue culture plates (Corning, Acton, USA) and were incubated at 37°C, 5% CO_2 to allow adherence. After 1.5 h, medium was changed to eliminate non-adherent cells. Subsequently, 10 ng/ml GM-CSF and 50 ng/ml IL-4 were added, and the cells were further incubated at 37°C, 5% CO_2. Every third day, half of the medium and cytokines was renewed until the end of the differentiation period (7 - 9 days). Due to the high purity, positive selected cells were not subject for the adherence step. Thus, positive isolated monocytes were cultured in T-125 flasks at a concentration of 1 x 10^6 cells/ml in monocyte medium containing 10 ng/ml GM-CSF and 50 ng/ml IL-4. After three days, the same volume of new medium and cytokines

was added. The differentiation process was phenotypically controlled by inverse microscopy and was also assessed by flow cytometric analysis of the expression of surface markers, such as CD14, CCR7, and CD83.

2.8 Transfection of cells

2.8.1 Transfection of A549 cells with the cationic lipid argfectin-50

For the transfection of A549 cells, the cationic lipid argfectin-50 (Atugen) was used, adapted to a protocol described elsewhere (Sonnemann et al., 2004a). In general, this technique of liposome-mediated transfection is also referred to as lipofection (Felgner et al., 1987). One day before lipofection, 1.5 x 10^5 A549 cells in a volume of 1.6 ml complemented medium were plated on Costar 3506 6-well tissue culture plates (Corning) for AS and siRNA knockdown experiments lasting 24 h. For 72 h experiments, 1 x 10^5 A549 cells were plated one day before lipofection. Final AS^{1st} concentrations (oligophosphorothioates, see chapter 2.1.6) were 200 nM, final AS^{2nd} concentrations (2'-alkoxy modified chimeric phosphorothioates, see chapter 2.1.6) were 50 - 100 nM. Final siRNA concentrations (Dharmacon 'SMARTpool' siRNAs, see chapter 2.1.6) were 5 - 100 nM. In all experiments, the argfectin-50 concentration of 0.9 µg/ml was used. Per sample, on day of lipofection, 250 µl 10 x AS or 10 x siRNA solution and 250 µl 10 x argfectin-50 solution were combined in polystyrene tubes (Sarstedt, Nuembrecht, Germany), mixed, and incubated at 37°C for 30 min. 10 x AS solution, 10 x siRNA solution, and 10 x argfectin solution were obtained by diluting AS (stock solution 80 µM in PBS), siRNA (stock solution 20 µM in 1 x siRNA buffer, Dharmacon), or argfectin-50 (stock solution 1 mg/ml, Atugen), respectively, in DMEM containing 20 mM HEPES (Invitrogen). After incubation, 400 µl of the combined AS/argfectin-50 or siRNA/argfectin-50 mixture were added to the plated A549 cells for 24 h or 72 h until harvest for downstream experiments. As control, only DMEM/20 mM HEPES (= untreated control) or DMEM/20 mM HEPES additionally containing 0.9 µg/ml argfectin-50 (= lipofection control) were applied.

2.8.2 Electroporation of $CD4^+$ T cells using the amaxa nucleofector (nucleofection)

Transfection of human peripheral, freshly isolated $CD4^+$ T cells was carried out using the nucleofector kit for unstimulated human T cells (Amaxa, Koeln, Germany), according to the instructions of the manufacturer (Gresch et al., 2004). 5 x 10^6 $CD4^+$ T cells per transfection sample were pelleted by centrifugation at RT for 15 min at 200 x g and resuspended in 100 µl of transfection solution (Amaxa). At standard condition, 97.1 µl of this cell solution were then added to an individual vial containing 7.9 µl of 20 µM siRNA, totaling in 105 µl of cell suspension and a final concentration of 1.5 µM siRNA. For higher siRNA concentrations,

60 µM siRNA was diluted with 1 x siRNA buffer (Dharmacon, Lafayette, USA) to the desired working concentration. For nucleofection (NF), each cell/siRNA suspension was transferred to a cuvette and electroporated using the program U-14 of the nucleofector device I (Amaxa). Immediately after NF, the samples were removed from the cuvette with 1 ml prewarmed T cell medium and transferred to 6-well plates (Corning Costar, Corning, USA) containing 1.5 ml of prewarmed medium. Cells were incubated in a humidified incubator at 37°C, 5% CO_2. For NF controls, only 1 x siRNA buffer, but no siRNA was added to the cell suspension prior transfection. For untreated controls, cells were resuspended in nucleofection solution, but no transfection was carried out. To test the transfection efficiency, different concentrations of FITC-labeled non-targeting siRNA (BLOCK-iT fluorescent oligo, Sequitur, Invitrogen) and different concentrations of a pmaxGFP plasmid (Amaxa) were nucleofected and the cells were analyzed by flow cytometry. After 24 h of culturing, cells were checked for viability by flow cytometry and diluted in prewarmed medium to a concentration of 1 x 10^6 cells/ml.

2.9 Stimulation of human primary immune cells

2.9.1 Anti-CD3/CD28 stimulation of T cells

For functional analysis, non-transfected and transfected human primary $CD4^+$ and $CD8^+$ T cells were stimulated via the CD3 chain of the T-cell receptor and the costimulatory molecule CD28, similar to a protocol described by Hatzelmann and Schudt (Hatzelmann and Schudt, 2001). In general, non-transfected T cells were stimulated on day of isolation, whereas transfected $CD4^+$ T cells were stimulated 24 h past nucleofection. To coat anti-CD3 monoclonal antibodies (Orthoclone OKT-3, Janssen-Cilag) on the surface of 96-well microtiter plates (Microtest tissue culture plate, Falcon, BD Biosciences, San Jose, USA), the plates were incubated for 2.5 h at 37°C, 5% CO_2 with 50 µl of a 6 or 60 µg/ml solution of anti-CD3 in PBS, corresponding to 0.3 or 3 µg anti-CD3/well, respectively. Afterwards, the plates were washed twice with PBS (150 µl/well). Subsequently, 200 µl of cultured cells (2 x 10^5 cells/well) were transferred into the pre-coated plates. Experiments were at least performed as duplicates. For costimulation, 10 µl soluble anti-CD28 mAb (diluted in medium to 6 µg/ml or 60 µg/ml, Immunotech) were added to each well, with the final concentration being ~0.3 µg anti-CD28/ml or ~3 µg anti-CD28/ml, respectively.

Optionally, the PDE4 inhibitor piclamilast (RP73401) and/or the PDE3 inhibitor motapizone were included at a final concentration of ~1 µM and/or ~10 µM, respectively. To achieve the final drug concentrations in the assays at a DMSO concentration of ~0.1% (v/v), stock solutions of piclamilast (10 mM in DMSO) and motapizone (100 mM in DMSO) were diluted 1:50 (v/v) in medium. For the combination of both, piclamilast and motapizone, equal volumes of piclamilast (20 mM) and motapizone (200 mM) were mixed and subsequently diluted

1:50 (v/v) in medium. Immediately after plating of the cells, 10 µl of the PDE inhibitor dilutions were applied. After incubation of the cells at 37°C, 5% CO_2 for 20 min, the costimulatory anti-CD28 mAb was added and the cells were further incubated for several time periods, as indicated (24 h - 72 h).

2.9.2 LPS stimulation of macrophages (MoMϕ) and dendritic cells (MoDCs)

Before use, the LPS stock solution (1 mg/ml, in PBS, 0.1% hydroxylamine) was homogenized in an ultrasonic bath for 30 sec. At day 6 - 8, monocyte-derived macrophages (MoMϕ) were stimulated with 1 µg LPS/ml medium for 22 h. Monocyte-derived dendritic cells (MoDCs) were harvested, counted, and plated on 6-well Costar tissue plates at a density of 5 x 10^5 cells/ml in monocyte medium. Stimulation of dendritic cells was performed with 1 µg LPS/ml medium for 24 - 44 h. After stimulation, cells were washed with PBS, lysed with 350 µl RLT buffer (Qiagen) complemented with 1% 2-mercaptoethanol, and stored at -80°C until RNA isolation (see chapter 2.2).

2.10 Bioinformatics

Averages are presented as mean ± SD. For statistical analysis, student's t-test or one-/two-way analysis of variance (ANOVA), a statistical tool of GraphPad Prism 4.0 (GraphPad Software, San Diego, USA), was used.

3 RESULTS

The aim of the study was to test the hypothesis that not all but individual PDE4 subtypes exert distinct cellular functions in human primary immune cells. For this purpose, at first, the expression profiles of PDE4 subtypes in several human primary immune cells were elucidated.

3.1 Validation of PCR primer and probes

For the quantification of gene expression on mRNA levels, PDE4 subtype-specific primer/probe sets were designed to bind at the 3' end of the open reading frame of each subtype, at positions where individual splice variants of one subtype are identical. By using the TaqMan polymerase chain reaction (PCR) technique from Applied Biosystems, as detailed in *Materials and Methods* in chapter 2.2, the fluorescent-labed probes facilitated the quantitative detection of mRNA expression levels of individual PDE4 subtypes.

In a series of experiments, the primer/probe sets detecting *PDE4A, PDE4B, PDE4C*, and *PDE4D* subtypes were validated. First, to test the specificity of the designed primer/probe sets, initial PCR experiments were performed with plasmids containing conserved C-terminal parts of the subtypes PDE4A, PDE4B, PDE4C, and PDE4D. As shown in Table 7, all tested primer/probe sets showed no cross-reactivity.

Table 7. Cross-reactivity test for PDE4A, PDE4B, PDE4C, and PDE4D primer/probe sets.[a]

Template	PDE4A detection (C_t)	PDE4B detection (C_t)	PDE4C detection (C_t)	PDE4D detection (C_t)
PDE4A	24	>40	>38	>40
PDE4B	>40	23	>40	>40
PDE4C	>40	>40	23	>40
PDE4D	>39	>40	>40	26

[a] Shown are threshold cycles (C_t) at which significant detection in quantitative PCR experiments was measured, as detailed in *Materials and Methods*. 2 ng of plasmids containing conserved C-terminal parts of the subtypes PDE4A, PDE4B, PDE4C, and PDE4D were diluted 1:12500 - 1:250000 and were taken as template for quantitative PCR reactions. The reaction was terminated after 40 cycles. Shown are mean values of three independent experiments.

Next, in order to test the efficiency of PCR reactions, total RNA of the human lung adenocarcinoma epithelial cell line A549 and of human primary $CD4^+$ T cells was reverse transcribed to cDNA, mixed with plasmid DNA, and used as template. For all quantitative PCR experiments in this study, ribosomal *18S rRNA* was used as internal standard of which earlier experiments in the laboratory of the Department of Biochemistry 2 (ALTANA Pharma AG, Konstanz) showed that it is not differentially expressed upon cell stimulation. *18S rRNA*

detection is commonly used to monitor the amount of template in different PCR reactions and is useful for normalization in quantitative PCR experiments (Bas et al., 2004).

At standard concentrations of 200 nM of the FAM-labeled probe, *PDE4A, PDE4C*, and *PDE4D* mRNA detection was optimal with forward and reverse primer concentrations of 900 nM. *PDE4B* detection was most efficient at 300 nM (forward primer) and 600 nM (reverse primer). Using the C_t (threshold cycle) slope method, amplification efficiency values for the primer/probe sets and their capability for duplex reactions (i.e., the combined detection of *18S rRNA* and a target gene within one PCR reaction) were measured. This method is based on the determination of C_t values in dilution series of the template. The primer/probe sets for *18S rRNA* and the respective PDE4 subtype were applied alone (singleplex) and in combination (duplex). The C_t values were plotted versus log cDNA input (Figure 10). Singleplex and duplex reactions of PDE4A (Figure 10*A*), PDE4B (Figure 10*B*), PDE4C (Figure 10*C*), or PDE4D (Figure 10*D*) primer/probe sets resulted in very similar C_t values, respectively. Moreover, linear regression of singleplex and duplex reactions produced similar slopes in all examined PDE4 subtype primer/probe sets.

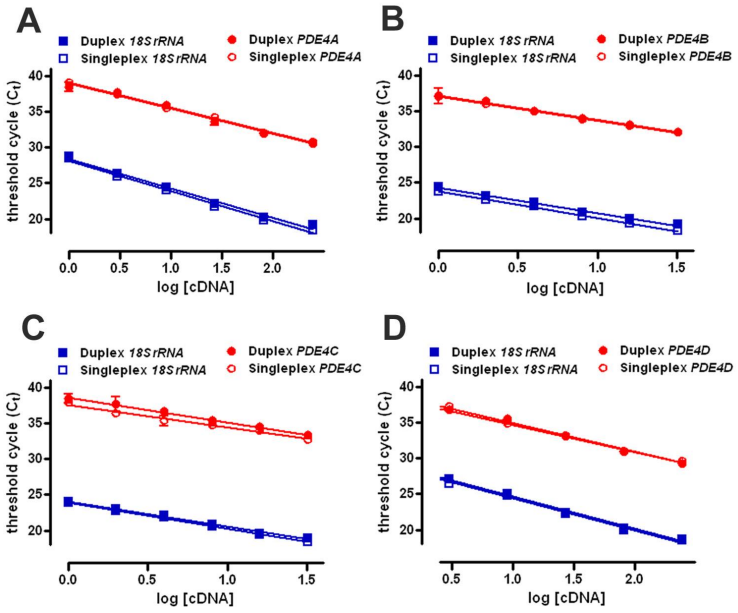

Figure 10. Validation of primer/probe sets for quantitative PCR experiments. Specific primer/probe sets detecting *PDE4A* (*A*), *PDE4B* (*B*), *PDE4C* (*C*), and *PDE4D* (*D*) were tested for their amplification efficiencies in quantitative PCR reactions when applied alone (singleplex reaction) or in combination with a primer/probe set specific for *18S rRNA* (duplex reaction). Dilution series (starting 1 x concentrated) were obtained from a mixed template (A549 cDNA, $CD4^+$ T cell cDNA, and plasmids). 50 nM forward primer, 50 nM reverse primer, and 50 nM VIC-labeled probe were used for the detection of *18S rRNA*. The FAM-labeled probes targeting PDE4 subtypes were applied at 200 nM. Forward and reverse primers for *PDE4A, PDE4C,* and *PDE4D* had the final concentration 900 nM; for *PDE4B* 300 nM (forward primer) and 600 nM (reverse primer). Linear regression was perfomed using a 95% confidence interval.

Amplification efficiencies were calculated using the equation $E = 10^{(-1/slope)} - 1$ (Application note, Applied Biosystems) and were $95 \pm 3\%$ for PDE4A, PDE4B, PDE4C, and PDE4D

primer/probe sets, independent of singleplex or duplex PCR reactions. Considering these validation experiments, the designed primer/probe sets detecting individual PDE4 subtypes were shown to be specific, highly efficient tools to study PDE4 expression levels in duplex reactions.

3.2 Selection of target cells and stimulation conditions

Various human primary immune cells have been linked to the pathophysiology of chronic inflammatory diseases (Tattersfield et al., 2002; Barnes et al., 2003). Because not all of these cells could exhaustively be addressed in the present study, human primary immune cells were chosen for experiments that are well-defined target cells for PDE4 inhibitors. In T cells and monocytes, the efficacy of PDE4 inhibitors is well documented (Torphy, 1998; Souness et al., 2000). $CD4^+$ T helper cells are essential cells in the orchestration of inflammatory cell responses (Tattersfield et al., 2002; Skapenko et al., 2005), can be transfected (Gresch et al., 2004), and were thus primarily used in the present study. However, also $CD8^+$ cytotoxic T cells are attractive target cells for PDE4 inhibitors because of their involvement in allergic responses in the lung (O'Sullivan et al., 2001; Gelfand and Dakhama, 2006) and their implication in the pathogenesis of COPD (Barczyk et al., 2006). Besides, $CD14^+$ monocytes have been shown to have profound pathophysiologic relevance as potent producers of the pro-inflammatory cytokine TNF-α (Beutler and Cerami, 1988; Haveman et al., 1999). All of these cells are available in sufficient amounts from peripheral blood and were used in the present study.
In contrast, it is considerable elaborative and difficult to obtain human primary macrophages or dendritic cells, although these two monocyte-derivatives have fundamental pathophysiological relevance (Banchereau et al., 2000; Barnes, 2004). However, *in vitro* monocyte-derived macrophages (MoMϕ) and dendritic cells (MoDCs) have been used to study the effects of PDE4 inhibition (Gantner et al., 1997a; Gantner et al., 1999). Thus, in the present study, MoMϕ and MoDCs were obtained by differentiating human primary monocytes.

To activate resting T lymphocytes, TCR- and CD28-costimulation was used in order to closely mimic the physiological conditions relevant to human in the experiments (June et al., 1994; Chambers and Allison, 1999; Acuto et al., 2003). Similarly, bacterial lipopolysaccharide (LPS), which is known to be a potent trigger of monocytes, macrophages, and dendritic cells (Haveman et al., 1999; Triantafilou and Triantafilou, 2002; Diks et al., 2004) was used as physiological stimulus for these cells.

3.3 Expression profiling in human primary CD4⁺ T cells

Human primary CD4⁺ T cells were isolated from human whole blood by negative selection using magnetic bead cell separation.

3.3.1 Isolation and stimulation of human primary CD4⁺ T cells

As assessed by flow cytometry, CD4⁺ T cells obtained by negative selection were 94% to 99% pure and showed low CD25 (IL-2 receptor α-chain) expression. Approx. 97% of the cells were viable (Figure 11*A*). In order to represent all cells, no gating was used for flow cytometric analysis.

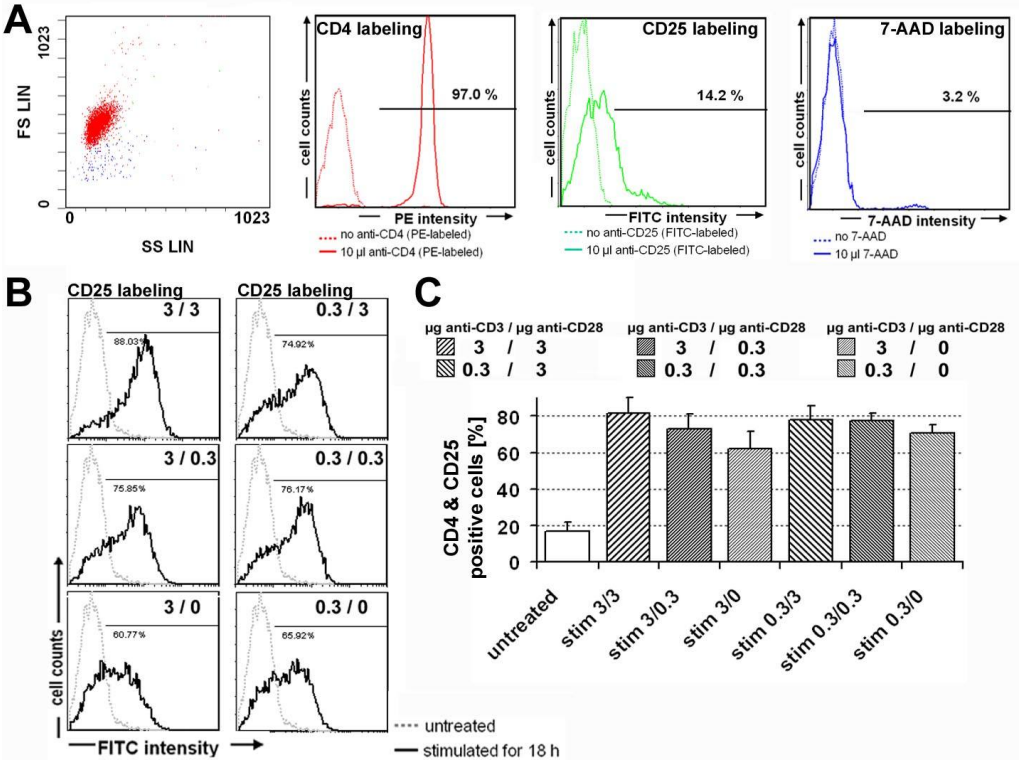

Figure 11. Determination of purity, cell viability, and anti-CD3/CD28 induced upregulation of CD25 surface expression of human primary CD4⁺ T lymphocytes by flow cytometry. *A*, CD4⁺ T cells were isolated by negative selection as described in *Materials and Methods* and were subject for flow cytometric analysis (left panel). Cells were labeled with antibodies specific for CD4 (PE-labeled anti-CD4; second panel from left) or CD25 (FITC-labeled anti-CD25; second panel from right). Additionally, cells were incubated with 7-AAD to determine cell viability (right panel). *B*, After treating the cells for 18 h with 3 µg anti-CD3/well and 3 µg anti-CD28/ml (3/3), with 3 µg anti-CD3/well and 0.3 µg anti-CD28/ml (3/0.3), with 3 µg anti-CD3/well alone (3/0), with 0.3 µg anti-CD3/well and 3 µg anti-CD28/ml (0.3/3), with 0.3 µg anti-CD3/well and 0.3 µg anti-CD28/ml (0.3/0.3), or with 0.3 µg anti-CD3/well alone (0.3/0), labeling was performed using FITC-labeled anti-CD25 antibodies and PE-labeled anti-CD4 antibodies to perform flow cytometric analysis. *C*, Experiments described in *B* were repeated and CD4 and CD25 double positive cells were summarized as mean ± SD of 4 independent experiments.

To mimic physiological conditions of T cell activation, cells were stimulated via the T-cell receptor (by plate-bound anti-CD3 antibodies) and the CD28 coreceptor (by soluble anti-CD28 antibodies). After anti-CD3/CD28 stimulation, T cells showed an upregulation of the surface expression marker CD25 within 18 h when compared to untreated $CD4^+$ T cells (Figure 11*B*). To obtain a comprehensive overview of anti-CD3/CD28 induced CD25-upregulation, $CD4^+$ T cells were activated with 3 µg anti-CD3/well and 3 µg anti-CD28/ml (= 3/3 stimulation), with 3 µg anti-CD3/well and 0.3 µg anti-CD28/ml (= 3/0.3 stimulation), or with 3 µg anti-CD3/well alone (= 3/0 stimulation). Additionally, the different anti-CD28 concentrations were used combined with a fixed concentration of 0.3 µg anti-CD3/well. As summarized in Figure 11*C*, the highest stimulation condition (= 3/3 stimulation) resulted in the highest number of CD25-upregulated CD4 cells (mean of double positive cells ± SD = 82 ± 9%), which was diminished by lowering the costimulatory anti-CD28 signal. The pronounced upregulation of CD25 on the cell surface measured by flow cytometry was used as stimulation control in further studies.

Phenotypically, the purity and viability of human primary $CD4^+$ T cells were assessed by microscopy. Untreated cells did not adhere to the bottom of the plate and were homogeneous in size (Figure 12*A*). After stimulation with anti-CD3/CD28, $CD4^+$ T cells gained in size and formed characteristic colonies (Figure 12*B* and *C*).

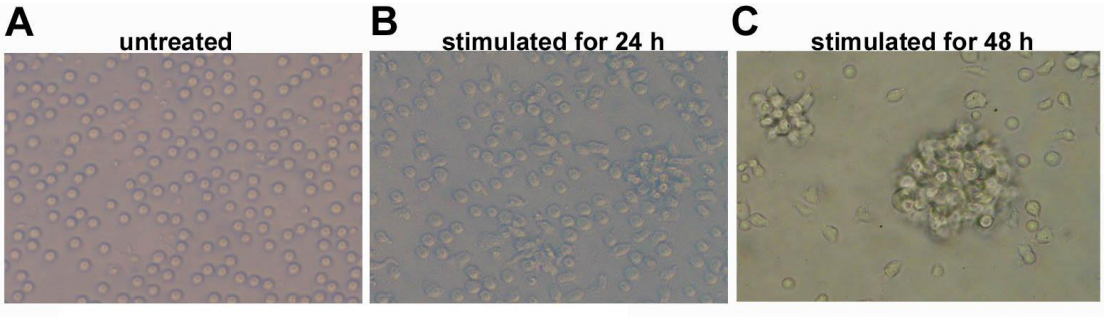

Figure 12. Phenotypical characterization of untreated and anti-CD3/CD28 stimulated human primary $CD4^+$ T lymphocytes by light microscopy. $CD4^+$ T cells were isolated by negative selection as described in *Materials and Methods* and were cultured in suspension. *A*, Shown are untreated cells after isolation. *B*, Cells were stimulated for 24 h with 3 µg anti-CD3/well in combination with 3 µg anti-CD28/ml. *C,* Cells were treated as in *B*, but stimulated for 48 h. Original magnification x 400 (Axiovert 25 inverse microscope).

3.3.2 PDE4 subtype mRNA expression and regulation in human primary $CD4^+$ T cells

First, the expression levels of the four PDE4 subtypes in untreated $CD4^+$ T cells were assessed. Because all PDE4 subtype primer/probe sets showed similar maximal efficiencies in standardized PCR reactions (see chapter 3.1), the PDE4 expression patterns were directly compared relative to the expression of *PDE4A* (Figure 13*A*). In untreated cells, the mRNA expression of the PDE4 subtypes *PDE4A*, *PDE4B,* and *PDE4D* was detected. The highest mRNA expression level was found for *PDE4D* (~12-fold higher than *PDE4A*), followed by *PDE4B* (~8-fold higher than *PDE4A*) and *PDE4A* (set 1 as reference). Although efficacy of the

PDE4C primer/probe set was shown in control experiments, no expression of *PDE4C* was detected in CD4$^+$ cells, regardless of whether the cells were stimulated or not.

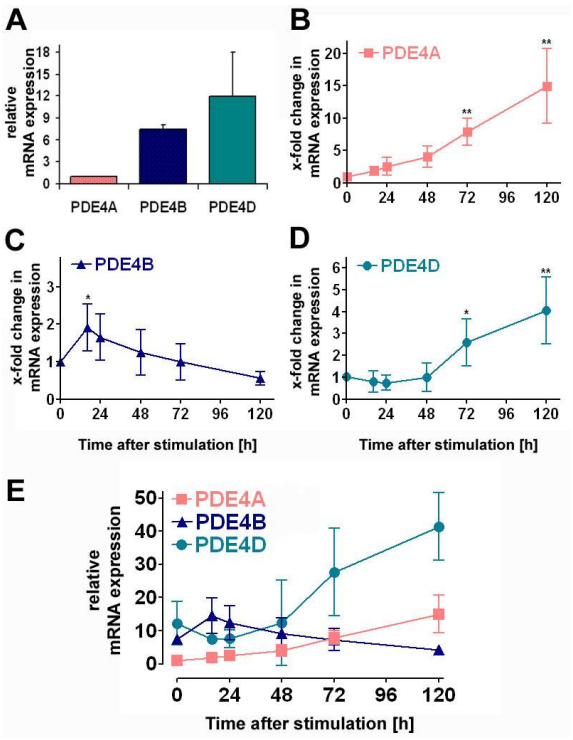

Figure 13. *PDE4A*, *PDE4B*, and *PDE4D* mRNA expression in untreated and anti-CD3/CD28 stimulated human primary CD4$^+$ T lymphocytes. Cells were separated from whole blood as described in *Materials and Methods* and were subject for total RNA isolation and cDNA transcription. Quantitative PCR was performed using ribosomal *18S rRNA* as internal standard (detected after 10 - 13 cycles) and specific primer/probe sets for *PDE4A*, *PDE4B*, *PDE4C*, or *PDE4D*. By comparing ΔC_t values, the expression levels of individual PDE4 subtypes were directly compared relative to *PDE4A*, which was detected after 27 - 30 cycles (mean ΔC_t of *PDE4A* ± SD = 16.7 ± 0.5) (*A*). After stimulation with 3 µg anti-CD3/well and 3 µg anti-CD28/ml, time-dependent mRNA expression for *PDE4A* (*B*), *PDE4B* (*C*), and *PDE4D* (*D*) was measured relative to untreated conditions (t = 0 h). *E,* The quantitative mRNA expression levels of *PDE4A*, *PDE4B,* and *PDE4D* in untreated cells (shown in *A*) were combined with the respective time courses (shown in *B-D*) to get a comprehensive picture of the PDE4 subtype expression after T cell stimulation. All data were expressed relative to the *PDE4A* expression level in untreated cells (t = 0 h). Thereby, the complete quantitative mRNA expression pattern of the PDE4 subtypes was obtained. *PDE4C* transcripts were not detected after 40 cycles. Results are expressed as mean ± SD of 4 donors. Significance of differences is indicated: *, $p < 0.05$; **, $p < 0.01$; *B*, *C*, *D*, compared to untreated cells (t = 0 h).

To ascertain whether the PDE4 subtypes are differentially expressed upon stimulation, human primary CD4$^+$ T cells were stimulated with anti-CD3/CD28 for different periods of time. For each gene, the expression in untreated cells (time point 0 h) was used as reference point. Upon stimulation, *PDE4A* mRNA was steadily upregulated and had a ~15-fold higher expression after 120 h (Figure 13*B*). *PDE4B* mRNA was upregulated ~2-fold within the first 16 h, returned to basal level after 48 h and further decreased during the time course, indicating a transient upregulation of this subtype (Figure 13*C*). *PDE4D* mRNA expression slightly decreased within the first 24 h after stimulation, but was then steadily upregulated and reached a ~4-fold higher expression after 120 h, indicating a long-term upregulation of this subtype

(Figure 13*D*). To obtain an overall picture of the PDE4 subtype expression after T cell stimulation, the different expression levels shown in Figure 13*A* were combined with the time courses of each individual subtype shown in Figure 13*B-D*, using the expression level of *PDE4A* in untreated cells as reference for all other data points (Figure 13*E*). Due to the considerably high *PDE4B* mRNA expression levels in untreated $CD4^+$ T cells, the ~2-fold upregulation after 16 h stimulation led to the predominant expression of this subtype at 16 h and 24 h. From 48 h onwards, the induction of *PDE4D* and the decrease of *PDE4B* resulted in *PDE4D* being the predominant subtype. *PDE4A* mRNA displayed the lowest expression level up to 48 h after stimulation. Due to the steady upregulation of this subtype and the downregulation of *PDE4B* mRNA at later time points, the expression level of *PDE4A* mRNA exceeded that of *PDE4B* mRNA at 120 h but still did not reach the high expression level of *PDE4D* mRNA.

3.3.3 Regulation of PDE4 subtypes after stimulation with different anti-CD3/CD28 ratios

To examine whether the distinct regulation of individual PDE4 mRNA levels is dependent on the anti-CD3:anti-CD28 ratio and subsequently on the costimulatory anti-CD28 stimulus, $CD4^+$ T cells were activated with different concentrations of anti-CD3 and anti-CD28 (Figure 14).

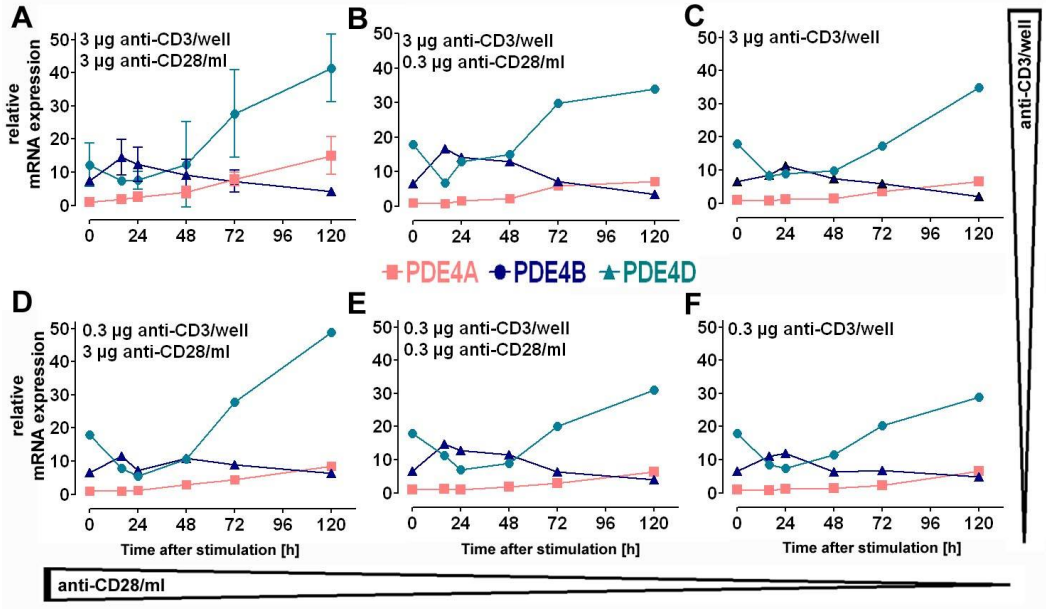

Figure 14. Time-dependent mRNA expression profiles of PDE4 subtypes in $CD4^+$ T cells after activation by different stimulation conditions. As detailed in the legend of Figure 13, complete quantitative mRNA expression patterns of the PDE4 subtypes were obtained relative to the expression of *PDE4A* in untreated cells (t = 0 h). *A*, Cells stimulated with 3 µg anti-CD3/well and 3 µg anti-CD28/ml (identical with Figure 13*E*, repeated here for easier comparison with other stimulation conditions). The same sets of experiments were performed for cells stimulated with 3 µg anti-CD3/well and 0.3 µg anti-CD28/ml (*B*), with 3 µg anti-CD3/well alone (*C*), with 0.3 µg anti-CD3/well and 3 µg anti-CD28/ml (*D*), with 0.3 µg anti-CD3/well and 0.3 µg anti-CD28/ml (*E*), or with 0.3 µg anti-CD3/well alone (*F*). Results in *A* are expressed as mean ± SD of 4 donors. Results in *B*, *C*, *D, E,* and *F* are the average of 2 donors.

Human primary CD4$^+$ T cells were treated with 3 µg anti-CD3/well and 3 µg anti-CD28/ml (Figure 14*A*, identical with Figure 13*E*), with 3 µg anti-CD3/well and 0.3 µg anti-CD28/ml (Figure 14*B*), with 3 µg anti-CD3/well alone (Figure 14*C*), with 0.3 µg anti-CD3/well and 3 µg anti-CD28/ml (Figure 14*D*), with 0.3 µg anti-CD3/well and 0.3 µg anti-CD28/ml (Figure 14*E*), or with 0.3 µg anti-CD3/well alone (Figure 14*F*). All conditions resulted in similar time-dependent expression patterns as were found for the strong stimulation with 3 µg anti-CD3/well in combination with 3 µg anti-CD28/ml shown in Figure 14*A,* hereby confirming the long-term induction of *PDE4A* and *PDE4D* and the transient upregulation of *PDE4B*. For all further experiments related to PDE4 subtype expression, either on mRNA or on protein level, this latter stimulation condition was used.

3.3.4 Regulation of PDE4 subtypes in human primary naïve and memory CD4$^+$ T cells

Since CD4$^+$ T cells isolated from human whole blood still represent a rather heterogeneous population of cells, different subpopulations of CD4$^+$ cells may regulate the PDE4 subtype expression specifically. Therefore, the expression patterns were studied separately in naïve CD4$^+$ T cells characterized by the surface marker CD45RA and in memory CD4$^+$ T cells expressing the marker CD45RO (Bell et al., 1998). Due to the isolation strategy (see *Materials and Methods*), CD45RA$^+$CD4$^+$ T cells were >95% pure and CD45RO$^+$CD4$^+$ T cells were >98% pure, whereas cells co-expressing CD4, CD45RA, and CD45RO were sorted out.
In untreated naïve CD4$^+$ T cells, slightly lower levels of *PDE4A*, *PDE4B,* and *PDE4D* transcripts were found compared to untreated memory CD4$^+$ T cells (Figure 15*A*-*C*).

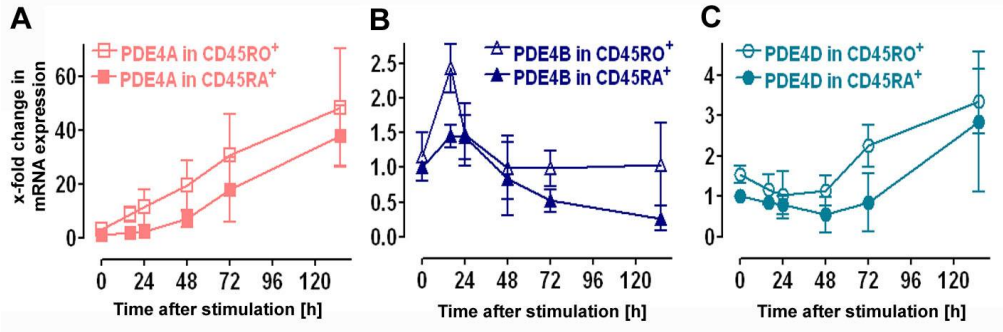

Figure 15. mRNA expression profiles of PDE4 subtypes in CD45RA$^+$ (naïve) and CD45RO$^+$ (memory) human primary CD4$^+$ T lymphocytes. CD4$^+$ cells were further purified by negative selection using either anti-CD45RA or anti-CD45RO microbeads. Cells were stimulated with 3 µg anti-CD3/well and 3 µg anti-CD28/ml for different periods of time. Subsequent experiments were performed as outlined in the legend of Figure 13. Expression profiles of *PDE4A* (*A*), *PDE4B* (*B*), and *PDE4D* (*C*) mRNA from both T cell subpopulations are shown. Results are expressed relative to untreated conditions in naïve T cells (t = 0 h), as mean ± SD of 4 donors. Differences between naïve and memory cells were statistically not significant.

After anti-CD3/CD28 stimulation, memory CD4$^+$ T cells showed a faster upregulation of *PDE4A* (Figure 15*A*) and *PDE4D* (Figure 15*C*) mRNA, as well as a more pronounced transient

upregulation of *PDE4B* mRNA (Figure 15*B*) compared to naïve $CD4^+$ T cells. However, these differences in the regulation of individual PDE4 subtypes between naïve and memory $CD4^+$ T cells were statistically not significant. Because the expression profiles of PDE4 subtypes both in naïve and memory $CD4^+$ T cells were found to be very similar, all following experiments were performed with $CD4^+$ cells that were not further separated.

3.3.5 PDE4 activity in human primary $CD4^+$ T cells

Changes in mRNA levels do not necessarily result in changes of the respective protein levels. Therefore, it was investigated whether the induction of PDE4 subtypes observed in quantitative PCR experiments translates in an increase in PDE4 enzyme activity. Upon stimulation, total cAMP-hydrolizing PDE activity (mean ± SD = 37 ± 16 pmol/min/mg in resting cells) was augmented in a time-dependent manner (Figure 16*A*), resulting in a significant higher activity 72 h and 120 h after stimulation. This increase was mainly due to an increase in PDE4 activity, whereas PDE4-independent enzyme activity initially decreased 24 h after stimulation and recovered to baseline levels during the time period studied.

To ascertain which PDE4 subtypes contribute to this upregulation, an immunoprecipitation strategy was applied with antibodies specific for PDE4A, PDE4B, or PDE4D. After precipitation, the samples were assayed for PDE4 cAMP hydrolyzing activity. In untreated $CD4^+$ T cells (time point 0 h in Figure 16*B*), the highest activity was measured in samples precipitated with the PDE4D-specific antibody. Whereas PDE4B activity was somewhat lower than PDE4D activity, PDE4A contributed least to the total PDE4 activity. However, after anti-CD3/CD28 stimulation, PDE4A activity was greatly induced starting at 72 h and reached a 4-fold higher activity at the end of the time period examined (Figure 16*B*). PDE4B activity was transiently upregulated, peaking with a 3.4-fold higher activity at 24 h followed by a decrease. After 120 h, PDE4B activity was similar to the level observed in untreated cells. At this time point, PDE4A activity exceeded the PDE4B activity. Compared to untreated cells, PDE4D activity remained relatively constant during the first 48 h after stimulation, and increased at 72 h and 120 h after stimulation totaling in a 1.5-fold upregulation.
Taken together, the pattern of PDE4 subtype-specific enzyme activities qualitatively closely resembled the mRNA expression profile reported in chapter 3.3.2.

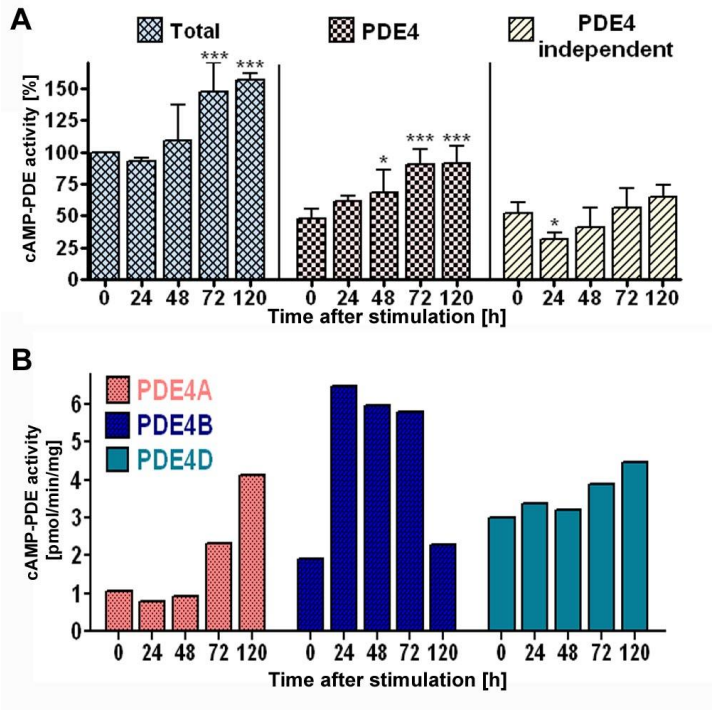

Figure 16. cAMP hydrolizing phosphodiesterase activity in untreated and anti-CD3/CD28 stimulated human primary CD4$^+$ T lymphocytes. Cells were stimulated with 3 µg anti-CD3/well and 3 µg anti-CD28/ml for different periods of time. *A,* Total cAMP-PDE hydrolyzing activity and PDE4 inhibitor-insensitive PDE activity (= PDE4 independent) in T cell lysates were measured as detailed in *Materials and Methods*. PDE4 activity was determined by subtracting the PDE4 independent activity from the total activity. Data are expressed as mean ± SD of 3-5 donors. *, $p < 0.05$; ***, $p < 0.001$ (compared to untreated cells, t = 0 h). *B*, Cell lysates were immunoprecipitated with Abs recognizing PDE4A (AC55), PDE4B (K118), or PDE4D (m3S1). The PDE activity recovered in the immunoprecipitated pellet was measured as detailed in *Materials and Methods*. Shown is one representative experiment out of three. For the experiment shown, CD4$^+$ cells of three donors were independently stimulated, but pooled for lysis and immunoprecipitation.

3.3.6 Immunodetection of PDE4 subtypes in human primary CD4$^+$ T cells

To elucidate which splice variants are expressed in untreated CD4$^+$ T lymphocytes and may account for the measured changes in mRNA levels and protein activities after stimulation, antibodies recognizing the conserved C-termini of the PDE4 subtypes were used to perform immunoblotting experiments (Figure 17*A* and *B*). These experiments were performed in cooperation with Dr. H. Tenor and B. Burgbacher (Department of Biochemistry 2, ALTANA Pharma AG, Konstanz).

In untreated T cells, a polyclonal antibody directed against PDE4A detected immunoreactivity at ~130 kDa and, with a very low density, below 100 kDa, which can be attributed to long (PDE4A4, PDE4A10, and/or PDE4A11) and short (PDE4A1) PDE4A forms, respectively. Contrary to the mRNA and enzyme activity measurements, the intensity of the immunodetected signals did not increase with time after stimulation with anti-CD3/CD28. A polyclonal antibody directed against PDE4B gave rise to two predominant bands. One band migrated slightly above 100 kDa and might be attributed to PDE4B long forms (PDE4B1 and/or

PDE4B3). The high immunoreactivity in untreated cells decreased after stimulation during the examined time period (0 h - 120 h). The other band, migrating at ~75 kDa (might be attributed to PDE4B2), was also present in untreated cells, but was strongly induced, peaking 24 h - 48 h after stimulation. At later time points, a reduction of this band was observed. Considering the transient induction of the subtype PDE4B measured by PCR and activity assays, the immunodetected downregulation of long PDE4B splice variants is compensated by a pronounced upregulation of the short splice variant and may result in a net upregulation between 24 h and 48 h after stimulation. A polyclonal antibody directed against PDE4D detected several bands of different molecular weights. One set of bands was in the range of ~60 - 75 kDa and likely corresponds to the short forms PDE4D6 (~59 kDa), PDE4D2 (~68 kDa), and PDE4D1 (~72 kDa). These short forms were upregulated in a time-dependent manner, with the middle band, assumingly PDE4D2, showing the most pronounced upregulation. The other set of bands was above ~85 kDa and may be the long splice variants of PDE4D (PDE4D3, PDE4D4, PDE4D5, PDE4D7, PDE4D8, and/or PDE4D9). These bands showed low immunoreactivites that were not, or only slightly, changed after stimulation. The unchanged immunodetection of β-Actin as loading control confirmed that the observed regulation of PDE4 subtypes was not due to different amounts of protein loaded onto the gel.

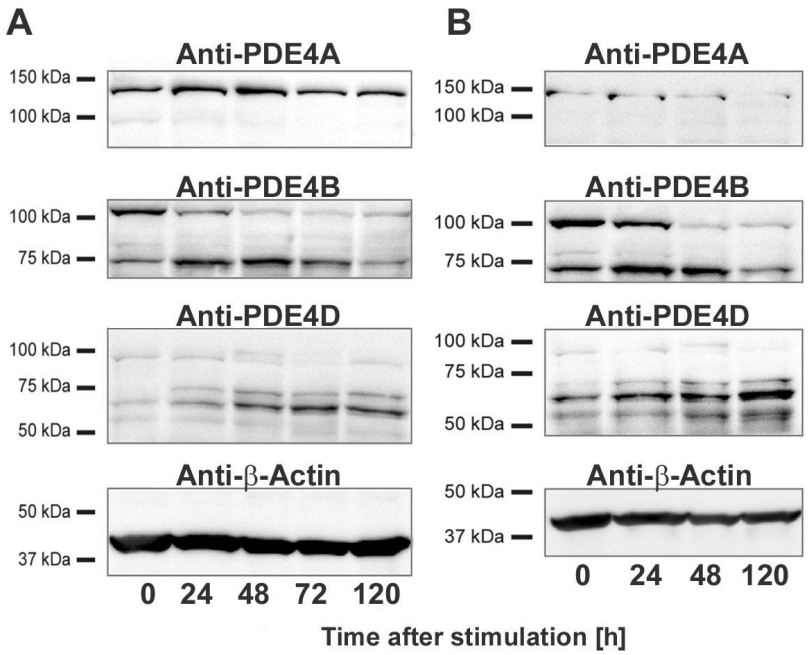

Figure 17. Detection of PDE4 splice variants in untreated and anti-CD3/CD28 stimulated human primary CD4$^+$ T lymphocytes by immunoblotting. Cells were stimulated with 3 µg anti-CD3/well and 3 µg anti-CD28/ml for different periods of time. Cells were lysed and 50 µg protein of the 1000 x g supernatant were separated by SDS-polyacrylamide gel electrophoresis. Immunodetection was performed using antibodies recognizing PDE4A, PDE4B, or PDE4D. β-Actin was used as loading control. Shown are two independent experiments (*A, B*), each with cells from three donors that have been independently stimulated, but pooled for lysis and immunoblotting.

3.4 Expression profiling in CD8⁺ T cells, monocytes, and monocyte-derived cells

3.4.1 PDE4 subtype mRNA expression and regulation in CD8⁺ T cells

As assessed by flow cytometry, CD8⁺ T cells isolated by negative selection were obtained 94 ± 2% (mean ± SD) pure (Figure 18).

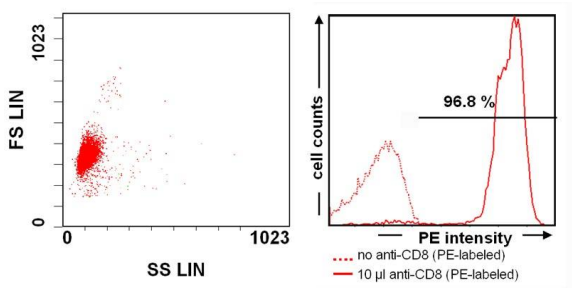

Figure 18. Determination of purity of human primary CD8⁺ T lymphocytes by flow cytometry. CD8⁺ T cells were isolated by negative selection as described in *Materials and Methods* and were subject for flow cytometric analysis (left panel). In order to represent all cells, no gating was used. For further analysis, cells were labeled with antibodies specific for CD8 (PE-labeled anti-CD8; right panel).

In unstimulated CD8⁺ T cells, the mRNA expression of the PDE4 subtypes *PDE4A*, *PDE4B,* and *PDE4D* was detected, whereas no expression of *PDE4C* was found. As specified in chapter 3.3.2 for CD4⁺ T cells, the PDE4 expression profile in untreated CD8⁺ T cells was directly compared relative to the expression of *PDE4A.* Both *PDE4B* mRNA and *PDE4D* mRNA were expressed ~10-fold higher than *PDE4A* mRNA, which was set 1 as reference (Figure 19*A*).

As detailed for the stimulation of CD4⁺ T cells (see chapter 3.3.2), human primary CD8⁺ T cells were stimulated via the T-cell receptor and the CD28 coreceptor for different periods of time. The mRNA expression in unstimulated cells (time point 0 h) was used as reference point for each PDE4 subtype. Anti-CD3/CD28 stimulation induced the steady upregulation of *PDE4A* mRNA, which had a ~12-fold higher expression at the end of the examined time period (84 h, Figure 19*B*). In contrast, *PDE4B* mRNA was upregulated ~2.4-fold within the first 16 h, but returned to basal level after 48 h, indicating a transient upregulation of this subtype (Figure 19*C*). *PDE4D* mRNA expression slightly increased within the first 16 h after stimulation, returned to basal level after 24 h, but was upregulated ~2.2-fold at 84 h, indicating a long-term upregulation of this subtype (Figure 19*D*). To get a comprehensive depiction of the PDE4 subtype expression after T cell stimulation, the expression levels in untreated cells shown in Figure 19*A* were combined with the time courses of each individual subtype shown in Figure 19*B-D* and were summarized in one diagram (Figure 19*E*). Because *PDE4B* mRNA expression was considerably high in untreated CD8⁺ T cells, the ~2-fold upregulation after 16 h

stimulation led to the predominant expression of this subtype at 16 h and 24 h. However, from 48 h onwards, the induction of *PDE4D* and the decrease of *PDE4B* resulted in *PDE4D* being the predominant subtype. Because of the low expression level of *PDE4A* in untreated cells, the steady upregulation of *PDE4A* after stimulation could not overpass the *PDE4D* level, but was similar to the *PDE4B* level after 48 h.

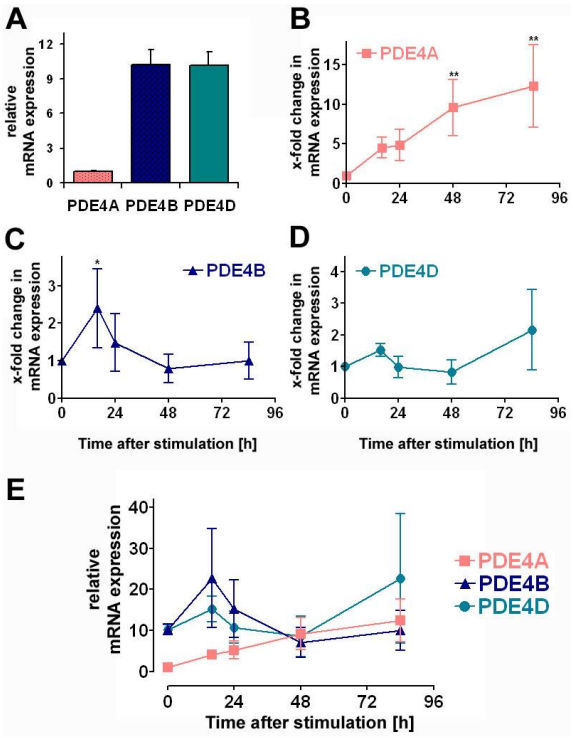

Figure 19. *PDE4A*, *PDE4B*, and *PDE4D* mRNA expression in untreated and anti-CD3/CD28 stimulated human primary CD8$^+$ T lymphocytes. Cells were separated from whole blood as described in *Materials and Methods.* Subsequent steps were performed as outlined in the legend of Figure 13. 18*S rRNA* was detected after 10 - 13 cycles. By comparing ΔC_t values, the expression levels of individual PDE4 subtypes were directly compared relative to *PDE4A* (mean ΔC_t of *PDE4A* ± SD = 15.2 ± 0.6) (*A*). After stimulation with 3 µg anti-CD3/well and 3 µg anti-CD28/ml, time-dependent mRNA expression for *PDE4A* (*B*), *PDE4B* (*C*), and *PDE4D* (*D*) was measured relative to untreated conditions (t = 0 h). *PDE4C* transcripts were not detected after 40 cycles. The quantitative mRNA expression levels of *PDE4A*, *PDE4B,* and *PDE4D* in untreated cells (shown in *A*) were combined with the respective time courses (shown in *B-D*) and were expressed relative to the *PDE4A* expression level in untreated cells (t = 0 h) (*E*). Results are expressed as mean ± SD of 4 donors. Significance of differences is indicated: *, $p < 0.05$; **, $p < 0.01$; *B*, *C*, *D*, compared to untreated cells (t = 0 h).

3.4.2 PDE4 subtype mRNA expression in monocytes, MoMϕ, and MoDCs

As assessed by flow cytometry, CD14$^+$ monocytes isolated by negative selection were obtained 89 ± 4% (mean ± SD) pure (Figure 20). CD14$^+$ cells isolated by positive selection were obtained 93 ± 2% pure. To increase the purity of monocytes for further downstream applications (e.g. mRNA isolation for quantitative PCR experiments or differentiation of

monocytes to monocyte-derived macrophages and dendritic cells), an adherence step was performed after isolation for 1.5 h and non-adherent cells were removed.

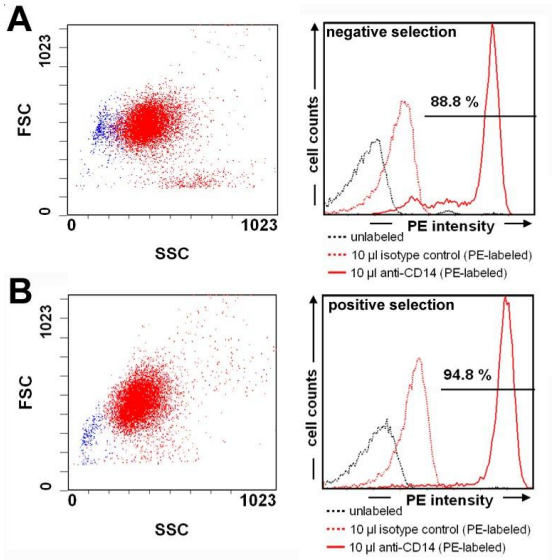

Figure 20. Determination of purity in human primary CD14$^+$ monocytes by flow cytometry. *A*, CD14$^+$ cells were isolated by negative selection as described in *Materials and Methods* and were subject for flow cytometric analysis (left panel). In order to represent all cells, no gating was used. For further analysis, cells were labeled with non-specific antibodies (PE-labeled isotype control) or antibodies specific for CD14 (PE-labeled anti-CD14; right panel). *B*, The same experiments were performed as in *A*, however, cells were isolated by positive selection as described in *Materials and Methods.*

In untreated CD14$^+$ monocytes, the mRNA expression of the PDE4 subtypes *PDE4A*, *PDE4B,* and *PDE4D* was detected (Figure 21*A*). As detailed in chapter 3.3.2 for CD4$^+$ T cells, the PDE4 expression patterns of freshly isolated CD14$^+$ cells were directly compared relative to the expression of *PDE4A* mRNA. In contrast to CD4$^+$ and CD8$^+$ T cells, the highest mRNA expression level in monocytes was found for *PDE4B* (~2.8-fold higher than *PDE4A*), followed by *PDE4A* (set 1 as reference) and *PDE4D* (~20-fold lower than *PDE4A*). No expression of *PDE4C* was detected in CD14$^+$ monocytes.

Upon culturing of CD14$^+$ monocytes in macrophage medium complemented with human AB serum (see *Materials and Methods*), the cells differentiated and developed a macrophage-like phenotype (e.g. strong adherence, increased size, and higher granularity) within 6 - 8 days (Figure 21*B*). In these monocyte-derived macrophages (MoMϕ), the expression levels of PDE4 subtypes dramatically changed compared to freshly isolated monocytes. The PDE4 expression profile in MoMϕ was compared relative to the expression of *PDE4A* mRNA in these cells, with *PDE4A* (set 1 as reference) being the predominant subtype, followed by a ~50-fold lower expression level of *PDE4D* mRNA and even a lower expression level of *PDE4B* mRNA (Figure 21*B*).

Similar to the differentiation of monocytes to macrophages, the differentiation of monocytes to monocyte-derived dendritic cells (MoDCs) by culturing $CD14^+$ cells in medium supplemented with GM-CSF and IL-4 (see *Materials and Methods*) for 7 - 9 days resulted in a change of the phenotype of the cells (Figure 21*C*). In these MoDCs, the expression profile of PDE4 subtypes differed from the expression profile examined in freshly isolated monocytes, but was similar to the expression levels found in MoMϕ. *PDE4A* mRNA (set 1 as reference) was the predominant subtype, followed by a ~30-fold lower expression level of *PDE4B* mRNA and a ~50-fold lower expression level of *PDE4D* mRNA (Figure 21*C*). Remarkably, the *PDE4A* mRNA expression level did not change markedly between monocytes, MoMϕ, and MoDCs.

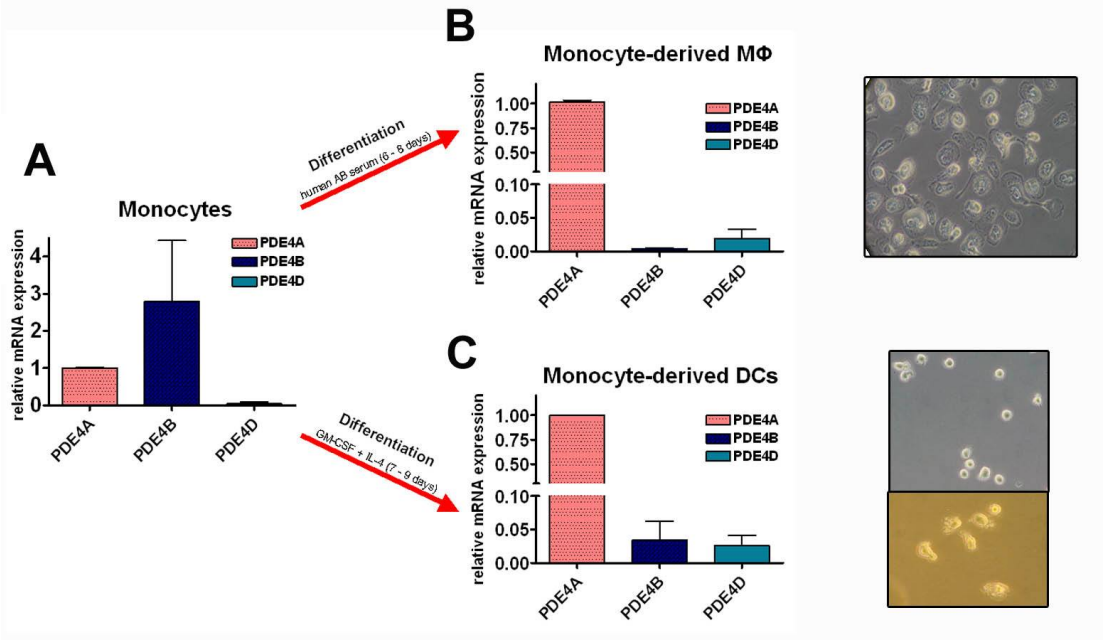

Figure 21. *PDE4A*, *PDE4B*, and *PDE4D* mRNA expression in untreated human primary monocytes, monocyte-derived macrophages (MoMϕ), and monocyte-derived dendritic cells (MoDCs). *A,* $CD14^+$ cells were separated from whole blood as described in *Materials and Methods* and were subject for total RNA isolation and cDNA transcription, as detailed in the legend of Figure 13. 18*S rRNA* was detected after 10 - 13 cycles. The mRNA expression level of individual PDE4 subtypes was directly compared relative to *PDE4A* (set 1 as reference), which was detected after 23 - 26 cycles (mean ΔC_t of *PDE4A* ± SD = 13.1 ± 1.3). *B*, Experiments were performed as described in *A*, however, human primary $CD14^+$ monocytes were differentiated for 6 - 8 days to monocyte-derived macrophages (MoMϕ). *PDE4A* mRNA expression in MoMϕ was set 1 as reference (mean ΔC_t of *PDE4A* ± SD = 12.6 ± 2.4). After differentiation, the phenotype was determined by light microscopy (original magnification x 400, Axiovert 25 inverse microscope). *C*, Experiments were performed as described in *A*, however, human primary $CD14^+$ monocytes were differentiated for 7 - 9 days to monocyte-derived dendritic cells (MoDCs). *PDE4A* mRNA expression in MoDCs was set 1 as reference (mean ΔC_t of *PDE4A* ± SD = 12.3 ± 1.4). After differentiation, the phenotype was determined by light microscopy (original magnification x 400, Axiovert 25 inverse microscope). In all experiments, *PDE4C* transcripts were not detected after 40 cycles. Results are expressed as mean ± SD of 5 donors.

3.4.3 PDE4 subtype mRNA regulation after LPS stimulation in MoMϕ and MoDCs

To ascertain whether PDE4 subtypes are differentially regulated in monocyte-derived macrophages (MoMϕ) and monocyte-derived dendritic cells (MoDCs) after stimulation,

physiological conditions of cell activation via CD14 binding and toll-like receptor 4 (TLR4) signaling were mimicked by the application of 1 µg LPS/ml medium. PDE4 subtype mRNA expression levels in MoMϕ stimulated for 22 h with LPS were compared to the corresponding PDE4 subtype expression level in MoMϕ that were not treated with LPS. LPS-stimulation resulted in slight changes of *PDE4A* and *PDE4D* mRNA levels that were not significant, but in a significant increase of *PDE4B* expression (~160-fold upregulation) (Figure 22*A*).

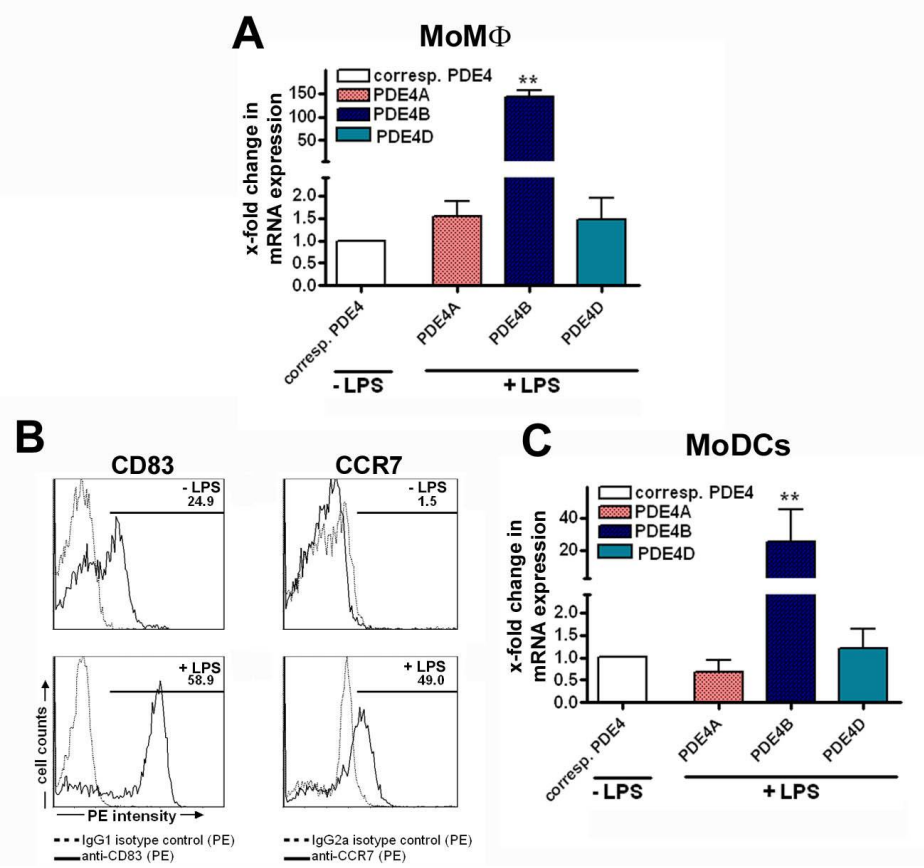

Figure 22. *PDE4A*, *PDE4B*, and *PDE4D* mRNA expression in monocyte-derived macrophages (MoMϕ) and monocyte-derived dendritic cells (MoDCs) after LPS stimulation. *In vitro* generated MoMϕ and MoDCs were obtained as detailed in the legend of Figure 21. *A*, After 7 - 9 days of culturing, MoMϕ were stimulated with 1 µg LPS/ml for 22 h and the mRNA expression levels of PDE4 subtypes were assessed as described in the legend of Figure 13. Results are expressed relative to the corresponding PDE4 subtype in MoMϕ not treated with LPS as mean ± SD of three donors. Significance of differences is indicated: **, $p < 0.01$; compared to cells not treated with LPS (- LPS, set 1 as reference). *B*, After 7 - 9 days of culturing, MoDCs were labeled with isotype controls or antibodies specific for CD83 (PE-labeled anti-CD83) or CCR7 (PE-labeled anti-CCR7) before and after LPS stimulation (1 µg LPS/ml for 44 h). *C*, MoDCs were treated as described in *A*, however, LPS stimulation was performed for 24 - 44 h. Results are expressed relative to the corresponding PDE4 subtype in MoDCs not treated with LPS as mean ± SD of five donors. Significance of differences is indicated: **, $p < 0.01$; compared to cells not treated with LPS (- LPS, set 1 as reference).

In monocyte-derived dendritic cells (MoDCs), staining of the surface markers CD83 and CCR7, respectively, and subsequent cytometric analysis assessed the differentiation process of MoDCs before and after LPS stimulation. To analyze the entire cultured population, no gating

was used for flow cytometry. Staining with PE-labeled anti-CD83 antibodies revealed that ~25% of 7 days old MoDCs had a PE intensity above the fluorescent level of the unspecific isotype control (Figure 22*B*, upper left panel), pointing to a low surface expression of CD83. After LPS stimulation, CD83 surface expression was upregulated, with ~59% of the cells being CD83-positive 44 h after stimulation (Figure 22*B*, lower left panel). Considering CCR7 expression, the same PE-fluorescent intensities of both the unspecific isotype control and the anti-CCR7 antibody indicated that the cells did not express CCR7 on the cell surface 7 days after culturing (Figure 22*B*, upper right panel). However, after 44 h of LPS stimulation, ~49% of the cells were CCR7-positive, indicating a pronounced upregulation of CCR7 surface expression after LPS treatment (Figure 22*B*, lower right panel). LPS stimulation affected the PDE4 subtype mRNA expression in MoDCs differently: Whereas *PDE4B* mRNA expression was significantly upregulated (~25-fold) after LPS stimulation, *PDE4A* and *PDE4D* mRNA levels were largely unaffected compared to the expression level of the corresponding PDE4 mRNA subtypes in cells not treated with LPS (Figure 22*C*).

3.5 Validation of PDE4 subtype-specific knockdown tools in A549

As detailed in chapters 3.3 and 3.4, PDE4 subtypes are differently expressed and differentially regulated in diverse human primary immune cells, suggesting a critical role of PDE4 subtypes for the attenuation of inhibitory cAMP signals and for the promotion of inflammatory cell responses. Indeed, the anti-inflammatory and immunomodulatory effects of PDE4 inhibition on a broad range of inflammatory and immunocompetent cells is well known (Torphy, 1998; Souness et al., 2000). However, current PDE4 inhibitors do not discriminate between individual PDE4 subtypes although several findings, primarily obtained in knockout mice, indicate that distinct PDE4 subtypes can have distinct functional relevance in mediating cellular functions. In the present study, to ascertain the functional impact of PDE4 subtypes in human cellular settings but due to the lack of subtype-specific inhibitors, two knockdown strategies were chosen as approach to specifically suppress the different PDE4 subtypes. Both an antisense (AS)- and a small interfering RNA (siRNA)-mediated PDE4 subtype knockdown strategy were tested for tolerability and efficiacy. These two techniques are widely used to induce mRNA and protein knockdown in various cellular contexts (Giles et al., 1995a; Micklefield, 2001; Dias and Stein, 2002; Dykxhoorn et al., 2003; Hannon and Rossi, 2004; Sioud, 2004). Because human primary immune cells are hard-to-transfect, have a comparatively high donor-dependent variability, and are technically more complex to handle, initial knockdown experiments were performed in the human lung adenocarcinoma epithelial cell line A549. This cell line is available in large amounts, has high PDE4 activity (mean $\pm$ SD = 51 $\pm$ 14 pmol/min/mg in untreated cells), is easy-to-transfect, and was expected to have stable readouts. Initial

experiments revealed that A549 expresses high levels of *PDE4D* mRNA (~12-fold higher than *PDE4A*), followed by *PDE4B* mRNA (~2-fold higher than *PDE4A*) and *PDE4A* mRNA (set 1 as reference). *PDE4A* was detected ~15 ± 1 cycles after *18S rRNA,* which was detected after 10 - 12 cycles. The transfection of eukaryotic cells with cationic lipids is a widely used technique (Felgner et al., 1987; de Lima et al., 1999; Rocha et al., 2002) and was also applied in the present study (also referred to as 'lipofection'). For transfection of A549 with the cationic lipid argfectin-50 (Atugen) in complex with either AS or siRNA, an optimized lipofection protocol was kindly provided by Drs. Gekeler and Hofmann (ALTANA Pharma AG, Konstanz).

3.5.1 Delivery of antisense and small interfering RNA into A549 cells via lipofection

First, the efficiency of the transfection method to deliver antisense (AS) and small interfering RNA (siRNA) into A549 cells with the cationic lipid argfectin-50 was investigated by using FITC-labeled AS^{2nd} (second generation antisense constructs, see chapter 3.5.3) and FITC-labeled siRNA, respectively. A549 cells were cultured in 6-well plates and 100 nM FITC-labeled AS^{2nd} or 100 nM FITC-labeled siRNA were transfected for 24 h with 0.9 µg/ml argfectin-50. To demonstrate the uptake of FITC-labeled AS^{2nd} and siRNA into A549 cells, an inverse microscope (Leica Microsystems) was used, both by using transmitted white light and fluorescent light (Figure 23*A* and *B*). The overlay revealed that both FITC-labeled AS^{2nd} and siRNA were found within the adherent A549 cells, and did not attach to the outer cell membrane of the cells.

To ascertain the transfection efficiency on a quantitative basis, A549 cells were treated for 24 h with 0.9 µg/ml atugen-50 lipid alone, with 100 nM FITC-labeled AS^{2nd} or siRNA alone, or with 100 nM FITC-labeled AS^{2nd} or siRNA in combination with 0.9 µg/ml atugen-50, respectively. After cells were detached by trypsin incubation, flow cytometric analysis was performed to determine the percentage of transfected (FITC-positive) cells in the population. The combined application of FITC-labeled AS^{2nd} and atugen-50 lipid increased the FITC intensity in the entire A549 cell population, and ~76% of the cells were above the FITC-threshold defined by the FITC signal of samples incubated with FITC-AS^{2nd}, but without atugen-50 lipid (Figure 23*C*). Likewise, the combined application of FITC-labeled siRNA and atugen-50 lipid increased the FITC intensity in the entire A549 cell population, with ~92% of the cells showing markedly higher FITC intensities than the control cells incubated with FITC-siRNA, but without atugen-50 lipid (Figure 23*D*).

In summary, these experiments revealed that the transfection of A549 cells with antisense and siRNA in combination with the cationic lipid argfectin-50 resulted in a high cellular uptake and was thus a feasible tool for knockdown studies in A549.

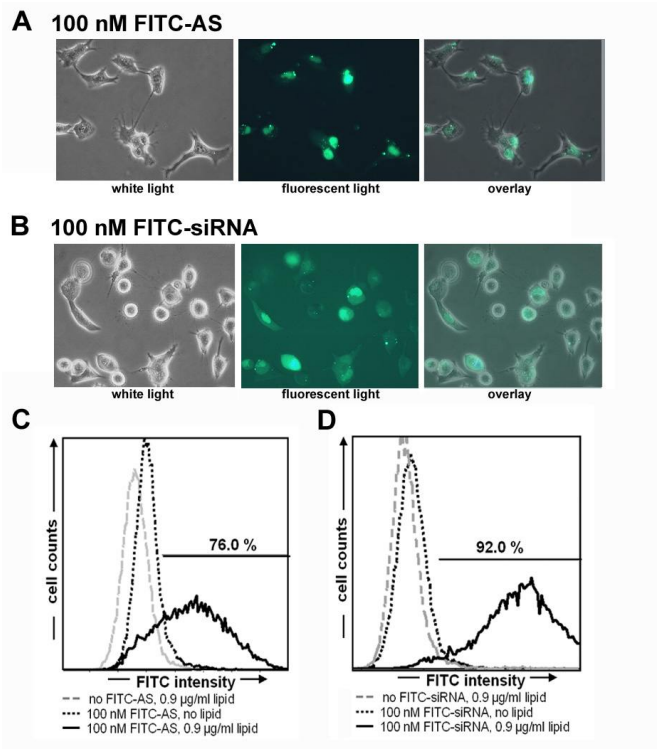

Figure 23. Delivery of FITC-labeled AS and siRNA into A549 cells by lipofection. A549 cells were plated as detailed in *Materials and Methods*, and were incubated with FITC-labeled AS^{2nd} or siRNA and with 0.9 µg/ml argfectin-50 for 24 h. *A*, Microscopic analysis of A549 cells transfected with 100 nM FITC-labeled AS^{2nd}. Original magnification x 400 (DMIL 1000 inverse microscope). *B*, Microscopic analysis of A549 cells transfected with 100 nM FITC-labeled siRNA. Original magnification x 400 (DMIL 1000 inverse microscope). *C,* Flow cytometric analysis of lipofection efficiency to deliver FITC-labeled AS^{2nd}. A549 cells treated with 0.9 µg/ml atugen-50 lipid alone, with 100 nM FITC-labeled AS^{2nd} alone, or with 100 nM FITC-labeled AS^{2nd} in combination with 0.9 µg/ml atugen-50 lipid were detached by trypsin incubation and were subject for flow cytometric analysis. *D*, Flow cytometric analysis of lipofection efficiency to deliver FITC-labeled siRNA. The same experimental setting was used as detailed in *C,* however, 100 nM FITC-labeled siRNAs were used. Data are representative of two independent experiments.

3.5.2 Validation of knockdown constructs directed against PDE4 subtypes in A549 cells

In order to induce PDE4 subtype-specific, substantial, and well-tolerated knockdown of PDE4 subtypes, antisense constructs and siRNAs directed against individual PDE4 subtypes were extensively validated following a multistage protocol (Figure 24).

The initial step in establishing the antisense technology was the synthesis of first generation oligophosphorothioates (AS^{1st}) based on sequence suggestions provided by Prof. Sczakiel (DGS Consulting e.K., Luebeck, Germany). In cooperation with the laboratory of Dr. Hofmann (ALTANA Pharma AG, Konstanz), 13 AS^{1st} targeting PDE4A, 10 AS^{1st} targeting PDE4B, 9 AS^{1st} targeting PDE4C, and 12 AS^{1st} targeting PDE4D were tested in a screening process by lipofecting A549 cells with 200 nM of the corresponding AS^{1st} (data not shown). By using quantitative PCR, the AS^{1st} were checked for efficacy to specifically knock down corresponding PDE4 subtype mRNA and the sequences of the most effective constructs were taken for the synthesis of second generation antisense constructs, namely 2'-alkoxy modified chimeric

phosphorothioate oligonucleotides (AS^{2nd}). As control, additional AS^{2nd} were synthesized with inverse sequences of the targeting antisense constructs. Although the efficacy of the PDE4C primer/probe set was shown in control experiments, *PDE4C* mRNA was not detected in A549 cells. Thus, AS^{2nd} from all suggested sequences targeting PDE4C were synthesized, but could not be further validated in A549. Because the final target cells for the mRNA knockdown strategy were $CD4^+$ T cells which do not express *PDE4C* mRNA (see chapter 3.3.2), the AS^{2nd} constructs targeting PDE4C were not further validated. The AS^{2nd} constructs directed against PDE4A, PDE4B, or PDE4D were tested for efficacy to specifically knock down PDE4 subtype mRNA by using quanitative PCR (see chapter 3.5.3). Additionally, PDE activity assays (see chapter 3.5.4) and immunoblotting experiments (see chapter 3.5.5) were carried out to determine whether the antisense constructs were also effective on protein level.

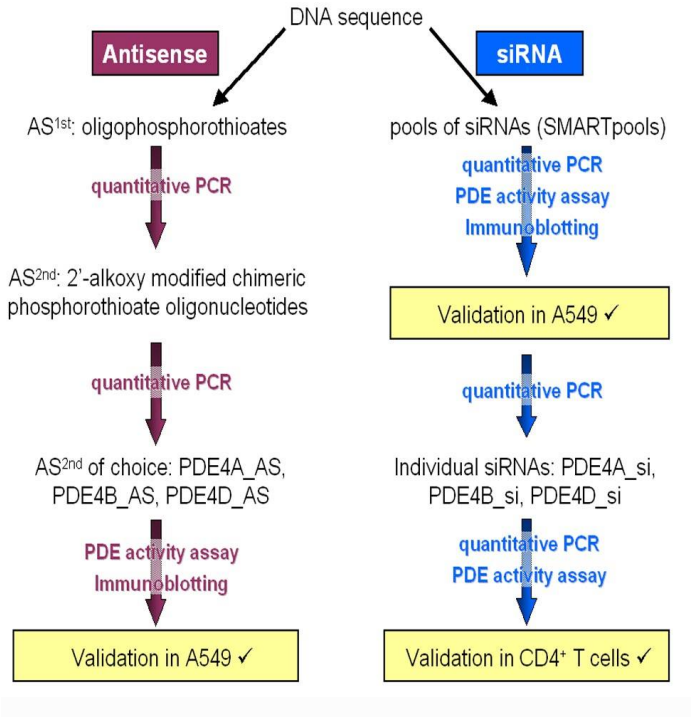

Figure 24. Flowchart of validation experiments to test antisense- and siRNA-mediated PDE4 subtype-specific knockdown efficacy on mRNA and protein level in A549 cells and in human primary $CD4^+$ T cells. Oligophosphorothioates (AS^{1st}) were screened for mRNA knockdown efficacy and specificity in A549 cells. From the most promising sequences, 2'-alkoxy modified chimeric phosphorothioate oligonucleotides (AS^{2nd}) were synthesized and tested for efficacy and specificity using quantitative PCR, PDE activity assays, and immunoblotting experiments (see chapters 3.5.3 - 3.5.5). Similarly, 'SMARTpool' siRNAs were validated in A549 cells (see chapters 3.5.3 - 3.5.5). As detailed in chapter 3.5.6, the siRNA technique proved to be the superior technique for the specific knockdown of PDE4 subtypes and was thus further validated in human primary $CD4^+$ T cells, as reported in chapter 3.6.

Similar to the experiments performed with antisense constructs, a siRNA-based technology to specifically knock down individual PDE4 subtypes was tested (Figure 24). Because self-designed, *in vitro* transcribed and duplexed siRNAs (*Silencer*™ siRNA construction kit,

Ambion, Austin, USA) had poor efficacies, pre-designed siRNA-Duplexes were purchased from Dharmacon (Lafayette, USA). Initially, to increase efficiency, Dharmacon 'SMARTpools' containing 4 individual siRNAs targeting one subtype were applied. Subsequently, 'SMARTpools' were tested for knockdown efficacy, specificity, and tolerability by quantitative PCR (see chapter 3.5.3), PDE activity assays (see chapter 3.5.4), and immunoblotting experiments (see chapter 3.5.5). Finally, because the siRNA-mediated knockdown strategy proved to be the superior technique in the experiments performed in the present study, as summarized in chapter 3.5.6, further validation experiments with siRNAs were performed in human primary $CD4^+$ T cells (see chapter 3.6).

3.5.3 mRNA knockdown of PDE4 subtypes in transfected A549 cells

Lipofection of A549 cells with 100 nM AS^{2nd} targeting PDE4A, PDE4B, or PDE4D resulted in the knockdown of corresponding mRNAs, when compared to untreated cells 24 h after lipofection (Figure 25*A*).

All targeting AS^{2nd} constructs used, i.e., three AS^{2nd} targeting PDE4A (PDE4A_AS1, PDE4A_AS2, and PDE4A_AS3), two AS^{2nd} targeting PDE4B (PDE4B_AS1 and PDE4B_AS2), and three AS^{2nd} targeting PDE4D (PDE4D_AS1, PDE4D_AS2, and PDE4D_AS3), caused substantial suppression of mRNA levels of corresponding PDE4 subtypes (73 - 91% knockdown of *PDE4A* mRNA, 74 - 78% knockdown of *PDE4B* mRNA, and 69 - 91% knockdown of *PDE4D* mRNA, respectively), whilst leaving the mRNA levels of other subtypes largely unaffected (Figure 25*A*). The lipofection procedure alone, tested by applying argfectin-50 lipid without AS^{2nd} constructs, or the transfection of AS^{2nd} constructs with inverse sequences (PDE4A_AS2_INV, PDE4B_AS2_INV, and PDE4D_AS2_INV) did not substantially affect the mRNA level of *PDE4A*, *PDE4B*, and *PDE4D* after 24 h of incubation.

To evaluate whether the knockdown effects of AS^{2nd} constructs on PDE4 mRNA were maintained for a longer time period, the lipofection experiments were repeated with an incubation time of 72 h (Figure 25*B*). At this latter time point, the reduction of PDE4 subtype mRNAs was similar to the effects observed after 24 h, however, the overall efficacies of the PDE4A- and PDE4B-AS^{2nd} constructs decreased (55 - 74% knockdown of *PDE4A*, 52 - 54% knockdown of *PDE4B*), whilst PDE4D-AS^{2nd} constructs were still highly effective (80 - 91% knockdown of *PDE4D*). The lipofection procedure alone and AS^{2nd} constructs with inverse sequences did overall not largely affect the mRNA level of *PDE4A*, *PDE4B*, and *PDE4D* after 72 h of incubation.

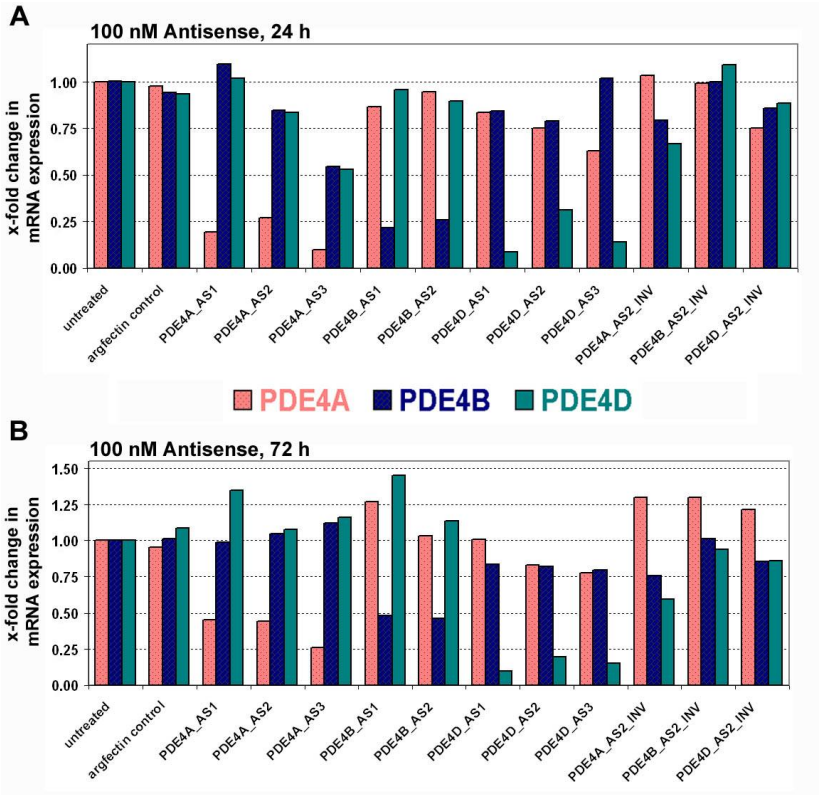

Figure 25. *PDE4A, PDE4B*, and *PDE4D* mRNA expression in untreated and antisense-transfected A549 cells. A549 cells were transfected in 6-well plates, as detailed in *Materials and Methods.* Quantitative PCR was performed to assess the mRNA levels of *PDE4A*, *PDE4B*, and *PDE4D*. All data are expressed relative to untreated cells (set 1 as reference). *A*, Lipofection was carried out for 24 h using 0.9 µg/ml argfectin-50 and 100 nM AS^{2nd} targeting PDE4A, PDE4B, or PDE4D, respectively. For control, only argfectin-50 (argfectin control) was applied. Additionally, AS^{2nd} constructs with inverse sequences (PDE4A_AS2_INV, PDE4B_AS2_INV, or PDE4D_AS2_INV) were used. *B*, Lipofection was carried out as described in *A*, however, for 72 h. All data are expressed as average of two independent experiments.

Similar to the experiments performed with antisense constructs, 'SMARTpools' containing 4 individual siRNAs targeting the same gene were transfected into A549 cells. Since siRNAs have been reported to act in the low nM range (Elbashir et al., 2001), 'SMARTpool' concentrations were tested in concentrations of 5 nM, 25 nM, 50 nM, and 100 nM. Compared to untreated cells, the argfectin control (cells only treated with 0.9 µg/ml argfectin-50) and the transfected PDE4C-SMARTpool had no effect on *PDE4A*, *PDE4B*, and *PDE4D* mRNA expression, measured after incubation for 24 h (Figure 26*A*). Remarkably, all applied concentrations of 'SMARTpools' targeting PDE4A, PDE4B, or PDE4D had similar high knockdown efficacies in suppressing the corresponding PDE4 subtype and were thus summarized within one diagram. Whilst leaving the expression of other PDE4 subtypes unaffected, the 'SMARTpools' targeting individual PDE4 subtypes caused substantial knockdowns of the corresponding mRNAs: ~73% knockdown of *PDE4A* mRNA, ~76% knockdown of *PDE4B* mRNA, and ~71% knockdown of *PDE4D* mRNA.

The knockdown effects of 'SMARTpools' were maintained for a longer time period, because after an incubation period of 72 h, all applied concentrations of 'SMARTpools' had similar effects than after 24 h (Figure 26*B*). Compared to untreated cells, no change in *PDE4A*, *PDE4B*, and *PDE4D* mRNA levels were observed in argfectin control cells or in cells transfected with the PDE4C-SMARTpool. In contrast, incubation with 'SMARTpools' targeting individual PDE4 subtypes for 72 h caused specific, similar high mRNA knockdown as measured for the 24 h incubation period: ~76% knockdown of *PDE4A* mRNA, ~69% knockdown of *PDE4B* mRNA, and ~84% knockdown of *PDE4D* mRNA.

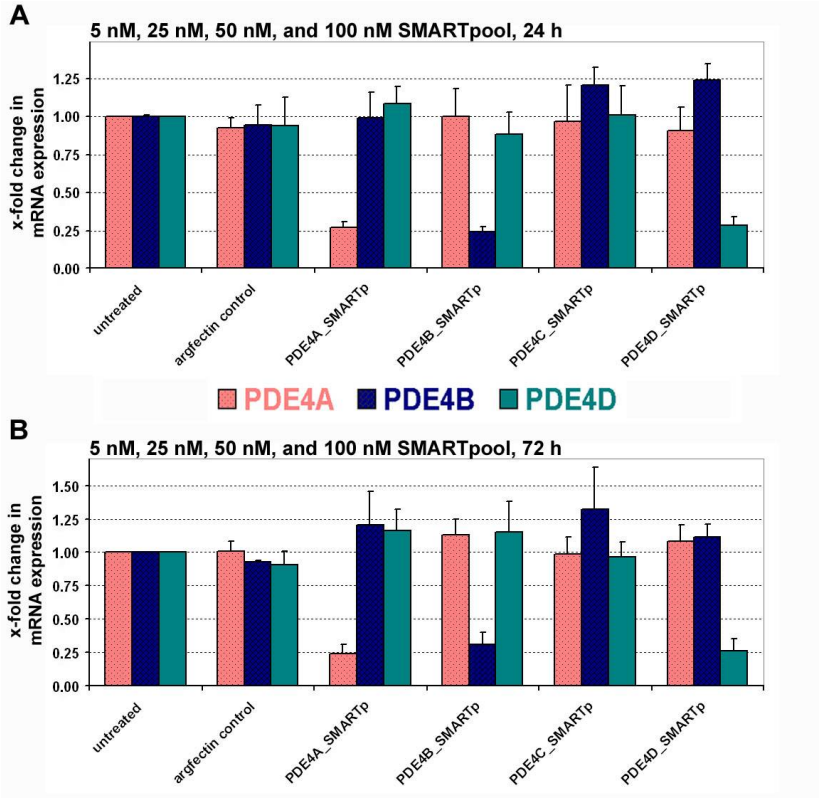

Figure 26. *PDE4A, PDE4B*, and *PDE4D* mRNA expression in untreated and 'SMARTpool'-transfected A549 cells. A549 cells were plated in 6-well plates and were subject for lipofection, as detailed in the legend of Figure 25. *A*, Lipofection was carried out for 24 h using 0.9 µg/ml argfectin-50 and 5 nM, 10 nM, 50 nM, or 100 nM 'SMARTpools' (pool of 4 individual siRNAs) targeting PDE4A, PDE4B, PDE4C, or PDE4D, respectively. For control, only argfectin-50 (argfectin control) was applied. *B*, Lipofection was carried out as described in *A*, however, with a 72 h incubation period. Because the different siRNA concentrations used in experiments resulted in very similar knockdown efficacies, individual experiments were summarized and are expressed as mean ± SD of four experiments.

3.5.4 PDE4 activity knockdown in transfected A549 cells

To ascertain whether observed mRNA knockdowns also affect PDE4 activity, cAMP-PDE activity assays were performed with lysates from untreated and AS^{2nd}- or siRNA-transfected A549 cells after 72 h of lipofection. PDE activities measured in lysates from untreated A549 cells were used as reference. Argfectin control cells (cells only treated with 0.9 µg/ml argfectin-

50) were analyzed to check whether lipofection alone effected cAMP-PDE activity (Figure 27). Whilst treatment with argfectin-50 alone did not effect cAMP-PDE activity, antisense (AS^{2nd}) constructs directed against PDE4A, PDE4B, or PDE4D significantly reduced total cAMP-PDE activity and PDE4 activity, with PDE4D-AS^{2nd} having the most pronounced effect (mean ± SD of PDE4 activity suppression: PDE4A-AS^{2nd} 44 ± 33%, PDE4B-AS^{2nd} 38 ± 16%, and PDE4D-AS^{2nd} 72 ± 10%; Figure 27*A*). Combined application of the AS^{2nd} constructs (PDE4A-AS^{2nd} + PDE4B-AS^{2nd} + PDE4D-AS^{2nd} = PDE4_all_AS in Figure 27*A*) did not result in higher knockdown efficacy. Remarkably, all AS^{2nd} constructs showed a trend to affect PDE4 independent activity.

In contrast, 'SMARTpool' siRNAs targeting PDE4A, PDE4B, or PDE4D did not affect PDE4 independent activity (Figure 27*B*). The PDE4D-SMARTpool significantly reduced total cAMP-PDE activity and PDE4 activity (mean ± SD of PDE4 activity suppression: 68 ± 8%), whereas the PDE4A- and PDE4B-SMARTpools had lower effects (13 ± 1% and 13 ± 4%, respectively). Combined application of the 'SMARTpools' (PDE4A_SMARTp + PDE4B_SMARTp + PDE4D_SMARTp = PDE4_all_SMARTp in Figure 27*B*) did not increase knockdown efficacy. Considering that the individual PDE4 subtypes contribute differently to the overall PDE4 activity (see introduction of chapter 3.5), it was expected that PDE4A- and PDE4B-AS^{2nd}/SMARTpools will have the smallest effects on PDE4 activity in A549 cells whereas the PDE4D-AS^{2nd}/SMARTpool will have larger effects even when the individual subtypes are diminished to the same extent.

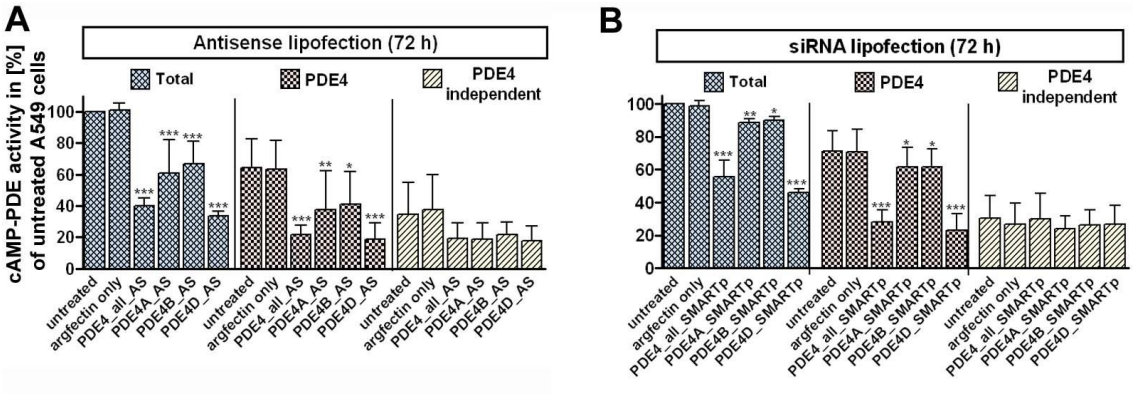

Figure 27. PDE activity knockdown, induced by PDE4 subtype specific antisense constructs and siRNA. A549 cells were transfected in 6-well plates, as detailed in *Materials and Methods.* After 72 h, cells were washed and harvested in lysis buffer IV (homogenization buffer), and 3 - 6 µg protein of the 1000 x g supernatant were assayed for cAMP-PDE activity. *A*, Antisense concentrations were 180 nM combined AS^{2nd} targeting PDE4A, PDE4B, and PDE4D (= PDE4_all_AS) and 120 nM combined AS^{2nd} targeting PDE4A (= PDE4A_AS), PDE4B (= PDE4B_AS), or PDE4D (= PDE4D_AS), respectively. *B*, 'SMARTpool' concentrations were 15 nM combined 'SMARTpools' targeting PDE4A, PDE4B, and PDE4D (= PDE4_all_SMARTp) and 5 nM 'SMARTpool' targeting PDE4A (= PDE4A_SMARTp), PDE4B (= PDE4B_ SMARTp), or PDE4D (= PDE4D_ SMARTp), respectively. Results are expressed as cAMP-PDE activity in [%] of untreated A549 cells, as mean ± SD of 3 independent experiments. Significant differences between untreated conditions and AS^{2nd}/SMARTpool-transfected cells are indicated (*, $p < 0.05$; **, $p < 0.01$; ***, $p < 0.001$; compared to untreated cells).

3.5.5 Immunodetection of PDE4D splice variants in untreated and transfected A549 cells

To ascertain whether AS^{2nd}- and siRNA-mediated mRNA and protein activity knockdown can be confirmed on the level of splice variants, immunodetection experiments were performed. Lysates from untreated A549 cells were used as reference, argfectin control cells (cells only treated with 0.9 µg/ml argfectin-50) were used to check whether lipofection alone affected protein levels. Immunoblotting with polyclonal antibodies directed against the conserved C-termini of PDE4A or PDE4B (FabGennix Inc., Shreveport, USA) failed to detect significant amounts of protein, which might be explained by the observation that A549 cells mainly express PDE4D (see introduction of chapter 3.5). Immunoblotting with a polyclonal antibody directed against the conserved C-termini of PDE4D detected several immunoreactive proteins of different molecular weights (Figure 28). In untreated A549 cells (lane 1, Figure 28*A* and *B*), immunoreactivity was detected in the range of ~115 - 130 kDa, which might be attributed to the long PDE4D4 splice variant (119 kDa). In the range of ~85 - 105 kDa, two immunoreactive bands were detected, which might correspond to different PDE4D long forms (PDE4D3 [~93 kDa], PDE4D5 [105 kDa], PDE4D7 [85 - 110 kDa], PDE4D8 [92 kDa], and/or PDE4D9 [90 kDa]). Three weaker immunoreactive bands were detected in the range of ~60 - 75 kDa, which might correspond to different PDE4D short forms (PDE4D1 [72 kDa], PDE4D2 [68 kDa], and/or PDE4D6 [59 kDa]).

For the investigation of maximal protein knockdown efficacies of antisense constructs, several AS^{2nd} constructs targeting one individual subtype were applied in combination (Figure 28*A*). Additionally, to target all expressed PDE4 subtypes simultaneously, A549 cells were treated with a pool of AS^{2nd} constructs targeting PDE4A, PDE4B, and PDE4D (termed PDE4_all_AS). Considering the limited space on minigels and the low protein concentrations from lysed AS^{2nd} samples, only 17 µg of protein were loaded per lane for antisense experiments. Subsequently, the immunoreactive signals in the AS^{2nd} samples were comparably low (Figure 28*A*). Compared to untreated A549 cells (lane 1), no substantial changes in the amount of PDE4D splice variants were observed in argfectin control cells (lane 2) and in cells treated with AS^{2nd} constructs targeting PDE4A or PDE4B (PDE4A_AS, lane 4 and PDE4B_AS, lane 5, respectively). However, a substantial decrease in immunoreactivity was found for the cells treated with PDE4D_AS (indicated with arrows, lane 6). A decrease in immunoreactivity in cells treated with all AS^{2nd} (PDE4_all_AS, lane 3) was not clearly observed.

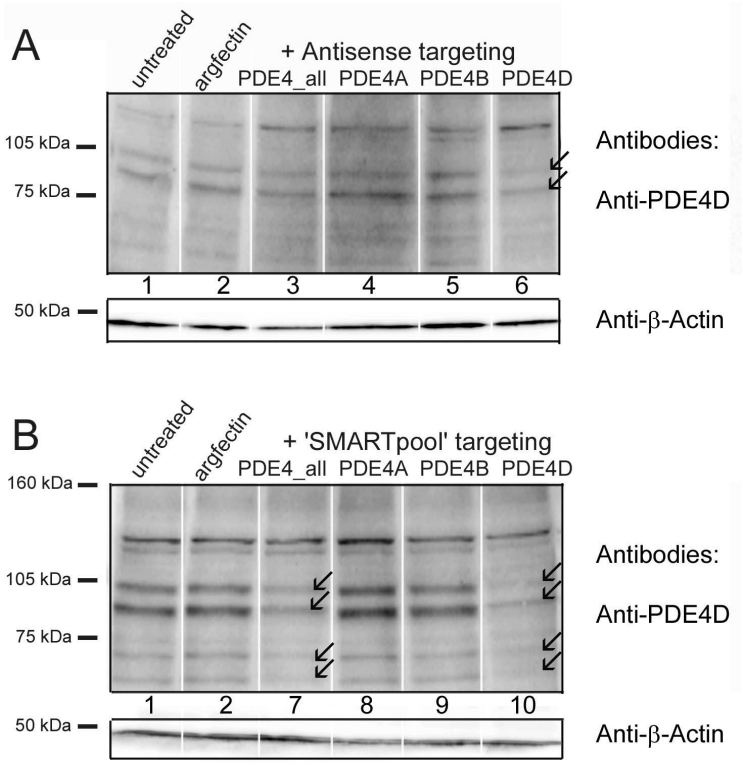

Figure 28. Detection of PDE4D splice variants in untreated and transfected A549 cells. A549 cells were transfected in 6-well plates, as detailed in *Materials and Methods.* After 72 h, cells were washed and harvested in lysis buffer III (RIPA buffer), and protein was separated by SDS-polyacrylamide gel electrophoresis. Immunodetection was performed using commercial antibodies recognizing PDE4D. ß-Actin was used as loading control. Antisense (*A*) and siRNA (*B*) concentrations were as detailed in the legend of Figure 27. Arrows indicate knockdown of PDE4D splice variants.

Similarly to the AS^{2nd} experiments, A549 cells were treated with individual 'SMARTpools' targeting corresponding PDE4 subtypes or with the combined 'SMARTpools' (termed PDE4_all_SMARTpool) (Figure 28*B*). Because lysates from siRNA samples were more concentrated, 31 µg of protein per lane were loaded for siRNA experiments, resulting in increased immunoreactive signals (Figure 28*B*). Compared to untreated A549 cells, no substantial changes in the amount of PDE4D splice variants were observed in argfectin control cells (lane 2) and in cells treated with 'SMARTpools' targeting PDE4A (lane 8) or PDE4B (lane 9). However, a substantial decrease in immunoreactivity was found for cells treated with combined 'SMARTpool' siRNAs (PDE4_all_SMARTp, indicated with arrows, lane 7) and for cells treated with the individual 'SMARTpool' targeting PDE4D (indicated with arrows, lane 10). Interestingly, the PDE4D-SMARTpool showed efficacy to knock down long and short forms, i.e., no selectivity to knock down distinct PDE4D splice variants was observed. In all experiments, the immunodetection of ß-Actin demonstrated that observed knockdowns in PDE4D protein were not due to lower amounts of protein loaded onto the gel.

3.5.6 Summary: Antisense versus siRNA in transfected A549 cells

As summarized in Table 8, both the AS^{2nd} and siRNA strategy induced substantial, PDE4 subtype-specific knockdown. Quantitatively, some AS^{2nd} constructs had higher efficacies to knock down mRNA and protein activity than siRNAs. However, the efficacies of AS^{2nd} constructs slightly decreased time-dependently and were qualitatively more variable than siRNAs in knocking down corresponding PDE4 subtypes. Furthermore, AS^{2nd} constructs slightly affected PDE4 independent activity. In contrast, the application of siRNAs was effective at lower concentrations, showed less variability in between experiments, and was better tolerated (Table 8). By comparing all examined parameters, the siRNA-based technique was preferred in the present study for the knockdown of PDE4 subtypes in human primary $CD4^+$ T cells and was further validated in these cells (see chapter 3.6).

Table 8. Comparison: AS^{2nd} versus siRNA knockdown technique in transfected A549 cells[a]

Parameter	Antisense (AS^{2nd})	siRNA
Delivery	~76%	~92%
Knockdown specificity (mRNA)	yes	yes
Knockdown efficacy (mRNA) after 24 h	69 - 91%	71 - 76%
Knockdown efficacy (mRNA) after 72 h	52 - 91%	69 - 84%
Knockdown efficacy (protein activity) after 72 h	up to 72 ± 10%	up to 68 ± 8%
Effect on PDE4 independent activity	not significant, but trend of suppression	not significant, no trend of suppression
Overall variability of experiments	more variable than siRNA	less variable than AS^{2nd}
Overall tolerability	less tolerated than siRNA (~30% of cells detached)	better tolerated than AS^{2nd} (no cells detached)

[a] A549 cells were transfected with AS^{2nd} constructs or siRNAs, as detailed in *Materials and Methods*. Delivery of knockdown constructs was determined by using FITC-labeled AS^{2nd} and siRNA and subsequent flow cytometrical analysis. Knockdown specificity and efficacy on mRNA level was ascertained by quantitative PCR. Immunodetection experiments and activity assays measured knockdown efficacy on protein level. The tolerability of the cells towards treatment with knockdown constructs was phenotypically analyzed by using an inverse microscope and by estimating the confluency and percentage of detached cells.

3.6 Validation of PDE4 subtype-specific siRNAs in $CD4^+$ T cells

Although T cells have been recognized as critical regulators of inflammatory responses, the functional impact of PDE4 subtypes in human primary $CD4^+$ T cells is largely unknown. To address the question whether the specific expression patterns of PDE4 subtypes in human primary $CD4^+$ T cells (see chapter 3.3) correlate with a respective relevance for different T cell functions, the siRNA strategy, validated initially in A549 (see chapter 3.5), was applied to T cells. To transfect human primary $CD4^+$ T cells with siRNAs, an electroporation technique (Amaxa nucleofection [NF]) was used (Gresch et al., 2004). In a series of control experiments, this siRNA-based strategy was validated. Whilst a comparatively high stimulation condition (3 µg anti-CD3/well in combination with 3 µg anti-CD28/ml) was used for all PDE4 expression

and activity studies to detect maximal effects in the regulation of PDE4 subtypes (see Figure 13, Figure 16, Figure 17), a weaker stimulation condition (0.3 µg anti-CD3/well in combination 0.3 µg anti-CD28/ml) was used for all functional studies and therefore also for all siRNA validation experiments in T cells. This weaker stimulation was chosen because strong stimulation decreases the efficacy of PDE4 inhibitors (unpublished observations of Dr. Hatzelmann, ALTANA Pharma AG, Konstanz), and will thus also decrease functional effects of PDE4 subtype-specific siRNAs on T cell responses.

3.6.1 Delivery of a GFP-plasmid and of FITC-siRNA into CD4$^+$ T cells via nucleofection

The transfection efficiency of the amaxa nucleofection (NF) technique was tested with a pmaxGFP plasmid (Amaxa) and with FITC-labeled non-targeting siRNA (Sequitur). 24 h after nucleofection, cells were analyzed by flow cytometry, resulting in ~83% GFP-expressing CD4$^+$ T cells (Figure 29*A*). The nucleofection of FITC-labeled siRNA resulted in ~85% FITC positive cells when treated with 200 nM FITC-siRNA (Figure 29*B*) and in ~97% FITC positive cells when treated with 2 µM FITC-siRNA (Figure 29*C*). CD4$^+$ T cells did not show spontaneous siRNA uptake (without nucleofection) and FITC-siRNA applied after nucleofection did also not enter the cells.

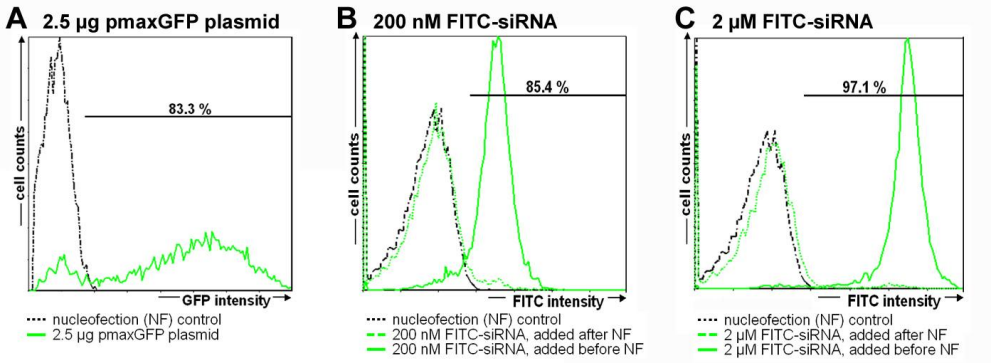

Figure 29. Delivery of a GFP-plasmid and of FITC-labeled siRNA into human primary CD4$^+$ T lymphocytes by amaxa nucleofection. Nucleofection (NF) was performed with freshly isolated human primary CD4$^+$ T cells, as detailed in *Materials and Methods*. *A*, Transfection efficiency, tested by using 2.5 µg plasmid-DNA coding for GFP. Expression of GFP was measured by flow cytometry 24 h after transfection. *B*, Transfection efficiency, tested by using 200 nM FITC-labeled siRNA. Uptake of siRNA was measured by flow cytometry 24 h after transfection. *C*, Transfection efficiency, tested as detailed in *B*, but with 2 µM FITC-labeled siRNA.

3.6.2 Selection of individual PDE4 subtype-specific siRNAs

As detailed in chapter 3.5, 'SMARTpools', i.e., sets of 4 individual siRNAs targeting the same PDE4 subtype, were used for initial siRNA validation experiments in the cell line A549. Because it was not expected that all four individual siRNAs of one PDE4 subtype-specific 'SMARTpool' set have the same knockdown efficacies, the individual siRNAs from the

'SMARTpool' sets were transfected into human primary CD4$^+$ T cells and were tested for efficacy to downregulate the respective PDE4 subtype mRNA. Indeed, the nucleofection of individual siRNAs targeting PDE4 subtypes resulted in different knockdown efficacies when compared to nucleofection (NF) control cells, which were set 1 as reference (Figure 30). The individual siRNAs PDE4A_si4, PDE4B_si4, and PDE4D_si2 were most effective in specifically knocking down the corresponding subtype and were selected for further experiments. These findings were confirmed in A549 cells transfected with the individual siRNAs (data not shown). For more convenient labeling of figures and tables, PDE4A_si4 was subsequently termed PDE4A_si, PDE4B_si4 was termed PDE4B_si, and PDE4D_si2 was termed PDE4D_si in further experiments. The application of a set of non-targeting siRNAs (NEG_SMARTp) did not influence the expression of the PDE4 subtypes.

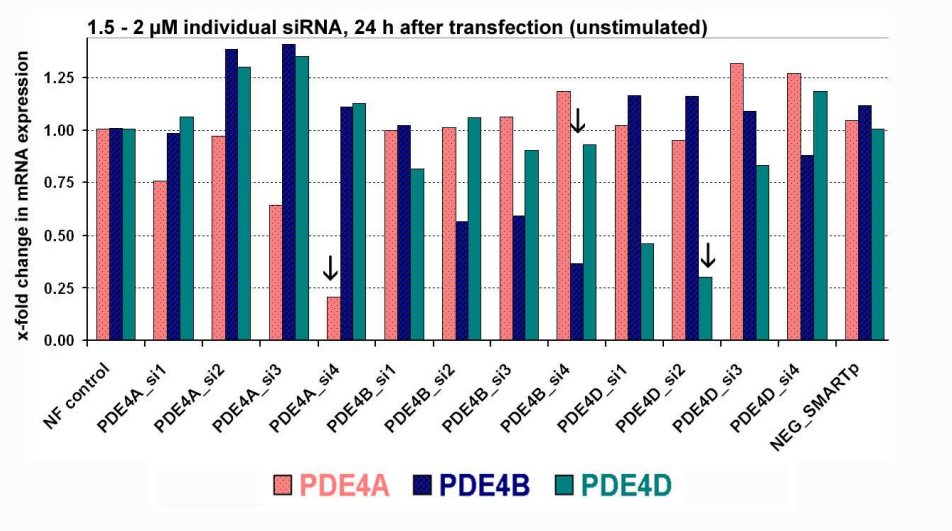

Figure 30. Selection of individual siRNAs from sets of 'SMARTpools'. Human primary CD4$^+$ T cells were transfected as described in *Materials and Methods*. 24 h after transfection, cells were harvested and quantitative PCR was performed to assess the mRNA levels of *PDE4A*, *PDE4B*, and *PDE4D*. All data are expressed relative to the nucleofection (NF) control, where no siRNA was applied (set 1 as reference). NF was carried out with individual siRNAs targeting PDE4A (1.5 µM of PDE4A_si1, PDE4A_si2, PDE4A_si3, or PDE4A_si4, respectively), PDE4B (2 µM of PDE4B_si1, PDE4B_si2, PDE4B_si3, or PDE4B_si4, respectively), and PDE4D (2 µM of PDE4D_si1, PDE4D_si2, PDE4D_si3, or PDE4D_si4, respectively). For control, a set of non-targeting siRNAs (1.5 µM - 2 µM of NEG_SMARTp) was applied. Arrows indicate the selected individuals used for further studies. Shown are average values of two independent experiments with the exception of PDE4D-siRNA data, which represent one experiment.

3.6.3 Tolerability of amaxa nucleofection in CD4$^+$ T cells

To ascertain the tolerability of the nucleofection procedure and to test whether the additional application of siRNAs *per se* had effects, several functional read-out parameters were analyzed to validate the siRNA knockdown technique in human primary CD4$^+$ T cells. The nucleofection procedure alone (without siRNA) produced a considerable loss (mean ± SD = 37 ± 10%) of cells. However, nucleofection (NF control in Figure 31*A*) had only a minor effect

(5 ± 3%) on cell mortality of recovered cells compared to untreated cells, as measured by 7-AAD staining 24 h and 48 h after nucleofection. The nucleofection of siRNAs had no additional effect on cell mortality when compared to NF control cells (Figure 31*A*). The expression of surface markers, such as CD4 and CD25 measured by flow cytometry was not significantly changed by the nucleofection procedure or by the additional application of siRNAs 24 h and 48 h after nucleofection (Figure 31*B*).

To verify whether nucleofection affected T cell proliferation and the release of cytokines after anti-CD3/CD28 stimulation, [^{3}H]-thymidine incorporation and enzyme-linked immunosorbent assays, respectively, were performed. The proliferation rate and IL-2, IFN-γ, and IL-5 cytokine synthesis measured in cells that were not nucleofected, but stimulated with anti-CD3/CD28 were set to 100% (no NF in Figure 31*C*). In parallel, cells were nucleofected (NF in Figure 31*C*, no siRNAs applied). Additionally, NF cells were incubated with 0.1% DMSO (NF + DMSO in Figure 31*C*) to ascertain the impact of DMSO in the final assay concentration (see chapter 3.8). The proliferation rate of stimulated CD4$^+$ T cells was neither affected by the nucleofection procedure nor by the application of DMSO (Figure 31*C*). In contrast, the release of cytokines at different time points was significantly affected by the nucleofection procedure, ranging from 32% to 39% suppression of IL-2 release, 42% to 49% suppression of IFN-γ release, and ~39% suppression of IL-5 release, when compared to untreated cells. The overall effect of the nucleofection procedure on the suppression of anti-CD3/CD28 induced cytokines was averaged to be 42 ± 5%. The additional application of DMSO did not significantly affect cytokine release.

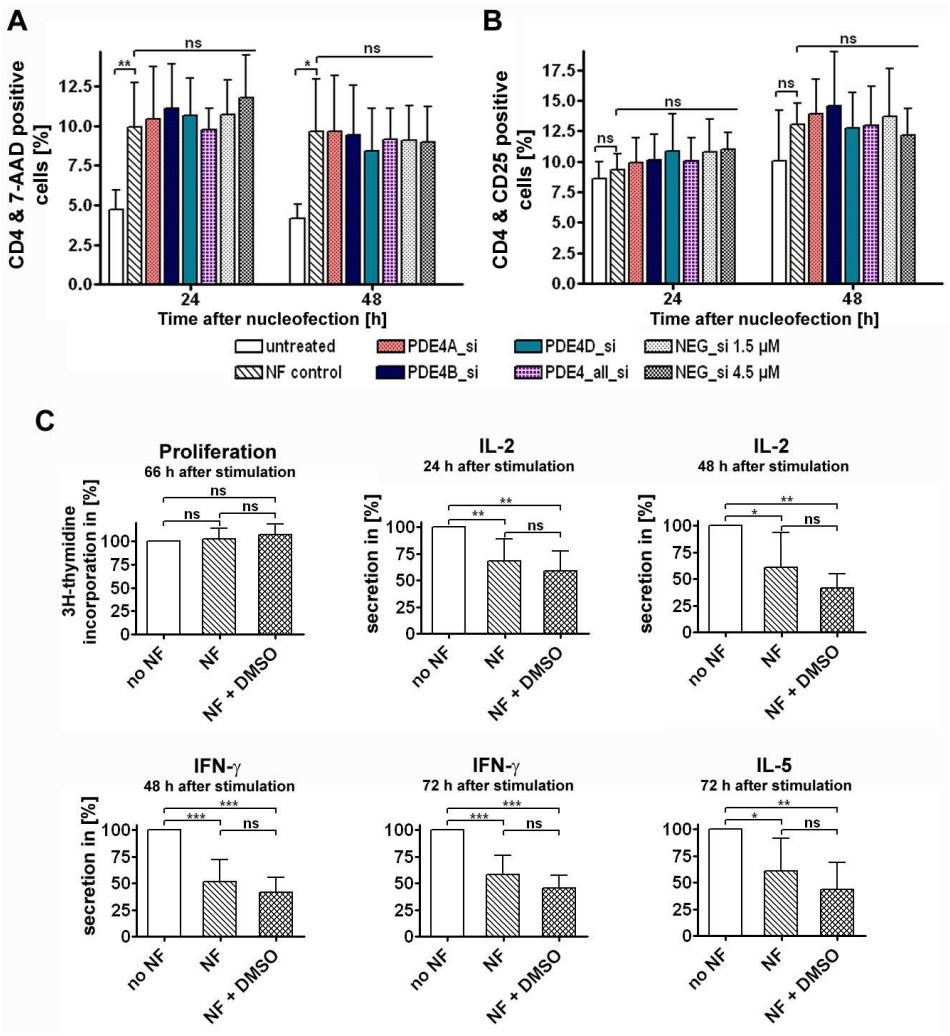

Figure 31. Validation of the nucleofection procedure in human primary CD4⁺ T lymphocytes. *A,* Tolerability of the nucleofection procedure. $CD4^+$ T cells were left untreated or were nucleofected without siRNA (NF control) or with 1.5 µM of PDE4 subtype-specific siRNAs (PDE4A_si, PDE4B_si, or PDE4D_si, respectively). The individual PDE4 subtype-specific siRNAs were also applied in combination (PDE4A_si + PDE4B_si + PDE4D_si, each 1.5 µM = PDE4_all_si). For control, non-targeting siRNA was applied (1.5 µM and 4.5 µM = NEG_si). 24 h and 48 h after nucleofection, the viability of the cells was determined by 7-AAD staining and flow cytometric analysis. Data are mean ± SD of 3 - 5 independent experiments. Significance of difference is indicated: ns, not significant; *, $p < 0.05$; **, $p < 0.01$. *B,* Effect of nucleofection on surface markers. The same experiments were performed as detailed in *A*, however, PE-labeled anti-CD4 and FITC-labeled anti-CD25 antibodies were used for flow cytometric analysis. Data are mean ± SD of 3 - 5 independent experiments, which were not significantly different (ns). *C*, Effect of nucleofection and DMSO on anti-CD3/CD28 induced T cell responses. Cells were left untreated (no NF), were nucleofected (NF), or were nucleofected and additionally treated with 0.1% DMSO. 24 h past nucleofection, all cells were stimulated for different periods of time using 0.3 µg anti-CD3/well and 0.3 µg anti-CD28/ml. For the determination of the proliferation rate, [^{3}H]-thymidine was added 48 h after stimulation for 18 h. For the determination of cytokines, supernatants were collected and subject for enzyme-linked immunosorbent assays (see *Materials and Methods*). The proliferation rate and cytokine level of the cells that were not nucleofected (no NF) were set to 100%. Data are mean ± SD of 5 - 6 independent experiments. Significance of difference is indicated: ns, not significant; *, $p < 0.05$; **, $p < 0.01$; ***, $p < 0.001$.

Although the nucleofection procedure alone had substantial effects on some of the measured parameters, the application of siRNA *per se* had no additional effects on any of the parameters investigated besides expected effects of PDE4 subtype-specific siRNAs on cytokine release and on proliferation correlated with PDE4 subtype knockdown (see chapter 3.8). For better comparison, the effects of the nucleofection procedure on various T cell functions and additional effects of siRNAs are summarized in Table 9.

Table 9. Validation of the nucleofection procedure[a]

Functional parameter	Effect of nucleofection	Additional effect of siRNA
Loss of cells	37 ± 10%	no effect
Mortality of recovered cells	5 ± 3% increased	no effect
Expression of CD4 and CD25	no effect	no effect
Proliferation	no effect	no effect (NEG_si)
Cytokine release	42 ± 5% decreased	no effect (NEG_si)

[a] $CD4^+$ T cells were treated by the nucleofection procedure without the addition of siRNA (column: 'effect of nucleofection') or with the addition of siRNA (column: 'additional effect of siRNA'). The loss of cells due to the transfection procedure was determined by counting the recovered cells 24 h after nucleofection. 24 - 48 h after nucleofection, 7-AAD was used to determine the mortality of recovered cells. Additionally, cells were stained with Abs recognizing CD4 and CD25 and the expression of these surface markers were measured by flow cytometry. Cytokine release and the proliferation rate were determined as detailed in *Materials and Methods*. NEG_si, non-targeting control siRNA. Data are mean ± SD of several independent experiments (n > 8).

Taking some technical restrictions into account, these data suggest that the nucleofection technique can be considered to be a suitable tool to transfect human primary $CD4^+$ T cells.

3.6.4 PDE4 subtype-specific mRNA knockdown in nucleofected $CD4^+$ T cells

To determine the optimal concentration needed for mRNA knockdown, different siRNA concentrations were tested (Figure 32*A*). In unstimulated $CD4^+$ cells, individual siRNAs directed against PDE4A, PDE4B, or PDE4D concentration-dependently induced specific mRNA-knockdowns of each respective PDE4 subtype 24 h after transfection compared to nucleofection controls (NF control, cells nucleofected without siRNA), whilst leaving the mRNA level of other expressed PDE4 subtypes unaffected (Figure 32*A*). Nontargeting siRNA used as a negative control did not largely affect the expression of *PDE4A*, *PDE4B*, and *PDE4D* mRNA (Figure 32*A*). Maximal mRNA knockdown was achieved with 1.5 µM siRNA. Notably, the knockdown efficacy for every individual siRNA was within the same range of ~62 - 65%.

To test whether the PDE4 subtype-specific siRNAs were also effective after stimulation, transfected cells were left unstimulated for 24 h to allow siRNA-mediated mRNA knockdown before the addition of the anti-CD3/CD28 stimulus. Subsequently, the mRNA knockdown effects were determined at 24 h, 48 h and 72 h after stimulation and were compared to the NF controls (Figure 32*B*) taken at the respective time point. Significant mRNA knockdowns were achieved up to 48 h after stimulation with all applied siRNAs. 72 h after stimulation, siRNA-

mediated knockdown effects started to diminish for every subtype although effects for PDE4B and PDE4D were still significant.

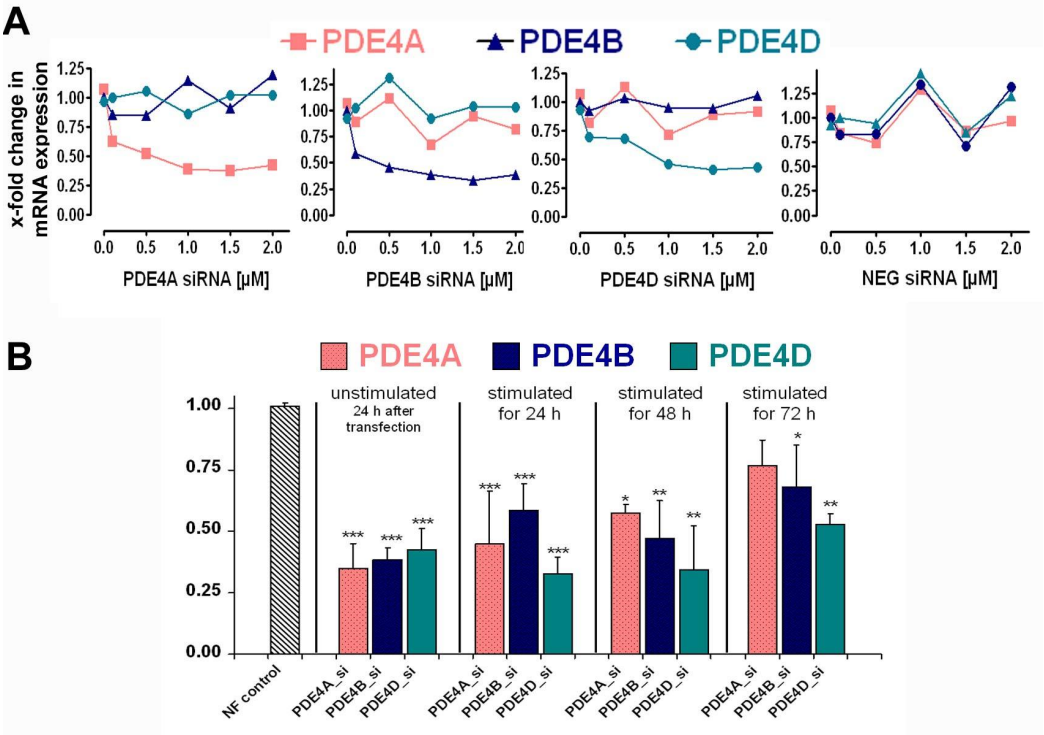

Figure 32. mRNA knockdown in unstimulated and stimulated human primary CD4⁺ T cells. *A*, Concentration-dependent siRNA-mediated mRNA knockdown in unstimulated CD4⁺ T cells 24 h after nucleofection. Data are shown relative to each nucleofection (NF) control, as average of two experiments. *B*, Time-dependent siRNA-mediated mRNA knockdown after stimulation with 0.3 µg anti-CD3/well and 0.3 µg anti-CD28/ml. Results are expressed relative to the respective NF control as mean ± SD of 2 - 6 donors. Significant differences between NF control and siRNA-nucleofected cells are indicated; *, $p < 0.05$; **, $p < 0.01$; ***, $p < 0.001$; compared to NF control of each time point.

3.6.5 siRNA-mediated PDE4 activity knockdown in nucleofected CD4⁺ T cells

To ascertain whether the mRNA knockdown translates into a decrease in protein level, cAMP-PDE activity assays with lysates from siRNA-transfected CD4⁺ T cells were performed. Lysates from T cells treated only with the nucleofection procedure were used as reference. 24 h after stimulation, a marginal reduction of total cAMP-PDE activity and PDE4 activity (mean ± SD = 10 ± 13%, ns) was achieved with siRNA directed against PDE4A (Figure 33*A*). SiRNAs directed against PDE4B or PDE4D significantly reduced total cAMP-PDE activity and PDE4 activity (PDE4B-siRNA: 28 ± 5%, PDE4D-siRNA: 51 ± 11%). To evaluate whether the knockdown effects on PDE4 activity were maintained for a longer time period, the PDE activity measurements were repeated at 72 h after stimulation (Figure 33*B*). At this latter time point, the reduction of PDE4 enzyme activity by the different siRNAs was similar to the 24 h time point (PDE4A-siRNA: 18 ± 9%, PDE4B-siRNA: 27 ± 14%, PDE4D-siRNA: 46 ± 7%).

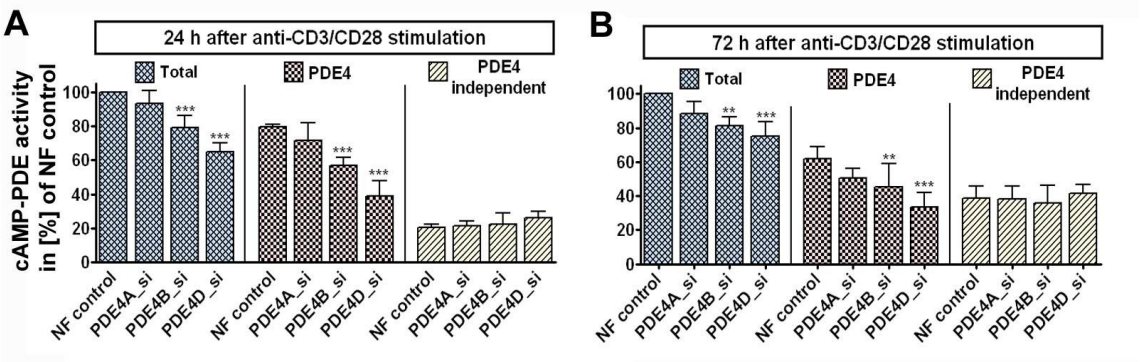

Figure 33. Protein activity knockdown in unstimulated and stimulated human primary CD4$^+$ T cells. PDE activity knockdown, induced by PDE4 subtype-specific siRNAs, in CD4$^+$ T cells 24 h (*A*) and 72 h (*B*) after anti-CD3/CD28 stimulation. Results are expressed as cAMP-PDE activity in [%] of the NF control, as mean ± SD of 3 donors. Significant differences between NF control and siRNA-transfected cells are indicated (**, $p < 0.01$; ***, $p < 0.001$; compared to NF control).

Considering that the individual PDE4 subtypes contribute quite differently to the overall PDE4 activity (see chapter 3.3), it is expected that PDE4A-siRNA will have the smallest effect on PDE4 activity whereas PDE4B- and PDE4D-siRNAs will have larger effects even when the individual subtypes are diminished to the same extent. Indeed, the collective effects of all individual PDE4-siRNAs sum up to about 90% both after 24 h and 72 h, indicating a pronounced efficacy of the siRNAs to downregulate their respective subtype. Taken together, the strategy to selectively knock down individual PDE4 subtypes in primary CD4$^+$ T cells was shown to be well tolerated, specific, and efficient. Because enzymatic activity was effectively reduced 72 h after stimulation but mRNA levels started to recover at the same time, the siRNA approach can be considered to be suitable for the application on functional T cell assays in a time period of up to 72 h.

3.7 Anti-CD3/CD28 induced release of cytokines and the effect of PDE inhibition on T cells

3.7.1 Time-dependent release of cytokines after anti-CD3/CD28 stimulation of CD4$^+$ T cells

To determine how human primary CD4$^+$ T cells functionally respond to different anti-CD3/CD28 stimulation conditions, levels of IL-2 (Figure 34*A*), IFN-γ (Figure 34*B*), and IL-5 (Figure 34C) were measured in supernatants of stimulated cells at different time points. In untreated cells (time point 0 h), cytokine levels were below the detection limit. After stimulation with different anti-CD3:anti-CD28 ratios, IL-2, IFN-γ, and IL-5 secretion was time-dependently upregulated, however, to a different extent and with different kinetics.

Strong stimulation with 3 µg anti-CD3/well and 3 µg anti-CD28/ml (= 3/3 stimulation) resulted in highest IL-2 levels with maximal concentrations of ~11 ng/ml after 48 h of stimulation (Figure 34*A*). Treatment with 0.3 µg anti-CD3/well and 3 µg anti-CD28/ml (= 0.3/3 stimulation) led to a faster upregulation but slightly lower peak concentrations of IL-2, when compared to the 3/3 stimulation. Because treatment with 3 µg anti-CD3/well and 0.3 µg anti-CD28/ml (= 3/0.3 stimulation) or with 0.3 µg anti-CD3/well and 0.3 µg anti-CD28/ml (= 0.3/0.3 stimulation) resulted in similar but overall lower IL-2 levels, anti-CD3/CD28 induced IL-2 secretion might be independent of the anti-CD3 strength, but dependent on the costimulatory anti-CD28 stimulus. Using the 3/0.3 stimulation, peak concentrations were reached at 48 h; using the 0.3/0.3 stimulation at 24 h. Treatment of $CD4^+$ T cells with anti-CD3 alone (= 3/0 stimulation or 0.3/0 stimulation) only weakly induced IL-2 secretion, confirming the anti-CD28 dependency of IL-2 induction. Remarkably, anti-CD3/CD28 induced IL-2 synthesis was transiently induced, because IL-2 levels declined at 72 h and 134 h after stimulation.

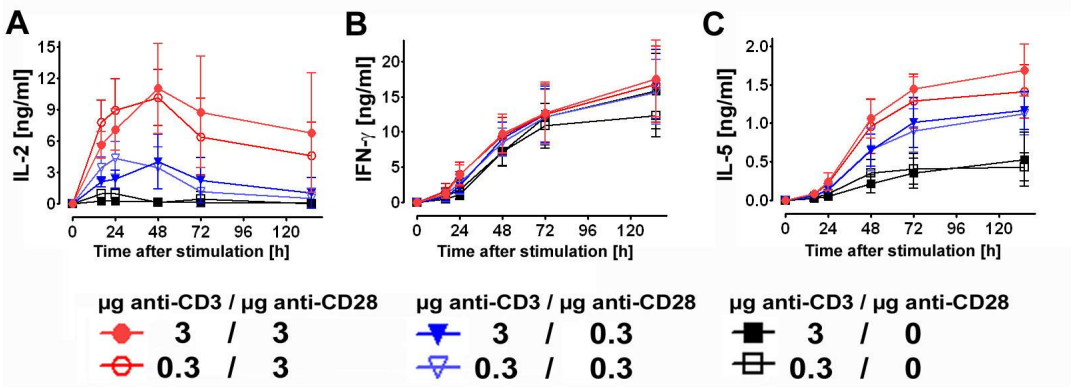

Figure 34. Time course of IL-2, IFN-γ, and IL-5 release after treatment of human primary $CD4^+$ T lymphocytes with different anti-CD3/CD28 concentrations. Shown is the time-dependent cytokine secretion of IL-2 (*A*), IFN-γ (*B*), and IL-5 (*C*) after stimulation of $CD4^+$ T cells with different stimulation conditions, as indicated. Supernatants were collected at different time points and cytokine concentrations were determined by enzyme-linked immunosorbent assays. Results are expressed as mean ± SD of 4 donors.

Compared to IL-2 secretion, IFN-γ synthesis was substantially induced at later time points, but was from 24 h onwards steadily upregulated and reached maximal levels at the end of the examined time period (12 - 17 ng/ml at 134 h) (Figure 34*B*). Because the measured IFN-γ concentrations were similar after treatment with different anti-CD3:anti-CD28 ratios, the upregulation of IFN-γ might be independent of the strength of the anti-CD3 stimulus and independent of the anti-CD28 costimulatory signal.

Similar to IFN-γ secretion, IL-5 release was substantially induced at later time points and was from 24 h onwards steadily upregulated with maximal levels at the end of the examined time period (0.4 - 1.7 ng/ml at 134 h) (Figure 34*C*). However, IL-5 cytokine levels were dependent on the costimulatory anti-CD28 signal: strong costimulation (3/3 and 0.3/3 stimulation, see above) caused highest IL-5 levels, whereas weaker costimulation (3/0.3 and 0.3/0.3

stimulation) resulted in lower IL-5 levels. IL-5 levels were lowest after stimulation with 3 µg or 0.3 µg anti-CD3/well alone.

3.7.2 Suppression of cytokine release and proliferation by PDE4 and/or PDE3 inhibition

To investigate how T cell functions are affected by PDE4 inhibition, $CD4^+$ T cells were treated with the panPDE4 inhibitor RP73401 (piclamilast). Additionally, the PDE3 inhibitor motapizone and both, piclamilast combined with motapizone, were included in the experiments because findings indicate that the effects of PDE4 inhibition can be enforced by simultaneous inhibition of PDE3 (Hatzelmann and Schudt, 2001). In order to compare the effects of PDE inhibitors with the effects of PDE4 subtype-specific siRNAs (see chapter 3.8), transfected cells were used for these experiments, but no siRNA was applied. After a 24 h resting period, transfected cells were stimulated with anti-CD3/CD28. To adjust the control conditions for DMSO concentrations, transfected cells were treated with 0.1% DMSO and the measured cytokine level and proliferation rate of these cells was set to 100%. As in all siRNA validation experiments in $CD4^+$ T cells (see chapter 3.6), the stimulation condition 0.3 µg anti-CD3/well and 0.3 µg anti-CD28/ml was used for all functional studies.

1 µM RP73401 (a maximum concentration that guarantees PDE4 selectivity) significantly inhibited anti-CD3/CD28 induced IL-2 release 24 h and 48 h after stimulation (mean ± SD = ~39 ± 12% and ~65 ± 16% inhibition, respectively), IFN-γ release 48 h and 72 h after stimulation (~45 ± 9% and ~52 ± 11% inhibition, respectively), and IL-5 release 72 h after stimulation (~43 ± 13% inhibition; Figure 35 second bars). Under these conditions, proliferation was also inhibited, but to a lesser extent (~13 ± 4% inhibition 66 h after stimulation). 10 µM motapizone (a maximum concentration that guarantees PDE3 selectivity) significantly inhibited anti-CD3/CD28 induced IL-2 release 24 h and 48 h after stimulation (~30 ± 13% and ~44 ± 11% inhibition, respectively), IFN-γ release 48 h and 72 h after stimulation (~25 ± 11% and ~31 ± 12% inhibition, respectively), and IL-5 release 72 h after stimulation (~28 ± 14% inhibition), but hardly affected proliferation (~6 ± 6% inhibition 66 h after stimulation; Figure 35 third bars). The combined application of both 1 µM RP73401 and 10 µM motapizone had drastic effects on anti-CD3/CD28 induced T cell functions and significantly inhibited IL-2 release 24 h and 48 h after stimulation (~85 ± 2% and ~91 ± 9% inhibition, respectively), IFN-γ release 48 h and 72 h after stimulation (~86 ± 7% and ~88 ± 7% inhibition, respectively), IL-5 release 72 h after stimulation (~89 ± 13% inhibition), and proliferation 66 h after stimulation (~50 ± 20% inhibition) to an extent being overall overadditive to the individual inhibition of PDE4 or PDE3 (Figure 35 fourth bars).

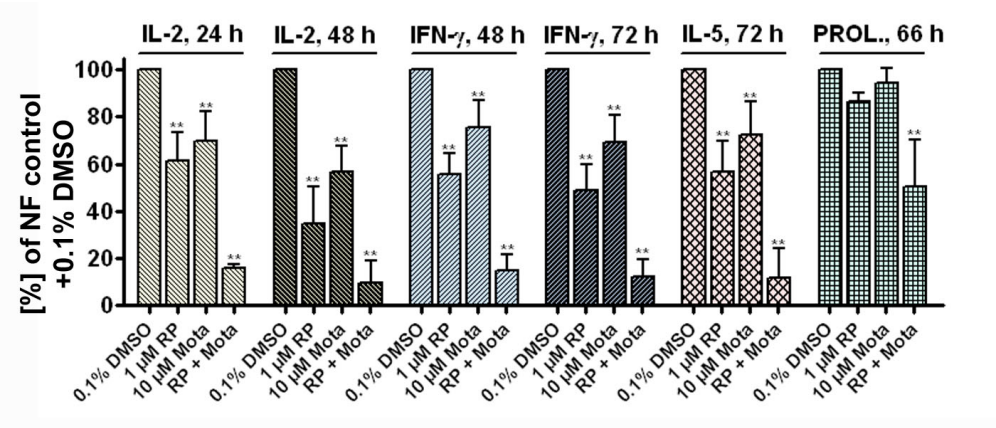

Figure 35. Suppression of CD4$^+$ T cell functions by PDE inhibition. Cells treated with the nucleofection procedure alone (NF control cells) were stimulated with 0.3 µg anti-CD3/well in combination with 0.3 µg anti-CD28/ml 24 h after nucleofection and cultured for the indicated periods of time either in the presence of 0.1% DMSO or additionally in the presence of 1 µM RP73401 (= RP, piclamilast), 10 µM motapizone (= Mota), or 1 µM RP73401 combined with 10 µM motapizone (= RP + Mota). Supernatants were collected and cytokine concentrations were determined by enzyme-linked immunosorbent assays. Alternatively, the proliferation rate was measured as detailed in *Materials and Methods*. Data are shown as mean ± SD (%) of 4 - 6 donors. Significance of differences is indicated: **, $p < 0.01$; compared to NF control (+ 0.1% DMSO).

3.7.3 Suppression of cytokine release and proliferation by Itk-specific siRNA

To ascertain how siRNAs can affect T cell functions, in addition to the application of PDE4 subtype-specific siRNAs (see chapter 3.8), control experiments were performed with siRNA specific for Itk (IL-2 inducible T cell kinase). Itk is a member of the Tec family kinases and has been shown to be involved in key regulatory signal pathways of T cell activation (Schwartzberg et al., 2005; Berg et al., 2005). Because T cells from mice deficient in Itk have a defective IL-2 secretion and an impaired TCR-mediated proliferation (Liao and Littman, 1995; Liu et al., 1998), siRNA targeting Itk was expected to have also a pronounced functional impact on these functional read-out parameters. The Itk-siRNA (Dharmacon) used in the present study was validated by Dr. O. Steinbach and J. Gilbert at the ALTANA Research Institute (Waltham, USA), who tested the Itk-siRNA for tolerability, efficacy, and off-target effects. The Itk-siRNA was shown to be specific, effective (~60 - 70% knockdown of both mRNA and protein), and well tolerated (personal communication). Thus, in the experiments performed in this study, Itk-siRNA served as positive control. In order to compare the effects of Itk-siRNA on T cell functions with the effects of the panPDE4 inhibitor RP73401 (see chapter 3.7.2), human primary CD4$^+$ T cells were nucleofected with non-targeting siRNA (NEG_si) or siRNA targeting Itk (Itk_si in Figure 36). After a 24 h resting period, transfected cells were stimulated with anti-CD3/CD28 for the indicated periods of time and IL-2 secretion and the proliferation rate were measured. To adjust for DMSO concentrations, transfected cells were treated with 0.1% DMSO. The measured cytokine level and proliferation rate of nucleofected control cells (no siRNA applied) was set to 100% (identical with first bar of respective read-out parameters in

Figure 35). Whereas 1.5 µM non-targeting siRNAs did not affect anti-CD3/CD28 induced cytokine release or proliferation, 1.5 µM Itk-siRNA significantly inhibited anti-CD3/CD28 induced IL-2 release 24 h and 48 h after stimulation (mean ± SD = ~74 ± 19% and ~63 ± 17% inhibition, respectively; Figure 36 fourth bars). Moreover, Itk-siRNA had anti-proliferative effects (~19 ± 13% inhibition 66 h after stimulation). Compared to the suppressive effects of the panPDE4 inhibitor RP73401 (identical with second bar of respective read-out parameters in Figure 35) on IL-2 release and proliferation, siRNA targeting Itk was similar effective (IL-2, 48 h and proliferation, 66 h) or even more effective (IL-2, 24 h) (Figure 36).

These experiments demonstrated that the application of the siRNA technique to human primary CD4$^+$ T cells is a powerful tool to study the functional significance of proteins in T cells.

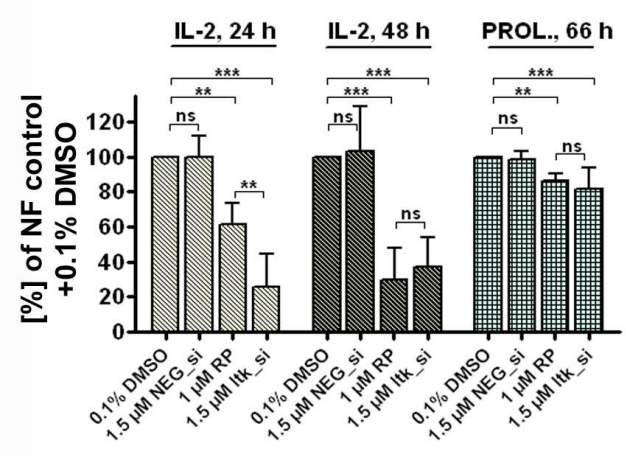

Figure 36. Suppression of CD4$^+$ T cell IL-2 release and proliferation by RP73401 and Itk-siRNA. Cells treated with the nucleofection procedure alone (NF control) were stimulated with 0.3 µg anti-CD3/well in combination with 0.3 µg anti-CD28/ml 24 h after nucleofection for the indicated periods of time either in the presence of 0.1% DMSO or additionally in the presence of 1 µM RP73401 (= RP, piclamilast). These data are identical to Figure 35 (first and second bars of functional read-out parameters). Alternatively, cells were nucleofected with 1.5 µM non-targeting siRNA (NEG_si) or with 1.5 µM siRNA targeting Itk (Itk_si) 24 h before stimulation. To adjust for DMSO concentrations, 0.1% DMSO was added to the siRNA-treated cells. Data are shown as mean ± SD (%) of 4 - 6 donors. Supernatants were collected and IL-2 concentrations were determined by enzyme-linked immunosorbent assays. The proliferation rate was measured as detailed in *Materials and Methods*. Significance of differences is indicated: ns, not significant; **, $p < 0.01$; ***, $p < 0.001$; compared to NF control (+ 0.1% DMSO) or Itk treatment compared to RP treatment.

3.8 Impact of PDE4 subtype-specific siRNAs on T cell functions

To ascertain which individual PDE4 subtype(s) mediate the inhibitory effect on T cell function, PDE4 subtype-specific siRNAs were nucleofected into human primary CD4$^+$ T cells. After a 24 h resting period, transfected cells were stimulated with anti-CD3/CD28. 1.5 µM non-targeting siRNA was used as control for statistical analysis (NEG_si). The functional impact of individual siRNAs on cytokine release (Figure 37, Figure 38, and Figure 39) and on cell proliferation (Figure 40) is reported in % of the RP73401 effect shown in Figure 35 (second bar

of experimental read-out parameters), which can be assumed to represent the maximal effect and was set therefore to 100%. Because additional application of the PDE3 inhibitor motapizone can enlarge the effects of PDE4 inhibition in an overadditive manner (see Figure 35, last column of experimental read-out parameters), all experiments were performed both in the absence and in the presence of 10 µM motapizone. The functional impact of individual siRNAs on cytokine release and on cell proliferation in the presence of motapizone is reported in % of the combined RP73401 and motapizone effect, which was set to 100% in these experiments.

The application of non-targeting siRNA (NEG_si in Figures) had no effect on any of the investigated functional read-out parameters. For better clarity, the individual effects of PDE4 subtype-specific siRNAs on T cell function will not only be reported in the following chapters, but will also be summarized in Table 10 (chapter 3.8.5, reported as mean ± SD).

3.8.1 Functional impact of PDE4 subtype-specific siRNAs on IL-2 release in $CD4^+$ T cells

Regarding IL-2 synthesis 24 h after stimulation, siRNA targeting PDE4A showed no significant inhibitory effect, however, knockdown of either PDE4B or PDE4D significantly suppressed anti-CD3/CD28 induced IL-2 release to an extent close to that observed with RP73401 (Figure 37*A*). Remarkably, the combined application of siRNAs targeting PDE4A, PDE4B, and PDE4D (PDE4_all_si), caused the most pronounced inhibitory effect on IL-2 release 24 h after stimulation. The additional application of motapizone qualitatively confirmed the effects of PDE4 subtype-specific siRNAs, however, the overall efficacy of the siRNAs to suppress IL-2 release 24 h after stimulation quantitatively decreased in the presence of motapizone when compared to the pronounced effects of the combined application of RP73401/motapizone (Figure 37*B*).

To study the functional effects of PDE4 subtype-specific siRNAs on IL-2 release at a later time point, cells were stimulated for 48 h. At this time point, the efficacies of PDE4 subtype-specific siRNAs to suppress anti-CD3/CD28 induced IL-2 release were overall less pronounced than the effects observed with 1 µM RP73401. However, whereas siRNA targeting PDE4A showed no significant inhibitory effect on IL-2 synthesis, knockdown of either PDE4B or PDE4D significantly suppressed anti-CD3/CD28 induced IL-2 release, with the combined application of all siRNAs being most effective (Figure 37*C*). Likewise to the experiments performed with the 24 h stimulation period, the additional application of motapizone qualitatively confirmed the individual effects of the applied PDE4-subtype specific siRNAs on IL-2 secretion 48 h after stimulation (Figure 37*D*).

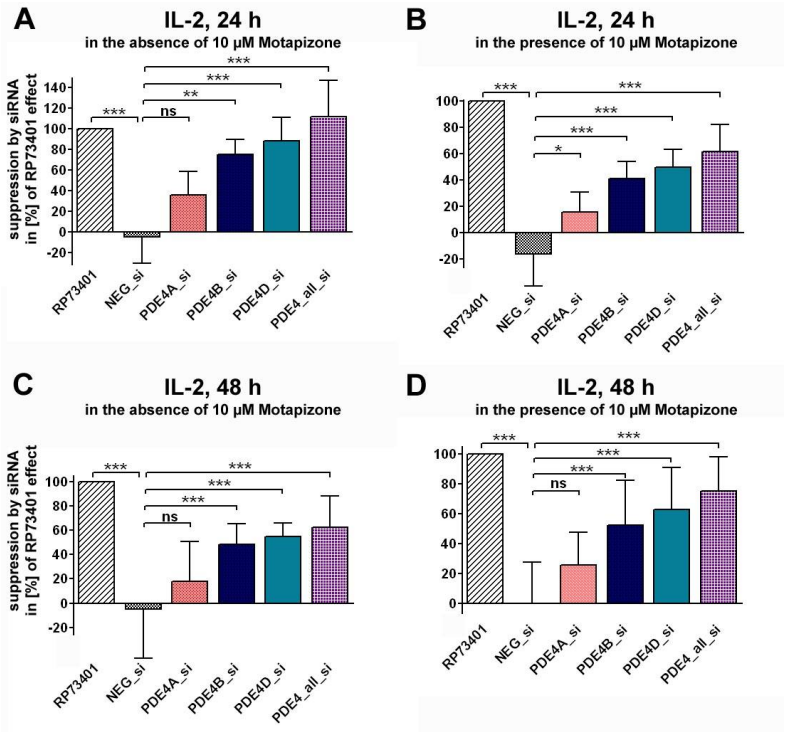

Figure 37. Suppression of anti-CD3/CD28 induced IL-2 synthesis by PDE4 subtype-specific siRNAs. 1.5 µM non-targeting siRNA (NEG_si) or PDE4 subtype-specific siRNAs were nucleofected into human primary $CD4^+$ T cells. Cells were left in culture for 24 h and were then stimulated with 0.3 µg anti-CD3/well in combination with 0.3 µg anti-CD28/ml. The siRNA-mediated suppression of IL-2 secretion after 24 h in the absence (*A*) or presence (*B*) of 10 µM motapizone and the siRNA-mediated suppression of IL-2 secretion after 48 h in the absence (*C*) or presence (*D*) of 10 µM motapizone is reported in % of the RP73401 effect. NEG_si, non-targeting control siRNA; PDE4_all_si, combined application of PDE4A_si, PDE4B_si, and PDE4D_si. Results are expressed as mean ± SD of 4 - 6 donors. Significance of differences is indicated: ns, not significant; *, $p < 0.05$; **, $p < 0.01$; ***, $p < 0.001$, compared to 1.5 µM NEG_si.

3.8.2 Functional impact of PDE4 subtype-specific siRNAs on IFN-γ release in $CD4^+$ T cells

Because substantial amounts of IFN-γ were only measured at later time points, the functional impact of PDE4 subtype-specific siRNAs on IFN-γ was investigated 48 h and 72 h after anti-CD3/CD28 stimulation. After stimulation for 48 h, siRNA targeting PDE4A and PDE4B had no significant inhibitory effect on IFN-γ release. In contrast, siRNA targeting PDE4D had a similar suppressive effect on IFN-γ synthesis than RP73401 (Figure 38*A*). However, the inhibitory effect of PDE4D-siRNA was increased by the combined application of all siRNAs. Although the overall efficacy of the PDE4 subtype-specific siRNAs quantitatively decreased by the additional application of motapizone, the predominant inhibitory effect of the siRNA targeting PDE4D was qualitatively confirmed (Figure 38*B*).

To ascertain whether the functional effects of PDE4 subtype-specific siRNAs on anti-CD3/CD28 induced IFN-γ generation were maintained for a longer time period, the experiments were repeated and cells were stimulated for 72 h. At this time point, similar results were observed than reported for the 48 h stimulation period. Whilst PDE4A-siRNA had again no significant inhibitory effect on IFN-γ release, PDE4B-siRNA had a slightly higher inhibitory

effect, and PDE4D-siRNA showed the most pronounced inhibitory effect on IFN-γ synthesis similar to RP73401 (Figure 38*C*). The combined application of all siRNAs was most effective in inhibiting IFN-γ release 72 h after stimulation. Considering the additional application of motapizone (Figure 38*D*), the results qualitatively confirmed the individual suppressive effects of the applied PDE4-subtype specific siRNAs on anti-CD3/CD28 induced IFN-γ synthesis observed in the absence of motapizone. However, the overall efficacies of the siRNAs decreased compared to the pronounced effect of RP73401 in combination with motapizone.

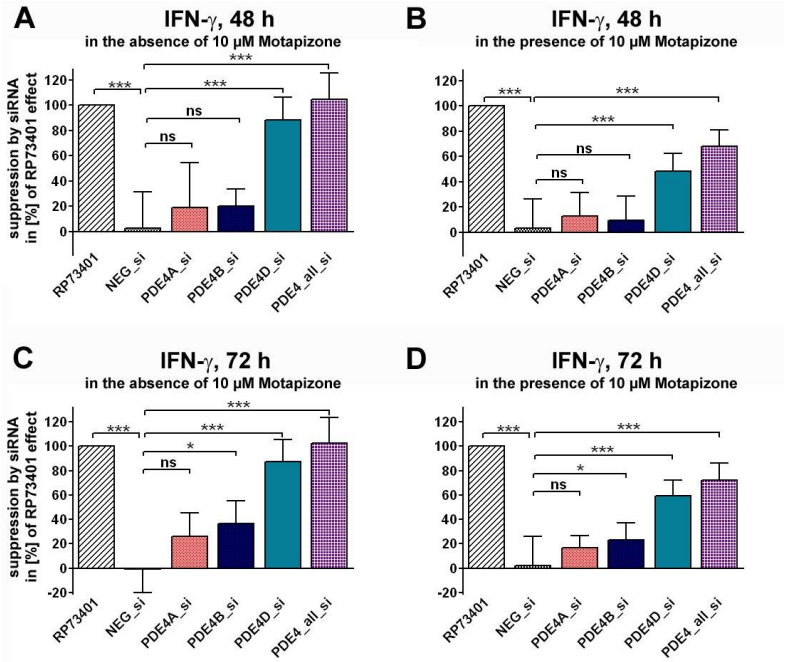

Figure 38. Suppression of anti-CD3/CD28 induced IFN-γ synthesis by PDE4 subtype-specific siRNAs. Experiments were performed as detailed in the legend of Figure 37, however, read-out parameters were the siRNA-mediated suppression of anti-CD3/CD28 induced IFN-γ secretion after 48 h in the absence (*A*) or presence (*B*) of 10 µM motapizone and after 72 h in the absence (*C*) or presence (*D*) of 10 µM motapizone. Results are expressed as mean ± SD of 5 - 6 donors. Significance of differences is indicated: ns, not significant; *, $p < 0.05$; ***, $p < 0.001$, compared to 1.5 µM NEG_si.

3.8.3 Functional impact of PDE4 subtype-specific siRNAs on IL-5 release in CD4$^+$ T cells

Although substantial amounts of IL-5 were measured in the supernatants of anti-CD3/CD28 stimulated human primary CD4$^+$ T cells at 48 h and 72 h (see Figure 34), the reported effects of the nucleofection procedure alone (see chapter 3.6.3) resulted in IL-5 levels that were at the detection limit at 48 h. Thus, the functional impact of PDE4 subtype-specific siRNAs on IL-5 release was only investigated at 72 h. At this time point, IL-5 synthesis was not significantly affected by the application of siRNAs targeting PDE4A and PDE4B, but was significantly inhibited by knockdown of PDE4D, to an extent close to that obtained with RP73401 (Figure 39*A*). The combined application of siRNAs targeting PDE4A, PDE4B, and PDE4D caused the most pronounced inhibitory effect on cytokine release. Whilst the combination of

RP73401 and motapizone was highly effective to suppress anti-CD3/CD28 induced IL-5 release, the combination of PDE4 subtype-specific siRNAs and motapizone was overall less effective (Figure 39*B*). However, the application of PDE4D-siRNA alone and the combined application of siRNAs were shown to significantly suppress IL-5 secretion in the presence of motapizone, which qualitatively confirmed the results obtained in the absence of motapizone.

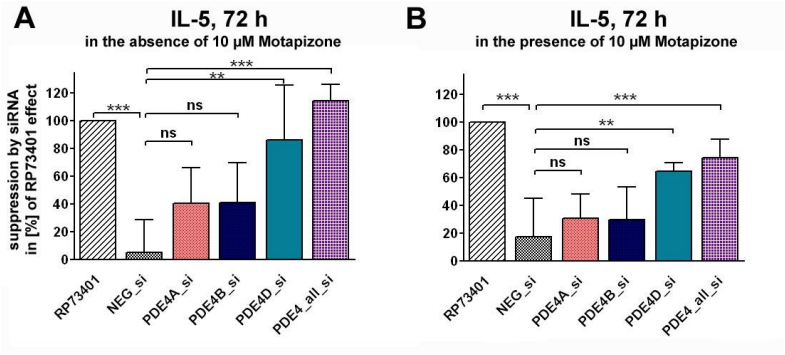

Figure 39. Suppression of anti-CD3/CD28 induced IL-5 synthesis by PDE4 subtype-specific siRNAs. Experiments were performed as detailed in the legend of Figure 37, however, read-out parameters were the siRNA-mediated suppression of anti-CD3/CD28 induced IL-5 secretion after 72 h in the absence (*A*) or presence (*B*) of 10 µM motapizone. Results are expressed as mean ± SD of 4 donors. Significance of differences is indicated: ns, not significant; **, $p < 0.01$; ***, $p < 0.001$, compared to 1.5 µM NEG_si.

3.8.4 Functional impact of PDE4 subtype-specific siRNAs on proliferation in $CD4^+$ T cells

Whereas in the latter experiments the determination of cytokine levels was taken as functional read-out parameter (as detailed in chapters 3.8.1 - 3.8.3), the functional impact of PDE4 subtype-specific siRNAs on anti-CD3/CD28 induced T cell proliferation was ascertained in the following set of experiments. Under the conditions applied, the relatively weak inhibitory effect of RP73401 on T cell proliferation after 66 h of anti-CD3/CD28 stimulation (compare Figure 35) was mimicked by PDE4D knockdown, whereas siRNA targeting PDE4A and PDE4B were hardly effective (Figure 40*A*). Furthermore, the addition of the latter two siRNAs to PDE4D-siRNA did not further increase the inhibitory effect on T cell proliferation. Although the additional application of motapizone qualitatively confirmed the effects of PDE4 subtype-specific siRNAs on proliferation 66 h after stimulation (Figure 40*B*), the overall anti-proliferative efficacy of the siRNAs quantitatively decreased in the presence of motapizone compared to the combined effects of RP73401 and motapizone.

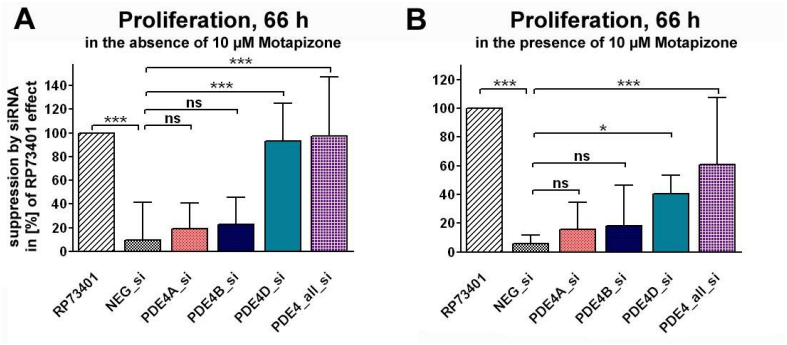

Figure 40. Suppression of anti-CD3/CD28 induced T cell proliferation by PDE4 subtype-specific siRNAs. Experiments were performed as detailed in the legend of Figure 37, however, read-out parameters were the siRNA-mediated suppression of anti-CD3/CD28 induced T cell proliferation ([^{3}H]-thymidine incorporation) after 66 h in the absence (*A*) or presence (*B*) of 10 µM motapizone. Results are expressed as mean ± SD of 6 donors. Significance of differences is indicated: ns, not significant; *, $p < 0.05$; ***, $p < 0.001$, compared to 1.5 µM NEG_si.

3.8.5 Summary: Impact of PDE4 subtype-specific siRNAs on T cell function

As detailed above (chapters 3.8.1 - 3.8.4), individual PDE4 subtype-specific siRNAs were shown to affect anti-CD3/CD28 induced T cell cytokine release (IL-2, IFN-γ, and IL-5) and T cell proliferation differently. For the purpose of clarity, the functional impact of the siRNAs was reported without the respective numerical values. To get a comprehensive overview of the experimental read-outs, the functional impact of individual siRNAs on cytokine release and on cell proliferation is summarized in Table 10.

Table 10. Summary of PDE4 subtype-specific, siRNA-mediated suppression of T cell functions[a]

		Mean suppression by siRNA in [%] of RP73401 effect ± SD (p-value)					
Parameter	Mota-pizone	NEG_si	PDE4A_si	PDE4B_si	PDE4D_si	PDE4_all_si	n
IL-2 (24 h)	no	-4.7 ± 25.7	35.5 ± 22.6 (ns)	75.1 ± 14.6 (**)	87.8 ± 23.1 (***)	111.3 ± 35.4 (***)	4
	yes	-16.0 ± 24.1	15.9 ± 15.0 (*)	41.0 ± 12.9 (***)	49.6 ± 13.9 (***)	62.0 ± 20.5 (***)	4
IL-2 (48 h)	no	-5.2 ± 40.1	17.8 ± 33.1 (ns)	48.4 ± 16.9 (***)	54.9 ± 11.4 (***)	62.5 ± 25.9 (***)	5
	yes	0.3 ± 27.2	25.8 ± 21.8 (ns)	52.5 ± 29.9 (***)	62.9 ± 28.3 (***)	75.3 ± 22.9 (***)	6
IFN-γ (48 h)	no	-7.0 ± 36.6	18.8 ± 35.6 (ns)	19.9 ± 13.9 (ns)	88.2± 18.4 (***)	105.5 ± 20.8 (***)	5
	yes	3.3 ± 22.9	12.9 ± 18.4 (ns)	9.5 ± 19.2 (ns)	48.6 ± 14.1 (***)	67.9 ± 13.2 (***)	6
IFN-γ (72 h)	no	-6.0 ± 24.7	26.1 ± 19.4 (ns)	36.8 ± 18.3 (*)	87.5 ± 18.0 (***)	102.4 ± 21.1 (***)	6
	yes	2.3 ± 23.6	16.6 ± 9.9 (ns)	23.2 ± 14.2 (*)	59.5 ± 12.4 (***)	72.2 ± 13.7 (***)	6
IL-5 (72 h)	no	-5.2 ± 23.7	40.5 ± 25.8 (ns)	41.2 ± 28.9 (ns)	86.3 ± 39.4 (**)	114.4 ± 12.1 (***)	4
	yes	17.6 ± 27.6	30.6 ± 17.6 (ns)	29.8 ± 23.5 (ns)	64.8 ± 5.8 (**)	74.6 ± 13.2 (***)	4
Proliferation (66 h)	no	9.4 ± 32.1	19.3 ± 21.7 (ns)	22.5 ± 23.4 (ns)	93.5 ± 31.4 (***)	97.3 ± 49.6 (***)	6
	yes	5.7 ± 6.2	15.9 ± 18.9 (ns)	18.3 ± 28.3 (ns)	40.5 ± 13.1 (*)	61.0 ± 46.4 (***)	6

[a] Human primary CD4$^+$ T cells were nucleofected with 1.5 µM non-targeting siRNA (NEG_si) or PDE4 subtype-specific siRNAs (PDE4A_si, PDE4B_si, or PDE4D_si, respectively). Additionally, PDE4A_si, PDE4B_si, and PDE4D_si siRNAs were applied in combination (PDE4_all_si). Cells were left in culture for 24 h and were then stimulated with 0.3 µg anti-CD3/well and 0.3 µg anti-CD28/ml. Besides, nucleofected cells (no siRNA applied) were treated with 0.1% DMSO or 1 µM RP73401 (see Figure 35). The siRNA-mediated suppression of T cell functions is reported in % of the RP73401 effect. In addition, 10 µM motapizone were included. For the latter experiments, the siRNA-effects are reported in % of the combined RP73401 and motapizone effect. Significance of differences is indicated: ns, not significant, $p > 0.05$; *, $p < 0.05$; **, $p < 0.01$; ***, $p < 0.001$, compared to 1.5 µM NEG_si.

4 DISCUSSION

One aim of this study was to clarify the time-dependent expression profile and regulation of the four PDE4 subtypes in human primary immune cells, such as $CD4^+$ T cells, $CD8^+$ T cells, monocytes, monocyte-derived macrophages, and monocyte-derived dendritic cells. Next, it was intended to validate an antisense- and a siRNA-mediated knockdown strategy to induce PDE4 subtype-specific mRNA and protein knockdown in the human lung adenocarcinoma epithelial cell line A549 and to transfer the superior strategy to human primary $CD4^+$ T cells. The final intension was to elucidate which PDE4 subtypes are of importance for immune cell functions such as T cell cytokine production and proliferation.

4.1 PDE4 subtype expression and regulation in human primary $CD4^+$ T cells

$CD4^+$ T helper cells play a key role as regulators of the immune system. A central task of $CD4^+$ T lymphocytes in initiating the adaptive immune response is the recognition of antigens, i.e., the interaction of the T cell antigen receptor (TCR) with a small foreign peptide bound to a cell surface protein of the class II histocompatibility complex (MHC II) expressed on an antigen-presenting cell (Davis and Bjorkman, 1988). Subsequently, released cytokines are potent mediators of immunity and inflammation (Larsen and Henson, 1983). Because $CD4^+$ T helper cells are essential cells in the orchestration of inflammatory cell responses (Tattersfield et al., 2002), are well-defined target cells for PDE4 inhibitors (Torphy, 1998; Souness et al., 2000), and can be transfected (Gresch et al., 2004), these cells were primarily addressed in the present study. Moreover, the functional relevance of individual PDE4 subtypes is largely unknown in $CD4^+$ T cells.

Primary $CD4^+$ T cells isolated from human whole blood by negative selection using magnetic bead cell separation were highly pure and showed low CD25 (IL-2 receptor α-chain) surface expression (see chapter 3.3.1). In general, CD25 expression can be attributed to a subpopulation of $CD4^+$ T cells that coexpress CD25 as surface marker, termed regulatory $CD4^+$ T cells (Sakaguchi et al., 1995), or to stimulated $CD4^+$ T cells (Taniguchi and Minami, 1993). The low CD25 expression that was observed indicates that only few regulatory T cells were in the isolated cell population and that other $CD4^+$ T cells were not stimulated by the isolation procedure. To activate resting $CD4^+$ T lymphocytes, TCR- and CD28-costimulation was used in order to closely mimic the physiological conditions relevant to human in the experiments (June et al., 1994; Chambers and Allison, 1999; Acuto et al., 2003). After anti-CD3 stimulation, CD25 surface expression of $CD4^+$ T cells was substantially upregulated.

However, the highest induction was observed when the cells were additionally treated with anti-CD28 antibodies, indicating that the upregulation of CD25 was dependent on costimulation. These findings are partly in agreement with a study of Liu and coworkers (Liu et al., 2001a), who reported an extensive upregulation of CD25 surface expression of human primary $CD4^+$ T cells after anti-CD3/CD28 stimulation, but no induction of CD25 surface expression after anti-CD3 stimulation alone. Because the upregulation of CD25 surface expression was a well defined and stable read-out parameter, cytometric analysis of CD25 expression was used in the present study to control the stimulation and activation status of $CD4^+$ T cells in the experiments.

4.1.1 PDE4 subtype mRNA expression and regulation in $CD4^+$ T cells

Using quantitative PCR, PDE activity assays combined with an immunoprecipitation protocol, and immunodetection experiments, it is demonstrated in this study that PDE4 subtypes are differently expressed in human primary $CD4^+$ T lymphocytes and are differentially regulated upon anti-CD3/CD28 stimulation.

Quantitative PCR (see chapter 3.3.2) revealed that *PDE4A*, *PDE4B*, and *PDE4D* mRNA are expressed in untreated $CD4^+$ T cells, whereas *PDE4C* was not detected, which is in agreement to an earlier report (Giembycz et al., 1996). The highest mRNA expression level was found for *PDE4D*, followed by *PDE4B* and *PDE4A*, the latter having a substantially lower expression level. These findings are partly in accordance with earlier studies based on semi-quantitative PCR experiments. Whereas Landells and coworkers (Landells et al., 2001) found high *PDE4D* mRNA expression in $CD4^+$ T cells, Gantner et al. (Gantner et al., 1997b) found *PDE4B* expression levels above *PDE4A*, but could not detect a substantial amount of *PDE4D*. Upon anti-CD3/CD28 stimulation, a time-dependent upregulation of *PDE4A*, *PDE4B*, and *PDE4D* mRNA expression was detected in the present study. Whereas *PDE4A* and *PDE4D* were upregulated within five days with the highest expression levels at 120 h (the latest time point measured), *PDE4B* only showed a transient upregulation with highest levels 16 - 24 h after stimulation. Although no comprehensive PDE4 subtype expression study with highly pure $CD4^+$ T cells has been reported to date, the induction of PDE4 subtypes observed in the present report is partly in agreement with other studies. Seybold and coworkers (Seybold et al., 1998) revealed an increase in PDE4 expression in mixed $CD4^+$ and $CD8^+$ T cells after treatment with fenoterol or 8-Bromo-cAMP, which caused an upregulation of *PDE4A* and *PDE4D* mRNA. Similarly, phytohemagglutinin, dibutyryl-cAMP, and 1-methyl-3-isobutylxanthine induced *PDE4A* and *PDE4D* mRNA in human peripheral blood lymphocytes (Jiang et al., 1998). In contrast, one study (Kanda and Watanabe, 2001) reported that phytohemagglutinin or anti-CD3/CD28 stimulation increased PDE4 activity 30 min after stimulation, but did not elevate *de novo* mRNA expression. Contrary to the present report, the

latter study did use a mixed $CD4^+$ and $CD8^+$ T cell population, another stimulation protocol, shorter stimulation periods, and a semi-quantitative PCR strategy.

Because different stimulation conditions can impact the efficacy of PDE4 inhibitors (unpublished observations of Dr. Hatzelmann, ALTANA Pharma AG, Konstanz), it was elucidated whether PDE4 subtypes are differently expressed and regulated in response to a wide array of anti-CD3 and anti-CD28 concentrations (see chapter 3.3.3). The time-dependent expression and regulation of PDE4 subtypes in $CD4^+$ T cells were not found to be influenced by the strength of the anti-CD3 stimulus nor the costimulatory anti-CD28 signal. Obviously, the above-described PDE4 subtype mRNA regulation can be induced by anti-CD3 stimulation alone as well as by medium and strong costimulation conditions. Thus, the susceptibility of PDE4 inhibitors to different anti-CD3/CD28 stimulation conditions cannot be explained on the level of PDE4 subtype mRNA expression.

Human primary $CD4^+$ T cells are a heterogeneous group of different subpopulations, among them naïve and memory T cells, which are distinguished by their surface markers CD45RA and CD45RO, respectively (Bell et al., 1998). These two subpopulations can be separated rather easily and in sufficient amounts. Considering the generally lower activation threshold dedicated to memory effector T cells (Lanzavecchia and Sallusto, 2000), it was asked whether PDE4 subtypes are differentially regulated in these two subpopulations. Although a marginally higher PDE4 subtype expression and a slightly faster and more pronounced induction of individual PDE4 subtypes in memory $CD4^+$ T cells was found, these differences were statistically not significant between naïve and memory T cells (see chapter 3.3.4). These findings indicate that naïve and memory $CD4^+$ T cells express the same set of PDE4 subtypes, and that PDE4 subtypes are similarly regulated after anti-CD3/CD28 stimulation. These findings are in line with a microarray study, in which Lui and coworkers (Liu et al., 2001a) analyzed over 54000 cDNAs and observed that similar numbers of transcripts were expressed in memory and naïve $CD4^+$ T cells at rest and after 16 h of anti-CD3/CD28 activation. However, the increase in mRNA levels of upregulated genes after anti-CD3/CD28 stimulation was greater in memory than in naïve $CD4^+$ T cells. Although *PDE4A* and *PDE4B* mRNA expression were substantially upregulated in the present study, this induction was not determined in the study by Liu, demonstrating that transcriptome-wide microarrays cannot substitute individual quantitative PCR experiments. Considering the similar expression and regulation of PDE4 subtypes both in naïve and memory $CD4^+$ T cells, it was decided to perform all further experiments with $CD4^+$ T cells not further purified into different subpopulations.

4.1.2 Protein activity of PDE4 subtypes in $CD4^+$ T cells

To ascertain whether the induction of PDE4 subtypes observed in quantitative PCR experiments translates in an increase in PDE4 enzyme activity, cAMP hydrolyzing PDE activity assays were performed (see chapter 3.3.5). After stimulation with anti-CD3/CD28, total cAMP hydrolyzing PDE activity increased time-dependently during the examined time period (0 - 120 h). The increase in total PDE activity was based on a pronounced upregulation of PDE4 activity, whereas PDE4 independent activity decreased 24 h after stimulation, was recovered to baseline levels 72 h after stimulation, and was only slightly increased at 120 h after stimulation. The PDE4 independent activity might be composed of several isoforms of cAMP-hydrolizing PDE families, of which PDE1, PDE3, PDE7, and PDE8 were described to be expressed in T cells (Schudt et al., 1995; Giembycz et al., 1996; Li et al., 1999; Glavas et al., 2001). The 'long-term' induction of PDE4 activity upon stimulation of T cells was also shown by others (Seybold et al., 1998). In contrast, one study (Kanda and Watanabe, 2001) reported that anti-CD3/CD28 stimulation increased PDE4 activity on a 'short-term' basis (30 min), but did not elevate *de novo* PDE4 protein. Long- and short-term regulation processes of PDE4 subtypes will be further discussed in chapter 4.1.4.

With the intension to assign the observed increase in PDE4 activity to the protein activities of individual PDE4 subtypes, PDE4 subtypes were immunoprecipitated with antibodies recognizing PDE4A, PDE4B, or PDE4D prior to activity assays (see chapter 3.3.5). Immunoprecipitation with these antibodies is a well-established technique in the laboratory of Prof. Conti (Stanford University School of Medicine, Stanford, USA) (Iona et al., 1998; Ariga et al., 2004; Jin et al., 2005). In order to test this immunoprecipitation technique in lysates of human primary $CD4^+$ T cells, a research training was carried out at the laboratory of Prof. Conti and the technique was transferred to ALTANA Pharma AG, Konstanz. Immunoprecipitation experiments revealed that in untreated $CD4^+$ T cells PDE4D had the predominant activity, followed by PDE4B activity, and lower levels of PDE4A activity. After anti-CD3/CD28 stimulation, PDE4A activity was greatly induced starting at 72 h, whereas PDE4B activity was transiently upregulated with highest activity 24 h after stimulation. PDE4D activity remained relatively constant during the first 48 h after stimulation, but increased at the end of the examined time period (72 h and 120 h). In general, the time-dependent PDE4 activity profiles determined in the present study measured by PDE4 subtype-specific immunoprecipitations closely resembled the PDE4 expression profiles found for mRNA levels measured by quantitative PCR. A time delay between changes of mRNA levels and enzyme activities was observed as expected since protein synthesis is subsequent to mRNA transcription. However, some differences were observed in the extent of mRNA and activity upregulation. Whereas *PDE4A* showed an approx. 15-fold induction and *PDE4D* an approx. 4-fold induction on mRNA level, PDE4 activities increased only 4-fold and 1.5-fold, respectively. In contrast, upregulation

of PDE4B activity was more pronounced than *PDE4B* mRNA upregulation (3.4-fold versus 2-fold). Whereas results by quantitative PCR directly reflect the number of mRNA molecules in the cell, PDE activity is not only influenced by the amount of the enzyme but also by other parameters such as phosphorylation and protein-protein interactions (see chapters 4.1.4 and 4.8). Therefore, changes on the mRNA level may not quantitatively reflect the changes in enzymatic activity. Taken together, PDE activity assays combined with an immmunoprecipitation protocol revealed that PDE4 subtypes have distinct protein activities that are differentially regulated after anti-CD3/CD28 stimulation in human primary $CD4^+$ T cells. Collectively, PDE4-subtype specific enzyme activities qualitatively resembled the determined mRNA expression profile in these cells.

4.1.3 Protein expression of PDE4 subtypes in $CD4^+$ T cells

Although the primary goal of the study was to analyze the different PDE4 subtypes, it was also assessed whether the observed subtype expression patterns can be attributed to certain splice variants (see chapter 3.3.6). Proteins of different lengths were detected in immunodetection experiments, indicating that multiple splice variants are expressed for each individual subtype. In untreated T cells, the antibody directed against PDE4A detected two bands, presumably corresponding to short and long forms of PDE4A. However, after stimulation, no increase of the amount of protein was observed. Since the induction of immunoprecipitated PDE4A activity is in good agreement with the upregulation of *PDE4A* mRNA, it may be possible that the antibody used for immunodetection experiments, which was different from the antibody used for immunoprecipitation, may not have detected all expressed PDE4A splice variants. Whereas for PDE4A this discrepancy was found between the mRNA and enzyme activity data versus the immunodetection data, the corresponding data sets were in good agreement for the PDE4B and PDE4D subtypes. If one considers the two prominent bands (slightly above 100 kDa and at ~75 kDa) displayed by the PDE4B antibody, an increase in the overall PDE4B protein amount 24 h after stimulation is comprehensible. A reduction is obvious at later time points. For PDE4D a clear induction is found for the proteins 60 - 75 kDa in size. Most remarkably, the different splice variants detected for PDE4B and PDE4D are not regulated uniformly. Especially, the immunoblot of PDE4B displays a time-dependent reduction of PDE4B long form(s) paralleled by a pronounced transient upregulation of the PDE4B short form. The immunoblot of PDE4D shows PDE4D long forms above 85 kDa in size, which are rather unaffected after stimulation. The detected proteins of 60 - 75 kDa in size may represent PDE4D short forms, which are clearly upregulated after stimulation. Whereas others used an antiserum recognizing all PDE4 isoenzymes with a preference for PDE4A splice variants and could only detect few PDE4 splice variants (Seybold et al., 1998), the application of PDE4 subtype-specific antibodies in the present study allowed the detection of several PDE4 splice

variants for each PDE4 subtype. Taken together, the immunoblots supplement the PCR and enzyme activity results. In addition, the data highlight that multiple splice variants further increase the complexity in the regulation of PDE4 subtypes in $CD4^+$ T cells.

4.1.4 Long- and short-term regulation of PDE4 subtypes

The present study indicates that PDE4 subtypes show a stimuli-induced transcriptionally upregulation of *PDE4A*, *PDE4B*, and *PDE4D* mRNA transcripts in $CD4^+$ T cells within different time periods (0 - 120 h examined). Transcriptional upregulation of PDE4 subtypes was first described by Conti and coworkers (Swinnen et al., 1989b). They observed a strong, long-term transcriptional upregulation of *PDE4* mRNA in rat sertoli cells after FSH or dibutyryl-cAMP stimulation, pointing to the presence of intronic cAMP- and hormone inducible promoters, as were found for *PDE4D1* and *PDE4D2* transcripts (Vicini and Conti, 1997). Le Jeune et al. identified a CRE- (cAMP-response element) containing, isoform specific promoter in *PDE4D5*, which is responsible for the cAMP-driven upregulation of *PDE4D5* in human airway smooth muscle cells (Le Jeune et al., 2002). Likewise, CREB was shown to regulate the short *PDE4B2* promoter in cortical neurons (D'Sa et al., 2002). In the *PDE4A* gene, Rena and co-workers described gene motifs with promoter-like activity (Rena et al., 2001). Because the present study shows transcriptional upregulation of *PDE4A*, *PDE4B*, and *PDE4D* mRNA, which resulted in increased PDE4 enzyme expression and activities in human primary $CD4^+$ T cells, several of the above described promoter-activities may also be involved in the regulation of PDE4 subtypes in human primary immune cells.

In addition to long-term regulation mechanism, short-term activation processes for PDE4 subtypes were described via PKA-dependent phosphorylation within minutes, providing quick negative feedback regulation in respond to cAMP stimuli (Sette and Conti, 1996; Ekholm et al., 1997; MacKenzie et al., 2002; Laliberte et al., 2002). Whereas a PKA phosphorylation site was found for all PDE4 long forms at the N-terminal end of UCR1, short forms of PDE4 lack this phosphorylation site. Additionally, ERK phosphorylation was shown to control PDE4B, PDE4C, and PDE4D long and short forms, by either inhibiting (long forms) or activating (short forms) PDE4 isozymes (Baillie et al., 2000). Recently, a novel phosphorylation site was found for the long PDE4D3 splice variant using PDE4D3-transfected COS cells. Phosphorylation of this site leads to an activation in response to oxidative oxygen species in these cells (Hill et al., 2006). In human primary T cells, Taskén and coworkers (Abrahamsen et al., 2004) confirmed that anti-CD3/CD28 stimulation activates PKA and increases PDE4 activity within 2 min, a process that was already described earlier (Kanda and Watanabe, 2001). In the present study, the action of PKA or ERK on PDE4 phosphorylation was not examined. Considering that the protein data obtained in human primary $CD4^+$ T cells qualitatively resemble the mRNA profile,

observed changes in PDE4 activity are likely at least in part the result of transcriptional induction of PDE4 subtypes.

By evaluating the comprehensive expression data, one can imply that the different expression levels of the PDE4 subtypes in untreated $CD4^+$ T cells and their different induction upon stimulation may have distinct effects on the regulation of T cell functions. For example, the high expression and activity level of PDE4D at all examined time points (0 - 120 h) may provide a constitutive high cAMP hydrolyzing capacity. PDE4B might be involved in regulating early T cell activation, because PDE4B mRNA and activity showed a substantial but only transient upregulation. Remarkably, PDE4A had the most pronounced x-fold upregulation of both mRNA and activity. This induction of PDE4A was highest 120 h after stimulation and may thus be involved in undefined long-term processes, which are beyond the scope of the examined time window.

4.2 PDE4 subtype expression and regulation in human primary $CD8^+$ T cells

Besides the effects on $CD4^+$ T lymphocytes, PDE4 inhibitors have also been shown to effect other immune cells such as $CD8^+$ T lymphocytes (Giembycz et al., 1996; Souness et al., 2000). $CD8^+$ T cells (cytotoxic T lymphocytes) are important mediators of adaptive immunity against viral, protozoan, and bacterial pathogens and participate in the elimination of transformed cells (Harty et al., 2000). Although still controversially discussed, it has been recognized that $CD8^+$ T cells may also be important contributors to the development of allergic responses in the lung (O'Sullivan et al., 2001; Gelfand and Dakhama, 2006). Furthermore, $CD8^+$ T cells were shown to be implicated in the pathogenesis of COPD (Barczyk et al., 2006).

In the present study, the expression and regulation of PDE4 subtypes in human primary $CD8^+$ T cells was elucidated using a quantitative PCR strategy. It was demonstrated that PDE4 subtypes are differently expressed in human primary $CD8^+$ T lymphocytes and are differentially regulated upon anti-CD3/CD28 stimulation (see chapter 3.4.1). Quantitative PCR data revealed that *PDE4A*, *PDE4B*, and *PDE4D* mRNA are expressed in untreated $CD8^+$ T cells, whereas *PDE4C* was not detected, which confirms an earlier report (Giembycz et al., 1996). The highest mRNA expression levels were found for *PDE4B* and *PDE4D*, whereas *PDE4A* had a substantial lower expression level. Compared to resting $CD4^+$ T cells, the basal expression level of *PDE4* subtypes in resting $CD8^+$ T cells was similar. These findings are partly in accordance with earlier studies based on semi-quantitative PCR experiments. Both Gantner et al. (Gantner et al., 1997b) and Landells et al. (Landells et al., 2001) found *PDE4A*, *PDE4B*, and *PDE4D* expression in human primary $CD8^+$ T cells. However, in the latter study, overall lower *PDE4* subtype mRNA expression in $CD8^+$ T cells was found when compared to

$CD4^+$ T cells. Upon anti-CD3/CD28 stimulation, a time-dependent upregulation of *PDE4A*, *PDE4B*, and *PDE4D* mRNA expression was detected, which was similar to the regulation of PDE4 subtypes in anti-CD3/CD28 treated $CD4^+$ T cells (as discussed in chapter 4.1.1). Whereas *PDE4A* and *PDE4D* were upregulated with the highest expression levels at 84 h (the latest time point measured), *PDE4B* only showed a transient upregulation with highest levels 16 - 24 h after stimulation. The induction of PDE4 subtypes upon stimulation of T cells shown in the present report is partly in agreement with other studies, where mixed $CD4^+$ and $CD8^+$ T cells were used (Seybold et al., 1998; Jiang et al., 1998; Kanda and Watanabe, 2001), as discussed in chapter 4.1.1. The notion that a higher intersubject variability was observed in $CD8^+$ T lymphocytes (Landells et al., 2001) was confirmed in the present study. As for PDE4 expression profiles in $CD4^+$ T cells, no comprehensive study using highly pure $CD8^+$ T cells for quantitative PCR experiments has been reported to date.

Evaluation of the expression data obtained in $CD8^+$ T cells concludes that the different PDE4 subtypes are similarly expressed in $CD4^+$ and $CD8^+$ T cells and are similarly regulated after anti-CD3/CD28 stimulation. These findings support the observation that $CD4^+$ and $CD8^+$ T cells, although differently affecting airway inflammation, are equally sensitive to PDE4 inhibition (Tenor et al., 1995b), and confirm the concept that $CD4^+$ and $CD8^+$ T cells may be equally sensitive targets for the effects of PDE4 inhibitors.

4.3 PDE4 subtype expression and regulation in human primary monocytes, macrophages, and dendritic cells

Because human primary monocytes, macrophages, and dendritic cells are crucial cellular components of the immune system that are affected by PDE4 inhibition (Giembycz et al., 1996; Souness et al., 2000), the expression and regulation of PDE4 subtypes in these immune cells was elucidated by quantitative PCR experiments.

4.3.1 PDE4 subtype mRNA expression in monocytes

Monocytes are potent producers of the pro-inflammatory cytokine TNF-α (Beutler and Cerami, 1988). Before migration into organs and differentiation into macrophages or dendritic cells, monocytes circulate in the blood and highly express the surface marker CD14, which is involved in the recognition of bacterial lipopolysaccharide (LPS) by the innate immune system (Triantafilou and Triantafilou, 2002). Human primary monocytes can be isolated in sufficient amounts from peripheral blood either by negative or by positive selection.

In the present study, negative isolation was initially performed to avoid potential activation signals possibly mediated by paramagnetic antibody binding. However, monocytes obtained by negative selection were less pure than monocytes isolated by positive selection using anti-

CD14 paramagnetic antibodies, which is a common caveat of negative isolation protocols (Gonzalez-Barderas et al., 2004). Because a microarray study (Gruetzkau et al., 2003) did not detect significant changes in overall mRNA expression levels between negatively and positively separated monocytes and because positive isolation had no effect on experimental read-outs in the present study, the latter isolation procedure was favored. To additionally increase the purity of monocyte preparations, isolated cells were left to adhere on culture dishes and non-adherent cells were removed.

Quantitative PCR data revealed that *PDE4A*, *PDE4B*, and *PDE4D* mRNA were expressed in untreated $CD14^+$ cells, whereas *PDE4C* mRNA was not detected (see chapter 3.4.2). In contrast to $CD4^+$ and $CD8^+$ T cells, the highest mRNA expression level in monocytes was found for *PDE4B*, followed by *PDE4A* and substantially lower levels of *PDE4D.* These observations in resting monocytes confirm semiquantitative RT-PCR results (Gantner et al., 1997b; Wang et al., 1999; Heystek et al., 2003), but are in variance to reports that showed predominant levels of *PDE4A* mRNA (Souness et al., 1996) or failed to detect *PDE4D* mRNA in human monocytes (Ma et al., 1999). Another study found low *PDE4C* mRNA expression in monocytes (Barber et al., 2004). In the present study, quantitative PCR experiments demonstrated that the overall expression level in resting monocytes was higher than in resting $CD4^+$ and $CD8^+$ T cells, suggesting an overall higher PDE4 enzyme expression in monocytes compared to T cells. Indeed, PDE4 activity analysis revealed higher PDE4 activities in resting monocytes than in T lymphocytes (Schudt et al., 1995; Gantner et al., 1997a; Gantner et al., 1997b).

4.3.2 PDE4 subtype mRNA expression in monocyte-derived macrophages (MoMϕ)

Whereas monocytes are mostly found in the peripheral blood, macrophages are located in tissues and may act directly at the site of inflammation. As a critical cellular source of TNF-α and other inflammatory mediators, alveolar macrophages have been recognized to play a pivotal role in the pathophysiology of COPD (Barnes et al., 2003; Barnes, 2003a). Because it is considerable elaborative to obtain human primary alveolar macrophages, *in vitro* monocyte-derived macrophages have been used to study the effects of PDE4 inhibition on macrophages (Gantner et al., 1997a). Interestingly, by application of human AB serum to the medium, the high PDE4 activity found in human primary monocytes decreased if differentiated into monocyte-derived macrophages (MoMϕ), which acquired a PDE profile very similar to that of alveolar macrophages (Tenor et al., 1995a; Gantner et al., 1997a).

In the present study, it was asked whether the reduction of PDE4 activity during differentiation is reflected in the amount of expressed PDE4 mRNAs. Thus, quantitative PCR experiments were performed with monocytes that were differentiated to MoMϕ (see chapter 3.4.2). In these macrophages (kept in culture for about one week), the expression profile was different from the

expression pattern observed in monocytes. *PDE4A*, *PDE4B*, and *PDE4D* mRNA were expressed in MoMϕ, whereas *PDE4C* mRNA was not significantly detected. The highest mRNA expression level was found for *PDE4A*, followed by very low levels of *PDE4B* and *PDE4D* mRNA. Obviously, during differentiation, *PDE4B* was substantially downregulated, whereas *PDE4A* and *PDE4D* mRNA expression were less affected. After LPS stimulation, only *PDE4B* mRNA was significantly upregulated, indicating that PDE4B is likely the only LPS-inducible PDE4 subtype in macrophages. These observations expand the proposition of Wang and coworkers, which implicated a specific role of PDE4B in monocytes (Ma et al., 1999; Wang et al., 1999). Interestingly, the latter study demonstrated that the short PDE4B2 form was responsible for this induction. The functional relevance of these observations will be further discussed in chapter 4.6.

4.3.3 PDE4 subtype mRNA expression in monocyte-derived dendritic cells (MoDCs)

Whilst macrophages can be derived from human primary monocytes without the application of exogenous cytokines, addition of GM-CSF and IL-4 initiates *in vitro* the differentiation of monocytes to cells with the phenotype and characteristics of immature dendritic cells (Sallusto and Lanzavecchia, 1994; Gantner et al., 1999). Because the frequency of human primary dendritic cells in peripheral blood is very low (Thomas et al., 1993; O'Doherty et al., 1993), monocyte-derived dendritic cells (MoDCs) are largely used, although the functional repertoire of MoDCs obtained with this differentiation protocol may be incomplete (Thurnher et al., 2001; Soruri and Zwirner, 2005). As professional antigen-presenting cells, dendritic cells are critical regulators for the induction of primary immune responses and the immunological tolerance: Immature dendritic cells reside in tissues, where they capture antigens. Afterwards, they can migrate to lymphoid organs and differentiate to mature dendritic cells (Banchereau and Steinman, 1998; Banchereau et al., 2000). Mature dendritic cells secrete large amounts of proinflammatory mediators and are capable to stimulate T cells. The analysis of CCR7 and CD83 surface expression are good markers for determination of the maturation status (Sallusto et al., 1998; Lechmann et al., 2002).

In the present study, *in vitro* monocyte-derived immature dendritic cells (immature MoDCs, kept in culture for about one week) showed low levels of CCR7 and CD83 surface expression, which were upregulated after 44 h of LPS stimulation, indicating that the cells differentiated into matured dendritic cells (see chapter 3.4.3). Because PDE4 activity was shown to be decreased in human MoDCs when compared to freshly isolated human primary monocytes (Gantner et al., 1999), it was tested in the present study whether the amount of expressed PDE4 subtype mRNAs was decreased as well. Quantitative PCR revealed that *PDE4A*, *PDE4B*, and *PDE4D* mRNA were expressed in immature MoDCs, whereas *PDE4C* mRNA was not detected. Overall, the PDE4 expression levels in MoDCs were similar to the

expression profile obtained in MoMϕ (as discussed in chapter 4.3.2). The highest mRNA expression level was found for *PDE4A*, followed by very low levels of *PDE4B* and *PDE4D* mRNA. These findings indicate that *PDE4B* was substantially downregulated during differentiation, whereas *PDE4A* and *PDE4D* mRNA expression were less affected. After LPS stimulation, *PDE4B* mRNA was significantly upregulated in mature monocyte-derived dendritic cells, pointing to PDE4B as the only subtype that is LPS-inducible, as was proposed for monocytes (Ma et al., 1999; Wang et al., 1999). As indicated previously, the relevance of these observations for cell function will be further discussed in chapter 4.6.

4.4 Application of mRNA knockdown strategies

As discussed in the previous sections, PDE4 subtypes are differently expressed in human primary immune cells and are differentially regulated after stimulation. Thus, several PDE4 subtypes may play critical and specific roles in inactivating cAMP action and may be involved in potentiating various cell responses by attenuating the negative constraint of cAMP. Indeed, the anti-inflammatory and immunomodulatory effect of PDE4 inhibitors is well described (Torphy, 1998; Souness et al., 2000). However, current PDE4 inhibitors do not discriminate between individual PDE4 subtypes, although several findings indicate that individual PDE4 subtypes may influence cell functions differently. Due to the lack of PDE4 subtype-specific small molecule (SMOL) inhibitors, the functional impact of individual PDE4 subtypes in immune cells cannot be assessed pharmacologically. However, because several mRNA knockdown techniques have been shown to effectively degrade mRNA and to subsequently suppress protein amount and activity of targeted genes, it was asked whether the application of antisense-constructs or siRNAs are reliable approaches to degrade PDE4 subtypes on a molecular basis in the present study. Initial knockdown experiments were performed in the human lung adenocarcinoma epithelial cell line A549, because A549 cells are available in large amounts, have a high PDE4 subtype expression, and can be transfected comparatively easily with cationic lipids. Furthermore, it was intended to transfer the superior knockdown technique (antisense or siRNA) to human primary $CD4^+$ T cells.

4.4.1 Lipofection of A549 cells with antisense-constructs

Antisense constructs applied in the present report were either first generation (AS^{1st}) or second generation (AS^{2nd}) antisense constructs directed against individual PDE4 subtypes. AS^{1st} constructs used in this study were phosphorothioate oligodeoxynucleotides, i.e., single stranded DNA-oligonucleotides of different lengths (17 - 21 bases) that were chemically modified to have a nonbridging oxygen atom of the DNA backbone phosphate group replaced

by a sulfur atom (Stein and Narayanan, 1994). Besides steric inhibition of the translation apparatus, target cells were shown to recognize DNA-mRNA hybrids, leading to subsequent degradation of targeted mRNA by RNAse H activation and cleaving of the DNA-mRNA hybrid (Crooke et al., 1995; Giles et al., 1995b). Phosphorothioates were shown to possess nuclease resistance and water solubility, to induce strong RNAse H activation and specific mRNA knockdown, and to have clinical relevance in molecular therapies (Alama et al., 1997; Patil et al., 2005). However, reports about immune stimulatory effects and other undesirable effects such as high protein binding capacities (Benimetskaya et al., 2004) have led to the development of second generation chimeric antisense (AS^{2nd}) constructs with high efficacy and tolerability (Giles et al., 1995a; Micklefield, 2001; Dias and Stein, 2002). In the present study, chimeric AS^{2nd} constructs were used that contained a phosphorothioate backbone and 2'-alkoxy modifications on the ribose residues at the first and last 4 - 6 bases in combination with an optimized lipofection protocol that was shown to have improved specificity and tolerability (Sonnemann et al., 2004a; Sonnemann et al., 2004b; Schmidt et al., 2006).

The efficiency to deliver antisense constructs into A549 cells in the experiments performed for the present study was very high (see chapter 3.5.1), confirming that lipofection with cationic lipids is an effective transfection technique (Felgner et al., 1987; de Lima et al., 1999; Rocha et al., 2002). To maximize knockdown efficacy, various first generation antisense (AS^{1st}) oligophosphorothioates were screened for their activity to reduce corresponding PDE4 subtype mRNA transcripts using quantitative PCR. From the most effective AS^{1st} sequences, chimeric AS^{2nd} constructs were synthesized and tested for efficacy (see chapters 3.5.3 - 3.5.5). Substantial and specific mRNA, protein, and activity knockdown were achieved using 100 nM of AS^{2nd} constructs, whereas lipofection alone had no effects on mRNA expression, which is in line with observations of others (Sonnemann et al., 2004a; Sonnemann et al., 2004b). Because A549 cells express mainly the PDE4D subtype, antisense targeting PDE4A and PDE4B are expected to have the smallest effect on PDE4 activity even when the individual PDE4 subtypes are diminished to a similar extent. Indeed, the most pronounced downregulation of PDE4 activity was observed with antisense targeting PDE4D. Although statistically not significant, the application of antisense constructs showed a trend to suppress PDE4 independent activity. Moreover, lipofection of antisense constructs led to the detachement of A549 cells, which were excluded from read-out parameters.

4.4.2 Lipofection of A549 cells with siRNAs

Besides antisense-mediated knockdown strategies, additional molecular approaches to specifically knock down target genes have been developed, of which the discovery of RNA interference (RNAi) (Fire et al., 1998) was the most profound innovation (Hannon, 2002; Couzin, 2002; Novina and Sharp, 2004; Mello and Conte, Jr., 2004). RNAi is the process of

sequence-specific post-transcriptional gene silencing triggered by double-stranded small interfering RNAs (siRNAs). Physiologically, siRNAs are ~21-nucleotide small interfering RNAs cleaved by ribonuclease III from longer dsRNAs that are recognized by a multienzyme complex termed RNA-induced silending complex (RISC), which specifically initiates the post-transcriptional gene silencing of sequence homologues of the parental siRNA (Hammond et al., 2000; Bernstein et al., 2001). Whereas long dsRNAs have been shown to be potent triggers of the interferon system (Stark et al., 1998), synthetic, small siRNAs can bypass these interferon responses and can induce specific downregulation of target genes (Elbashir et al., 2001). Since its discovery, the siRNA-mediated knockdown approach emerged as powerful tool to study gene functions in various cellular systems (Dykxhoorn et al., 2003; Hannon and Rossi, 2004) as well as to develop clinical therapies (Sioud, 2004; Leung and Whittaker, 2005). To test whether the application of siRNAs is able to reproduce or even to exceed the effects induced by antisense constructs in the present study, the A549 experiments were repeated with siRNAs targeting PDE4 subtypes (see chapters 3.5.1 - 3.5.5). For initial experiments, pools of four individual siRNAs targeting the same PDE4 subtype, termed 'SMARTpools', were used to maximize knockdown efficiency. All siRNAs were designed and manufactured by Dharmacon, following an algorithm that suggests improved efficacy of siRNAs (Reynolds et al., 2004). The delivery of siRNAs into A549 cells by lipofection was higher than the delivery of antisense constructs and siRNA-mediated PDE4 mRNA knockdowns were highly specific and similar in extent to the effects observed with antisense constructs. However, the overall efficacy to suppress PDE4 activity was less pronounced when siRNAs were used instead of antisense constructs. Yet, the siRNA-mediated effects were less variable, highly specific, and did not induce cell detaching. Remarkably, siRNAs were effective in the low nM range, confirming results of initial siRNA experiments performed by Tuschl and colleagues (Elbashir et al., 2001; Elbashir et al., 2002).

A definite evaluation of potential advantages and disadvantages of the antisense and siRNA technique, if possible at all, might depend on the targeted gene and/or on the cellular context and will require more detailed studies, such as extensive mRNA expression studies and functional experiments. In the present study, siRNAs were regarded to induce reliable knockdowns in the setting tested and were thus further validated in human primary $CD4^+$ T cells.

4.4.3 Amaxa nucleofection of $CD4^+$ T cells with siRNAs

Human primary $CD4^+$ T lymphocytes are difficult to transfect and various common transfection methods such as cationic lipids fail to transfect the cells efficiently. Since PDE4 inhibitors are tested in clinical trials and may provide future therapeutic options in diseases as asthma,

COPD, IBD, and others (Banner and Trevethick, 2004; Lipworth, 2005), it was important to closely mimic the physiological conditions relevant to human in the experiments performed in the present study. Consequently, although cell lines such as the Jurkat T cell line are functionally more stable and are easier to handle (e.g. to transfect), human primary $CD4^+$ T cells were preferred for this study, even though this approach is more time consuming, technically complex, and had a higher variability due to donor-dependent differences. A novel electroporation-based transfection method (nucleofection), optimized for the transfection of human T cells (Gresch et al., 2004; Yin et al., 2006), was used to validate siRNA-mediated PDE4 subtype mRNA and protein knockdown in human primary $CD4^+$ T cells. By using optimized buffers in combination with specific electroporation protocols of the nucleofector device (Amaxa), several primary and hard-to-transfect cells have been nucleofected with this technique, with varying efficacies and tolerabilities (Hamm et al., 2002; Gresch et al., 2004; Schakowski et al., 2004).

In the experiments performed for the present study (see chapter 3.6), the transfection procedure alone caused a considerable loss of cells, which is a common event associated with electroporation (Gehl, 2003). Additionally, the nucleofection procedure caused a substantial decrease in the anti-CD3/CD28 induced release of cytokines when compared to cells that were stimulated, but not nucleofected. Because the impact of the nucleofection procedure on IL-2, IFN-γ, and IL-5 synthesis was quantitatively similar, nucleofection had no selective inhibitory effects on cytokine release. Remarkably, cells recovered after nucleofection had a good viability and did not show CD25 upregulation. Furthermore, anti-CD3/CD28 induced proliferation of nucleofected cells was not affected by the nucleofection procedure, when compared to cells that were stimulated, but not nucleofected. Although the nucleofection technique was used in several studies for the transfection of $CD4^+$ T cells (Ganesh et al., 2003; Vang et al., 2004; Skapenko et al., 2004; Yin et al., 2006), considerably little information is available how the nucleofection procedure affects overall T cell function in these reports. In contrast, by measuring cell loss during nucleofection and determination of cell viability, CD25 surface expression, cytokine release, and proliferation of recovered cells, the impact of the nucleofection procedure was well characterized and controlled in the present study. The addition of DMSO to nucleofected cells did not significantly affect any investigated functional parameter. Taking the unavoidable effects of the procedure into account, it was important to demonstrate that the additional application of siRNAs had no additional effect on cell parameters (besides expected effects linked to PDE4 knockdown). Because it was not expected that all individual siRNAs from ‘SMARTpool’ sets targeting distinct PDE4 subtypes are equally effective, the most efficient individual siRNAs suppressing their corresponding PDE4 subtype were chosen for all further knockdown studies in human primary $CD4^+$ T cells. Whereas siRNA concentrations in the range from 100 nM to 4 µM have been used (Vang et al., 2004; Skapenko et al., 2004; Methi et al., 2005), 1.5 µM siRNA was determined as the

optimal concentration for maximal knockdown of PDE4 subtypes in the validation experiments performed in this study. Although a complete knockdown of the target PDE4 subtypes was not achieved, the mRNA and protein knockdown was substantial and specific. Noteworthy, in unstimulated $CD4^+$ T cells, all PDE4 subtype-specific siRNAs had the same efficacy in down-regulating the respective mRNA. However, after stimulation, the applied siRNAs not only had to reduce a stable basal mRNA level but also had to counteract the induction of the respective mRNAs, probably resulting in more variable knockdown effects under stimulatory conditions.

Whilst siRNAs are extensively applied for the examination of gene functions, there is still much controversy about specificity and potential off-target effects correlated to siRNAs (Leung and Whittaker, 2005). On the one hand, several studies indicate that individual siRNAs have a markedly high specificity and tolerability (Chi et al., 2003; Semizarov et al., 2003; Schwarz et al., 2003), on the other hand, some reports assigned off-target effects to siRNAs (Sledz et al., 2003; Jackson et al., 2003; Kariko et al., 2004). In the present study, the siRNA-mediated knockdown of PDE4 subtypes was extensively validated and all experiments were well controlled, with no indications of unspecific effects. In conclusion, the siRNA-mediated knockdown technique was shown to be an appropriate tool to generate PDE4 subtype-specific mRNA and protein knockdown in $CD4^+$ T cells and was thus considered to be a reliable strategy to study the function of PDE4 subtypes in immune cells.

4.5 Functional impact of PDE4 subtypes in $CD4^+$ T cells

$CD4^+$ T cell activation can be initiated by TCR-MHC interaction and can be multiplied by costimulatory signals triggered by accessory molecules present on the surface of the antigen-presenting cells (Davis and Bjorkman, 1988; Cantrell, 1996). Subsequently, both TCR and costimulatory signals can orchestrate intracellular signals that have profound effects on T cell function, such as cytokine release and proliferation (Larsen and Henson, 1983).

4.5.1 Anti-CD3/CD28 activation of $CD4^+$ T cells and IL-2, IFN-γ, and IL-5 synthesis

After the discovery that $CD4^+$ T helper cells can be characterized by their set of released cytokines, the terminology type 1 T helper (Th1) and type 2 T helper (Th2) cells was introduced to typify these differently polarized T cell subpopulations (Mosmann et al., 1986; Del Prete et al., 1991). Although the Th1-Th2 paradigm is widely accepted, there is increasing evidence that the strict Th1/Th2 dichotomy may be oversimplified (Gor et al., 2003; Crane and Forrester, 2005). However, Th1 cells and Th1 cytokines, such as IL-2 and IFN-γ, have been linked to cell-mediated immunity and have been shown to have pathophysiological relevance

in autoimmunity and chronic inflammatory diseases (Romagnani, 1994; Lafaille, 1998). In contrast, Th2 cells and Th2 cytokines, such as IL-4 and IL-5, have been linked to humoral immunity and have been shown to have pathopysiological relevance in allergic disorders like asthma or atopic dermatitis (Romagnani, 2000; Renauld, 2001). Although not absolutely required for activation, the costimulatory receptor CD28 was implicated as a classical component of the two-signal model for T cell activation that originates from the immunological synapse, i.e., the nanometer scale gap between TCR and APC (Bromley et al., 2001).

In the present study, (patho)physiological TCR/CD28 stimulation was mimicked by treating human primary $CD4^+$ T cells with different anti-CD3/CD28 concentrations. Subsequently, IL-2, IFN-γ, and IL-5 cytokine concentrations in the supernatant were determined at different time points (see chapter 3.7.1). This selection of cytokines was chosen to represent Th1 cytokines (IL-2 and IFN-γ) as well as a Th2 cytokine (IL-5) as functional read-out parameters and to test if the stimulation of human primary $CD4^+$ T cells affects these cytokines differently. Whereas no cytokines were detected in untreated $CD4^+$ T cells, substantial amounts of cytokines were found after stimulation. IL-2 secretion was strongly, but transiently induced with maximal levels 24 - 48 h after stimulation. For the highest induction of IL-2, costimulation with anti-CD28 antibodies was necessary. These findings are in accordance to and extend earlier studies (Thompson et al., 1989; Fraser et al., 1991; Jenkins et al., 1991; Norton et al., 1992). As partly depicted in Figure 6 (see chapter 1.4), the regulation of cytokine transcription is under the control of PKA action, but can also be controlled by various processes such as chromatin remodeling, costimulation, activation and cooperation of transcription factors, and the existence of multiple promoter and enhancer regions (Salomon and Bluestone, 2001; Holloway et al., 2002). Via the trimeric IL-2 receptor, IL-2 has been shown to support crucial signals for cell survival and proliferation (Taniguchi and Minami, 1993).

Compared to IL-2 secretion, IFN-γ levels were substantially induced at later time points in the present study, but were from 24 h onwards steadily upregulated. IFN-γ concentrations were maximal at the end of the examined time period and were not dependent on costimulation. These findings support and expand previous observations that CD28 costimulation is not required for IFN-γ induction, especially under conditions of strong or sustained TCR stimulation (Salomon and Bluestone, 2001; Frauwirth and Thompson, 2002). IFN-γ has been recognized as the principal, tightly regulated Th1 effector cytokine that has pleiotropic effects on immune cells (Boehm et al., 1997; Teixeira et al., 2005). Similar to IFN-γ, substantial levels of IL-5 were only detected after 24 h of stimulation in the present report. IL-5 concentrations were maximal at the end of the examined time period and were shown to be dependent on costimulation. This findings are in line with and extend experiments performed by others (Inami et al., 2004). Because IL-5 is mainly involved in the activation and regulation of eosinophils, IL-5 has been

recognized as a key Th2 cytokine in atopic diseases (Sanderson, 1992; Mordvinov and Sanderson, 2001).

4.5.2 Anti-inflammatory effects of PDE4 inhibitors and the consequences of PDE3 inhibition

As detailed in chapter 4.5.1, cytokines are not only pivotal messengers of the immune system, but are also pathophysiological key mediators of various chronic inflammatory diseases (Lafaille, 1998; Romagnani, 2000; Renauld, 2001). By attenuating the inhibitory constraint of cAMP on inflammatory cell responses, PDE4 subtypes play a crucial role in such signaling processes. Subsequently, the anti-inflammatory effect of PDE4 inhibition on inflammatory and immunocompetent cells by elevating cAMP levels was the rationale for the development of PDE4 inhibitors (Torphy, 1998; Essayan, 1999; Souness et al., 2000; Houslay et al., 2005). However, under certain conditions, the efficacy of PDE4 inhibitors to suppress inflammatory cell functions was found to be reduced: Whilst in monocytes PDE4 inhibition largely suppresses LPS-induced TNF-α release, efficacy of PDE4 inhibitors in monocyte-derived macrophages and dendritic cells to suppress TNF-α is diminished (Gantner et al., 1997a; Gantner et al., 1999; Hatzelmann and Schudt, 2001). Considering the downregulation of PDE4 mRNA and protein activity in the latter cells, as discussed in chapter 4.3, a decreased efficacy of PDE4 inhibitors is comprehensible if one assumes that less protein may also have less functional relevance. Remarkably, the efficacy of a PDE4 inhibitor in these cells can be substantially increased by the additional application of a PDE3 inhibitor, supporting the concept of overadditive PDE3/4 inhibition that has been proposed for clinical therapy (Schudt et al., 1991; Giembycz, 1992; Tenor and Schudt, 1999). In human primary $CD4^+$ T cells, although PDE4 inhibitors alone show efficacy, the anti-inflammatory effect on T cell function can be enhanced by combined PDE3 inhibition (Robicsek et al., 1991; Giembycz et al., 1996; Hatzelmann and Schudt, 2001). The two subtypes PDE3A and PDE3B are high affinity phosphodiesterase for both, cGMP and cAMP, but it is suggested that *in vivo* the hydrolysis of cAMP is inhibited by cGMP (Degerman et al., 1997; Bender and Beavo, 2006). Moreover, PDE3 subtypes are involved in various cellular processes and have been shown to be activated by PKA, Akt, and PI3K (Degerman et al., 1997; Bender and Beavo, 2006). PDE3 subtypes have been recognized as therapeutic targets since they are widely expressed with substantial (mostly membrane-bound) activity in macrophages, dendritic cells, smooth muscle cells, and to a lower extent in T cells (Schudt et al., 1995; Gantner et al., 1997a; Gantner et al., 1999; Schmidt et al., 1999).

In the present study, the secretion of IL-2, IFN-γ, and IL-5 and the proliferation rate were used as functional read-out parameters. The maximum inhibition of these parameters by complete suppression of PDE4 activity was determined by the panPDE4 inhibitor RP73401 (piclamilast), which does not discriminate between distinct PDE4 subtypes (see chapter 3.7.2). Additionally,

to check whether PDE3 inhibition alone is effective in suppressing T cell functions, the panPDE3 inhibitor motapizone (Borbe et al., 1986) was included in the experiments. Finally, the efficacy of the combined application of the two inhibitors was examined. Whereas PDE4 inhibition had significant suppressive effects on anti-CD3/CD28 induced release of IL-2, IFN-γ, and IL-5, the anti-proliferative effect was considerably smaller. Compared to the effects of RP73401, motapizone had consistently lower effects. However, combination of both inhibitors resulted in the most pronounced suppressive effects on T cell function, which were overadditive. These observations are mostly in accordance with and extend former reports (Robicsek et al., 1991; Giembycz et al., 1996; Hatzelmann and Schudt, 2001). In the latter study, 1 µM RP73401 alone had substantially higher efficacy to suppress anti-CD3/CD28 induced proliferation than in the present report. Although the same TCR stimulation protocol was used in both studies, these variances might be explained by the use of different charges of plastic dishes and monoclonal anti-CD3 antibodies in the studies, possibly resulting in different adherence of the anti-CD3 antibodies and subsequently in different TCR stimulation conditions. Because increased strength of anti-CD3 stimulation can reduce the efficacy of RP73401 to suppress the proliferation rate (unpublished observations of Dr. Hatzelmann, ALTANA Pharma AG, Konstanz), the stimulation of the TCR might have been considerably stronger in the present study. Besides, Hatzelmann and Schudt (Hatzelmann and Schudt, 2001) reported that 1 µM motapizone alone had no significant effects on T cell functions. In the present study, motapizone alone had also effects, which might be explained by the use of a higher motapizone concentration (10 µM). At this concentration, motapizone may partially inhibit other PDEs, although inhibitory effects on these PDEs are expected to be very small (below 20%, personal communication). In accordance with the latter report, no preferential inhibition of either Th1- or Th2-cytokines was found in the present study. These findings confirm earlier observations indicating that human Th1 and Th2 cells appear to be equally responsive to the cytokine-suppressing and anti-proliferative effects of PDE4 inhibition (Torphy, 1998).

4.5.3 The impact of PDE4 subtype-specific siRNAs on $CD4^+$ T cell functions

As detailed before, the suppression of cytokine release and proliferation by PDE4 inhibition and the therapeutic rationale for the development of PDE4 inhibitors as anti-inflammatory and immunomodulatory compounds is well known. However, no individual PDE4 subtypes were yet functionally attributed to these effects in T cells. Because extensive validation experiments showed that the siRNA technique was a reliable tool to study $CD4^+$ T cell functions in the present study, PDE4 subtype-specific siRNAs were nucleofected into $CD4^+$ T cells and their functional impact on IL-2, IFN-γ, and IL-5 secretion and on the proliferation rate was compared to the effects of complete suppression of PDE4 activity by RP73401 (piclamilast), as reported

in chapter 3.8. It was demonstrated that siRNA-mediated knockdown of both PDE4B and PDE4D resulted in significant suppression of anti-CD3/CD28 induced IL-2 release 24 h and 48 h after stimulation; the effect of PDE4A-siRNA was not statistically significant. These data indicate that for IL-2 synthesis PDE4B and PDE4D may have a partially overlapping function. For IFN-γ and IL-5, the present study demonstrates that PDE4D-siRNA had a predominant effect in suppressing anti-CD3/CD28 induced IFN-γ and IL-5 generation. Thus, PDE4 subtypes may have nonredundant functional roles, which cannot be compensated by other expressed PDE4 subtypes. However, the inhibition of cytokines was most effective when PDE4 subtype-specific siRNAs were applied in combination, pointing to complementary functions of PDE4 subtypes. In the present study, the weak suppression of anti-CD3/CD28 induced proliferation by inhibition of PDE4 enzyme activity (as discussed in chapter 4.5.2) could be fully mimicked by PDE4D-siRNA, whereas siRNAs targeting PDE4A or PDE4B were not effective. Because many studies showed that IL-2 is a major inducer of T cell proliferation (Mookerjee and Pauly, 1990; Taniguchi and Minami, 1993; Nelson, 2004), the anti-proliferative effect of PDE4D-siRNA may be directed via lowered IL-2 levels. In contrast, it was shown that supraphysiologic doses of recombinant IL-2 cannot overcome the suppressive effect of PDE4 inhibition (Essayan et al., 1994), indicating that the anti-proliferative effect of PDE4D-siRNA could also be mediated via an IL-2 independent process. In line with this observation, T cell proliferation has been recognized to be a multilayered process that can be initiated by a magnitude of IL-2 dependent and IL-2 independent mechanisms (Boothby et al., 2001; Frauwirth and Thompson, 2002; Fruman, 2004; Marrack and Kappler, 2004).

The suppressive effect of PDE4 subtype-specific siRNAs on T cell cytokine production and proliferation was qualitatively not changed by the presence of the PDE3 inhibitor motapizone. However, whereas the combination of RP73401 with motapizone overadditively suppressed T cell functions (as discussed in chapter 4.5.2), the suppressive effects of combined PDE4 subtype-specific siRNAs with motapizone were not overadditive. A possible explanation for this observation might be that PDE4 subtype-specific siRNAs alone and RP73401 alone may increase cAMP concentrations to a level above a ‘primary’ threshold that is sufficient to suppress anti-CD3/CD28 induced cell responses to an extent discussed above. Because both PDE4 subtype-specific siRNAs and RP73401 mediate the exceeding of this supposed cAMP threshold, both have similar functional efficacies. However, chances are that total PDE4 inhibition by RP73401 may generate cAMP levels even above the siRNA-mediated cAMP elevation, which have no functional relevance as long as RP73401 is applied alone. Yet, if motapizone is applied additionally to RP73401, it might be that the combined PDE3/4 inhibition increases cAMP concentrations to a level above a ‘second, superior’ threshold that overadditively suppresses T cell functions. Assumingly, the combined application of PDE4 subtype-specific siRNAs and motapizone is not sufficient to elevate cAMP levels above this

proposed second cAMP threshold, resulting in the absence of overadditive effects. However, the effects of motapizone and PDE4 subtype-specific siRNAs in increasing cAMP levels were not further examined in the present study and their interactions remain speculative. Qualitatively, the additional application of motapizone confirmed the functional impact of individual PDE4 subtypes on T cell cytokine release and proliferation.

The key findings of the present study in respect to the functional impact of distinct PDE4 subtypes in human primary $CD4^+$ T cells are summarized in Figure 41.

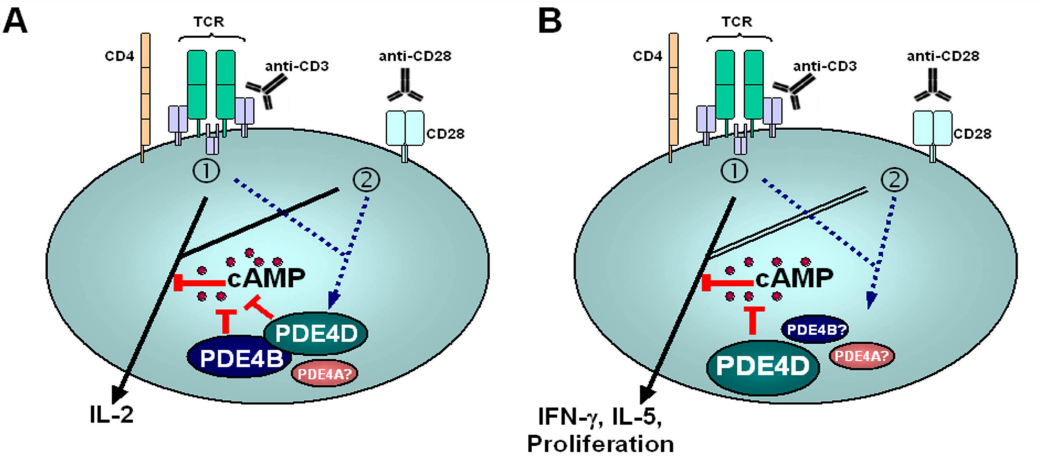

Figure 41. Proposed mechanisms of cAMP regulation by distinct PDE4 subtypes in anti-CD3/CD28 activated human primary $CD4^+$ T cells. The cartoon depicts the basic pathways that may be induced after TCR stimulation (signal ①) and CD28 costimulation (signal ②) and that result in the generation of cytokines and T cell proliferation. The inhibitory constraint of cAMP on T cell function can be attenuated by anti-CD3 or anti-CD3/CD28 induced upregulation of distinct PDE4 subtypes. *A*, Anti-CD3/CD28 induced generation of IL-2 may be regulated by the PDE4 subtypes PDE4B and PDE4D, which may have an overlapping role. *B*, Anti-CD3/CD28 induced generation of IFN-γ and IL-5 and proliferation is likely predominantly regulated by the PDE4D subtype. However, also PDE4A and PDE4B may have functional relevance, indicating that PDE4 subtypes seem to have overall nonredundant, but complementary roles. For IFN-γ induction, no costimulatory signal is necessary. Because PDE4 subtypes have different functional impact on T cell functions at different time points (i.e., 'early' versus 'late' signals), PDE4 subtypes may also have time-dependent roles. ⊣ = Inhibitory effects; full arrow = induction of cytokine release/proliferation; dotted arrow = induction of PDE4 subtypes.

In conclusion, because PDE4B- and PDE4D-siRNA both had pronounced effects on IL-2 release, the two subtypes may have overlapping roles in controlling the synthesis of this 'early' cytokine. Considering the regulation of 'later' cytokines and of the proliferation rate, the functional impact of PDE subtypes changed: because PDE4D-siRNA had the predominant effects, PDE4 subtypes may have nonredundant roles. However, the most pronounced effects on cytokine release were observed when all siRNAs were applied in combination, negotiating an exclusive role for PDE4D, but pointing to complementary functions of PDE4 subtypes. In summary, these findings indicate that the regulation and function of individual PDE4 subtypes might be a complex interplay leading to overall nonredundant, complementary, and time-dependent roles.

4.5.4 The role of PDE4 subtypes for T cell function: Comparison to other studies

The relevance of PDE4 subtypes for T cell function has not been extensively described either in mice or in humans. However, in human primary T cells and T cell lines, two reports localize PDE4B2 at the TCR and the immunological synapse (Baroja et al., 1999; Arp et al., 2003). Interestingly, the latter study correlated overexpression of PDE4B2 in Jurkat cells with an increase in IL-2 production. Another study reported that TCR and CD28 stimulation in human peripheral T cells recruits PDE4A4, PDE4B2, PDE4D1, and PDE4D2 in complex with β-arrestin to lipid rafts, pointing to a potential role of PDE4 in counteracting C-terminal Src kinase (Csk) mediated inhibition of Lck (Abrahamsen et al., 2004). Interestingly, the immunoblot analyses performed in the present study showed that especially the short forms of PDE4B and PDE4D are responsible for or contribute to the time-dependent upregulation of these subtypes in $CD4^+$ T cells. Furthermore, one study revealed that PDE4 subtypes can interact with AKAPs and PKA in T lymphocytes, indicating that PDE4 subtypes might be compartmentalized in T cells (Asirvatham et al., 2004). In view of the general concept of compartmentalized PDE4 subtypes, this finding will be discussed in more detail in chapter 4.8.

The results of the present study seem to be in discrepancy to a study of Manning and coworkers (Manning et al., 1999), who claimed that suppression of T cell proliferation with 'PDE4 subtype-selective inhibitors' correlated with the inhibition of PDE4A and PDE4B. This contradiction might be explained by the low selectivity of the inhibitors used in that study and/or by different stimulation conditions. In the Manning study, mononuclear cells from allergic donors were stimulated by antigen. In the present study, the impact of stimulation conditions (anti-CD3 ± costimulation with anti-CD28 in different strengths, see chapter 3.3.3) has been evaluated and no differences with respect to regulation of PDE4 subtypes were found. For functional studies, a 'medium' costimulation protocol was used by applying 0.3 µg anti-CD3/well and 0.3 µg anti-CD28/ml. One cannot exclude the possibility that - in contrast to the mRNA expression profiles - the impact of various PDE4 subtypes/splice variants may depend on the stimulation condition used. In addition, this argument might be supported by the unexpected observation that, although PDE4B-siRNA was shown to significantly inhibit IL-2 release in the present study, no anti-proliferative effect of PDE4B-siRNA was observed. As discussed above, this finding can be explained by potential IL-2 independent induction of proliferation under the stimulation conditions applied. With regard to the anti-CD/CD28 costimulation in the present study, the small efficacy of RP73401 on proliferation might further limit the analysis of functional relevance of PDE4 subtype-specific siRNAs, and possibly underrepresent potential effects of other PDE4 subtypes than PDE4D. Finally, it may also be that for different stimulation conditions small (undefined) subpopulations of $CD4^+$ T cells may respond differently which cannot be resolved by the used protocol. In view of these

circumstances, siRNA-mediated knockdown experiments with altered stimulation conditions and/or with different subpopulations (which may be more difficult to obtain in sufficient amounts) should allow further information concerning the involvement of PDE4 subtypes in regulating T cell functions.

4.6 Beyond $CD4^+$ T cells: Functional impact of PDE4 subtypes

Although PDE4 subtype-specific knockdown experiments were exclusively performed in $CD4^+$ T cells in the present study, the revealed mRNA expression profiles in $CD8^+$ T cells, monocytes, macrophages, and dendritic cells may help in addition to data reported by others to evaluate the functional relevance of PDE4 subtypes in other immune cells than $CD4^+$ T cells. Considering the experiments performed in $CD8^+$ T cells, the present study demonstrates that the mRNA expression of PDE4 subtypes is very similar in $CD8^+$ and $CD4^+$ T cells. Although the functional relevance of PDE4 subtypes has to be unravelled in $CD8^+$ T cells, the findings presented in the present study may indicate that the functional roles of PDE4 subtypes are likely to be similar in $CD8^+$ and $CD4^+$ T cells. This assumption is supported by the observation that $CD8^+$ and $CD4^+$ T cells are equally sensitive to PDE4 inhibition (Tenor et al., 1995b).

In monocytes, monocyte-derived macrophages, and monocyte-derived dendritic cells, the PDE4 subtype mRNA expression profile determined in the present study along with former reports (Ma et al., 1999; Wang et al., 1999) may suggest that PDE4B likely plays a predominant role, because it is the only largely regulated subtype and exclusively responds to LPS in these cells. Indeed, a genetical approach using mice deficient in either PDE4A, PDE4B, or PDE4D showed that only PDE4B ablation effectively suppressed LPS-induced TNF-α release (Jin and Conti, 2002; Jin et al., 2005). Ablation of PDE4A or PDE4D did not affect TNF-α synthesis in murine monocytes, macrophages, and dendritic cells. Remarkably, complementary, but nonredundant roles of PDE4 subtypes have been described in mice deficient in PDE4B and PDE4D, in which neutrophil recruitment to the inflamed lung is impaired (Ariga et al., 2004). In the latter study, although ablation of PDE4B substantially effected neutrophil function, ablation of PDE4D had the predominant effects.

However, data derived from knockout experiments cannot intuitively be assigned to the human situation. Although the PDE4 subtype mRNA expression data in the present study and data from former reports may assign a predominant role for PDE4B in human primary monocytes, monocyte-derived macrophages, and monocyte-derived dendritic cells, one study demonstrated that *PDE4A4* mRNA transcripts were found to be significantly upregulated in lung macrophages of smokers with COPD when compared to control smokers (Barber et al., 2004). Besides, in this latter study, *PDE4B2* and *PDE4A4* mRNA levels were upregulated in

monocytes of smokers when compared to nonsmokers. In atopic subjects, PDE4 subtypes were found to be induced in leukocytes (Grewe et al., 1982; Holden et al., 1986), but whether an atopic disease status correlates with higher PDE4 activity is still controversially discussed and the functional relevance of individual PDE4 subtypes is unclear (Gantner et al., 1997b; Landells et al., 2000; Landells et al., 2001). Treatment of human primary monocytes with cAMP elevating agents induced a long PDE4A splice variant and a short PDE4B splice variant (Manning et al., 1996). Similarly, in the human monocytic cell line Mono Mac 6, treatment with dibytyryl-cAMP induced a long PDE4A splice variant and short PDE4B and PDE4D splice variants within 24 h (Verghese et al., 1995). Comparable desensitization mechanisms upon increased cAMP levels have been proposed in the monocytic cell line U937 (Torphy et al., 1995). However, cell line models may not reflect the physiological situation in human primary monocytes, since the PDE4 subtype expression profile during monocyte-macrophage differentiation of human U937 cells (Shepherd et al., 2004) differed from the expression profile of human monocyte-derived macrophages reported in the present study. Moreover, because LPS stimulation, as performed in the present report, may not be representive for other stimulation conditions, further studies with different stimulation conditions might reveal further information about PDE4 subtype expression patterns in human primary monocytes, macrophages, and dendritic cells. Knockdown studies in these cells might help to test whether PDE4B is exclusively involved in cell signaling or whether other subtypes also play a role for cell function.

Beyond human primary immune cells, functional relevance of individual PDE4 subtypes has been found for haplotypes of the human *PDE4D* gene, which were shown to confer increased risk of ischemic stroke (Gretarsdottir et al., 2003). Moreover, the *PDE4D* gene was implicated in bone density and osteoporosis (Reneland et al., 2005). On the other hand, only PDE4B has been found to be involved in schizophrenia (Millar et al., 2005).

In knockout mice, an exclusive role for PDE4D has been described for airway smooth muscle contraction (Hansen et al., 2000; Mehats et al., 2003), for β_2-adrenergic signaling in cardiac myocytes (Xiang et al., 2005), and for lowered progression of heart failure (Lehnart et al., 2005). However, although PDE4 subtype structure and expression are considerably conserved within different species (see chapter 1.3), PDE4 subtype functions may differ between different species. Thus, to obtain conclusive information about the functional impact of PDE4 subtypes in human primary inflammatory and immunocompetent cells, further studies including PDE4 subtype-specific knockdown experiments will be necessary.

In conclusion, data generated in several cellular systems indicate that distinct subtypes and splice variants may have different functional roles, underpinning the complexity of the PDE4 family.

4.7 Future options for the development of PDE4 inhibitors

Although the development of PDE4 inhibitors has a long history, the medicinal use of PDE4 inhibitors has been hampered by adverse gastrointestinal and emetic side effects or due to the lack of clinical efficacy (Torphy, 1998; Souness et al., 2000). Thus, the synthesis of PDE4 inhibitors with an improved therapeutic ratio is essential for the development of novel low-molecular-weight compounds targeting PDE4.

As early studies with rolipram were initiated, the existence of a high- and a low-affinity binding site for rolipram was suggested (Schneider et al., 1986; Muller et al., 1996). It is now established that the catalytical unit of PDE4 splice variants has only one rolipram binding site, but can adopt at least two conformational states, termed high-affinity rolipram-binding state (HARBS) and low-affinity rolipram-binding state (LARBS) (Souness and Rao, 1997; Houslay and Adams, 2003; Conti et al., 2003). Both HARBS and LARBS can be identified by their distinct affinities for rolipram, characterised by an IC_{50} of ~1 - 50 nM for HARBS and an IC_{50} of ~0.1 - 10 µM for LARBS (Houslay and Adams, 2003). The HARBS conformational state likely corresponds to the active site of the holoenzyme (i.e., the enzyme bound to cofactors such as Mg^{2+}), whereas the LARBS conformational state has been linked to the active site of the apoenzyme (i.e., the free enzyme) (Laliberte et al., 2000). Several molecular mechanisms have been suggested to explain the existence of these multiple conformers, including the possible involvement of bivalent-metal-ion centers (Laliberte et al., 2000; Xu et al., 2000; Liu et al., 2001b), of phosphorylation events (Sette and Conti, 1996; Laliberte et al., 2002), and/or of the amino termini of PDE4 isoforms (Houslay and Adams, 2003; Conti et al., 2003). The therapeutic relevance of multiple conformations of PDE4 is reflected by the observation that LARBS may be predominantly present in immune cells (mediating desired anti-inflammatory therapeutic effects) (Barnette et al., 1995b; Barnette et al., 1996), whereas HARBS was assigned to parietal glands and the CNS (mediating undesired effects such as gastric acid secretion and emesis) (Barnette et al., 1995a; Souness and Rao, 1997; Torphy, 1998). However, also HARBS inhibiton has been linked to therapeutic effects, mediating bronchodilation (Harris et al., 1989), decreased neutrophil degranulation (Barnette et al., 1996), or cAMP accumulation in macrophages (Kelly et al., 1996). Post-rolipram PDE4 inhibitors like piclamilast have been designed to exhibit a different HARBS/LARBS ratio (Souness et al., 1995; Souness and Rao, 1997).

Besides, other studies suggested that side effects of PDE4 inhibitors might be attributed to individual PDE4 subtypes. Robichaud and colleagues linked emesis in mice to the deletion of PDE4D (Robichaud et al., 2002), supporting the hypothesis that PDE4D might mediate adverse effects rather than other PDE4 subtypes. This observation in line with reports proposing an improved therapeutic ratio of PDE4 subtype-selective inhibitors led to the suggestion to develop PDE4B-selective low-molecular-weight compounds (Manning et al.,

1999; Jin et al., 2005). Yet, this approach is challenging because of the highly conserved catalytical site of PDE4 subtypes (Bender and Beavo, 2006). Although catachol-based PDE4A/PDE4B-, naphtyridine-based PDE4D-, or nicotinamide-based PDE4D-preferred inhibitors have been reported (Manning et al., 1999; Hersperger et al., 2000; Chambers et al., 2006), no highly PDE4 subtype-selective inhibitors have been developed to date. Therefore, the hypothesis of improved therapeutic efficacy of such PDE4 inhibitors remains to be tested *in vivo*. The successful development of novel PDE4 subtype-selective compounds certainly depends on the better understanding of the catalytic pocket of PDE4 subtypes (Zhang et al., 2004; Conti, 2004), but prospects arise that specificity could also be achieved by blocking interactions of PDE4 subtypes with other proteins (Richter et al., 2001; MacKenzie, 2004).

The results of the present study in line with several other findings (as discussed in chapters 4.5 and 4.6) suggest that several PDE4 subtypes might mediate the broad anti-inflammatory effects of PDE4 inhibitors in immune and immunocompetent cells. In this view, the concept to develop PDE4 subtype-selective inhibitors may result in increased selectivity and in improved tolerability, but at the same time in lowered anti-inflammatory and immunomodulatory efficacy. However, as demonstrated in the present study and in accordance to previous studies (see chapters 4.5 and 4.6), distinct PDE4 splice variants are regulated differentially in human primary immune cells. Thus, although not primarily addressed in the present study, PDE4 short forms of different PDE4 subtypes may be functionally even more relevant as therapeutic targets than the affilitation to a subtype alone. The confirmation of this correlation in various immune cells would help to define the rationale to develop PDE4 short form-selective inhibitors instead of PDE4 subtype-selective inhibitors. Whether this concept holds true and whether the synthesis of such compounds is a feasible approach has to be awaited.

4.8 Compartmentalization of PDE4 subtypes

Although the intracellular localization of PDE4 subtypes was not addressed in the present study, several reports indicate that PDE4 splice variants may be compartmentalized in human T cells, both temporally and spatially (Conti et al., 2003; Asirvatham et al., 2004; Abrahamsen et al., 2004; Baillie et al., 2005; Tasken and Stokka, 2006). These findings support the observation that in immune cells of PDE4 knockout mice no changes in overall cAMP levels were measured, but that only subtle cAMP pools might be affected by PDE4 subtype ablation (Jin et al., 2005). In conclusion, these findings would suggest that PDE4 subtypes are highly compartmentalized in immune cells – a concept, that is well established in many cellular settings (Houslay and Adams, 2003; Baillie et al., 2005; Lynch et al., 2006).

Several reports showed that various A kinase anchoring proteins (AKAPs) can bind regulatory subunits of PKA isoenzymes and control their intracellular targeting, thus affecting the

selective activation of these PKA isoforms at discrete subcellular locations (Michel and Scott, 2002; Tasken and Aandahl, 2004; Wong and Scott, 2004). Much evidence arises that also PDE4 splice variants can be found associated to AKAP-PKA complexes, thus forming spatially constrained signaling modules which enable a local negative feedback loop to terminate cAMP action (Jurevicius and Fischmeister, 1996; Tasken et al., 2001; Kapiloff et al., 2001; Dodge et al., 2001; Carlisle Michel et al., 2004; Barnes et al., 2005; Bajpai et al., 2006; Willoughby et al., 2006; McSorley et al., 2006). In immune cells, such multi-component signaling complexes of AKAP, PKA, and PDE4 might be an effective system to decrease the negative constraint of cAMP on immune functions (Baillie et al., 2005).

Another example of intracellular targeting of PDE4 subtypes and thus compartmentalized PDE4 action is the interaction of PDE4 splice variants with $ß_2$-adrenergic receptor ($ß_2$-AR) associated scaffold proteins, called ß-arrestins (Perry et al., 2002). $ß_2$-ARs transduce fundamental signals, but are tightly regulated by various receptor attenuation/desensitization mechanisms to limit the magnitude of $ß_2$-adrenergic signaling (Freedman and Lefkowitz, 1996; Perry et al., 2002; Lefkowitz and Shenoy, 2005). In general, all PDE4 isoforms can associate with ß-arrestins through a common motif located within their conserved catalytic domain, but due to its unique N-terminal end, PDE4D5 is the preferred isoform (Bolger et al., 2003a). PKA-phosphorylated $ß_2$-AR not only uncouples the signaling to G_s, but was shown to enhance the coupling to G_i, thus activating G_i-linked pathways involving ERK1/2 or Akt (Baillie et al., 2003; Baillie and Houslay, 2005). As indicated previsouly, Abrahamsen and coworkers (Abrahamsen et al., 2004) found ß-arrestin and PDE4 splice variants preassembled in human primary T cells. These ß-arrestin/PDE4 signaling complexes were shown to be recruited to lipid rafts after anti-CD3/CD28 stimulation and can thus potentiate T cell immune responses by abrogating the negative impact of cAMP (Tasken and Stokka, 2006).

Regarding the unique N-terminal regions of PDE4 isoforms, it can be expected that PDE4 splice variants also interact with other proteins as well. Indeed, some PDE4 long isoforms (PDE4A4/5, PDE4D4) contain a polyproline motif that can interact with SH3 (Src homology 3) domains of Fyn/Lyn/Src kinases (Houslay and Adams, 2003). Besides, binding of Lyn and Src to human PDE4A4 was shown to alter the sensitivity to inhibition by rolipram (McPhee et al., 1999). Moreover, rat PDE4A5 can associate with immunophilins, such as XAP2, which attenuates the activity status of the enzyme (Bolger et al., 2003b). PDE4D5 has been found to interact with RACK1, a scaffold protein involved in binding of protein kinase C and other proteins (Yarwood et al., 1999; Bolger et al., 2006). The unique amino terminus of PDE4A1 has been shown to include a microdomain, termed TAPAS-1, mediating membrane association and binding of phosphatidic acid (Baillie et al., 2002).

Taken together, the regulation of the activation status of PDE4 subtypes and their intracellular targeting to different signaling modules is highly complex, allowing a precise control of compartmentalized cAMP pools for the orchestration of a multitude of signals. However, the

functional relevance of such protein-protein interactions in human primary immune cells has to be further evaluated.

4.9 Conclusions

The combination of several mechanisms, including the upregulation of the amount of different PDE4 subtypes, the regulation of PDE4 activity by e.g. phosphorylation, and the intracellular targeting of distinct PDE4 splice variants to specific microdomains may be involved in the subtle and complex regulation necessary for opposing the inhibitory tonus of cAMP in immune cells. The present study indicates that PDE4 subtypes are differently expressed and differentially regulated in human primary immune cells such as $CD4^+$ and $CD8^+$ T cells, monocytes, monocyte-derived macrophages, and monocyte-derived dendritic cells. In human primary $CD4^+$ T cells, the PDE4B and PDE4D short forms were found to be mainly responsible for the time-dependent upregulation of PDE4 subtypes. To study the functional impact of PDE4 subtypes in these cells, a siRNA-mediated knockdown strategy using PDE4 subtype-specific siRNAs was validated and proved to be a reliable tool for knockdown experiments. Using this strategy, it was demonstrated that individual PDE4 subtypes have overall nonredundant, but complementary, time-dependent roles in propagating various T cell functions. Both PDE4B and PDE4D were shown to be involved in anti-CD3/CD28 induced IL-2 synthesis, whereas PDE4D is the form that likely plays a predominant role in other T cell functions such as IFN-γ release, IL-5 release, and proliferation. Thus, the present study extends the complexity of individual PDE4 subtypes and multiple splice variants for the control of cAMP levels.

5 SUMMARY

As a second messenger, adenosine 3'-5' cyclic monophosphate (cAMP) plays a crucial role for intracellular signaling and determines various cellular functions by activating several effector systems. In immune cells, such as T cells, monocytes, macrophages, or dendritic cells, cAMP has mainly inhibitory properties on cellular responses. Thus, type 4 phosphodiesterases (PDE4), which are capable to hydrolyze cAMP, are critical regulators of inflammatory cell signals by attenuating the negative constraint of cAMP. The PDE4 isoenzyme family consists of four distinct subtypes, each encoded by one gene. Because PDE4 subtypes are widely expressed in inflammatory cells, the PDE4 family became an attractive drug target for the treatment of chronic inflammatory diseases, such as asthma or COPD. In fact, PDE4 inhibitors have been shown to have anti-inflammatory and immunomodulatory effects on a broad range of inflammatory and immunocompetent cells and have proved efficacy in clinical trials. However, it is largely unknown which PDE4 subtype(s) mediate(s) the inhibitory effects in a defined immune cell. Whilst data obtained from knockout mice indicate that PDE4 subtypes have indeed different functional impact in different immune cells, the functional significance of PDE4 subtypes in T cells and generally in immune cells of human origin is largely elusive.

The objectives of the present study were i) to ascertain the expression patterns of PDE4 subtypes in different human primary immune cells via quantitative PCR, PDE activity assays, and immunodetection experiments; ii) to validate an antisense- and a siRNA-mediated, PDE4 subtype-specific knockdown technique in the cell line A549 and to transfer the superior knockdown strategy to human primary $CD4^+$ T cells; and iii) to elucidate the functional impact of PDE4 subtypes in human primary $CD4^+$ T cells.

The study revealed that whilst *PDE4C* mRNA expression was never detected in human primary $CD4^+$ T cells, $CD8^+$ T cells, monocytes, monocyte-derived macrophages, and monocyte-derived dendritic cells, the mRNAs of the subtypes *PDE4A*, *PDE4B*, and *PDE4D* were differently expressed and differentially regulated after stimulation. In resting human primary $CD4^+$ T cells, low levels of *PDE4A* were detected, whereas *PDE4B* and *PDE4D* mRNA expression and protein activity were substantially higher, with PDE4D being the predominant subtype. After anti-CD3/CD28 stimulation of human primary $CD4^+$ T cells, the expression of *PDE4A*, *PDE4B*, and *PDE4D* was induced in a specific time-dependent manner: *PDE4A* and *PDE4D* mRNA as well as protein activity were upregulated within five days, whereas *PDE4B* mRNA and activity showed a transient upregulation with highest levels 24 h after stimulation. The induction of PDE4 subtypes was shown to be independent of costimulation and the anti-

CD3/CD28 ratio and was similar in naïve ($CD45RA^+$) and memory ($CD45RO^+$) T cell subpopulations. Remarkably, the PDE4B and PDE4D short forms were found to contribute largely to the time-dependent upregulation of PDE4 subtypes in human primary $CD4^+$ T cells. These data underline the complexity of the composition and regulation of individual PDE4 subtypes and multiple splice variants in these cells. In resting human primary $CD8^+$ T cells, *PDE4B* and *PDE4D* mRNA were predominantly expressed, whereas *PDE4A* mRNA had low expression levels. After anti-CD3/CD28 stimulation, the induction of PDE4 subtypes in $CD8^+$ T cells resembled, also not equal in a quantitative manner, the induction of PDE4 subtypes in $CD4^+$ T cells. In contrast to T cells, *PDE4B* mRNA was the predominantly expressed PDE4 subtype in freshly isolated human primary monocytes, followed by *PDE4A* and very low levels of *PDE4D*. During differentiation of monocytes to macrophages or to dendritic cells, *PDE4B* mRNA expression dramatically decreased, whereas *PDE4A* and *PDE4D* mRNA levels were less regulated. LPS stimulation of macrophages or dendritic cells strongly induced *PDE4B*, but not *PDE4A* and *PDE4D* mRNA. Taken together, these experiments revealed that PDE4 subtypes have distinct expression patterns in human primary immune cells and that the expressed subtypes are transcriptionally differentially regulated after stimulation.

With the intention to elucidate the impact of individual PDE4 subtypes on cell function and because of the lack of PDE4 subtype-specific inhibitors, two strategies were evaluated to specifically knock down PDE4 subtypes. Initially, several second generation antisense (AS^{2nd}) constructs or pools of short interfering RNAs (siRNAs) targeting *PDE4A*, *PDE4B*, or *PDE4D* mRNA were transfected into the human lung adenocarcinoma epithelial cell line A549 and were tested for efficacy, specificity, and tolerability. AS^{2nd} constructs as well as siRNAs were shown to induce substantial, PDE4 subtype-specific knockdown of mRNA and protein 24 h and 72 h after transfection. Because siRNAs were effective in lower concentrations, were well tolerated, and showed less variability in between experiments, the siRNA-mediated knockdown strategy was transferred to human primary $CD4^+$ T cells. The transfection of individual siRNAs into $CD4^+$ T cells with the nucleofector electroporation technique resulted in significant, specific, and well-tolerated knockdown of PDE4 subtypes on mRNA and protein level. In conclusion, the siRNA-mediated knockdown technique was a reliable tool specifically knock down PDE4 subtypes in human T cells.

Finally, the validated siRNA-mediated knockdown technique was used to ascertain the functional relevance of PDE4 subtypes in human primary $CD4^+$ T cells. SiRNA-mediated knockdown of either PDE4B or PDE4D inhibited anti-CD3/CD28 induced IL-2 release 24 h after stimulation to an extent overall similar to that observed with the panPDE4 inhibitor RP73401 (piclamilast), pointing to an overlapping function of PDE4B and PDE4D for IL-2 synthesis. At 48 h after stimulation, efficacies of PDE4B- and PDE4D-siRNAs to suppress IL-2

release were slightly diminished. Because substantial levels of IFN-γ and IL-5 were only measured at later time points, the effects of PDE4 subtype-specific siRNAs on these cytokines were determined at 48 h and 72 h. Considering the anti-CD3/CD28 induced generation of IFN-γ and IL-5, PDE4D-siRNA showed a predominant inhibitory effect, suggesting nonredundant roles of PDE4 subtypes for T cell cytokine production. However, the inhibition of cytokines was most effective when PDE4 subtype-specific siRNAs were applied in combination, indicating complementary functions of PDE4 subtypes. Although the effect of PDE4 inhibition on T cell proliferation was small, the PDE4D-targeting siRNA alone had similar anti-proliferative effects than RP73401, whereas PDE4A- or PDE4B-siRNAs were hardly effective. In all experiments, the additional application of the panPDE3 inhibitor motapizone had qualitatively no effect on the functional roles of individual PDE4 subtypes.

In conclusion, the present study demonstrates that individual PDE4 subtypes have overall nonredundant, but complementary, time-dependent roles in propagating various T cell functions, such as IL-2, IFN-γ, and IL-5 release and proliferation, and that PDE4D is the form that likely plays a predominant role in T cell function.

6 ZUSAMMENFASSUNG

Als sekundärer Botenstoff spielt zyklisches Adenosinmonophosphat (cAMP) eine entscheidende Rolle für die intrazelluläre Signalweiterleitung und steuert durch die Aktivierung von nachgeschalteten Systemen verschiedene Zellfunktionen. In Immunzellen wie T-Zellen, Monozyten, Makrophagen oder Dendritische Zellen hat cAMP hauptsächlich hemmende Eigenschaften auf zelluläre Funktionen. Da Typ 4 Phosphodiesterasen (PDE4) cAMP hydrolisieren und dadurch den hemmenden Einfluss von cAMP abschwächen können, sind sie kritische Regler von Entzündungssignalen. Die PDE4-Familie besteht aus vier Subtypen, die von jeweils einem Gen kodiert werden. Da PDE4-Subtypen in einer Vielzahl von entzündlichen Zellen exprimiert werden, wurde die PDE4-Familie ein attraktives Ziel für die Arzneimittelforschung für die Behandlung von chronisch entzündlichen Krankheiten wie Asthma oder chronische Bronchitis (COPD). In der Tat haben PDE4-Inhibitoren entzündungshemmende und immunmodulatorische Effekte in einer Reihe von entzündlichen und immunkompetenten Zellen und bewiesen Wirksamkeit in klinischen Studien. Allerdings ist größtenteils unbekannt, welche PDE4-Subtypen in einer bestimmten Immunzelle die inhibitorischen Effekte vermitteln. Während Befunde aus Knockout-Mäusen darauf hinweisen, dass PDE4-Subtypen tatsächlich verschiedene funktionelle Bedeutung in verschiedenen Immunzellen haben, ist die funktionelle Signifikanz von PDE4-Subtypen in T-Zellen und generell in Immunzellen menschlichen Ursprungs bisher schwer nachvollziehbar.

Die Ziele der vorliegenden Arbeit waren a) durch die Anwendung von quantitativen PCR-Experimenten, von PDE Aktivitätstests und von Immundetektionsanalysen das Expressionsmuster von PDE4-Subtypen in verschiedenen humanen primären Immunzellen herauszufinden; b) eine Antisense- und siRNA-vermittelte Technik zur spezifischen Herunterregulation (‚Knockdown') von PDE4-Subtypen in der Zelllinie A549 zu validieren und die besser geeignete Knockdownstrategie auf humane primäre $CD4^+$ T-Zellen zu überführen; und c) die funktionelle Bedeutung von PDE4-Subtypen in humanen primären $CD4^+$ T-Zellen herauszufinden.

Die vorliegende Arbeit zeigte, dass die mRNA der Subtypen *PDE4A*, *PDE4B* und *PDE4D* in humanen primären $CD4^+$ T-Zellen, $CD8^+$ T-Zellen, Monozyten, aus Monozyten differenzierten Makrophagen und aus Monozyten differenzierten Dendritischen Zellen unterschiedlich exprimiert war und differentiell reguliert wurde nach Stimulation, während die Expression von *PDE4C* mRNA nie detektierbar war. In ruhenden humanen primären $CD4^+$ T-Zellen wurde die geringste Expression und Enzymaktivität für *PDE4A* gemessen, während die *PDE4B*- und

PDE4D-Expression und Proteinaktivität größer waren und PDE4D als der vorherrschende Subtyp vorlag. Nach Stimulation der Zellen mit anti-CD3/CD28 wurde die Expression der PDE4-Subtypen zeitabhängig induziert. Sowohl Expression als auch Enzymaktivität von *PDE4A* und *PDE4D* wurden innerhalb von fünf Tagen hochreguliert, während *PDE4B* nur vorübergehend hochreguliert und 24 Stunden nach Stimulation am höchsten war. Die Induktion von PDE4-Subtypen war unabhängig von der Kostimulation und von den eingesetzten Mengen von anti-CD3/CD28 und ähnlich ausgeprägt in naiven ($CD45RA^+$) T-Zellen und T-Gedächtniszellen ($CD45RO^+$). Bemerkenswerterweise waren es hauptsächlich die kurzen Isoformen von PDE4B und PDE4D, die für die beobachtete zeitabhängige Hochregulation von PDE4-Subtypen in humanen primären $CD4^+$ T-Zellen beitrugen. Diese Befunde unterstreichen die Komplexität in Zusammensetzung und Regulation der PDE4-Subtypen und der vielfältigen Splice-Varianten in diesen Zellen. In ruhenden humanen primären $CD8^+$ T-Zellen wurde die geringste mRNA-Expression für *PDE4A* gemessen, während sie für *PDE4B* und *PDE4D* etwa gleich groß war. Nach Stimulation der Zellen mit anti-CD3/CD28 wurde die Expression der PDE4-Subtypen nach ähnlichem Muster wie in den $CD4^+$ T-Zellen zeitabhängig induziert, wenn auch nicht qualitativ im gleichen Ausmaß. Im Gegensatz zu T-Zellen war *PDE4B* der vorherrschend exprimierte Subtyp in frisch isolierten humanen primären Monozyten, gefolgt von *PDE4A* und einem sehr geringen Expressionsniveau von *PDE4D*. Während der Differenzierung von Monozyten zu Makrophagen oder Dendritischen Zellen nahm die *PDE4B*-Expression drastisch ab, während die *PDE4A*- und *PDE4B*-Expression weniger reguliert wurde. Stimulation mit LPS induzierte in diesen Makrophagen oder Dendritischen Zellen stark *PDE4B* mRNA, aber nicht *PDE4A* und *PDE4D* mRNA. Zusammengefasst zeigten diese Experimente, dass PDE4-Subtypen verschiedene Expressionsmuster in humanen primären Immunzellen haben und dass die PDE4-Subtypen transkriptionell unterschiedlich reguliert werden nach Stimulation.

Mit dem Ziel, die Bedeutung von individuellen PDE4-Subtypen auf die Zellfunktion aufzuklären, und durch das Fehlen von PDE4-Subtyp-spezifischen Inhibitoren wurden zwei Strategien evauliert, um spezifisch PDE4-Subtypen herunterzuregulieren. Zunächst wurden mehrere Antisense-Konstrukte oder Kombinationen von kurzen doppelsträngigen RNAs (siRNAs), die gegen PDE4-Subtypen gerichtet waren, in die humane epitheliale Lungenadenokarzinom-zelllinie A549 transfiziert und auf Effizienz, Spezifität und Verträglichkeit geprüft. Es wurde gezeigt, dass sowohl Antisense-Konstrukte als auch siRNAs beträchtliche, spezifische Herunterregulationen von PDE4-Subtypen auf mRNA- und Proteinebene 24 und 72 Stunden nach Transfektion bewirken konnten. Da siRNAs in geringeren Konzentrationen wirksam und gut verträglich waren und geringere Variabilitäten in den Experimenten zeigten, wurde die siRNA-vermittelte Knockdownstrategie auf humane primäre $CD4^+$ T-Zellen übertragen. Die Transfektion von einzelnen siRNAs in $CD4^+$ T-Zellen resultierte in signifikanten, spezifischen,

und gut verträglichen Herunterregulationen von mRNA und Protein der PDE4-Subtypen. Insgesamt wurde gezeigt, dass die Knockdown-Technik eine zuverlässige Methode war, um spezifisch PDE4-Subtypen in humanen T-Zellen herunterzuregulieren.

Letztendlich wurde die validierte siRNA-vermittelte Knockdowntechnik benutzt, um die funktionelle Relevanz von PDE4-Subtypen in humanen primären $CD4^+$ T-Zellen zu ermitteln. Sowohl die siRNA-vermittelte Herunterregulation von PDE4B als auch von PDE4D hemmten die anti-CD3/CD28 induzierte IL-2 Freisetzung 24 Stunden nach Stimulation in ähnlichem Ausmaß wie der panPDE4-Inhibitor RP73401 (Piclamilast). Dieser Befund deutet auf eine überlappende Rolle von PDE4B und PDE4D für die IL-2 Synthese hin. Nach 48-stündiger Stimulation waren die hemmenden Effekte von PDE4B- und PDE4D-siRNAs auf die IL-2 Synthese etwas schwächer. Da wesentliche Mengen von IFN-γ und IL-5 nur zu späteren Zeitpunkten messbar waren, wurden die Effekte von PDE4-Subtyp-spezifischen siRNAs auf diese Zytokine nach 48 und 72 Stunden bestimmt. Betrachtet man die anti-CD3/CD28 induzierte Bildung von IFN-γ und IL-5, so zeigte die gegen PDE4D gerichtete siRNA einen vorwiegenden inhibitorischen Effekt auf diese Zytokine. Dies lässt vermuten, dass die PDE4-Subtypen keine redundanten Rollen für die Zytokinproduktion innehaben. Allerdings war die Hemmung der Zytokine dann am größten, wenn alle PDE4-Subtyp-spezifischen siRNAs zusammen angewendet wurden, was auf komplementäre Funktionen der PDE4-Subtypen hindeutet. Obwohl die Effekte der PDE4-Hemmung auf die T-Zellproliferation gering waren, hatte nur die gegen PDE4D gerichtete siRNA eine ähnliche anti-proliferative Wirkung wie RP73401, während PDE4A- oder PDE4B-siRNAs kaum effektiv waren. In allen Experimenten hatte die zusätzliche Anwendung des panPDE3-Inhibitors Motapizone keinen qualitativen Einfluss auf die funktionellen Rollen der individuellen PDE4-Subtypen.
Schlussfolgernd legt die vorliegende Arbeit dar, dass individuelle PDE4-Subtypen insgesamt nicht redundante, aber komplementäre, zeitabhängige Rollen spielen bezüglich der Weiterleitung von zahlreichen T-Zellfunktionen, wie die IL-2, IFN-γ und IL-5 Freisetzung und der T-Zellproliferation, und dass PDE4D der Subtyp ist, der wahrscheinlich eine übergeordnete Rolle für die T-Zellfunktion spielt.

7 REFERENCES

Aandahl,E.M., Moretto,W.J., Haslett,P.A., Vang,T., Bryn,T., Tasken,K., and Nixon,D.F. (2002). Inhibition of antigen-specific T cell proliferation and cytokine production by protein kinase A type I. J. Immunol. *169*, 802-808.

Abrahamsen,H., Baillie,G., Ngai,J., Vang,T., Nika,K., Ruppelt,A., Mustelin,T., Zaccolo,M., Houslay,M., and Tasken,K. (2004). TCR- and CD28-mediated recruitment of phosphodiesterase 4 to lipid rafts potentiates TCR signaling. J. Immunol. *173*, 4847-4858.

Acuto,O., Mise-Omata,S., Mangino,G., and Michel,F. (2003). Molecular modifiers of T cell antigen receptor triggering threshold: the mechanism of CD28 costimulatory receptor. Immunol. Rev. *192*, 21-31.

Alama,A., Barbieri,F., Cagnoli,M., and Schettini,G. (1997). Antisense oligonucleotides as therapeutic agents. Pharmacol. Res. *36*, 171-178.

Ariga,M., Neitzert,B., Nakae,S., Mottin,G., Bertrand,C., Pruniaux,M.P., Jin,S.L., and Conti,M. (2004). Nonredundant function of phosphodiesterases 4D and 4B in neutrophil recruitment to the site of inflammation. J. Immunol. *173*, 7531-7538.

Arp,J., Kirchhof,M.G., Baroja,M.L., Nazarian,S.H., Chau,T.A., Strathdee,C.A., Ball,E.H., and Madrenas,J. (2003). Regulation of T-cell activation by phosphodiesterase 4B2 requires its dynamic redistribution during immunological synapse formation. Mol. Cell. Biol. *23*, 8042-8057.

Asirvatham,A.L., Galligan,S.G., Schillace,R.V., Davey,M.P., Vasta,V., Beavo,J.A., and Carr,D.W. (2004). A-Kinase anchoring proteins interact with phosphodiesterases in T lymphocyte cell lines. J. Immunol. *173*, 4806-4814.

Aubier,M. and Barnes,P.J. (1995). Theophylline and phosphodiesterase inhibitors. Eur. Respir. J. *8*, 347-348.

Baillie,G., MacKenzie,S.J., and Houslay,M.D. (2001). Phorbol 12-myristate 13-acetate triggers the protein kinase A-mediated phosphorylation and activation of the PDE4D5 cAMP phosphodiesterase in human aortic smooth muscle cells through a route involving extracellular signal regulated kinase (ERK). Mol. Pharmacol. *60*, 1100-1111.

Baillie,G.S. and Houslay,M.D. (2005). Arrestin times for compartmentalised cAMP signalling and phosphodiesterase-4 enzymes. Curr. Opin. Cell Biol. *17*, 129-134.

Baillie,G.S., MacKenzie,S.J., McPhee,I., and Houslay,M.D. (2000). Subfamily selective actions in the ability of Erk2 MAP kinase to phosphorylate and regulate the activity of PDE4 cyclic AMP-specific phosphodiesterases. Br. J. Pharmacol. *131*, 811-819.

Baillie,G.S., Scott,J.D., and Houslay,M.D. (2005). Compartmentalisation of phosphodiesterases and protein kinase A: opposites attract. FEBS Lett. *579*, 3264-3270.

Baillie,G.S., Sood,A., McPhee,I., Gall,I., Perry,S.J., Lefkowitz,R.J., and Houslay,M.D. (2003). beta-Arrestin-mediated PDE4 cAMP phosphodiesterase recruitment regulates beta-adrenoceptor switching from Gs to Gi. Proc. Natl. Acad. Sci. USA *100*, 940-945.

Baillie,G.S., Huston,E., Scotland,G., Hodgkin,M., Gall,I., Peden,A.H., MacKenzie,C., Houslay,E.S., Currie,R., Pettitt,T.R., Walmsley,A.R., Wakelam,M.J.O., Warwicker,J., and Houslay,M.D. (2002). TAPAS-1, a novel microdomain within the unique N-terminal region of the PDE4A1 cAMP-specific phosphodiesterase that allows rapid, Ca^{2+}-triggered membrane association with selectivity for interaction with phosphatidic acid. J. Biol. Chem. *277*, 28298-28309.

Bajpai,M., Fiedler,S.E., Huang,Z., Vijayaraghavan,S., Olson,G.E., Livera,G., Conti,M., and Carr,D.W. (2006). AKAP3 selectively binds PDE4A isoforms in bovine spermatozoa. Biol. Reprod. *74*, 109-118.

Banchereau,J., Briere,F., Caux,C., Davoust,J., Lebecque,S., Liu,Y.J., Pulendran,B., and Palucka,K. (2000). Immunobiology of dendritic cells. Annu. Rev. Immunol. *18*, 767-811.

Banchereau,J. and Steinman,R.M. (1998). Dendritic cells and the control of immunity. Nature *392*, 245-252.

Banner,K.H. and Trevethick,M.A. (2004). PDE4 inhibition: a novel approach for the treatment of inflammatory bowel disease. Trends Pharmacol. Sci. *25*, 430-436.

Barber,R., Baillie,G.S., Bergmann,R., Shepherd,M.C., Sepper,R., Houslay,M.D., and Heeke,G.V. (2004). Differential expression of PDE4 cAMP phosphodiesterase isoforms in inflammatory cells of smokers with COPD, smokers without COPD, and nonsmokers. Am J Physiol Lung Cell Mol Physiol *287*, L332-L343.

Barczyk,A., Pierzchala,W., Kon,O.M., Cosio,B., Adcock,I.M., and Barnes,P.J. (2006). Cytokine production by bronchoalveolar lavage T lymphocytes in chronic obstructive pulmonary disease. J. Allergy Clin. Immunol. *117*, 1484-1492.

Barnes,A.P., Livera,G., Huang,P., Sun,C., O'Neal,W.K., Conti,M., Stutts,M.J., and Milgram,S.L. (2005). Phosphodiesterase 4D forms a cAMP diffusion barrier at the apical membrane of the airway epithelium. J. Biol. Chem. *280*, 7997-8003.

Barnes,P.J. (2003a). New concepts in chronic obstructive pulmonary disease. Annu. Rev. Med. *54*, 113-129.

Barnes,P.J. (2003b). Theophylline: new perspectives for an old drug. Am. J. Respir. Cell Mol. Biol. *167*, 813-818.

Barnes,P.J. (2004). Alveolar macrophages as orchestrators of COPD. COPD. *1*, 59-70.

Barnes,P.J. and Pauwels,R.A. (1994). Theophylline in the management of asthma: time for reappraisal? Eur. Respir. J. *7*, 579-591.

Barnes,P.J., Shapiro,S.D., and Pauwels,R.A. (2003). Chronic obstructive pulmonary disease: molecular and cellular mechanisms. Eur. Respir. J. *22*, 672-688.

Barnette,M.S., Grous,M., Cieslinski,L.B., Burman,M., Christensen,S.B., and Torphy,T.J. (1995a). Inhibitors of phosphodiesterase IV (PDE IV) increase acid secretion in rabbit isolated gastric glands: correlation between function and interaction with a high-affinity rolipram binding site. J. Pharmacol. Exp. Ther. *273*, 1396-1402.

Barnette,M.S., Manning,C.D., Cieslinski,L.B., Burman,M., Christensen,S.B., and Torphy,T.J. (1995b). The ability of phosphodiesterase IV inhibitors to suppress superoxide production in guinea pig eosinophils is correlated with inhibition of phosphodiesterase IV catalytic activity. J. Pharmacol. Exp. Ther. *273*, 674-679.

Barnette,M.S., Bartus,J.O., Burman,M., Christensen,S.B., Cieslinski,L.B., Esser,K.M., Prabhakar,U.S., Rush,J.A., and Torphy,T.J. (1996). Association of the anti-inflammatory activity of phosphodiesterase 4 (PDE4) inhibitors with either inhibition of PDE4 catalytic activity or competition for [^{3}H]rolipram binding. Biochem. Pharmacol. *51*, 949-956.

Barnette,M.S., Christensen,S.B., Essayan,D.M., Grous,M., Prabhakar,U., Rush,J.A., Kagey-Sobotka,A., and Torphy,T.J. (1998). SB 207499 (Ariflo), a potent and selective second-generation phosphodiesterase 4 inhibitor: in vitro anti-inflammatory actions. J. Pharmacol. Exp. Ther. *284*, 420-426.

Baroja,M.L., Cieslinski,L.B., Torphy,T.J., Wange,R.L., and Madrenas,J. (1999). Specific CD3 (epsilon) association of a phosphodiesterase 4B isoform determines its selective tyrosine phosphorylation after CD3 ligation. J. Immunol. *162*, 2016-2023.

Bas,A., Forsberg,G., Hammarstrom,S., and Hammarstrom,M.L. (2004). Utility of the housekeeping genes 18S rRNA, beta-actin and glyceraldehyde-3-phosphate-dehydrogenase for normalization in real-time quantitative reverse transcriptase-polymerase chain reaction analysis of gene expression in human T lymphocytes. Scand. J. Immunol. *59*, 566-573.

Bateman,E.D., Izquierdo,J.L., Harnest,U., Hofbauer,P., Magyar,P., Schmid-Wirlitsch,C., Leichtl,S., and Bredenbroker,D. (2006). Efficacy and safety of roflumilast in the treatment of asthma. Ann. Allergy Asthma. Immunol. *96*, 679-686.

Bauer,A.C. and Schwabe,U. (1980). An improved assay of cyclic 3',5'-nucleotide phosphodiesterases with QAE-Sephadex columns. N. Schmied. Arch. Pharmacol. *311*, 193-198.

Beard,M.B., Olsen,A.E., Jones,R.E., Erdogan,S., Houslay,M.D., and Bolger,G.B. (2000). UCR1 and UCR2 domains unique to the cAMP-specific phosphodiesterase family form a discrete module via electrostatic interactions. J. Biol. Chem. *275*, 10349-10358.

Beavo,J.A., Hardman,J.G., and Sutherland,E.W. (1970). Hydrolysis of cyclic guanosine and adenosine 3',5'-monophosphates by rat and bovine tissues. J. Biol. Chem. *245*, 5649-5655.

Beavo,J.A. and Brunton,L.L. (2002). Cyclic nucleotide reasearch - still expanding after half a century. Nat. Rev. Mol. Cell Biol. *3*, 710-718.

Beavo,J.A. and Reifsnyder,D.H. (1990). Primary sequence of cyclic nucleotide phosphodiesterase isozymes and the design of selective inhibitors. Trends Pharmacol. Sci. *11*, 150-155.

Bell,E.B., Sparshott,S.M., and Bunce,C. (1998). $CD4^+$ T-cell memory, CD45R subsets and the persistence of antigen--a unifying concept. Immunol. Today *19*, 60-64.

Bender,A.T. and Beavo,J.A. (2006). Cyclic nucleotide phosphodiesterases: molecular regulation to clinical use. Pharmacol. Rev. *58*, 488-520.

Benimetskaya,L., Wittenberger,T., Stein,C.A., Hofmann,H.P., Weller,C., Lai,J.C., Miller,P., and Gekeler,V. (2004). Changes in gene expression induced by phosphorothioate oligodeoxynucleotides (including G3139) in PC3 prostate carcinoma cells are recapitulated at least in part by treatment with interferon-beta and -gamma. Clin. Cancer Res. *10*, 3678-3688.

Berg,L.J., Finkelstein,L.D., Lucas,J.A., and Schwartzberg,P.L. (2005). Tec family kinases in T lymphocyte development and function. Annu. Rev. Immunol. *23*, 549-600.

Bernstein,E., Caudy,A.A., Hammond,S.M., and Hannon,G.J. (2001). Role for a bidentate ribonuclease in the initiation step of RNA interference. Nature *409*, 363-366.

Beutler,B. and Cerami,A. (1988). The common mediator of shock, cachexia, and tumor necrosis. Adv. Immunol. *42*, 213-231.

Bhattacharya,M., Babwah,A.V., and Ferguson,S.S. (2004). Small GTP-binding protein-coupled receptors. Biochem. Soc. Trans. *32*, 1040-1044.

Bloom,T. and Beavo,J. (1996). Identification and tissue-specific expression of PDE7 phosphodiesterase splice variants. Proc. Natl. Acad. Sci. USA *93*, 14188-14192.

Boehm,U., Klamp,T., Groot,M., and Howard,J.C. (1997). Cellular responses to interferon-gamma. Annu. Rev. Immunol. *15*, 749-795.

Bolger,G., Michaeli,T., Martins,T., St John,T., Steiner,B., Rodgers,L., Riggs,M., Wigler,M., and Ferguson,K. (1993). A family of human phosphodiesterases homologous to the dunce learning and memory gene product of Drosophila melanogaster are potential targets for antidepressant drugs. Mol. Cell. Biol. *13*, 6558-6571.

Bolger,G.B., Baillie,G.S., Li,X., Lynch,M.J., Herzyk,P., Mohamed,A., Mitchell,L.H., McCahill,A., Hundsrucker,C., Klussmann,E., Adams,D.R., and Houslay,M.D. (2006). Scanning peptide array analyses identify overlapping binding sites for the signalling scaffold proteins, beta-arrestin and RACK1, in cAMP-specific phosphodiesterase PDE4D5. Biochem. J. *398*, 23-36.

Bolger,G.B., McCahill,A., Huston,E., Cheung,Y.F., McSorley,T., Baillie,G.S., and Houslay,M.D. (2003a). The unique amino-terminal region of the PDE4D5 cAMP phosphodiesterase isoform confers preferential interaction with beta-arrestins. J. Biol. Chem. *278*, 49230-49238.

Bolger,G.B., Peden,A.H., Steele,M.R., MacKenzie,C., McEwan,D.G., Wallace,D.A., Huston,E., Baillie,G.S., and Houslay,M.D. (2003b). Attenuation of the activity of the cAMP-specific phosphodiesterase PDE4A5 by interaction with the immunophilin XAP2. J. Biol. Chem. *278*, 33351-33363.

Boothby,M., Mora,A.L., and Stephenson,L.M. (2001). Lymphokine-dependent proliferation of T-lymphoid cells: regulated responsiveness and role in vivo. Crit. Rev. Immunol. *21*, 487-522.

Borbe,H.O., Hilboll,G., and Prop,G. (1986). Inhibition of human platelet aggregation by motapizone via an increase in intracellular cAMP. Agents Actions Suppl. *20*, 249-257.

Boswell-Smith,V., Spina,D., and Page,C.P. (2006). Phosphodiesterase inhibitors. Br. J. Pharmacol. *147 Suppl 1*, S252-S257.

Bourne,H.R. (1997). How receptors talk to trimeric G proteins. Curr. Opin. Cell Biol. *9*, 134-142.

Bradford,M.M. (1976). A rapid and sensitive method for the quantitation of microgram quantities of protein utilizing the principle of protein-dye binding. Anal. Biochem. *72*, 248-254.

Bradley,J., Reisert,J., and Frings,S. (2005). Regulation of cyclic nucleotide-gated channels. Curr. Opin. Neurobiol. *15*, 343-349.

Bredenbröker,D., Syed,J., Leichtl,S., Rathgeb,F., and Wurst,W. (2002). Roflumilast, a new orally active phosphodiesterase 4 inhibitor, is effective in the treatment of chronic obstructive pulmonary disease. Eur. Respir. J. *20*, Suppl. 38, 374s.

Bromley,S.K., Burack,W.R., Johnson,K.G., Somersalo,K., Sims,T.N., Sumen,C., Davis,M.M., Shaw,A.S., Allen,P.M., and Dustin,M.L. (2001). The immunological synapse. Annu. Rev. Immunol. *19*, 375-396.

Bundschuh,D.S., Eltze,M., Barsig,J., Wollin,L., Hatzelmann,A., and Beume,R. (2001). In vivo efficacy in airway disease models of roflumilast, a novel orally active PDE4 inhibitor. J. Pharmacol. Exp. Ther. *297*, 280-290.

Burnett,A.L. (2005). Phosphodiesterase 5 mechanisms and therapeutic applications. Am. J. Cardiol. *96*, 29-31.

Cantrell,D. (1996). T cell antigen receptor signal transduction pathways. Annu. Rev. Immunol. *14*, 259-274.

Carlisle Michel,J.J., Dodge,K.L., Wong,W., Mayer,N.C., Langeberg,L.K., and Scott,J.D. (2004). PKA-phosphorylation of PDE4D3 facilitates recruitment of the mAKAP signalling complex. Biochem. J. *381*, 587-592.

Chambers,C.A. and Allison,J.P. (1999). Costimulatory regulation of T cell function. Curr. Opin. Cell Biol. *11*, 203-210.

Chambers,R.J., Abrams,K., Castleberry,T.A., Cheng,J.B., Fisher,D.A., Kamath,A.V., Marfat,A., Nettleton,D.O., Pillar,J.D., and Salter,E.D. (2006). A new chemical tool for exploring the role of the PDE4D isozyme in leukocyte function. Bioorg. Med. Chem. Lett. *16*, 718-721.

Chi,J.T., Chang,H.Y., Wang,N.N., Chang,D.S., Dunphy,N., and Brown,P.O. (2003). Genomewide view of gene silencing by small interfering RNAs. Proc. Natl. Acad. Sci. USA *100*, 6343-6346.

Chow,C.W. and Davis,R.J. (2000). Integration of calcium and cyclic AMP signaling pathways by 14-3-3. Mol. Cell. Biol. *20*, 702-712.

Chrivia,J.C., Kwok,R.P., Lamb,N., Hagiwara,M., Montminy,M.R., and Goodman,R.H. (1993). Phosphorylated CREB binds specifically to the nuclear protein CBP. Nature *365*, 855-859.

Colicelli,J., Birchmeier,C., Michaeli,T., O'Neill,K., Riggs,M., and Wigler,M. (1989). Isolation and characterization of a mammalian gene encoding a high-affinity cAMP phosphodiesterase. Proc. Natl. Acad. Sci. USA *86*, 3599-3603.

Conti,M. (2004). A view into the catalytic pocket of cyclic nucleotide phosphodiesterases. Nat. Struct. Mol. Biol. *11*, 809-810.

Conti,M. and Jin,S.L. (1999). The molecular biology of cyclic nucleotide phosphodiesterases. Prog. Nucleic Acid Res. Mol. Biol. *63*, 1-38.

Conti,M., Kasson,B.G., and Hsueh,A.J. (1984). Hormonal regulation of 3',5'-adenosine monophosphate phosphodiesterases in cultured rat granulosa cells. Endocrinology *114*, 2361-2368.

Conti,M., Richter,W., Mehats,C., Livera,G., Park,J.Y., and Jin,C. (2003). Cyclic AMP-specific PDE4 phosphodiesterases as critical components of cyclic AMP signaling. J. Biol. Chem. *278*, 5493-5496.

Corbin,J.D., Keely,S.L., and Park,C.R. (1975). The distribution and dissociation of cyclic adenosine 3',5'-monophosphate-dependent protein kinases in adipose, cardiac, and other tissues. J. Biol. Chem. *250*, 218-225.

Couzin,J. (2002). Breakthrough of the year. Small RNAs make big splash. Science *298*, 2296-2297.

Crane,I.J. and Forrester,J.V. (2005). Th1 and Th2 lymphocytes in autoimmune disease. Crit. Rev. Immunol. *25*, 75-102.

Crooke,S.T., Lemonidis,K.M., Neilson,L., Griffey,R., Lesnik,E.A., and Monia,B.P. (1995). Kinetic characteristics of *Escherichia coli* RNase H1: cleavage of various antisense oligonucleotide-RNA duplexes. Biochem. J. *312 (Pt 2)*, 599-608.

D'Sa,C., Tolbert,L.M., Conti,M., and Duman,R.S. (2002). Regulation of cAMP-specific phosphodiesterases type 4B and 4D (PDE4) splice variants by cAMP signaling in primary cortical neurons. J. Neurochem. *81*, 745-757.

Davis,M.M. and Bjorkman,P.J. (1988). T-cell antigen receptor genes and T-cell recognition. Nature *334*, 395-402.

Davis,R.L., Takayasu,H., Eberwine,M., and Myres,J. (1989). Cloning and characterization of mammalian homologs of the Drosophila dunce+ gene. Proc. Natl. Acad. Sci. USA *86*, 3604-3608.

de Lima,M.C., Simoes,S., Pires,P., Gaspar,R., Slepushkin,V., and Duzgunes,N. (1999). Gene delivery mediated by cationic liposomes: from biophysical aspects to enhancement of transfection. Mol. Membr. Biol. *16*, 103-109.

de Rooij,J., Zwartkruis,F.J.T., Verheijen,M.H.G., Cool,R.H., Nijman,S.M.B., Wittinghofer,A., and Bos,J.L. (1998). Epac is a Rap1 guanine-nucleotide-exchange factor directly activated by cyclic AMP. Nature *396*, 474-477.

Degerman,E., Belfrage,P., and Manganiello,V.C. (1997). Structure, localization, and regulation of cGMP-inhibited phosphodiesterase (PDE3). J. Biol. Chem. *272*, 6823-6826.

Del Prete,G.F., De Carli,M., Mastromauro,C., Biagiotti,R., Macchia,D., Falagiani,P., Ricci,M., and Romagnani,S. (1991). Purified protein derivative of *Mycobacterium tuberculosis* and excretory-secretory antigen(s) of *Toxocara canis* expand in vitro human T cells with stable and opposite (type 1 T helper or type 2 T helper) profile of cytokine production. J. Clin. Invest. *88*, 346-350.

Dent,G., White,S.R., Tenor,H., Bodtke,K., Schudt,C., Leff,A.R., Magnussen,H., and Rabe,K.F. (1998). Cyclic nucleotide phosphodiesterase in human bronchial epithelial cells: characterization of isoenzymes and functional effects of PDE inhibitors. Pulmon. Pharmacol. Therap. *11*, 47-56.

Derian,C.K., Santulli,R.J., Rao,P.E., Solomon,H.F., and Barrett,J.A. (1995). Inhibition of chemotactic peptide-induced neutrophil adhesion to vascular endothelium by cAMP modulators. J. Immunol. *154*, 308-317.

Dhillon,A.S., Pollock,C., Steen,H., Shaw,P.E., Mischak,H., and Kolch,W. (2002). Cyclic AMP-dependent kinase regulates Raf-1 kinase mainly by phosphorylation of serine 259. Mol. Cell. Biol. *22*, 3237-3246.

Dias,N. and Stein,C.A. (2002). Antisense oligonucleotides: basic concepts and mechanisms. Mol. Canc. Therap. *1*, 347-355.

Diks,S.H., Richel,D.J., and Peppelenbosch,M.P. (2004). LPS signal transduction: the picture is becoming more complex. Curr. Top. Med. Chem. *4*, 1115-1126.

Dodge,K.L., Khouangsathiene,S., Kapiloff,M.S., Mouton,R., Hill,E.V., Houslay,M.D., Langeberg,L.K., and Scott,J.D. (2001). mAKAP assembles a protein kinase A/PDE4 phosphodiesterase cAMP signaling module. EMBO J. *20*, 1921-1930.

Dudai,Y., Jan,Y.N., Byers,D., Quinn,W.G., and Benzer,S. (1976). dunce, a mutant of Drosophila deficient in learning. Proc. Natl. Acad. Sci. USA *73*, 1684-1688.

Dykxhoorn,D.M., Novina,C.D., and Sharp,P.A. (2003). Killing the messenger: short RNAs that silence gene expression. Nat. Rev. Mol. Cell Biol. *4*, 457-467.

Eigler,A., Siegmund,B., Emmerich,U., Baumann,K.H., Hartmann,G., and Endres,S. (1998). Anti-inflammatory activities of cAMP-elevating agents: enhancement of IL-10 synthesis and concurrent suppression of TNF production. J. Leukoc. Biol. *63*, 101-107.

Ekholm,D., Belfrage,P., Manganiello,V., and Degerman,E. (1997). Protein kinase A-dependent activation of PDE4 (cAMP-specific cyclic nucleotide phosphodiesterase) in cultured bovine vascular smooth muscle cells. Biochim. Biophys. Acta *1356*, 64-70.

Elbashir,S.M., Harborth,J., Lendeckel,W., Yalcin,A., Weber,K., and Tuschl,T. (2001). Duplexes of 21-nucleotide RNAs mediate RNA interference in cultured mammalian cells. Nature *411*, 494-498.

Elbashir,S.M., Harborth,J., Weber,K., and Tuschl,T. (2002). Analysis of gene function in somatic mammalian cells using small interfering RNAs. Methods *26*, 199-213.

Essayan,D.M. (2001). Cyclic nucleotide phosphodiesterases. J. Allergy Clin. Immunol. *108*, 671-680.

Essayan,D.M., Huang,S.K., Undem,B.J., Kagey-Sobotka,A., and Lichtenstein,L.M. (1994). Modulation of antigen- and mitogen-induced proliferative responses of peripheral blood mononuclear cells by nonselective and isozyme selective cyclic nucleotide phosphodiesterase inhibitors. J. Immunol. *153*, 3408-3416.

Essayan,D.M. (1999). Cyclic nucleotide phosphodiesterase (PDE) inhibitors and immunomodulation. Biochem. Pharmacol. *57*, 965-973.

Fain,G.L., Matthews,H.R., Cornwall,M.C., and Koutalos,Y. (2001). Adaptation in vertebrate photoreceptors. Physiol. Rev. *81*, 117-151.

Fawcett,L., Baxendale,R., Stacey,P., McGrouther,C., Harrow,I., Soderling,S., Hetman,J., Beavo,J.A., and Phillips,S.C. (2000). Molecular cloning and characterization of a distinct human phosphodiesterase gene family: PDE11A. Proc. Natl. Acad. Sci. USA *97*, 3702-3707.

Felgner,P.L., Gadek,T.R., Holm,M., Roman,R., Chan,H.W., Wenz,M., Northrop,J.P., Ringold,G.M., and Danielsen,M. (1987). Lipofection: A highly efficient, lipid-mediated DNA-transfection procedure. Proc. Natl. Acad. Sci. USA *84*, 7413-7417.

Fine,J.S., Byrnes,H.D., Zavodny,P.J., and Hipkin,R.W. (2001). Evaluation of signal transduction pathways in chemoattractant-induced human monocyte chemotaxis. Inflammation *25*, 61-67.

Fire,A., Xu,S., Montgomery,M.K., Kostas,S.A., Driver,S.E., and Mello,C.C. (1998). Potent and specific genetic interference by double-stranded RNA in *Caenorhabditis elegans*. Nature *391*, 806-811.

Fisher,D.A., Smith,J.F., Pillar,J.S., Denis,S.H., and Cheng,J.B. (1998a). Isolation and characterization of PDE9A, a novel human cGMP-specific phosphodiesterase. J. Biol. Chem. *273*, 15559-15564.

Fisher,D.A., Smith,J.F., Pillar,J.S., St.Denis,S.H., and Cheng,J.B. (1998b). Isolation and characterization of PDE8A, a novel human cAMP-specific phosphodiesterase. Biochem. Biophys. Res. Commun. *246*, 570-577.

Francis,S.H., Turko,I.V., and Corbin,J.D. (2001). Cyclic nucleotide phosphodiesterases: relating structure and function. Prog. Nucleic Acid Res. Mol. Biol. *65*, 1-52.

Fraser,J.D., Irving,B.A., Crabtree,G.R., and Weiss,A. (1991). Regulation of interleukin-2 gene enhancer activity by the T cell accessory molecule CD28. Science *251*, 313-316.

Frauwirth,K.A. and Thompson,C.B. (2002). Activation and inhibition of lymphocytes by costimulation. J. Clin. Invest. *109*, 295-299.

Freedman,N.J. and Lefkowitz,R.J. (1996). Desensitization of G protein-coupled receptors. Recent Prog. Horm. Res. *51*, 319-351.

Fruman,D.A. (2004). Phosphoinositide 3-kinase and its targets in B-cell and T-cell signaling. Curr. Opin. Immunol. *16*, 314-320.

Fujishige,K., Kotera,J., Michibata,H., Yuasa,K., Takebayashi,S.i., Okumura,K., and Omori,K. (1999). Cloning and characterization of a novel human phosphodiesterase that hydrolyzes both cAMP and cGMP (PDE10A). J. Biol. Chem. *274*, 18438-18445.

Ganesh,L., Burstein,E., Guha-Niyogi,A., Louder,M.K., Mascola,J.R., Klomp,L.W., Wijmenga,C., Duckett,C.S., and Nabel,G.J. (2003). The gene product Murr1 restricts HIV-1 replication in resting CD4+ lymphocytes. Nature *426*, 853-857.

Gantner,F., Gotz,C., Gekeler,V., Schudt,C., Wendel,A., and Hatzelmann,A. (1998). Phosphodiesterase profile of human B lymphocytes from normal and atopic donors and the effects of PDE inhibition on B cell proliferation. Br. J. Pharmacol. *123*, 1031-1038.

Gantner,F., Kupferschmidt,R., Schudt,C., Wendel,A., and Hatzelmann,A. (1997a). *In vitro* differentiation of human monocytes to macrophages: change of PDE profile and its relationship to suppression of tumour necrosis factor-alpha release by PDE inhibitors. Br. J. Pharmacol. *121*, 221-231.

Gantner,F., Schudt,C., Wendel,A., and Hatzelmann,A. (1999). Characterization of the phosphodiesterase (PDE) pattern of *in vitro*-generated human dendritic cells (DC) and the influence of PDE inhibitors on DC function. Pulm. Pharmacol. Ther. *12*, 377-386.

Gantner,F., Tenor,H., Gekeler,V., Schudt,C., Wendel,A., and Hatzelmann,A. (1997b). Phosphodiesterase profiles of highly purified human peripheral blood leukocyte populations from normal and atopic individuals: A comparative study. J. Allergy Clin. Immunol. *100*, 527-535.

Gehl,J. (2003). Electroporation: theory and methods, perspectives for drug delivery, gene therapy and research. Acta Physiol. Scand. *177*, 437-447.

Gelfand,E.W. and Dakhama,A. (2006). $CD8^+$ T lymphocytes and leukotriene B4: novel interactions in the persistence and progression of asthma. J. Allergy Clin. Immunol. *117*, 577-582.

Giembycz,M.A. (2002). Development status of second generation PDE4 inhibitors for asthma and COPD: the story so far. Monaldi Arch. Chest Dis. *57*, 48-64.

Giembycz,M.A., Corrigan,C.J., Seybold,J., Newton,R., and Barnes,P.J. (1996). Identification of cyclic AMP phosphodiesterases 3, 4 and 7 in human $CD4^+$ and $CD8^+$ T-lymphocytes: role in regulating proliferation and the biosynthesis of interleukin-2. Br. J. Pharmacol. *118*, 1945-1958.

Giembycz,M.A. (1992). Could isoenzyme-selective phosphodiesterase inhibitors render bronchodilator therapy redundant in the treatment of bronchial asthma? Biochem. Pharmacol. *43*, 2041-2051.

Giles,R.V., Spiller,D.G., Green,J.A., Clark,R.E., and Tidd,D.M. (1995a). Optimization of antisense oligodeoxynucleotide structure for targeting bcr-abl mRNA. Blood *86*, 744-754.

Giles,R.V., Spiller,D.G., and Tidd,D.M. (1995b). Detection of ribonuclease H-generated mRNA fragments in human leukemia cells following reversible membrane permeabilization in the presence of antisense oligodeoxynucleotides. Antisense Res. Dev. *5*, 23-31.

Glavas,N.A., Ostenson,C., Schaefer,J.B., Vasta,V., and Beavo,J.A. (2001). T cell activation up-regulates cyclic nucleotide phosphodiesterases 8A1 and 7A3. Proc. Natl. Acad. Sci. USA *98*, 6319-6324.

Gonzalez,G.A. and Montminy,M.R. (1989). Cyclic AMP stimulates somatostatin gene transcription by phosphorylation of CREB at serine 133. Cell *59*, 675-680.

Gonzalez-Barderas,M., Gallego-Delgado,J., Mas,S., Duran,M.C., Lazaro,A., Hernandez-Merida,S., Egido,J., and Vivanco,F. (2004). Isolation of circulating human monocytes with high purity for proteomic analysis. Proteomics *4*, 432-437.

Gor,D.O., Rose,N.R., and Greenspan,N.S. (2003). TH1-TH2: a procrustean paradigm. Nat. Immunol. *4*, 503-505.

Grange,M., Sette,C., Cuomo,M., Conti,M., Lagarde,M., Prigent,A.F., and Nemoz,G. (2000). The cAMP-specific phosphodiesterase PDE4D3 is regulated by phosphatidic acid binding. Consequences for cAMP signaling pathway and characterization of phosphatidic acid binding site. J. Biol. Chem. *275*, 33379-33387.

Gresch,O., Engel,F.B., Nesic,D., Tran,T.T., England,H.M., Hickman,E.S., Korner,I., Gan,L., Chen,S., and Castro-Obregon,S. (2004). New non-viral method for gene transfer into primary cells. Methods *33*, 151-163.

Gretarsdottir,S., Thorleifsson,G., Reynisdottir,S.T., Manolescu,A., Jonsdottir,S., Jonsdottir,T., Gudmundsdottir,T., Bjarnadottir,S.M., Einarsson,O.B., Gudjonsdottir,H.M., Hawkins,M., Gudmundsson,G., Gudmundsdottir,H., Andrason,H., Gudmundsdottir,A.S., Sigurdardottir,M., Chou,T.T., Nahmias,J., Goss,S., Sveinbjornsdottir,S., Valdimarsson,E.M., Jakobsson,F., Agnarsson,U., Gudnason,V., Thorgeirsson,G., Fingerle,J., Gurney,M., Gudbjartsson,D., Frigge,M.L., Kong,A., Stefansson,K., and Gulcher,J.R. (2003). The gene encoding phosphodiesterase 4D confers risk of ischemic stroke. Nat. Genet. *35*, 131-138.

Grewe,S.R., Chan,S.C., and Hanifin,J.M. (1982). Elevated leukocyte cyclic AMP-phosphodiesterase in atopic disease: a possible mechanism for cyclic AMP-agonist hyporesponsiveness. J. Allergy Clin. Immunol. *70*, 452-457.

Gruetzkau, A., Gerstmayer, B., Moewes B., Kaiser T., Raba K., Bosio A., Scheffold A., and Radbruch A. What happens with highly purified monocytes on their way from blood to the bench? Heidelberg Cytometry Symposium (HCS) . 2003.
Ref Type: Abstract

Guipponi,M., Scott,H.S., Kudoh,J., Kawasaki,K., Shibuya,K., Shintani,A., Asakawa,S., Chen,H., Lalioti,M.D., Rossier,C., Minoshima,S., Shimizu,N., and Antonarakis,S.E. (1998). Identification and characterization of a novel cyclic nucleotide phosphodiesterase gene (PDE9A) that maps to 21q22.3: alternative splicing of mRNA transcripts, genomic structure and sequence. Hum. Gen. *103*, 386-392.

Hamm,A., Krott,N., Breibach,I., Blindt,R., and Bosserhoff,A.K. (2002). Efficient transfection method for primary cells. Tissue Eng. *8*, 235-245.

Hammond,S.M., Bernstein,E., Beach,D., and Hannon,G.J. (2000). An RNA-directed nuclease mediates post-transcriptional gene silencing in Drosophila cells. Nature *404*, 293-296.

Hannon,G.J. (2002). RNA interference. Nature *418*, 244-251.

Hannon,G.J. and Rossi,J.J. (2004). Unlocking the potential of the human genome with RNA interference. Nature *431*, 371-378.

Hanoune,J. and Defer,N. (2001). Regulation and role of adenylyl cyclase isoforms. Ann. Rev. Pharmacol. Toxicol. *41*, 145-174.

Hansen,G., Jin,S., Umetsu,D.T., and Conti,M. (2000). Absence of muscarinic cholinergic airway responses in mice deficient in the cyclic nucleotide phosphodiesterase PDE4D. Proc. Natl. Acad. Sci. USA *97*, 6751-6756.

Harris,A.L., Connell,M.J., Ferguson,E.W., Wallace,A.M., Gordon,R.J., Pagani,E.D., and Silver,P.J. (1989). Role of low Km cyclic AMP phosphodiesterase inhibition in tracheal relaxation and bronchodilation in the guinea pig. J. Pharmacol. Exp. Ther. *251*, 199-206.

Harty,J.T., Tvinnereim,A.R., and White,D.W. (2000). $CD8^+$ T cell effector mechanisms in resistance to infection. Annu. Rev. Immunol. *18*, 275-308.

Harvath,L., Robbins,J.D., Russell,A.A., and Seamon,K.B. (1991). cAMP and human neutrophil chemotaxis. Elevation of cAMP differentially affects chemotactic responsiveness. J. Immunol. *146*, 224-232.

Hata,A.N. and Breyer,R.M. (2004). Pharmacology and signaling of prostaglandin receptors: Multiple roles in inflammation and immune modulation. Pharmacol. Ther. *103*, 147-166.

Hatzelmann,A. and Schudt,C. (2001). Anti-inflammatory and immunomodulatory potential of the novel PDE4 inhibitor roflumilast in vitro. J. Pharmacol. Exp. Ther. *297*, 267-279.

Haveman,J.W., Muller Kobold,A.C., Cohen Tervaert,J.W., van den Berg,A.P., Tulleken,J.E., Kallenberg,C.G.M., and The,T.H. (1999). The central role of monocytes in the pathogenesis of sepsis: consequences for immunomonitoring and treatment. Neth. J. Med. *55*, 132-141.

Heid,C.A., Stevens,J., Livak,K.J., and Williams,P.M. (1996). Real time quantitative PCR. Genome Res. *6*, 986-994.

Hermans,E. (2003). Biochemical and pharmacological control of the multiplicity of coupling at G-protein-coupled receptors. Pharmacol. Ther. *99*, 25-44.

Hersperger,R., Bray-French,K., Mazzoni,L., and Muller,T. (2000). Palladium-catalyzed cross-coupling reactions for the synthesis of 6, 8-disubstituted 1,7-naphthyridines: a novel class of potent and selective phosphodiesterase type 4D inhibitors. J. Med. Chem. *43*, 675-682.

Hetman,J.M., Soderling,S.H., Glavas,N.A., and Beavo,J.A. (2000a). Cloning and characterization of PDE7B, a cAMP-specific phosphodiesterase. Proc. Natl. Acad. Sci. USA *97*, 472-476.

Hetman,J.M., Robas,N., Baxendale,R., Fidock,M., Phillips,S.C., Soderling,S.H., and Beavo,J.A. (2000b). Cloning and characterization of two splice variants of human phosphodiesterase 11A. Proc. Natl. Acad. Sci. USA *97*, 12891-12895.

Heystek,H.C., Thierry,A.C., Soulard,P., and Moulon,C. (2003). Phosphodiesterase 4 inhibitors reduce human dendritic cell inflammatory cytokine production and Th1-polarizing capacity. Int. Immunol. *15*, 827-835.

Hill,E.V., Sheppard,C.L., Cheung,Y.F., Gall,I., Krause,E., and Houslay,M.D. (2006). Oxidative stress employs phosphatidyl inositol 3-kinase and ERK signalling pathways to activate cAMP phosphodiesterase-4D3 (PDE4D3) through multi-site phosphorylation at Ser239 and Ser579. Cell. Signal. *18*, 2056-2069.

Hoffmann,R., Baillie,G.S., MacKenzie,S.J., Yarwood,S.J., and Houslay,M.D. (1999). The MAP kinase ERK2 inhibits the cyclic AMP-specific phosphodiesterase HSPDE4D3 by phosphorylating it at Ser579. EMBO J. *18*, 893-903.

Holden,C.A., Chan,S.C., and Hanifin,J.M. (1986). Monocyte localization of elevated cAMP phosphodiesterase activity in atopic dermatitis. J. Invest. Dermatol. *87*, 372-376.

Holloway,A.F., Rao,S., and Shannon,M.F. (2002). Regulation of cytokine gene transcription in the immune system. Mol. Immunol. *38*, 567-580.

Honda,A., Sugimoto,Y., Namba,T., Watabe,A., Irie,A., Negishi,M., Narumiya,S., and Ichikawa,A. (1993). Cloning and expression of a cDNA for mouse prostaglandin E receptor EP2 subtype. J. Biol. Chem. *268*, 7759-7762.

Houslay,M.D. (2001). PDE4 cAMP-specific phosphodiesterases. Prog. Nucleic Acid Res. Mol. Biol. *69*, 249-315.

Houslay,M.D. and Adams,D.R. (2003). PDE4 cAMP phosphodiesterases: modular enzymes that orchestrate signalling cross-talk, desensitization and compartmentalization. Biochem. J. *370*, 1-18.

Houslay,M.D. and Baillie,G.S. (2003). The role of ERK2 docking and phosphorylation of PDE4 cAMP phosphodiesterase isoforms in mediating cross-talk between the cAMP and ERK signalling pathways. Biochem. Soc. Trans. *31*, 1186-1190.

Houslay,M.D., Schafer,P., and Zhang,K.Y. (2005). Keynote review: phosphodiesterase-4 as a therapeutic target. Drug Discov. Today *10*, 1503-1519.

Hurley,J.H. (1999). Structure, Mechanism, and Regulation of Mammalian Adenylyl Cyclase. J. Biol. Chem. *274*, 7599-7602.

Inami,M., Yamashita,M., Tenda,Y., Hasegawa,A., Kimura,M., Hashimoto,K., Seki,N., Taniguchi,M., and Nakayama,T. (2004). CD28 costimulation controls histone hyperacetylation of the interleukin 5 gene locus in developing Th2 cells. J. Biol. Chem. *279*, 23123-23133.

Iona,S., Cuomo,M., Bushnik,T., Naro,F., Sette,C., Hess,M., Shelton,E.R., and Conti,M. (1998). Characterization of the rolipram-sensitive, cyclic AMP-specific phosphodiesterases: Identification and differential expression of immunologically distinct forms in the rat brain. Mol. Pharmacol. *53*, 23-32.

Jackson,A.L., Bartz,S.R., Schelter,J., Kobayashi,S.V., Burchard,J., Mao,M., Li,B., Cavet,G., and Linsley,P.S. (2003). Expression profiling reveals off-target gene regulation by RNAi. Nat. Biotech. *21*, 635-637.

Jenkins,M.K., Taylor,P.S., Norton,S.D., and Urdahl,K.B. (1991). CD28 delivers a costimulatory signal involved in antigen-specific IL-2 production by human T cells. J. Immunol. *147*, 2461-2466.

Jiang,X., Paskind,M., Weltzien,R., and Epstein,P.M. (1998). Expression and regulation of mRNA for distinct isoforms of cAMP-specific PDE-4 in mitogen-stimulated and leukemic human lymphocytes. Cell Biochem. Biophys. *28*, 135-160.

Jin,S.L. and Conti,M. (2002). Induction of the cyclic nucleotide phosphodiesterase PDE4B is essential for LPS-activated TNF-alpha responses. Proc. Natl. Acad. Sci. USA *99*, 7628-7633.

Jin,S.L., Lan,L., Zoudilova,M., and Conti,M. (2005). Specific role of phosphodiesterase 4B in lipopolysaccharide-induced signaling in mouse macrophages. J. Immunol. *175*, 1523-1531.

Johnston,L.A., Erdogan,S., Cheung,Y.F., Sullivan,M., Barber,R., Lynch,M.J., Baillie,G.S., Van Heeke,G., Adams,D.R., Huston,E., and Houslay,M.D. (2004). Expression, intracellular distribution and basis for lack of catalytic activity of the PDE4A7 isoform encoded by the human PDE4A cAMP-specific phosphodiesterase gene. Biochem. J. *380*, 371-384.

June,C.H., Bluestone,J.A., Nadler,L.M., and Thompson,C.B. (1994). The B7 and CD28 receptor families. Immunol. Today *15*, 321-331.

Jurevicius,J. and Fischmeister,R. (1996). cAMP compartmentation is responsible for a local activation of cardiac Ca2+ channels by beta -adrenergic agonists. Proc. Natl. Acad. Sci. USA *93*, 295-299.

Kakiuchi,S. and Yamazaki,R. (1970). Calcium dependent phosphodiesterase activity and its activating factor (PAF) from brain studies on cyclic 3',5'-nucleotide phosphodiesterase (3). Biochem. Biophys. Res. Commun. *41*, 1104-1110.

Kakkar,R., Raju,R.V., and Sharma,R.K. (1999). Calmodulin-dependent cyclic nucleotide phosphodiesterase (PDE1). Cell Mol. Life Sci. *55*, 1164-1186.

Kalinski,P., Hilkens,C.M., Snijders,A., Snijdewint,F.G., and Kapsenberg,M.L. (1997). IL-12-deficient dendritic cells, generated in the presence of prostaglandin E2, promote type 2 cytokine production in maturing human naive T helper cells. J. Immunol. *159*, 28-35.

Kammer,G.M. (1988). The adenylate cyclase-cAMP-protein kinase A pathway and regulation of the immune response. Immunol. Today *9*, 222-229.

Kammer,G.M., Boehm,C.A., Rudolph,S.A., and Schultz,L.A. (1988). Mobility of the human T lymphocyte surface molecules CD3, CD4, and CD8: Regulation by a cAMP-dependent pathway. Proc. Natl. Acad. Sci. USA *85*, 792-796.

Kanda,N. and Watanabe,S. (2001). Regulatory roles of adenylate cyclase and cyclic nucleotide phosphodiesterases 1 and 4 in interleukin-13 production by activated human T cells. Biochem. Pharmacol. *62*, 495-507.

Kapiloff,M.S., Jackson,N., and Airhart,N. (2001). mAKAP and the ryanodine receptor are part of a multi-component signaling complex on the cardiomyocyte nuclear envelope. J. Cell Sci. *114*, 3167-3176.

Kariko,K., Bhuyan,P., Capodici,J., and Weissman,D. (2004). Small interfering RNAs mediate sequence-independent gene suppression and induce immune activation by signaling through toll-like receptor 3. J. Immunol. *172*, 6545-6549.

Karish,S.B. and Gagnon,J.M. (2006). The potential role of roflumilast: the new phosphodiesterase-4 inhibitor. Ann. Pharmacother. *40*, 1096-1104.

Kaupp,U.B. and Seifert,R. (2002). Cyclic nucleotide-gated ion channels. Physiol. Rev. *82*, 769-824.

Kawasaki,H., Springett,G.M., Mochizuki,N., Toki,S., Nakaya,M., Matsuda,M., Housman,D.E., and Graybiel,A.M. (1998). A family of cAMP-binding proteins that directly activate Rap1. Science *282*, 2275-2279.

Kelly,J.J., Barnes,P.J., and Giembycz,M.A. (1996). Phosphodiesterase 4 in macrophages: relationship between cAMP accumulation, suppression of cAMP hydrolysis and inhibition of [^{3}H]R-(-)-rolipram binding by selective inhibitors. Biochem. J. *318 (Pt 2)*, 425-436.

Kenan,Y., Murata,T., Shakur,Y., Degerman,E., and Manganiello,V.C. (2000). Functions of the N-terminal Region of Cyclic Nucleotide Phosphodiesterase 3 (PDE 3) Isoforms. J. Biol. Chem. *275*, 12331-12338.

Kopperud,R., Krakstad,C., Selheim,F., and Doskeland,S.O. (2003). cAMP effector mechanisms. Novel twists for an 'old' signaling system. FEBS Lett. *546*, 121-126.

Kovala,T., Sanwal,B.D., and Ball,E.H. (1997). Recombinant expression of a type IV, cAMP-specific phosphodiesterase: characterization and structure-function studies of deletion mutants. Biochemistry *36*, 2968-2976.

Kumar,R.K., Herbert,C., Thomas,P.S., Wollin,L., Beume,R., Yang,M., Webb,D.C., and Foster,P.S. (2003). Inhibition of inflammation and remodeling by roflumilast and dexamethasone in murine chronic asthma. J. Pharmacol. Exp. Ther. *307*, 349-355.

Laemmli,U.K. (1970). Cleavage of structural proteins during the assembly of the head of bacteriophage T4. Nature *227*, 680-685.

Lafaille,J.J. (1998). The role of helper T cell subsets in autoimmune diseases. Cytokine Growth Factor Rev. *9*, 139-151.

Laliberte,F., Han,Y., Govindarajan,A., Giroux,A., Liu,S., Bobechko,B., Lario,P., Bartlett,A., Gorseth,E., Gresser,M., and Huang,Z. (2000). Conformational difference between PDE4 apoenzyme and holoenzyme. Biochemistry *39*, 6449-6458.

Laliberte,F., Liu,S., Gorseth,E., Bobechko,B., Bartlett,A., Lario,P., Gresser,M.J., and Huang,Z. (2002). *In vitro* PKA phosphorylation-mediated human PDE4A4 activation. FEBS Lett. *512*, 205-208.

Landells,L.J., Spina,D., Souness,J.E., O'Connor,B.J., and Page,C.P. (2000). A biochemical and functional assessment of monocyte phosphodiesterase activity in healthy and asthmatic subjects. Pulm. Pharmacol. Ther. *13*, 231-239.

Landells,L.J., Szilagy,C.M., Jones,N.A., Banner,K.H., Allen,J.M., Doherty,A., O'Connor,B.J., Spina,D., and Page,C.P. (2001). Identification and quantification of phosphodiesterase 4 subtypes in CD4 and CD8 lymphocytes from healthy and asthmatic subjects. Br. J. Pharmacol. *133*, 722-729.

Lang,P., Gesbert,F., Delespine-Carmagnat,M., Stancou,R., Pouchelet,M., and Bertoglio,J. (1996). Protein kinase A phosphorylation of RhoA mediates the morphological and functional effects of cyclic AMP in cytotoxic lymphocytes. EMBO J. *15*, 510-519.

Lanzavecchia,A. and Sallusto,F. (2000). Dynamics of T lymphocyte responses: intermediates, effectors, and memory cells. Science *290*, 92-97.

Larsen,G.L. and Henson,P.M. (1983). Mediators of inflammation. Annu. Rev. Immunol. *1*, 335-359.

Laudanna,C., Campbell,J.J., and Butcher,E.C. (1997). Elevation of Intracellular cAMP Inhibits RhoA Activation and Integrin-dependent Leukocyte Adhesion Induced by Chemoattractants. J. Biol. Chem. *272*, 24141-24144.

Lazaar,A.L. and Panettieri,R.A., Jr. (2006). Airway smooth muscle as a regulator of immune responses and bronchomotor tone. Clin. Chest Med. *27*, 53-69, vi.

Le Jeune,I.R., Shepherd,M., Van Heeke,G., Houslay,M.D., and Hall,I.P. (2002). Cyclic AMP-dependent transcriptional up-regulation of phosphodiesterase 4D5 in human airway smooth muscle cells. Identification and characterization of novel PDE4D5 promoter. J. Biol. Chem. *277*, 35980-35989.

Lechmann,M., Zinser,E., Golka,A., and Steinkasserer,A. (2002). Role of CD83 in the immunomodulation of dendritic cells. Int. Arch. Allergy Immunol. *129*, 113-118.

Ledbetter,J.A., Parsons,M., Martin,P.J., Hansen,J.A., Rabinovitch,P.S., and June,C.H. (1986). Antibody binding to CD5 (Tp67) and Tp44 T cell surface molecules: effects on cyclic nucleotides, cytoplasmic free calcium, and cAMP-mediated suppression. J. Immunol. *137*, 3299-3305.

Lee,K.A. and Masson,N. (1993). Transcriptional regulation by CREB and its relatives. Biochim. Biophys. Acta *1174*, 221-233.

Lefkowitz,R.J. and Shenoy,S.K. (2005). Transduction of receptor signals by beta-arrestins. Science *308*, 512-517.

Legler,D.F., Krause,P., Scandella,E., Singer,E., and Groettrup,M. (2006). Prostaglandin E2 is generally required for human dendritic cell migration and exerts its effect via EP2 and EP4 receptors. J. Immunol. *176*, 966-973.

Lehnart,S.E., Wehrens,X.H., Reiken,S., Warrier,S., Belevych,A.E., Harvey,R.D., Richter,W., Jin,S.L., Conti,M., and Marks,A.R. (2005). Phosphodiesterase 4D deficiency in the ryanodine-receptor complex promotes heart failure and arrhythmias. Cell *123*, 25-35.

Leung,R.K.M. and Whittaker,P.A. (2005). RNA interference: From gene silencing to gene-specific therapeutics. Pharmacol. Ther. *107*, 222-239.

Li,L., Yee,C., and Beavo,J.A. (1999). CD3- and CD28-dependent induction of PDE7 required for T cell activation. Science *283*, 848-851.

Liao,X.C. and Littman,D.R. (1995). Altered T cell receptor signaling and disrupted T cell development in mice lacking Itk. Immunity *3*, 757-769.

Lim,J., Pahlke,G., and Conti,M. (1999). Activation of the cAMP-specific phosphodiesterase PDE4D3 by phosphorylation. Identification and function of an inhibitory domain. J. Biol. Chem. *274*, 19677-19685.

Lin,C.S., Chow,S., Lau,A., Tu,R., and Lue,T.F. (2002). Human PDE5A gene encodes three PDE5 isoforms from two alternate promoters. Int. J. Impot. Res. *14*, 15-24.

Lipworth,B.J. (2005). Phosphodiesterase-4 inhibitors for asthma and chronic obstructive pulmonary disease. Lancet *365*, 167-175.

Liu,J.O. (2005). The yins of T cell activation. Sci. STKE *2005*, re1.

Liu,K.Q., Bunnell,S.C., Gurniak,C.B., and Berg,L.J. (1998). T cell receptor-initiated calcium release is uncoupled from capacitative calcium entry in Itk-deficient T cells. J. Exp. Med. *187*, 1721-1727.

Liu,K., Li,Y., Prabhu,V., Young,L., Becker,K.G., Munson,P.J., and Weng,N.p. (2001a). Augmentation in expression of activation-induced genes differentiates memory from naive $CD4^+$ T cells and is a molecular mechanism for enhanced cellular response of memory $CD4^+$ T cells. J. Immunol. *166*, 7335-7344.

Liu,M. and Simon,M.I. (1996). Regulation by cAMP-dependent protein kinase of a G-protein-mediated phospholipase C. Nature *382*, 83-87.

Liu,S., Laliberte,F., Bobechko,B., Bartlett,A., Lario,P., Gorseth,E., Van Hamme,J., Gresser,M.J., and Huang,Z. (2001b). Dissecting the cofactor-dependent and independent bindings of PDE4 inhibitors. Biochemistry *40*, 10179-10186.

Livak,K.J. and Schmittgen,T.D. (2001). Analysis of relative gene expression data using real-time quantitative PCR and the 2 ($^{-\Delta\Delta Ct}$) method. Methods *25*, 402-408.

Loughney,K., Martins,T.J., Harris,E.A.S., Sadhu,K., Hicks,J.B., Sonnenburg,W.K., Beavo,J.A., and Ferguson,K. (1996). Isolation and characterization of cDNAs corresponding to two human calcium, calmodulin-regulated, 3`,5`-cyclic nucleotide phosphodiesterases. J. Biol. Chem. *271*, 796-806.

Loza,M.J., Foster,S., Peters,S.P., and Penn,R.B. (2006). Beta-agonists modulate T-cell functions via direct actions on type 1 and type 2 cells. Blood *107*, 2052-2060.

Lugnier,C. (2006). Cyclic nucleotide phosphodiesterase (PDE) superfamily: a new target for the development of specific therapeutic agents. Pharmacol. Ther. *109*, 366-398.

Lynch,M.J., Hill,E.V., and Houslay,M.D. (2006). Intracellular targeting of phosphodiesterase 4 underpins compartmentalized cAMP signaling. In Curr. Top. Dev. Biol., P.S.Gerald, ed. Academic Press), pp. 225-259.

Ma,D., Wu,P., Egan,R.W., Billah,M.M., and Wang,P. (1999). Phosphodiesterase 4B gene transcription is activated by lipopolysaccharide and inhibited by interleukin-10 in human monocytes. Mol. Pharmacol. *55*, 50-57.

MacKenzie,S.J. (2004). Phosphodiesterase 4 cAMP phosphodiesterases as targets for novel anti-inflammatory therapeutics. Allergol. Int. *53*, 101-110.

MacKenzie,S.J., Baillie,G.S., McPhee,I., MacKenzie,C., Seamons,R., McSorley,T., Millen,J., Beard,M.B., Van Heeke,G., and Houslay,M.D. (2002). Long PDE4 cAMP specific phosphodiesterases are activated by protein kinase A-mediated phosphorylation of a single serine residue in Upstream Conserved Region 1 (UCR1). Br. J. Pharmacol. *136*, 421-433.

MacKenzie,S.J., Baillie,G.S., McPhee,I., Bolger,G.B., and Houslay,M.D. (2000). ERK2 mitogen-activated protein kinase binding, phosphorylation, and regulation of the PDE4D cAMP-specific phosphodiesterases. The involvement of COOH-terminal docking sites and NH2-terminal UCR regions. J. Biol. Chem. *275*, 16609-16617.

Manganiello,V.C., Taira,M., Degerman,E., and Belfrage,P. (1995). Topical review type III cGMP-inhibited cyclic nucleotide phosphodiesterases (PDE 3 gene family). Cell. Signal. *7*, 445-455.

Manning,C.D., Burman,M., Christensen,S.B., Cieslinski,L.B., Essayan,D.M., Grous,M., Torphy,T.J., and Barnette,M.S. (1999). Suppression of human inflammatory cell function by subtype-selective PDE4 inhibitors correlates with inhibition of PDE4A and PDE4B. Br. J. Pharmacol. *128*, 1393-1398.

Manning,C.D., McLaughlin,M.M., Livi,G.P., Cieslinski,L.B., Torphy,T.J., and Barnette,M.S. (1996). Prolonged beta adrenoceptor stimulation up-regulates cAMP phosphodiesterase activity in human monocytes by increasing mRNA and protein for phosphodiesterases 4A and 4B. J. Pharmacol. Exp. Ther. *276*, 810-818.

Marrack,P. and Kappler,J. (2004). Control of T cell viability. Annu. Rev. Immunol. *22*, 765-787.

Martorana,P.A., Beume,R., Lucattelli,M., Wollin,L., and Lungarella,G. (2005). Roflumilast fully prevents emphysema in mice chronically exposed to cigarette smoke. Am. J. Respir. Crit. Care Med. *172*, 848-853.

Mayr,B. and Montminy,M. (2001). Transcriptional regulation by the phosphorylation-dependent factor CREB. Nat. Rev. Mol. Cell Biol. *2*, 599-609.

McPhee,I., Yarwood,S.J., Scotland,G., Huston,E., Beard,M.B., Ross,A.H., Houslay,E.S., and Houslay,M.D. (1999). Association with the Src family tyrosyl kinase Lyn triggers a conformational change in the catalytic region of human cAMP-specific phosphodiesterase HSPDE4A4B. Consequences for rolipram inhibition. J. Biol. Chem. *274*, 11796-11810.

McSorley,T., Stefan,E., Henn,V., Wiesner,B., Baillie,G.S., Houslay,M.D., Rosenthal,W., and Klussmann,E. (2006). Spatial organisation of AKAP18 and PDE4 isoforms in renal collecting duct principal cells. Eur. J. Cell Biol. *85*, 673-678.

Meacci,E., Taira,M., Moos,M., Jr., Smith,C.J., Movsesian,M.A., Degerman,E., per,B., and Manganiello,V. (1992). Molecular cloning and expression of human myocardial cGMP-inhibited cAMP phosphodiesterase. Proc. Natl. Acad. Sci. USA *89*, 3721-3725.

Mehats,C., Jin,S.L., Wahlstrom,J., Law,E., Umetsu,D.T., and Conti,M. (2003). PDE4D plays a critical role in the control of airway smooth muscle contraction. FASEB J. *17*, 1831-1841.

Mello,C.C. and Conte,D., Jr. (2004). Revealing the world of RNA interference. Nature *431*, 338-342.

Methi,T., Ngai,J., Mahic,M., Amarzguioui,M., Vang,T., and Tasken,K. (2005). Short-interfering RNA-mediated Lck knockdown results in augmented downstream T cell responses. J. Immunol. *175*, 7398-7406.

Michel,J.J.C. and Scott,J.D. (2002). AKAP mediated signal transduction. Ann. Rev. Pharmacol. Toxicol. *42*, 235-257.

Micklefield,J. (2001). Backbone modification of nucleic acids: synthesis, structure and therapeutic applications. Curr. Med. Chem. *8*, 1157-1179.

Millar,J.K., Pickard,B.S., Mackie,S., James,R., Christie,S., Buchanan,S.R., Malloy,M.P., Chubb,J.E., Huston,E., Baillie,G.S., Thomson,P.A., Hill,E.V., Brandon,N.J., Rain,J.C., Camargo,L.M., Whiting,P.J., Houslay,M.D., Blackwood,D.H., Muir,W.J., and Porteous,D.J. (2005). DISC1 and PDE4B are interacting genetic factors in schizophrenia that regulate cAMP signaling. Science *310*, 1187-1191.

Mookerjee,B.K. and Pauly,J.L. (1990). Mitogenic effect of interleukin-2 on unstimulated human T cells: an editorial review. J. Clin. Lab. Anal. *4*, 138-149.

Mordvinov,V.A. and Sanderson,C.J. (2001). Regulation of IL-5 expression. Arch. Immunol Ther. Exp. (Warsz.) *49*, 345-351.

Mosmann,T.R., Cherwinski,H., Bond,M.W., Giedlin,M.A., and Coffman,R.L. (1986). Two types of murine helper T cell clone. I. Definition according to profiles of lymphokine activities and secreted proteins. J. Immunol. *136*, 2348-2357.

Muller,T., Engels,P., and Fozard,J.R. (1996). Subtypes of the type 4 cAMP phosphodiesterases: structure, regulation and selective inhibition. Trends Pharmacol. Sci. *17*, 294-298.

Neer,E.J. (1995). Heterotrimeric G proteins: organizers of transmembrane signals. Cell *80*, 249-257.

Nelson,B.H. (2004). IL-2, regulatory T cells, and tolerance. J. Immunol. *172*, 3983-3988.

Norton,A.W., D'Amours,M.R., Grazio,H.J., Hebert,T.L., and Cote,R.H. (2000). Mechanism of transducin activation of frog rod photoreceptor phosphodiesterase. Allosteric interactions between the inhibitory gamma subunit and the noncatalytical cGMP-binding sites. J. Biol. Chem. *275*, 38611-38619.

Norton,S.D., Zuckerman,L., Urdahl,K.B., Shefner,R., Miller,J., and Jenkins,M.K. (1992). The CD28 ligand, B7, enhances IL-2 production by providing a costimulatory signal to T cells. J. Immunol. *149*, 1556-1561.

Novina,C.D. and Sharp,P.A. (2004). The RNAi revolution. Nature *430*, 161-164.

O'Doherty,U., Steinman,R.M., Peng,M., Cameron,P.U., Gezelter,S., Kopeloff,I., Swiggard,W.J., Pope,M., and Bhardwaj,N. (1993). Dendritic cells freshly isolated from human blood express CD4 and mature into typical immunostimulatory dendritic cells after culture in monocyte-conditioned medium. J. Exp. Med. *178*, 1067-1076.

O'Sullivan,S., Cormican,L., Faul,J.L., Ichinohe,S., Johnston,S.L., Burke,C.M., and Poulter,L.W. (2001). Activated, cytotoxic $CD8^+$ T lymphocytes contribute to the pathology of asthma death. Am. J. Respir. Cell Mol. Biol. *164*, 560-564.

Obernolte,R., Ratzliff,J., Baecker,P.A., Daniels,D.V., Zuppan,P., Jarnagin,K., and Shelton,E.R. (1997). Multiple splice variants of phosphodiesterase PDE4C cloned from human lung and testis. Biochim. Biophys. Acta *1353*, 287-297.

Owens,R.J., Lumb,S., Rees-Milton,K., Russell,A., Baldock,D., Lang,V., Crabbe,T., Ballesteros,M., and Perry,M.J. (1997). Molecular cloning and expression of a human phosphodiesterase 4C. Cell. Signal. *9*, 575-585.

Panettieri,J. (2003). Airway smooth muscle: immunomodulatory cells that modulate airway remodeling? Resp. Physiol. Neurobiol. *137*, 277-293.

Patil,S.D., Rhodes,D.G., and Burgess,D.J. (2005). DNA-based therapeutics and DNA delivery systems: a comprehensive review. AAPS. J. *7*, E61-E77.

Perry,S.J., Baillie,G.S., Kohout,T.A., McPhee,I., Magiera,M.M., Ang,K.L., Miller,W.E., McLean,A.J., Conti,M., Houslay,M.D., and Lefkowitz,R.J. (2002). Targeting of cyclic AMP degradation to beta 2-adrenergic receptors by beta-arrestins. Science *298*, 834-836.

Platzer,C., Fritsch,E., Elsner,T., Lehmann,M.H., Volk,H.D., and Prosch,S. (1999). Cyclic adenosine monophosphate-responsive elements are involved in the transcriptional activation of the human IL-10 gene in monocytic cells. Eur. J. Immunol. *29*, 3098-3104.

Procopio,D.O., Teixeira,M.M., Camargo,M.M., Travassos,L.R., Ferguson,M.A.J., Almeida,I.C., and Gazzinelli,R.T. (1999). Differential inhibitory mechanism of cyclic AMP on TNF-[alpha] and IL-12 synthesis by macrophages exposed to microbial stimuli. Br. J. Pharmacol. *127*, 1195-1205.

Rabe,K.F., Bateman,E.D., O'Donnell,D., Witte,S., Bredenbroker,D., and Bethke,T.D. (2005). Roflumilast - an oral anti-inflammatory treatment for chronic obstructive pulmonary disease: a randomised controlled trial. Lancet *366*, 563-571.

Rabe,K.F., Tenor,H., Dent,G., Schudt,C., Nakashima,M., and Magnussen,H. (1994). Identification of PDE isozymes in human pulmonary artery and effect of selective PDE inhibitors. Am J Physiol Lung Cell Mol Physiol *266*, L536-L543.

Raeburn,D., Underwood,S.L., Lewis,S.A., Woodman,V.R., Battram,C.H., Tomkinson,A., Sharma,S., Jordan,R., Souness,J.E., Webber,S.E., and . (1994). Anti-inflammatory and bronchodilator properties of RP 73401, a novel and selective phosphodiesterase type IV inhibitor. Br. J. Pharmacol. *113*, 1423-1431.

Regan,J.W., Bailey,T.J., Pepperl,D.J., Pierce,K.L., Bogardus,A.M., Donello,J.E., Fairbairn,C.E., Kedzie,K.M., Woodward,D.F., and Gil et,a. (1994). Cloning of a novel human prostaglandin receptor with characteristics of the pharmacologically defined EP2 subtype. Mol. Pharmacol. *46*, 213-220.

Reimann,E.M., Walsh,D.A., and Krebs,E.G. (1971). Purification and properties of rabbit skeletal muscle adenosine 3',5'-monophosphate-dependent protein kinases. J. Biol. Chem. *246*, 1986-1995.

Rena,G., Begg,F., Ross,A., MacKenzie,C., McPhee,I., Campbell,L., Huston,E., Sullivan,M., and Houslay,M.D. (2001). Molecular cloning, genomic positioning, promoter identification, and characterization of the novel cyclic amp-specific phosphodiesterase PDE4A10. Mol. Pharmacol. *59*, 996-1011.

Renauld,J.C. (2001). New insights into the role of cytokines in asthma. J. Clin. Pathol. *54*, 577-589.

Reneland,R.H., Mah,S., Kammerer,S., Hoyal,C.R., Marnellos,G., Wilson,S.G., Sambrook,P.N., Spector,T.D., Nelson,M.R., and Braun,A. (2005). Association between a variation in the phosphodiesterase 4D gene and bone mineral density. BMC. Med. Genet. *6*, 9.

Reynolds,A., Leake,D., Boese,Q., Scaringe,S., Marshall,W.S., and Khvorova,A. (2004). Rational siRNA design for RNA interference. Nat. Biotech. *22*, 326-330.

Richter,W. and Conti,M. (2002). Dimerization of the type 4 cAMP-specific phosphodiesterases is mediated by the upstream conserved regions (UCRs). J. Biol. Chem. *277*, 40212-40221.

Richter,W. and Conti,M. (2004). The oligomerization state determines regulatory properties and inhibitor sensitivity of type 4 cAMP-specific phosphodiesterases. J. Biol. Chem. *279*, 30338-30348.

Richter,W., Jin,S.L., and Conti,M. (2005). Splice variants of the cyclic nucleotide phosphodiesterase PDE4D are differentially expressed and regulated in rat tissue. Biochem. J. *388*, 803-811.

Richter,W., Unciuleac,L., Hermsdorf,T., Kronbach,T., and Dettmer,D. (2001). Identification of inhibitor binding sites of the cAMP-specific phosphodiesterase 4. Cell. Signal. *13*, 287-297.

Robichaud,A., Stamatiou,P.B., Jin,S.L., Lachance,N., MacDonald,D., Laliberte,F., Liu,S., Huang,Z., Conti,M., and Chan,C.C. (2002). Deletion of phosphodiesterase 4D in mice shortens alpha(2)-adrenoceptor-mediated anesthesia, a behavioral correlate of emesis. J. Clin. Invest. *110*, 1045-1052.

Robicsek,S.A., Blanchard,D.K., Djeu,J.Y., Krzanowski,J.J., Szentivanyi,A., and Polson,J.B. (1991). Multiple high-affinity cAMP-phosphodiesterases in human T-lymphocytes. Biochem. Pharmacol. *42*, 869-877.

Rocha,A., Ruiz,S., and Coll,J.M. (2002). Improvement of DNA transfection with cationic liposomes. J. Physiol. Biochem. *58*, 45-56.

Romagnani,S. (1994). Lymphokine production by human T cells in disease states. Annu. Rev. Immunol. *12*, 227-257.

Romagnani,S. (2000). The role of lymphocytes in allergic disease. J. Allergy Clin. Immunol. *105*, 399-408.

Rosman,G.J., Martins,T.J., Sonnenburg,W.K., Beavo,J.A., Ferguson,K., and Loughney,K. (1997). Isolation and characterization of human cDNAs encoding a cGMP-stimulated 3',5'-cyclic nucleotide phosphodiesterase. Gene *191*, 89-95.

Sakaguchi,S., Sakaguchi,N., Asano,M., Itoh,M., and Toda,M. (1995). Immunologic self-tolerance maintained by activated T cells expressing IL-2 receptor alpha-chains (CD25). Breakdown of a single mechanism of self-tolerance causes various autoimmune diseases. J. Immunol. *155*, 1151-1164.

Sallusto,F. and Lanzavecchia,A. (1994). Efficient presentation of soluble antigen by cultured human dendritic cells is maintained by granulocyte/macrophage colony-stimulating factor plus interleukin 4 and downregulated by tumor necrosis factor alpha. J. Exp. Med. *179*, 1109-1118.

Sallusto,F., Schaerli,P., Loetscher,P., Schaniel,C., Lenig,D., Mackay,C.R., Qin,S., and Lanzavecchia,A. (1998). Rapid and coordinated switch in chemokine receptor expression during dendritic cell maturation. Eur. J. Immunol. *28*, 2760-2769.

Salomon,B. and Bluestone,J.A. (2001). Complexities of CD28/B7: CTLA-4 costimulatory pathways in autoimmunity and transplantation. Annu. Rev. Immunol. *19*, 225-252.

Sanderson,C.J. (1992). Interleukin-5, eosinophils, and disease. Blood *79*, 3101-3109.

Scandella,E., Men,Y., Gillessen,S., Forster,R., and Groettrup,M. (2002). Prostaglandin E2 is a key factor for CCR7 surface expression and migration of monocyte-derived dendritic cells. Blood *100*, 1354-1361.

Schakowski,F., Buttgereit,P., Mazur,M., Marten,A., Schottker,B., Gorschluter,M., and Schmidt-Wolf,I.G. (2004). Novel non-viral method for transfection of primary leukemia cells and cell lines. Genet. Vaccines. Ther. *2*, 1.

Schmidt,D., Dent,G., and Rabe,K.F. (1999). Selective phosphodiesterase inhibitors for the treatment of bronchial asthma and chronic obstructive pulmonary disease. Clin. Exp. Allergy *29 Suppl 2*, 99-109.

Schmidt,M., Hofmann,H.P., Sanders,K., Sczakiel,G., Beckers,T.L., and Gekeler,V. (2006). Molecular alterations after Polo-like kinase 1 mRNA suppression versus pharmacologic inhibition in cancer cells. Mol. Cancer Ther. *5*, 809-817.

Schneider,H.H., Schmiechen,R., Brezinski,M., and Seidler,J. (1986). Stereospecific binding of the antidepressant rolipram to brain protein structures. Eur. J. Pharmacol. *127*, 105-115.

Schudt,C., Tenor,H., and Hatzelmann,A. (1995). PDE isoenzymes as targets for anti-asthma drugs. Eur. Resp. J. *8*, 1179-1183.

Schudt,C., Winder,S., Eltze,M., Kilian,U., and Beume,R. (1991). Zardaverine: a cyclic AMP specific PDE III/IV inhibitor. Agents Actions Suppl. *34*, 379-402.

Schwabe,U., Miyake,M., Ohga,Y., and Daly,J.W. (1976). 4-(3-Cyclopentyloxy-4-methoxyphenyl)-2-pyrrolidone (ZK 62711): a potent inhibitor of adenosine cyclic 3',5'-monophosphate phosphodiesterases in homogenates and tissue slices from rat brain. Mol. Pharmacol. *12*, 900-910.

Schwartzberg,P.L., Finkelstein,L.D., and Readinger,J.A. (2005). TEC-family kinases: regulators of T-helper-cell differentiation. Nat. Rev. Immunol. *5*, 284-295.

Schwarz,D.S., Hutvagner,G., Du,T., Xu,Z., Aronin,N., and Zamore,P.D. (2003). Asymmetry in the assembly of the RNAi enzyme complex. Cell *115*, 199-208.

Selliah,N., Bartik,M.M., Carlson,S.L., Brooks,W.H., and Roszman,T.L. (1995). cAMP accumulation in T-cells inhibits anti-CD3 monoclonal antibody-induced actin polymerization. J. Neuroimmunol. *56*, 107-112.

Semizarov,D., Frost,L., Sarthy,A., Kroeger,P., Halbert,D.N., and Fesik,S.W. (2003). Specificity of short interfering RNA determined through gene expression signatures. Proc. Natl. Acad. Sci. USA *100*, 6347-6352.

Sette,C. and Conti,M. (1996). Phosphorylation and activation of a cAMP-specific phosphodiesterase by the cAMP-dependent protein kinase. Involvement of serine 54 in the enzyme activation. J. Biol. Chem. *271*, 16526-16534.

Seybold,J., Newton,R., Wright,L., Finney,P.A., Suttorp,N., Barnes,P.J., Adcock,I.M., and Giembycz,M.A. (1998). Induction of phosphodiesterases 3B, 4A4, 4D1, 4D2, and 4D3 in Jurkat T-cells and in human peripheral blood T-lymphocytes by 8-bromo-cAMP and Gs-coupled receptor agonists. Potential role in beta2-adrenoreceptor desensitization. J. Biol. Chem. *273*, 20575-20588.

Shakur,Y., Takeda,K., Kenan,Y., Yu,Z.X., Rena,G., Brandt,D., Houslay,M.D., Degerman,E., Ferrans,V.J., and Manganiello,V.C. (2000). Membrane localization of cyclic nucleotide phosphodiesterase 3 (PDE3). Two N-terminal domains are required for the efficient targeting to, and association of, PDE3 with endoplasmic reticulum. J. Biol. Chem. *275*, 38749-38761.

Shaywitz,A.J. and Greenberg,M.E. (1999). CREB: A stimulus-induced transcription factor activated by a diverse array of extracellular signals. Annu. Rev Biochem. *68*, 821-861.

Shepherd,M., McSorley,T., Olsen,A.E., Johnston,L.A., Thomson,N.C., Baillie,G.S., Houslay,M.D., and Bolger,G.B. (2003). Molecular cloning and subcellular distribution of the novel PDE4B4 cAMP-specific phosphodiesterase isoform. Biochem. J. *370*, 429-438.

Shepherd,M.C., Baillie,G.S., Stirling,D.I., and Houslay,M.D. (2004). Remodelling of the PDE4 cAMP phosphodiesterase isoform profile upon monocyte-macrophage differentiation of human U937 cells. Br. J. Pharmacol. *142*, 339-351.

Simonds,W.F. (1999). G protein regulation of adenylate cyclase. Trends Pharmacol. Sci. *20*, 66-73.

Sioud,M. (2004). Therapeutic siRNAs. Trends Pharmacol. Sci. *25*, 22-28.

Skalhegg,B.S., Landmark,B.F., Doskeland,S.O., Hansson,V., Lea,T., and Jahnsen,T. (1992). Cyclic AMP-dependent protein kinase type I mediates the inhibitory effects of 3',5'-cyclic adenosine monophosphate on cell replication in human T lymphocytes. J. Biol. Chem. *267*, 15707-15714.

Skalhegg,B.S. and Tasken,K. (2000). Specificity in the cAMP/PKA signaling pathway. Differential expression, regulation, and subcellular localization of subunits of PKA. Front Biosci. *5*, D678-D693.

Skalhegg,B.S., Tasken,K., Hansson,V., Huitfeldt,H.S., Jahnsen,T., and Lea,T. (1994). Location of cAMP-dependent protein kinase type I with the TCR-CD3 complex. Science *263*, 84-87.

Skapenko,A., Leipe,J., Lipsky,P.E., and Schulze-Koops,H. (2005). The role of the T cell in autoimmune inflammation. Arthritis Res. Ther. *7 Suppl 2*, S4-14.

Skapenko,A., Leipe,J., Niesner,U., Devriendt,K., Beetz,R., Radbruch,A., Kalden,J.R., Lipsky,P.E., and Schulze-Koops,H. (2004). GATA-3 in human T cell helper type 2 development. J. Exp. Med. *199*, 423-428.

Sledz,C.A., Holko,M., de Veer,M.J., Silverman,R.H., and Williams,B.R. (2003). Activation of the interferon system by short-interfering RNAs. Nat. Cell Biol. *5*, 834-839.

Soderling,S.H., Bayuga,S.J., and Beavo,J.A. (1998a). Cloning and characterization of a cAMP-specific cyclic nucleotide phosphodiesterase. Proc. Natl. Acad. Sci. USA *95*, 8991-8996.

Soderling,S.H., Bayuga,S.J., and Beavo,J.A. (1998b). Identification and characterization of a novel family of cyclic nucleotide phosphodiesterases. J. Biol. Chem. *273*, 15553-15558.

Soderling,S.H., Bayuga,S.J., and Beavo,J.A. (1999). Isolation and characterization of a dual-substrate phosphodiesterase gene family: PDE10A. Proc. Natl. Acad. Sci. USA *96*, 7071-7076.

Sombroek,C.C., Stam,A.G.M., Masterson,A.J., Lougheed,S.M., Schakel,M.J.A.G., Meijer,C.J.L.M., Pinedo,H.M., van den Eertwegh,A.J.M., Scheper,R.J., and de Gruijl,T.D. (2002). Prostanoids play a major role in the primary tumor-induced inhibition of dendritic cell differentiation. J. Immunol. *168*, 4333-4343.

Sonnemann,J., Gekeler,V., Ahlbrecht,K., Brischwein,K., Liu,C., Bader,P., Muller,C., Niethammer,D., and Beck,J.F. (2004a). Down-regulation of protein kinase Ceta by antisense oligonucleotides sensitises A549 lung cancer cells to vincristine and paclitaxel. Cancer Lett. *209*, 177-185.

Sonnemann,J., Gekeler,V., Sagrauske,A., Muller,C., Hofmann,H.P., and Beck,J.F. (2004b). Down-regulation of protein kinase Ceta potentiates the cytotoxic effects of exogenous tumor necrosis factor-related apoptosis-inducing ligand in PC-3 prostate cancer cells. Mol. Cancer Ther. *3*, 773-781.

Soruri,A. and Zwirner,J. (2005). Dendritic cells: limited potential in immunotherapy. Int. J. Biochem. Cell Biol. *37*, 241-245.

Souness,J.E., Aldous,D., and Sargent,C. (2000). Immunosuppressive and anti-inflammatory effects of cyclic AMP phosphodiesterase (PDE) type 4 inhibitors. Immunopharmacology *47*, 127-162.

Souness,J.E., Griffin,M., Maslen,C., Ebsworth,K., Scott,L.C., Pollock,K., Palfreyman,M.N., and Karlsson,J.A. (1996). Evidence that cyclic AMP phosphodiesterase inhibitors suppress TNF alpha generation from human monocytes by interacting with a 'low-affinity' phosphodiesterase 4 conformer. Br. J. Pharmacol. *118*, 649-658.

Souness,J.E., Maslen,C., Webber,S., Foster,M., Raeburn,D., Palfreyman,M.N., Ashton,M.J., and Karlsson,J.A. (1995). Suppression of eosinophil function by RP 73401, a potent and selective inhibitor of cyclic AMP-specific phosphodiesterase: comparison with rolipram. Br. J. Pharmacol. *115*, 39-46.

Souness,J.E. and Rao,S. (1997). Proposal for pharmacologically distinct conformers of PDE4 cyclic AMP phosphodiesterases. Cell. Signal. *9*, 227-236.

Stark,G.R., Kerr,I.M., Williams,B.R., Silverman,R.H., and Schreiber,R.D. (1998). How cells respond to interferons. Annu. Rev. Biochem. *67*, 227-264.

Stein,C.A. and Narayanan,R. (1994). Antisense oligodeoxynucleotides. Curr. Opin. Oncol. *6*, 587-594.

Steinbrink,K., Paragnik,L., Jonuleit,H., Tuting,T., Knop,J., and Enk,A.H. (2000). Induction of dendritic cell maturation and modulation of dendritic cell-induced immune responses by prostaglandins. Arch. Dermatol. Res. *292*, 437-445.

Sullivan,M., Olsen,A.S., and Houslay,M.D. (1999). Genomic organisation of the human cyclic AMP-specific phosphodiesterase PDE4C gene and its chromosomal localisation to 19p13.1, between RAB3A and JUND. Cell. Signal. *11*, 735-742.

Sutherland,E.W. and Rall,T.W. (1958). Fractionation and characterization of a cyclic adenine ribonucleotide formed by tissue particles. J. Biol. Chem. *232*, 1077-1092.

Swinnen,J.V., Joseph,D.R., and Conti,M. (1989a). Molecular cloning of rat homologues of the *Drosophila melanogaster* Dunce cAMP phosphodiesterase: Evidence for a family of genes. Proc. Natl. Acad. Sci. USA *86*, 5325-5329.

Swinnen,J.V., Joseph,D.R., and Conti,M. (1989b). The mRNA encoding a high-affinity cAMP phosphodiesterase is regulated by hormones and cAMP. Proc. Natl. Acad. Sci. USA *86*, 8197-8201.

Taira,M., Hockman,S.C., Calvo,J.C., Taira,M., Belfrage,P., and Manganiello,V.C. (1993). Molecular cloning of the rat adipocyte hormone-sensitive cyclic GMP- inhibited cyclic nucleotide phosphodiesterase. J. Biol. Chem. *268*, 18573-18579.

Takahashi,N., Tetsuka,T., Uranishi,H., and Okamoto,T. (2002). Inhibition of the NF-kappaB transcriptional activity by protein kinase A. Eur. J. Biochem. *269*, 4559-4565.

Tamir,A. and Isakov,N. (1994). Cyclic AMP inhibits phosphatidylinositol-coupled and -uncoupled mitogenic signals in T lymphocytes. Evidence that cAMP alters PKC- induced transcription regulation of members of the jun and fos family of genes. J. Immunol. *152*, 3391-3399.

Taniguchi,T. and Minami,Y. (1993). The IL-2/IL-2 receptor system: a current overview. Cell *73*, 5-8.

Tasken,K. and Aandahl,E.M. (2004). Localized effects of cAMP mediated by distinct routes of protein kinase A. Physiol. Rev. *84*, 137-167.

Tasken,K. and Stokka,A.J. (2006). The molecular machinery for cAMP-dependent immunomodulation in T-cells. Biochem. Soc. Trans. *34*, 476-479.

Tasken,K.A., Collas,P., Kemmner,W.A., Witczak,O., Conti,M., and Tasken,K. (2001). Phosphodiesterase 4D and protein kinase A type II constitute a signaling unit in the centrosomal area. J. Biol. Chem. *276*, 21999-22002.

Tattersfield,A.E., Knox,A.J., Britton,J.R., and Hall,I.P. (2002). Asthma. Lancet *360*, 1313-1322.

Taylor,S.S., Yang,J., Wu,J., Haste,N.M., Radzio-Andzelm,E., and Anand,G. (2004). PKA: a portrait of protein kinase dynamics. Biochim. Biophys. Acta Protein Proteomics *1697*, 259-269.

Teixeira,L.K., Fonseca,B.P., Barboza,B.A., and Viola,J.P. (2005). The role of interferon-gamma on immune and allergic responses. Mem. Inst. Oswaldo Cruz. *100 Suppl 1*, 137-144.

Tempel,B.L., Bonini,N., Dawson,D.R., and Quinn,W.G. (1983). Reward learning in normal and mutant *Drosophila*. Proc. Natl. Acad. Sci. USA *80*, 1482-1486.

Tenor,H., Hatzelmann,A., Kupferschmidt,R., Stanciu,L., Djukanovic,R., Schudt,C., Wendel,A., Church,M.K., and Shute,J.K. (1995a). Cyclic nucleotide phosphodiesterase isoenzyme activities in human alveolar macrophages. Clin. Exp. Allergy *25*, 625-633.

Tenor,H., Hedbom,E., Hauselmann,H.J., Schudt,C., and Hatzelmann,A. (2002). Phosphodiesterase isoenzyme families in human osteoarthritis chondrocytes--functional importance of phosphodiesterase 4. Br. J. Pharmacol. *135*, 609-618.

Tenor, H. and Schudt, C. Phosphodiesterases in asthma. Sampson, A. P. and Church, M. K. Anti-Inflammatory Drugs in Asthma, 87-135. 1999. Birkhäuser Verlag, Basel, Switzerland.
Ref Type: Serial (Book,Monograph)

Tenor,H., Staniciu,L., Schudt,C., Hatzelmann,A., Wendel,A., Djukanovic,R., Church,M.K., and Shute,J.K. (1995b). Cyclic nucleotide phosphodiesterases from purified human $CD4^+$ and $CD8^+$ T lymphocytes. Clin. Exp. Allergy *25*, 616-624.

Tesmer,J.J., Sunahara,R.K., Gilman,A.G., and Sprang,S.R. (1997). Crystal structure of the catalytic domains of adenylyl cyclase in a complex with Gsα·GTPS. Science *278*, 1907-1916.

Thomas,R., Davis,L.S., and Lipsky,P.E. (1993). Isolation and characterization of human peripheral blood dendritic cells. J. Immunol. *150*, 821-834.

Thompson,C.B., Lindsten,T., Ledbetter,J.A., Kunkel,S.L., Young,H.A., Emerson,S.G., Leiden,J.M., and June,C.H. (1989). CD28 activation pathway regulates the production of multiple T-cell-derived lymphokines/cytokines. Proc. Natl. Acad. Sci. USA *86*, 1333-1337.

Thompson,W.J. and Appleman,M.M. (1971a). Multiple cyclic nucleotide phosphodiesterase activities from rat brain. Biochemistry *10*, 311-316.

Thompson,W.J., Terasaki,W.L., Epstein,P.M., and Strada,S.J. (1979). Assay of cyclic nucleotide phosphodiesterase and resolution of multiple molecular forms of the enzyme. Adv. Cyclic Nucleotide Res. *10*, 69-92.

Thompson,W.J. and Appleman,M.M. (1971b). Characterization of cyclic nucleotide phosphodiesterases of rat tissues. J. Biol. Chem. *246*, 3145-3150.

Thurnher,M.A., Zelle-Rieser,C.L., Ramoner,R.E., Bartsch,G.E., and Holtl,L.O. (2001). The disabled dendritic cell. FASEB J. *15*, 1054-1061.

Timmer,W., Leclerc,V., Birraux,G., Neuhauser,M., Hatzelmann,A., Bethke,T., and Wurst,W. (2002). The new phosphodiesterase 4 inhibitor roflumilast is efficacious in exercise-induced asthma and leads to suppression of LPS-stimulated TNF-alpha ex vivo. J. Clin. Pharmacol. *42*, 297-303.

Torgersen,K.M., Vang,T., Abrahamsen,H., Yaqub,S., and Tasken,K. (2002). Molecular mechanisms for protein kinase A-mediated modulation of immune function. Cell. Signal. *14*, 1-9.

Torphy,T.J. (1998). Phosphodiesterase isozymes. Molecular targets for novel antiasthma agents. Am. J. Respir. Crit. Care Med. *157*, 351-370.

Torphy,T.J., Zhou,H.L., Foley,J.J., Sarau,H.M., Manning,C.D., and Barnette,M.S. (1995). Salbutamol up-regulates PDE4 activity and induces a heterologous desensitization of U937 cells to prostaglandin E2. Implications for the therapeutic use of beta-adrenoceptor agonists. J. Biol. Chem. *270*, 23598-23604.

Triantafilou,M. and Triantafilou,K. (2002). Lipopolysaccharide recognition: CD14, TLRs and the LPS-activation cluster. Trends Immunol. *23*, 301-304.

van Schalkwyk,E., Strydom,K., Williams,Z., Venter,L., Leichtl,S., Schmid-Wirlitsch,C., Bredenbroker,D., and Bardin,P.G. (2005). Roflumilast, an oral, once-daily phosphodiesterase 4 inhibitor, attenuates allergen-induced asthmatic reactions. J. Allergy Clin. Immunol. *116*, 292-298.

Vang,T., Abrahamsen,H., Myklebust,S., Enserink,J., Prydz,H., Mustelin,T., Amarzguioui,M., and Tasken,K. (2004). Knockdown of C-terminal Src kinase by siRNA-mediated RNA interference augments T cell receptor signaling in mature T cells. Eur. J. Immunol. *34*, 2191-2199.

Vassiliou,E., Jing,H., and Ganea,D. (2003). Prostaglandin E2 inhibits TNF production in murine bone marrow-derived dendritic cells. Cell. Immunol. *223*, 120-132.

Veillette,A., Latour,S., and Davidson,D. (2002). Negative regulation of immunoreceptor signaling. Annu. Rev. Immunol. *20*, 669-707.

Verde,I., Pahlke,G., Salanova,M., Zhang,G., Wang,S., Coletti,D., Onuffer,J., Jin,S.-L.C., and Conti,M. (2001). Myomegalin is a novel protein of the Golgi/centrosome that interacts with a cyclic nucleotide phosphodiesterase. J. Biol. Chem. *276*, 11189-11198.

Verghese,M.W., McConnell,R.T., Lenhard,J.M., Hamacher,L., and Jin,S.L. (1995). Regulation of distinct cyclic AMP-specific phosphodiesterase (phosphodiesterase type 4) isozymes in human monocytic cells. Mol. Pharmacol. *47*, 1164-1171.

Vicini,E. and Conti,M. (1997). Characterization of an intronic promoter of a cyclic adenosine 3',5'-monophosphate (cAMP)-specific phosphodiesterase gene that confers hormone and cAMP inducibility. Mol. Endocrinol. *11*, 839-850.

Vo,N. and Goodman,R.H. (2001). CREB-binding Protein and p300 in Transcriptional Regulation. J. Biol. Chem. *276*, 13505-13508.

Wallace,D.A., Johnston,L.A., Huston,E., MacMaster,D., Houslay,T.M., Cheung,Y.F., Campbell,L., Millen,J.E., Smith,R.A., Gall,I., Knowles,R.G., Sullivan,M., and Houslay,M.D. (2005). Identification and characterization of PDE4A11, a novel, widely expressed long isoform encoded by the human PDE4A cAMP phosphodiesterase gene. Mol. Pharmacol. *67*, 1920-1934.

Wang,D., Deng,C., Bugaj-Gaweda,B., Kwan,M., Gunwaldsen,C., Leonard,C., Xin,X., Hu,Y., Unterbeck,A., and De Vivo,M. (2003). Cloning and characterization of novel PDE4D isoforms PDE4D6 and PDE4D7. Cell. Signal. *15*, 883-891.

Wang,P., Wu,P., Ohleth,K.M., Egan,R.W., and Billah,M.M. (1999). Phosphodiesterase 4B2 is the predominant phosphodiesterase species and undergoes differential regulation of gene expression in human monocytes and neutrophils. Mol. Pharmacol. *56*, 170-174.

Wei,J.Y., Roy,D.S., Leconte,L., and Barnstable,C.J. (1998). Molecular and pharmacological analysis of cyclic nucleotide-gated channel function in the central nervous system. Prog. Neurobiol. *56*, 37-64.

Wess,J. (1998). Molecular basis of receptor/G-protein-coupling selectivity. Pharmacol. Therapeut. *80*, 231-264.

Weston,M.C., Anderson,N., and Peachell,P.T. (1997). Effects of phosphodiesterase inhibitors on human lung mast cell and basophil function. Br. J. Pharmacol. *121*, 287-295.

Willoughby,D., Wong,W., Schaack,J., Scott,J.D., and Cooper,D.M. (2006). An anchored PKA and PDE4 complex regulates subplasmalemmal cAMP dynamics. EMBO J. *25*, 2051-2061.

Wong,W. and Scott,J.D. (2004). AKAP signalling complexes: focal points in space and time. Nat. Rev. Mol. Cell Biol. *5*, 959-970.

Xiang,Y., Naro,F., Zoudilova,M., Jin,S.L., Conti,M., and Kobilka,B. (2005). Phosphodiesterase 4D is required for beta2 adrenoceptor subtype-specific signaling in cardiac myocytes. Proc. Natl. Acad. Sci. USA *102*, 909-914.

Xu,R.X., Hassell,A.M., Vanderwall,D., Lambert,M.H., Holmes,W.D., Luther,M.A., Rocque,W.J., Milburn,M.V., Zhao,Y., Ke,H., and Nolte,R.T. (2000). Atomic structure of PDE4: insights into phosphodiesterase mechanism and specificity. Science *288*, 1822-1825.

Yarfitz,S. and Hurley,J.B. (1994). Transduction mechanisms of vertebrate and invertebrate photoreceptors. J. Biol. Chem. *269*, 14329-14332.

Yarwood,S.J., Steele,M.R., Scotland,G., Houslay,M.D., and Bolger,G.B. (1999). The RACK1 signaling scaffold protein selectively interacts with the cAMP-specific phosphodiesterase PDE4D5 isoform. J. Biol. Chem. *274*, 14909-14917.

Yin,J., Ma,Z., Selliah,N., Shivers,D.K., Cron,R.Q., and Finkel,T.H. (2006). Effective gene suppression using small interfering RNA in hard-to-transfect human T cells. J. Immunol. Methods *312*, 1-11.

Yuasa,K., Ohgaru,T., Asahina,M., and Omori,K. (2001). Identification of rat cyclic nucleotide phosphodiesterase 11A (PDE11A): comparison of rat and human PDE11A splicing variants. Eur. J. Biochem. *268*, 4440-4448.

Yue,C., Dodge,K.L., Weber,G., and Sanborn,B.M. (1998). Phosphorylation of serine 1105 by protein kinase A inhibits phospholipase Cβ3 stimulation by Gαq. J. Biol. Chem. *273*, 18023-18027.

Zhang,K.Y., Card,G.L., Suzuki,Y., Artis,D.R., Fong,D., Gillette,S., Hsieh,D., Neiman,J., West,B.L., Zhang,C., Milburn,M.V., Kim,S.H., Schlessinger,J., and Bollag,G. (2004). A glutamine switch mechanism for nucleotide selectivity by phosphodiesterases. Mol. Cell *15*, 279-286.

Zitt,C., Strauss,B., Schwarz,E.C., Spaeth,N., Rast,G., Hatzelmann,A., and Hoth,M. (2004). Potent inhibition of Ca^{2+} release-activated Ca^{2+} channels and T-lymphocyte activation by the pyrazole derivative BTP2. J. Biol. Chem. *279*, 12427-12437.